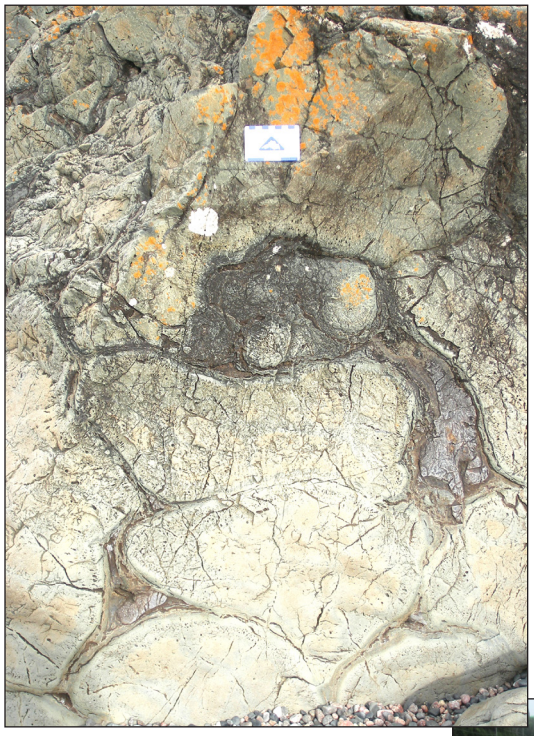
65th Annual Meeting

Terrace Bay, Ontario - May 8-9, 2019

Institute on Lake Superior Geology

Part 2 – Field Trip Guidebook







www.lakesuperiorgeology.org

Thank you to our sponsors!

































Individual contributors to student travel scholarship:

Al MacTavish, Mary Kay Arthur, L. Gordon Medaris, Jr., Nick Swanson-Hysell



www.lakesuperiorgeology.org

65th Annual Meeting

Institute on Lake Superior Geology

May 8-9, 2019

Terrace Bay, Ontario

HOSTED BY:

Mark Smyk and Pete Hollings

Co-Chairs

Ontario Geological Survey and Lakehead University

Proceedings - Volume 65

Part 2 – Field Trip Guidebook

Compiled and edited by Al MacTavish and Pete Hollings

Cover Photos: Left - Pillowed Archean metabasalt, Schreiber Beach, Middle - Layered Eastern Border Gabbro, Coldwell Complex. Right - Foliated Archean metavolcanic rocks, Slate Islands.

65th Institute on Lake Superior Geology

Volume 65 consists of:

Part 1: Program and Abstracts

Part 2: Field Trip Guidebook

Trip 1: The Slate Islands

Trip 2: Midcontinent Rift-Related Carbonatites and Diatremes

Trip 3: Geology of the Western Schreiber-Hemlo Greenstone Belt

Trip 4: Geology of the Nipigon Area

Trip 5: A stratigraphic transect across the Northern flank of the Midcontinent Rift near Rossport

Trip 6: Geology of the Coldwell alkaline complex

Trip 7: Building and ornamental stone sites of the Marathon Area, Ontario

Trip 8: Geology of the past-producing Winston Lake Cu-Zn Mine

Reference to material in Part 2 should follow the example below:

Magnus, S., 2019. Geology of the Western Schreiber-Hemlo Greenstone Belt. In; MacTavish, A. and Hollings, P. (Eds.), Institute on Lake Superior Geology Proceedings, 65th Annual Meeting, Terrace Bay, Ontario, Part 2 - Field trip guidebook, v.65, part 2, 3-31.

Published by the 65th Institute on Lake Superior Geology and distributed by the ILSG Secretary:

Pete Hollings - ILSG Secretary
Department of Geology
Lakehead University
955 Oliver Road
Thunder Bay, ON P7B 5E1
Canada
Email: peter.hollings@lakeheadu.ca

ILSG website: www.lakesuperiorgeology.org
ISSN 1042-9964

Table of Contents

65th Annual Meeting ..... A

Introduction, safety considerations and acknowledgements 1

Field trip 1 - The Slate Islands 2

Field trip 2 - Midcontinent Rift-Related Carbonatites and Diatremes 3

Field trip 3 - Geology of the Western Schreiber-Hemlo Greenstone Belt 14

Field trip 4 - Geology of the Nipigon Area 43

Field trip 5 - A stratigraphic transect across the Northern flank of the Midcontinent Rift near Rossport 60

Field trip 6 - Geology of the Coldwell alkaline complex 75

Field trip 7 - Building and ornamental stone sites of the Marathon Area, Ontario 105

Field trip 8 - Geology of the past-producing Winston Lake Cu-Zn Mine 113

Introduction, safety considerations and acknowledgements

Pete Hollings

Department of Geology, Lakehead University, Thunder Bay, Ontario, P7B 5E1, Canada

and

Mark Smyk

Resident Geologist Program, Ontario Geological Survey, Ministry of Energy, Northern Development and Mines, Thunder Bay, Ontario, P7E 6S7, Canada

This volume is intended to serve not only as a guide for 65th ILSG field trip participants but also as a reference for those planning to revisit these areas at a later date. Consequently we have included UTM coordinates in the NAD 83 datum for stops, as well as instructions on how to reach them. As some of the stops are on private and staked land, please be sure to obtain the land owners' permission before entering their land. Contact the staff of the Resident Geologist Program in Thunder Bay for current ownership information.

We are once again offering field trips onto Lake Superior. This creates a number of unique safety issues. Please exercise caution when getting in and out of the boats as the outcrops are often extremely slippery. Personal flotation devices must be worn in the boats at all times. If you are planning to revisit these sites please be very careful, as Lake Superior is dangerous; waves can often be many metres high and even in mid-summer fog can appear very quickly.

The other field trips will be visiting stops along either major highways or busy logging roads. Please take care when crossing or parking along these roads.

We would like to thank all the other authors who contributed to this field guide, all those who provided comments and/or assisted with the running of the field trips themselves (Shannon Zurevinski, Rob Cundari, Phil Fralick, Dorothy Campbell, Mark Puumala, Robert Lodge, Al MacTavish, Dave Good, John McBride, Peter Hinz, Seamus Magnus, Bill Skrepichuk). We appreciate the assistance and cooperation of the exploration and mining companies in providing us access and information concerning their properties, particularly Superior Lake Resources Ltd. (Winston Lake Mine), Plato Gold Corp. (Good Hope Niobium), Rudy Wahl (Madonna), Jerry Blakely (Shack Lake), Red Rock Indian Band (Ruby Lake), Alex Pleson (Stenlund), John Ternowesky (Dead Horse North) , Stillwater-Sibanye (Marathon) and Ontario Parks (Slate Islands and Neys).

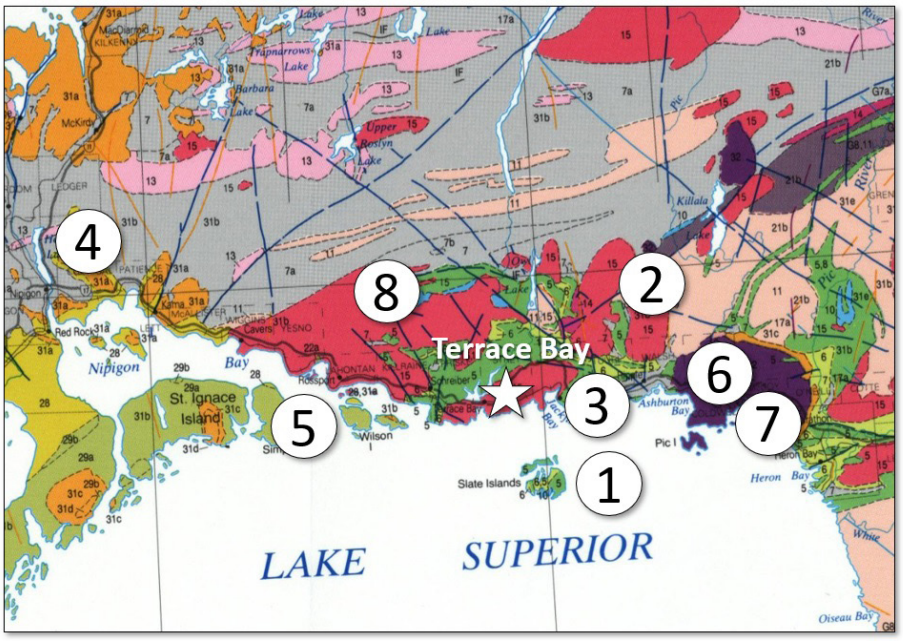


Figure 1. Map showing the location of the eight field trips offered in 2019.

Field trip 1 - The Slate Islands

Pete Hollings

Department of Geology, Lakehead University, Thunder Bay, Ontario, P7B 5E1, Canada

Mark Smyk

Resident Geologist Program, Ontario Geological Survey, Ministry of Northern Development and Mines, Thunder Bay, Ontario, P7E 6S7, Canada

Bill Addison

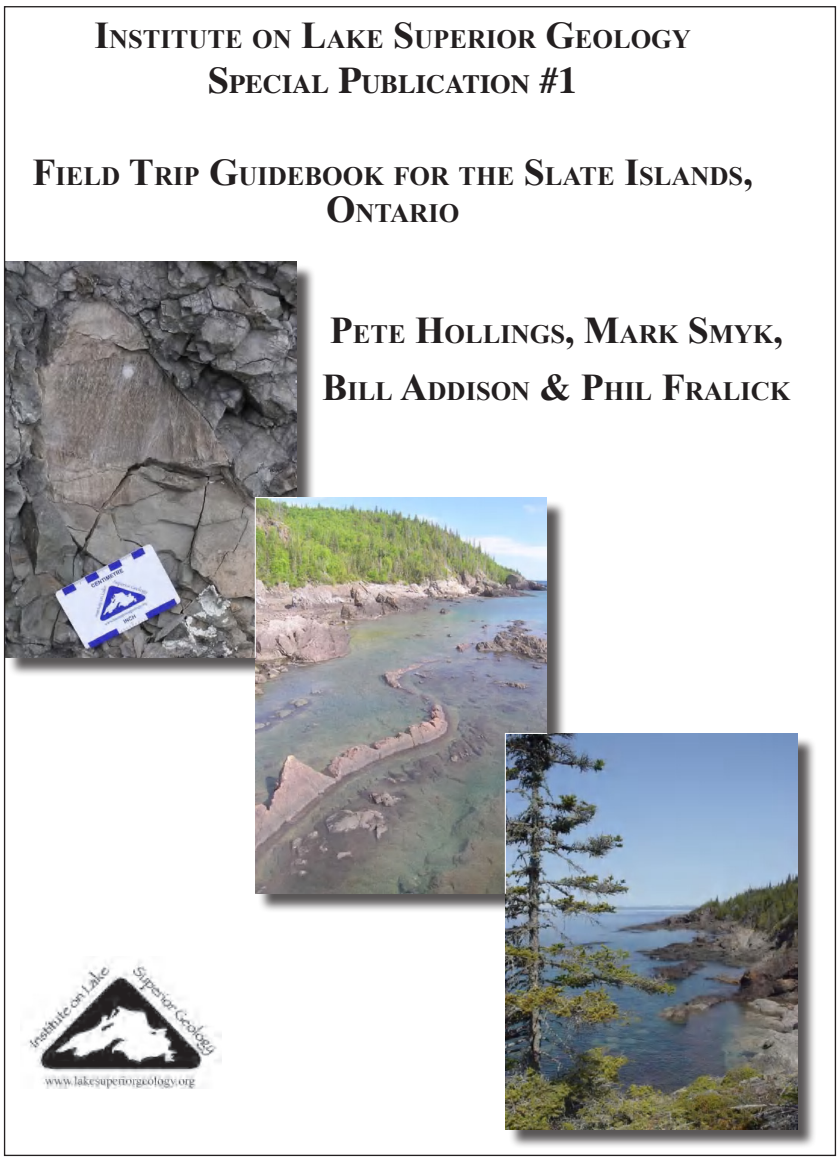
and

Phil Fralick

Department of Geology, Lakehead University, Thunder Bay, Ontario, P7B 5E1, Canada

---

The field guide for the Slate Islands has previously been published as ILSG Special Publication #1 and is available on the ILSG website - www.lakesuperiorgeology.org



Field trip 2 - Midcontinent Rift-Related Carbonatites and Diatremes

Shannon Zurevinski

Department of Geology, Lakehead University, Thunder Bay, Ontario, P7B 5E1, Canada

Dorothy Campbell and Mark Puumala

Resident Geologist Program, Ontario Geological Survey, Ministry of Northern Development and Mines, Thunder Bay, Ontario, P7E 6S7, Canada

Introduction

The Midcontinent Rift System (MCR) of North America is one of the largest known aborted rifts, and extends ~2200km from Kansas, north to the Lake Superior area. There are several MCR-related fault systems in Lake Superior and the surrounding terrain, as evidenced by seismic reflections, gravity and various magnetic anomalies.

Some of the most fascinating geology of the Terrace Bay-Marathon area of Northwestern Ontario is where Archean rocks of the Superior Province are intruded by diatremes, alkalic rocks, carbonatites and ultramafic lamprophyres, which are mostly related to the MCR and the Trans-Superior Tectonic Zone (TSTZ). Many of these intrusions are located along the strike of the Big Bay-Ashburton Fault (which is the proposed northern extension of the Thiel Fault), representing the most northerly component of the TSTZ (Sage, 1982). The Coldwell Alkalic Complex, Killala Lake Alkalic Complex, Chipman, Prairie Lake and Good Hope Carbonatite occurrences, the Dead Horse Creek Diatreme, and various ultramafic lamprophyres lie along the extrapolated arm of the fault system (Fig. 1).

We would like to acknowledge the earlier work of Ron Sage and David H. Watkinson, who guided an extensive field trip into the Alkalic rocks of the MCR during the 41st Annual Meeting of the Institute in 1995. This field trip will serve as an update to the prospecting and exploration completed over the last 25 years and will visit: 1) the North Dead Horse property; 2) the diamondiferous Madonna dyke; 3) the Prairie Lake Carbonatite; and 4) the Good Hope Carbonatite (Fig. 2). We also acknowledge Rudy Wahl for his hard work and boots-on-the-ground prospecting that has led to the discoveries of both the Madonna dyke and Good Hope Carbonatite. A special thanks to Seamus Magnus for providing assistance with the descriptions of the North Dead Horse subcomplex trenches.

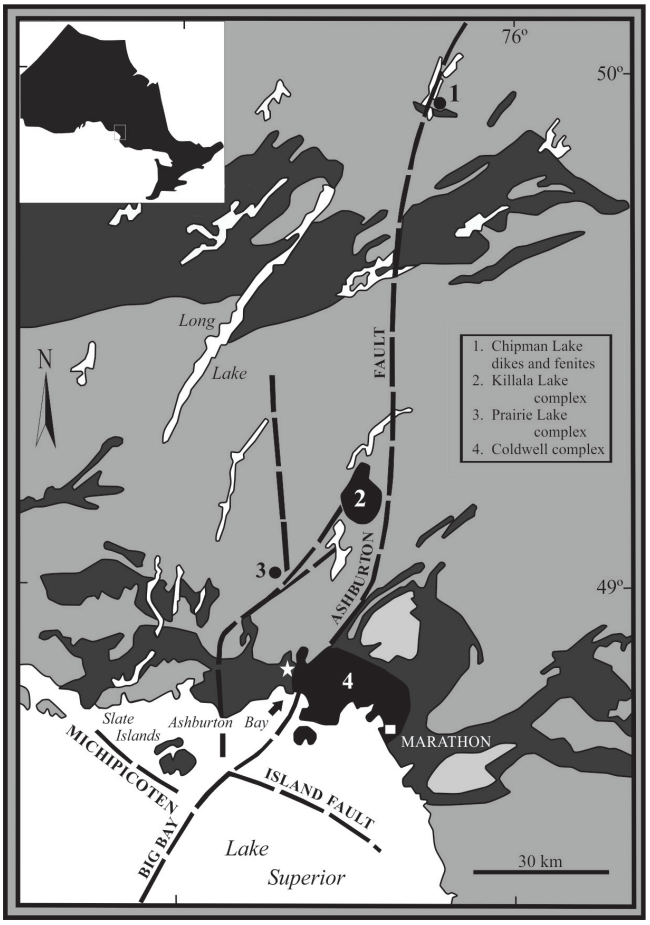


Figure 1. A regional map of the area north of Lake Superior between Terrace Bay and Marathon, showing the alkaline complexes, diatremes, carbonatites and ultramafic lamprophyres of the area. (modified from Smyk et al., 1993).

Acknowledgements

We are grateful to Rudy Wahl (Madonna dyke and Good Hope Carbonatite), John Ternowsky (North Dead Horse Property) and Nuinsco Resources (Prairie Lake Carbonatite) for permissions to access the properties for this field trip.

Stop descriptions

Stop 1: The North Dead Horse Creek Diatreme

UTM Coordinates 523959E 5409978N (parking lot)

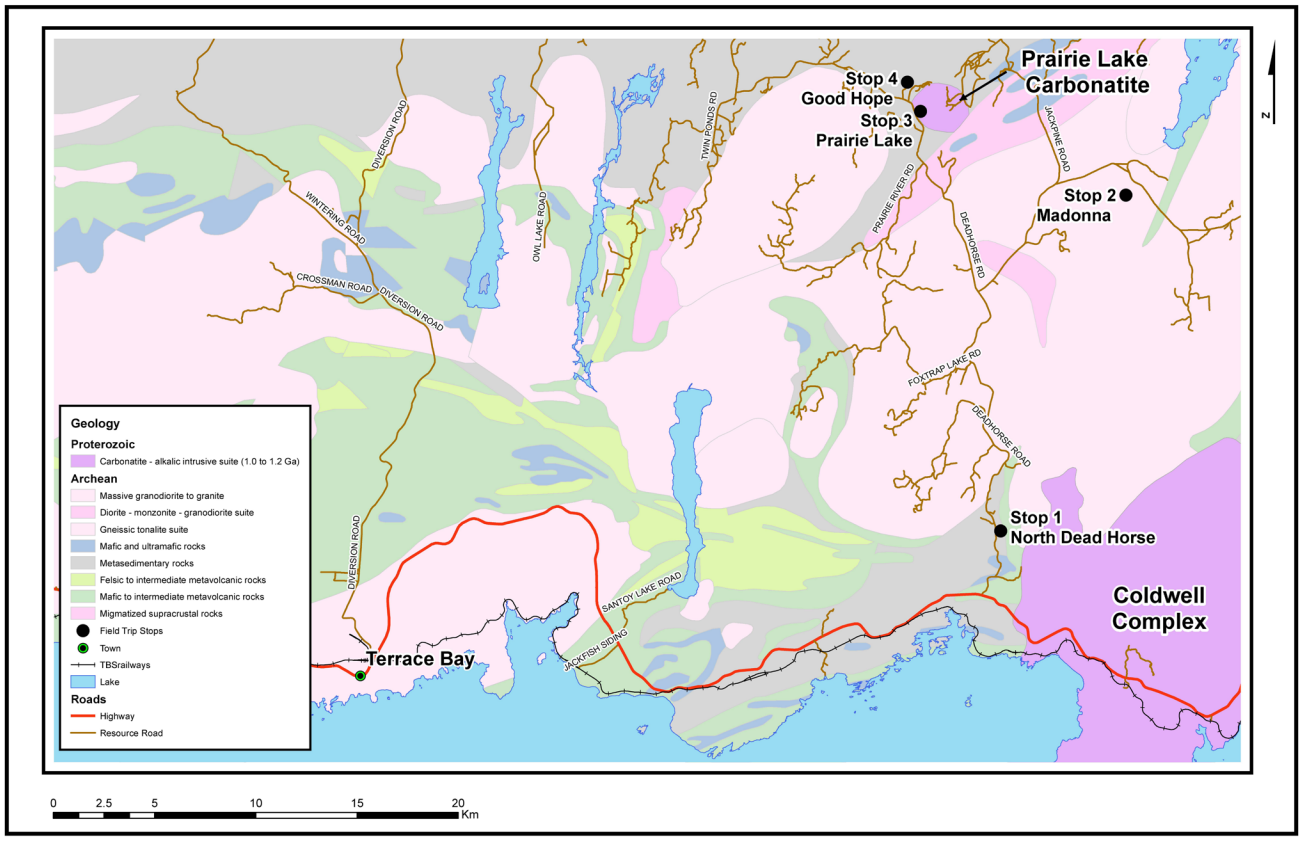


Figure 2. General geology with field trip stops (geology from the Ontario Geological Survey).

Introduction

The Dead Horse Creek Diatreme is hosted by the metasedimentary and metavolcanic rocks of the Schreiber-White River greenstone belt, within the Wawa Subprovince (Sage, 1982). It is located approximately 1km from the western margin of the Coldwell Alkalic Complex (Fig. 2). Sage (1982) describes the complex as a broad spectrum of heterolithic breccias that have undergone varying degrees of alteration and are variably radioactive, and subsequently divided the complex into five subcomplexes (North, South, East, West, and Central; Fig. 3). Past exploration programs by Gulf Minerals Canada (1977) focused on the uranium mineralization of the West Dead Horse and the North Dead Horse subcomplexes (Fig. 3). Subsequent exploration on the property by Highwood Resources Ltd. (1985) focused on exploration for beryllium, yttrium, and cerium; Unocal Canada's (1987) main interest was exploring the potential for yttrium; while Canadian International Mining (2011) focused on exploration for the Rare Earth Elements (REEs). The mineralized zone of the West Dead Horse subcomplex has been described as "diverse, exotic, hydrothermally altered, and rare metal mineralized" (Sage, 1982). Unpublished U-Pb geochronology of zircons from the

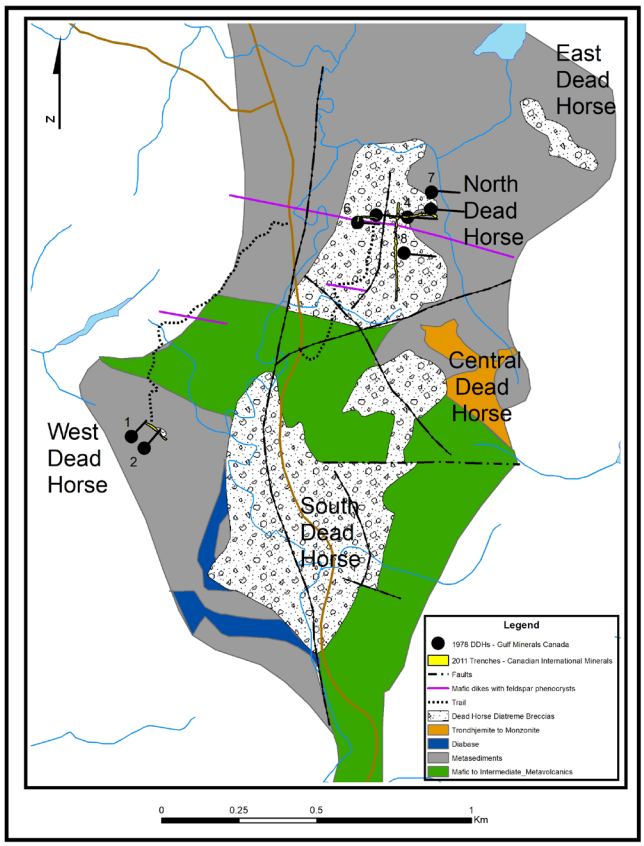


Figure 3. The Dead Horse Creek Diatreme geology map. Shown here are the 5 subcomplexes. Also note the Gulf minerals drilling program (investigated for U). After Sage (1982)

Dead Horse Creek West subcomplex, were found to be 1128.7 ± 6 Ma (Sage, 1995).

The West Dead Horse subcomplex (400m x 1600m elongate in a N-NE direction) has been the focus of extensive geochemical and mineralogical studies, and is described as an occurrence of heterolithic and carbonate-rich breccias and veins (Smyk et al., 1993; Potter and Mitchell, 2005). Smyk et al. (1993) reported Heavy Rare Earth Element (HREE) enrichment from the mineralized zone of the West Dead Horse occurrence to be up to 1004ppm ΣHREE. Potter and Mitchell (2005) summarized the REE mineralogy of the occurrence, including a phenakite-bearing quartz vein, Ca-zirconosilicate, zircon, thorite, uraninite, apatite, xenotime-Y, monazite-Ce and rutile. Smyk et al. (1993) proposed that the volcaniclastic breccia formed during the early stages of the MCR event and incorporated clasts of Archean metasedimentary and granitic rocks. They proposed that after the emplacement of the volcaniclastic breccia, U-Be-Zr mineralization occurred along fault structures after being introduced via A-type granitic fluids, and was followed by alkaline metasomatism. The mineralized zone is not related to the igneous activity that produced the volcaniclastic breccia, rather the porous breccia allowed for the deposition of the U-Be-Zr mineralization. Potter and Mitchell (2005) provide a genetic model for the complex based on the exotic mineral suite present (including the accessory REE mineralogy), and concluded that upon emplacement of the nearby Coldwell Alkalic complex (1108 ±1 Ma; Heaman & Machado, 1992), the Dead Horse volcaniclastic breccia was subjected to thermal metamorphism and post-Pleistocene supergene alteration. Nb-Ti-V-Cr-bearing alkaline fluids were introduced into the same fault system and reacted with the initial mineralization, creating the suite of exotic minerals which was further diversified by supergene alteration (Potter and Mitchell, 2005).

The remaining question: What is the source of these Nb-Ti-V-Cr-bearing fluids? While the Coldwell Alkalic Complex does contain the A-type granitic rocks that would produce these fluids, the timing of the emplacement of both the Coldwell Alkalic Complex and the Dead Horse Creek diatreme would need further geochronological studies to constrain this relationship.

Canadian International Minerals Inc. (CIM) recently conducted an extensive exploration program on the North Dead Horse property, including trenching, assaying, and geophysical surveys. The showing is arranged in a cross, and the E-W trending stripping is ~250m, while the N-S stripping is ~320m in length (Fig. 4). This recently exposed trenching provides an

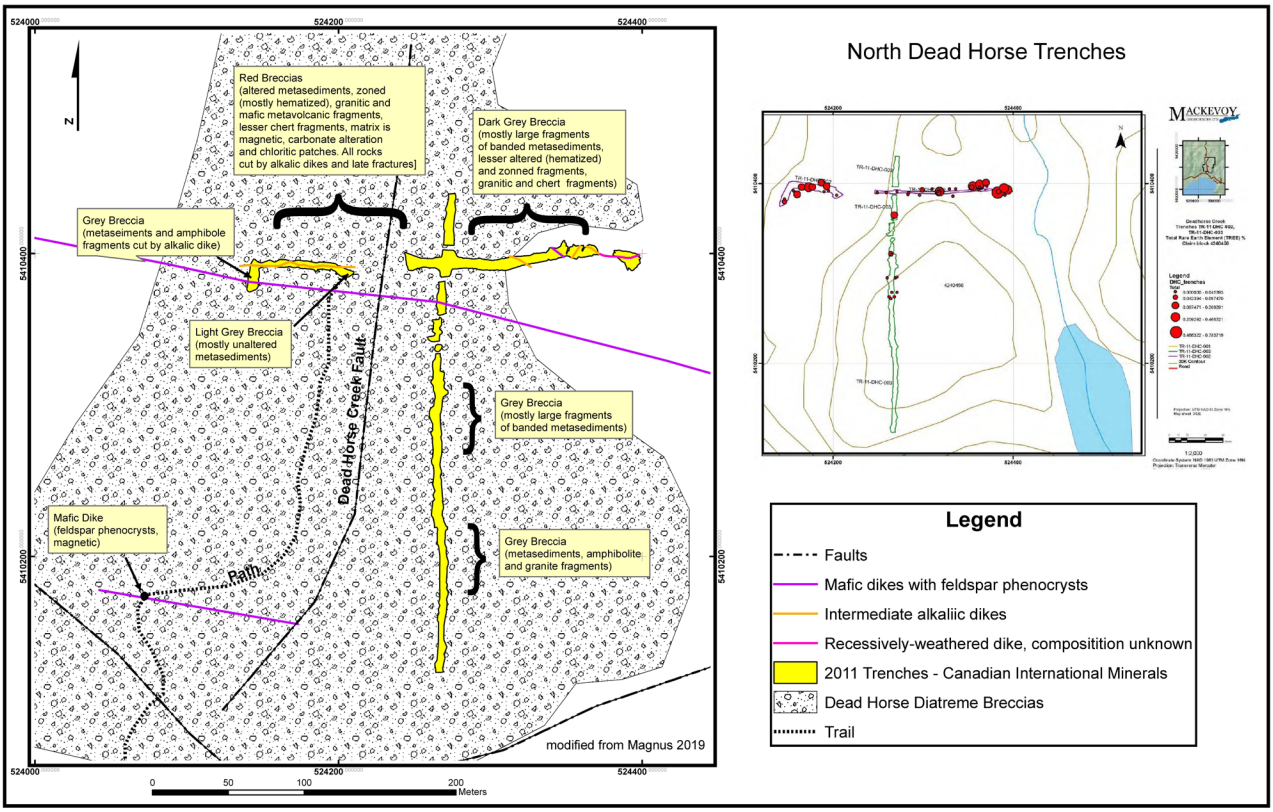


Figure 4. The North Dead Horse Creek trench map (modified from Magnus 2019).

excellent opportunity to observe the breccia and its various components.

Stop 1a: North Dead Horse: Trachytic Diabase Dyke

UTM Coordinates 524072E 5410174N

Occurring along the trail from the parking area is a trachytic diabase dyke. This is described as a mafic dyke containing feldspar phenocrysts with a magnetic matrix (Fig. 5). These dykes are widespread throughout the area and also occur within the Coldwell Alkalic Complex.



Figure 5. (a - top) Photograph of the Trachytic diabase dyke from Stop #1. (b - bottom) Close-up photograph of the feldspar phenocrysts of the Trachytic diabase dyke.

Stop 1b: North Dead Horse: East-West Trench

UTM Coordinates 524210E 5410389N

Grey and red heterolithic breccias are found at the North Dead Horse trenches, cut by various mafic and intermediate dykes (Fig. 4).

The light grey breccia is host to relatively unaltered clasts that show their primary and structural fabrics

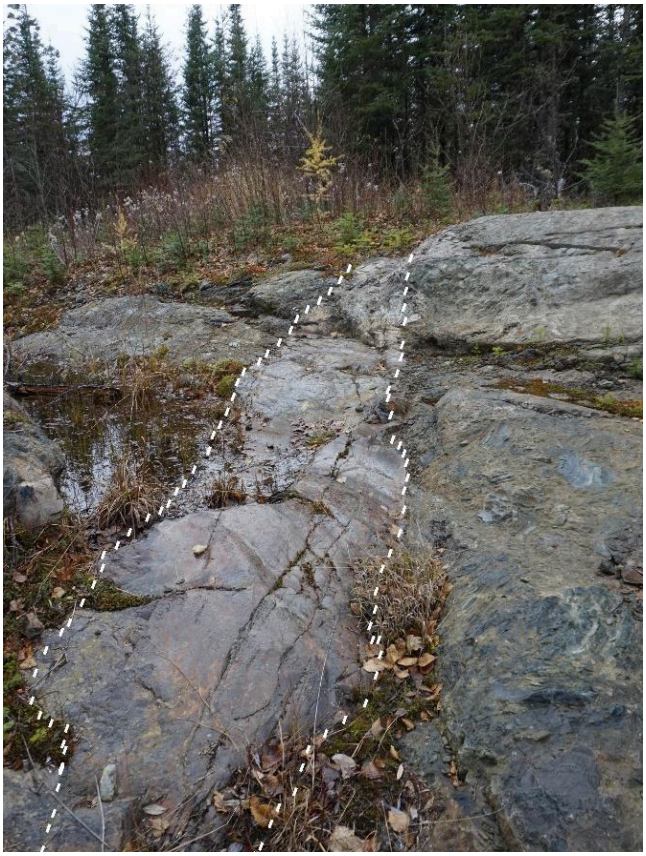


Figure 6. Photograph of the grey breccia from the North Dead Horse trench, cut by an alkalic dyke.



Figure 7. Photograph of the dark grey breccia from the North Dead Horse trench, showing large clasts of banded metasediments, and hematized and zoned fragments, as well as chert fragments.

(Figs. 6 and 7). CIM describes the matrix of the grey breccias as carbonate-rich. The clasts are generally composed of amphibolite, wacke, and granitoid rocks (Fig. 6). Some wacke clasts are several meters in length. Brecciation of the various clasts appears to be found along bedding and schistosity planes.

The red breccia is dominant in the western part of the trench and is highly altered (Fig. 8). The clasts are



Figure 8. Photographs of the red breccia from the North Dead Horse trench, showing altered hematized metasediments, and both granitic and mafic metavolcanic clasts.

composed of granitic and mafic metavolcanics, altered metasediment, and lesser chert. The metasedimentary clasts are hematized and heavily altered at the rims, with the degree of alteration reduced towards the core of the clasts. Some clasts are sulphide-rich. The matrix is magnetic and there is carbonate and chlorite alteration present.

Rare earth mineralization on the property appears to be associated with areas containing the red breccia unit (Fig. 4). Minerals identified by Potter and Mitchell (2005) on the property include albite, potassium feldspar, quartz, calcite, apatite, phenakite, aegirine-jervisite, aegirine-natalyite, allanite, barite, barylite, coffinite, Ca-Mn-silicate, magnetite, monazite-(Ce), niobian vanadium rutile, pyrite, thorite, thoro-gummite, thortveitite, uraninite, vanadium crichtonite, xenotime-(Y), ankerite-dolomite and zircon (Quist, 2011).

North-South trench

The north-south trench contains mostly grey breccias. The grey breccia has large, relatively unaltered metasediment, amphibolite, and granitic clasts (as described above).

Intermediate alkalic dykes, mafic dykes, and late fractures crosscut all breccias. The mafic dykes are similar to the dyke from Stop 1a (and occur throughout the area and within the Coldwell Alkalic Complex). The intermediate alkalic dykes are fine-grained and grey to pink in colour. The intermediate dykes are less common than the mafic dykes. Preliminary studies have shown the intermediate alkalic dykes to have up to 2000ppm ΣREEs, and it is reported that the altered and mineralized zones of North Dead Horse are coincident with these intermediate REE-enriched alkalic dykes (S. Magnus, personal communication). The east end of the E-W trench is host to a recessively weathered dyke with an unknown, possibly carbonatitic composition.

Stop 2: The Madonna Dyke

UTM Coordinates 530377E 5427200N

Introduction

Located approximately 30kms northwest of Marathon, the Madonna Dyke was discovered by Rudy Wahl in 2007 (Fig. 9). The Madonna Dyke is



Figure 9. Photo of the Madonna dyke (photo courtesy of R. Wahl).

approximately 1 to 2m in width, outcrops for ~50m, strikes 009°, and dips 65° towards the west (Wahl website). Sampling recovered 66 diamonds from a 1205.80 kg sample, which includes white, green, yellow, brown and grey diamonds (http://users.renegadeisp.com/~rwahl/Kimberlite%20Targets%20Available%20for%20Option.htm). In 2018, R. Wahl completed drilling 82m to the southwest of the Madonna Dyke and intersected the same diamondiferous dyke over a width of 2.78m. The dyke is underlain by Neoarchean biotite granite gneiss and hornblende granite gneiss, as well as post tectonic quartz monzonites (Coates, 1970). The dyke intrudes near lineament intersections that could represent zones of crustal weakness that may have acted as a pathway for the ascent of mantle-derived magmas (Kozlowski, 2016).

Classification

The Madonna dyke been classified as a diamondiferous alnöite ultramafic lamprophyre (Kozlowski, 2016). It is described as a mafic hypabyssal rock with medium- to fine-grained rounded phenocrysts and a fine-grained dark-green to black groundmass (Fig. 10). The dyke has an orange-brown rind on its weathered surface. The phenocrysts (1 to 10mm in diameter) are estimated to make up to 50% of the modal abundance and are identified as pseudomorphs after olivine, pyroxene, and oxides rimmed by carbonate and lesser late-stage calcic amphiboles (Kozlowski, 2016). The groundmass consists of calcite (after melilite), phlogopite, magnetite, apatite and some alteration products (Kozlowski, 2016).



Figure 10. Photo of the Madonna dyke showing rounded phenocrysts set in a dark green groundmass. Also note the orange-brown rind on the weathered surface (photo courtesy of R. Wahl).

Mineralogy of the Madonna Dyke

Kozlowski (2016) summarizes the mineral chemistry of the Madonna dyke used to provide proper classification of the dyke. Pseudomorphed olivine occurs as microphenocrysts, phenocrysts, and rare macrocrysts replaced by serpentine, magnetite, and calcite. A few fresh olivine macrocrysts show mantle compositions ranging from Fo_{91} to Fo_{92} (Kozlowski, 2016). Clinopyroxenes are aluminous diopside with Al_2O_3 ranging from 3.11 to 14.47 wt.%. Groundmass micas have kinoshitalite–phlogopite compositions, with up to 4 wt.% BaO and 20.9 wt.% Al_2O_3. Spinel-group mineral compositions follow Magnetic Trend #2 – the Titanomagnetite Trend, where spinels range in composition from aluminous magnesian chromite to titanian magnesian chromite to titanian chromite to members of the ulvöspinel-magnetite series (Fig. 11; Kozlowski, 2016). Spinel-group minerals occur as red chromium spinel phenocrysts to macrocrysts with magnesium-rich cores and iron-rich rims, often associated with olivine phenocrysts and macrocrysts. They also occur as fine-grained opaque groundmass titanomagnetites with altered cores, and as reaction products forming a necklace texture around olivine. Atoll spinel is present. Although the Madonna dyke shows some textural and petrogenetic features of kimberlites, the mineralogy, including the presence of calcite after melilite and amphibole, are analogous with an ultramafic lamprophyre of alnöitic affinity

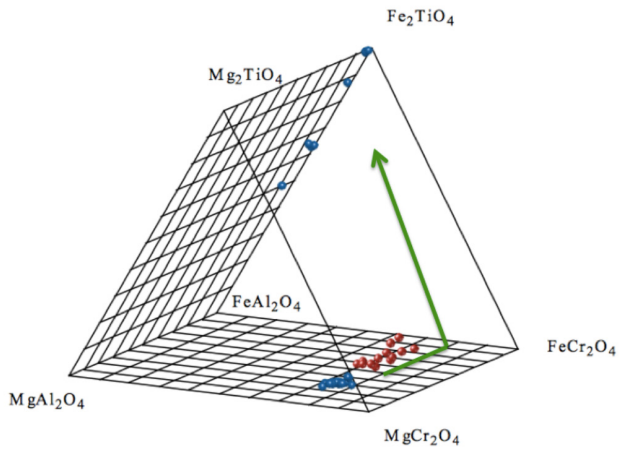


Figure 11. Reduced spinel prism with compositions of Madonna dyke spinels (blue = core; red = rim) showing a magmatic trend 2 – the titanomagnetite trend (green arrow) with a hiatus in the middle (classification after Mitchell, 1986).

Table 1 Summary of petrographic features of the Madonna Dyke compared to kimberlite and UML (ultramafic lamprophyre). After Mitchell (1995b) and Birkett et al. (2004).

	Kimberlites	UML	Madonna Dyke
Olivine (macrocrysts)	common	rare	rare
(phenocrysts)	common	common	common
Mica (phenocrysts)	common phlogopite	common phlogopite	not observed
(groundmass)	common, phlogopite kinoshitalite	common Al-biotite	common, phlogopite kinoshitalite
Spinels	abundant, Mg-chromite to Mg ulvöspinel	common, Mg-chromite to Ti-magnetite	common, Mg-chromite to Ti-magnetite
(atoll)	very common	present	present
(necklace)	present	present	present
Perovskite	common, Sr- and REE-poor	common, Sr- and REE-poor	not observed
Diopside	absent	common, Al- and Ti-rich	common, Al- rich
Apatite	common, Sr- and REE-poor	common, Sr- and REE-poor	common, Sr- and REE-poor
(skeletal)	rare	rare	common
Calcite	abundant	common	common
Melilite	absent	common	common
Amphibole	absent	present	present

(Kozlowski, 2016). Table 1 provides a summary of the features of the Madonna dyke compared to kimberlite rocks and ultramafic lamprophyres.

Stop 3: The Prairie Lake Carbonatite Complex

UTM Coordinates 520150E 5431100N

Introduction

The Prairie Lake Carbonatite Complex is located ~26 km from the shores of Lake Superior (Figs. 1 & 2). It covers a surface area of ~8.8 km^2 and generally consists of foidolitic and carbonatitic rocks (Fig. 12; Sage, 1987). It is generally a small arcuate intrusion emplaced in Archean gneisses along the TSTZ (Sage, 1987). The complex has been actively explored since 1968 for U and Nb, and is considered 'multi-commodity' with its potential residual apatite deposits.

There is significant modal heterogeneity of the rocks at the Prairie Lake complex. Wu et al. (2017) summarize the variation of the rock types present: 1) calcite carbonatite; 2) biotite pyroxenite; 3) the ijolitic series rocks; 4) potassic syenites; 5) heterogeneous carbonatites; and 6) rare dolomitic carbonatite (Fig. 12). The niobium mineralization in the Prairie Lake Carbonatite complex includes Na- and Ca- pyrochlore, latrappite, loparite, U-pyrochlore, Ce-pyrochlore, Pb-pyrochlore, marianoite, and wohlerite (Mitchell, 2015). The pyrochlore has a wide range of compositions and are complexly zoned and resorbed. The Nb mineralization is distributed mainly between perovskite, pyrochlore, and Nb-Zirconolite and tends to be REE-poor with in situ alteration (Mitchell, 2015).

Zurevinski and Mitchell (2015) describe the only known worldwide occurrence of orbicular ijolite from within the Prairie Lake Complex (Fig. 13). This occurrence had been previously noted and described by Sage (1987, 1995). The orbicules occur in an ijolite matrix, and the mineralogy of the orbicules is similar to that of their host ijolite (nephelene, diopside, calcite, apatite, andradite-melanite garnet, titanite, etc.; Fig. 13; Zurevinski and Mitchell, 2015). Detailed mineralogy and petrology have shown that the orbicular ijolite represents an interaction of a partially crystallized quenched ijolitic melt, in contact with a second pulse

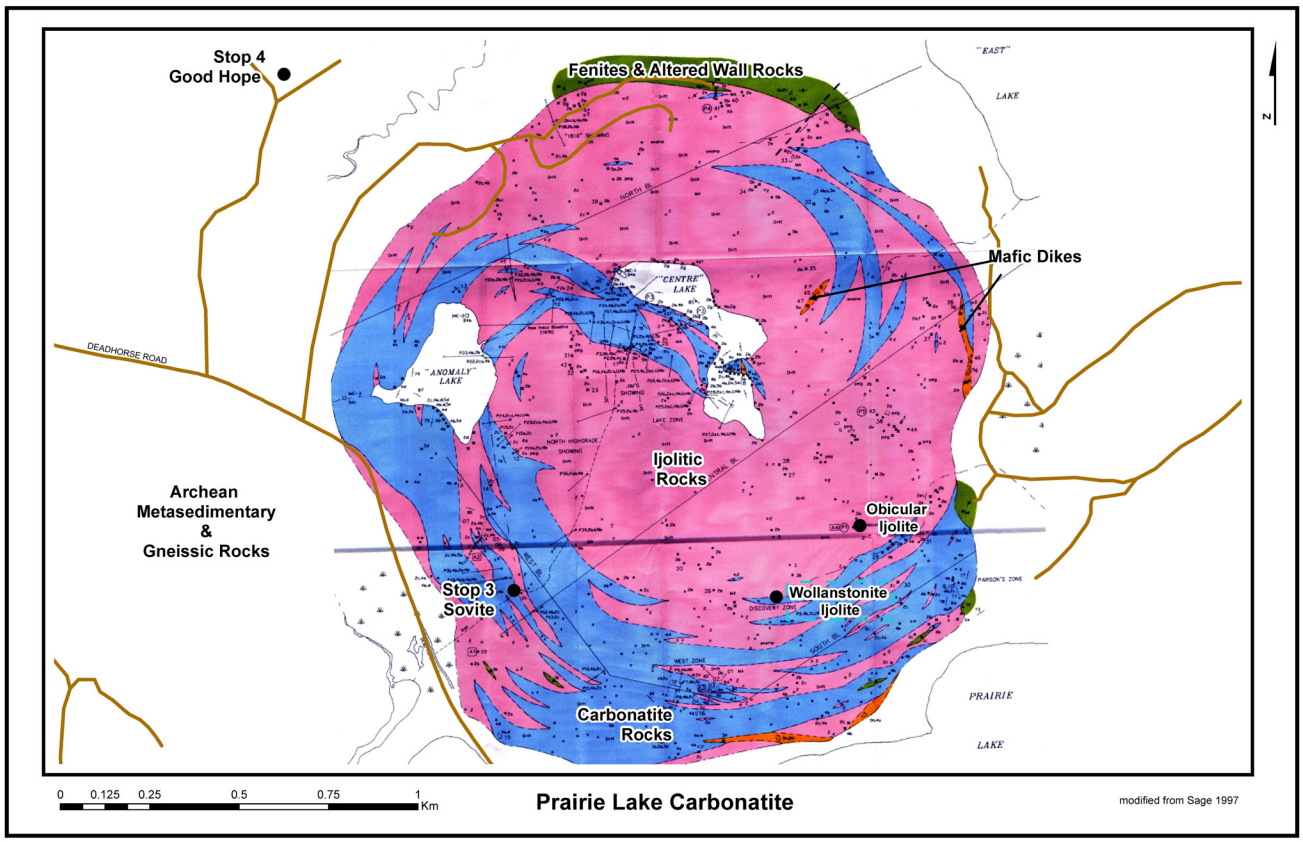


Figure 12. A map of the Prairie Lake Carbonatite complex. From Sage (1987).

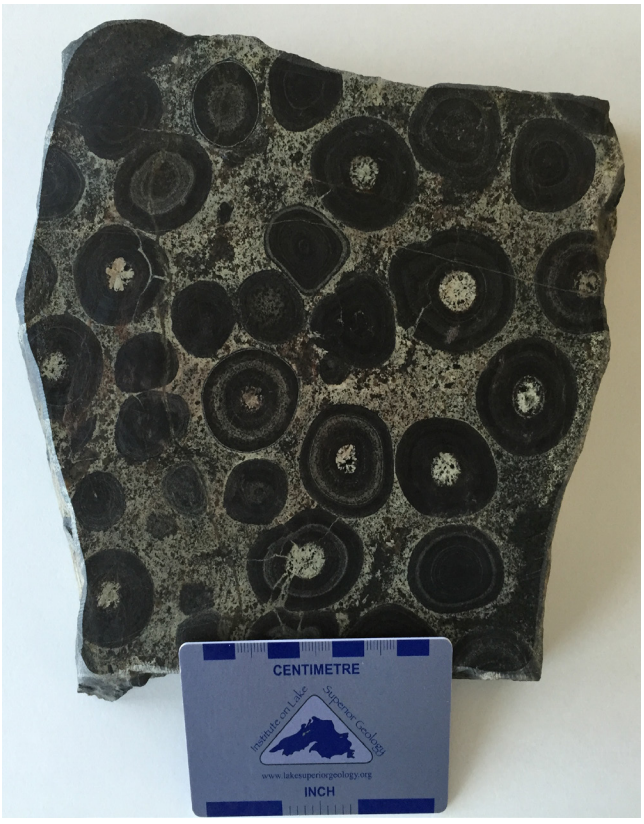


Figure 13. Orbicular ijolite from the Prairie Lake Carbonatite Complex (from Zurevinski and Mitchell, 2015).

of consanguineous ijolite magma. Immersion in the latter resulted in a sub-solidus diffusion and annealing recrystallization (i.e., magma mixing; Zurevinski and Mitchell, 2015).

Recent detailed geochronology has been completed on the Prairie Lake complex by Wu et al. (2016). In summary, U-Pb with baddeleyite from the carbonatite gave emplacement ages of 1157 ± 2.3 Ma and 1158 ± 3.8 Ma; baddeleyite from the ijolite-series rocks gave 1163 ± 3.6 Ma and U-Pb apatite from the carbonatite gave an emplacement age at ~1160 Ma. Therefore, the findings of Wu et al. (2016) reveal that all units were synchronously emplaced at ~1160 Ma. Furthermore, Sr-Nd-Hf tracer isotopic studies showed that the Prairie Lake carbonatites, ijolites, and syenite rocks had identical isotopic composition, therefore, the silicate and carbonatite rocks are co-genetic and thereby related by fractional crystallization processes (Wu et al., 2016). This data has reinforced the previous conclusions that Prairie Lake is the earliest manifestation of midcontinent rift magmatism, and is not genetically related to the nearby Coldwell or Killala Alkalic complexes (Rukhlov and Bell, 2010).

Stop 3: Prairie Lake Calciocarbonatite (Sövite) (West)

The area is noted by the prominent hill surrounded by low-lying marshy land. Generally, there is very sparse outcropping of extensively weathered calciocarbonatite. As you walk up the hill, you will view cobbles and boulders of calciocarbonatite and siliciocarbonatite rocks. (Figs. 14 and 15). The deep cuts on the right side of the trail will show deeply weathered carbonatite-rich soils, and in some areas, relict primary banding may be observed. The calcite carbonatite mineralogy varies throughout the complex, but generally contains calcite, apatite, olivine, phlogopite, pyrite, and magnetite. The modal layers and bands that are sometimes observed at Prairie Lake are represented by various oxides (commonly magnetite), interlayered between calcite-dominant layers.

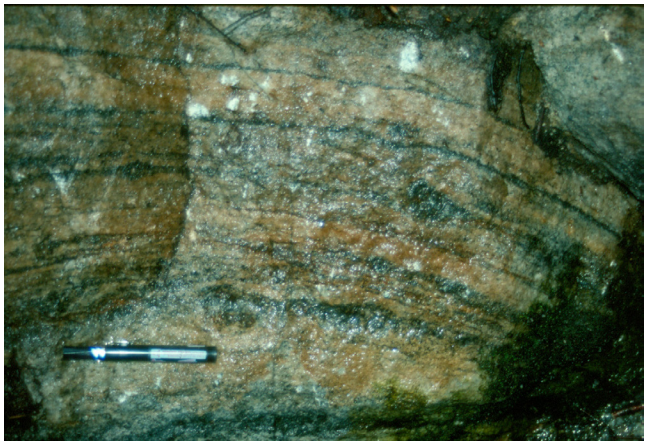


Figure 14. Banded sövite (calciocarbonatite) from the Prairie Lake Carbonatite Complex (photo courtesy of M. Smyk).



Figure 15. Weathered carbonatite from the Prairie Lake Carbonatite Complex (photo courtesy of M. Smyk).

Stop 4: The Good Hope Carbonatite

UTM Coordinates 519363 E 5431721 N (Parking area)

Introduction

The Good Hope Carbonatite is located approximately 28km North of Hwy 17 and was discovered in 2015 by Rudy Wahl (Fig. 2). It occurs within the magnetic "low" on the Northwestern flank of the Prairie Lake Carbonatite, in low-lying marshy land. The Nb property has undergone mapping, geophysical surveys, trenching, and drilling since its discovery. Plato Gold Corp. has an option agreement with Rudy Wahl and other claim holders on the property.

The Good Hope property is host to carbonatite, ijolite, and alkali granite. Alkali granite is fine- to medium-grained and characterized by the abundance of orange and red potassium feldspar and quartz (Selway, 2017). At surface, the medium-grained carbonatite has a reddish-brown rind and appears in some cases to be brecciated (Fig. 16). The brecciated material shows angular to subround fragments with buff-white carbonate stringers present (Puumala et al., 2015; Fig. 16). Investigations from the drill core samples have

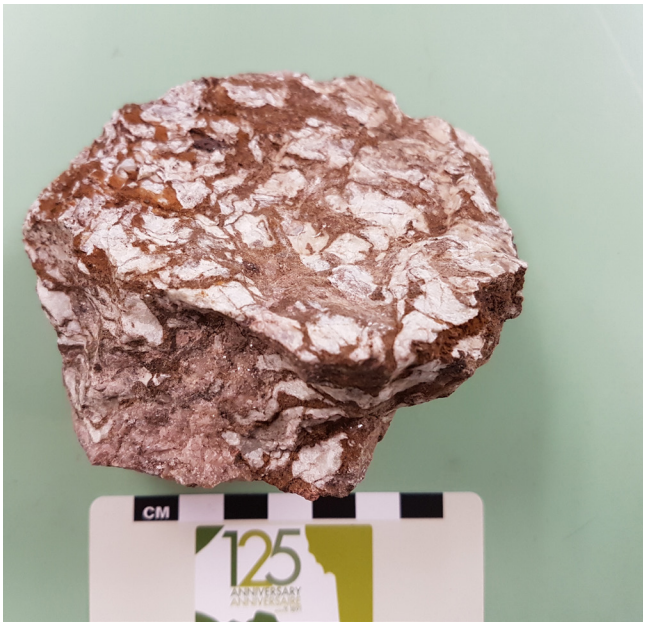


Figure 16. Brecciated carbonatite from the Good Hope Carbonatite.

led to the classification of the Good Hope carbonatitic rocks. Three types of carbonatite have been identified on the property: calciocarbonatite, ferrocarbonatite, and siliciocarbonatite (Cleaver, 2017). Alkali granitic breccia with carbonatite veins has been identified in the drill core (Selway, 2017). The veins correlate with the higher-grade mineralization (>1.0 wt. % Nb_2O_5) (Selway, 2017). Niobium mineralization is primarily concentrated in pyrochlore, which are characterized by low UO_3 and are ThO_2-free (https://www.platogold.com/projects/good-hope-niobium-project/). A pyrochlore-group mineral that has no ThO_2 and low UO_3 content is important as these radionuclides (Th, U) end up in the slag during processing and can be quite problematic. Other minerals found occurring within the carbonatite rocks include calcite, ferrodolomite, siderite, apatite, ferrocolumbite, mica, and pyrochlore-group minerals (Cleaver, 2017).

Cleaver (2017) divided the carbonatites into two paragenetic varieties, pyrochlore-rich and pyrochlore-poor. Mineralogical and petrological evidence from the pyrochlore-rich carbonatites show early crystallized cumulates of apatite and Na-Ca pyrochlore minerals, while the pyrochlore-poor carbonatites appear to represent a later stage of crystallization (Cleaver, 2017). Cleaver (2017) concluded that the mineralogy of the Good Hope occurrence is different to that of the carbonatites occurring in the western and southern margins of the Prairie Lake carbonatite. The differences in mineralogy, coupled with a different magnetic signature, carbonatite texture, weathering profile, and distinct topography, indicate that the Good Hope occurrence is perhaps not directly related to the Prairie Lake carbonatite, however, the genetic relationship remains unknown (Cleaver, 2017).

At this stop we will visit the areas that have been the focus of the exploration program over the last few years. Recent trenching has uncovered various outcrops of the ijolites, carbonatites and alkali granites present on the property.



Figure 17. Abundant pyrochlore in carbonatite at 102m, sample #1219065 (from Selway, 2017).

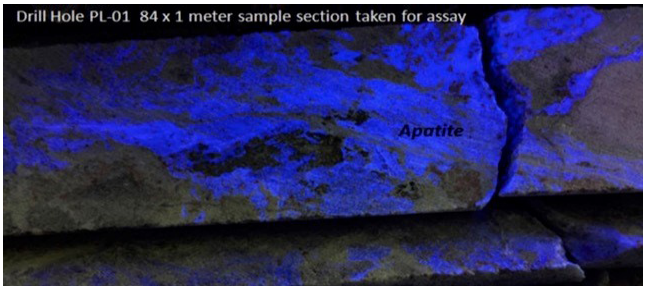


Figure 18. Apatite mineralization in a carbonatite vein, as shown with a UV light system. Photo courtesy of R. Wahl.

References

Birkett, T.C., McCandless, T.E., and Hood, C.T. 2004. Petrology of the Renard igneous bodies; host rocks for diamond in the northern Otish Mountains region, Quebec. Lithos 76 (1): 475-490.

Cleaver, A. 2017. Mineralogy and petrology of the Good Hope carbonatite occurrence, Marathon, Ontario. Unpublished HBSc. thesis, Lakehead University.

Coates, M.E. 1970. Geology of the Killala-Vein Lakes area, District of Thunder Bay, Ontario Department of Mines, Geology Report 81, 35p.

Heaman, L.M. and Machado, N. 1992. Timing and origin of midcontinent rift alkaline magmatism, North America: evidence from the Coldwell Alkaline Complex. Contributions to Mineralogy and Petrology 110:289-303.

Kozlowski, A. 2016. The mineralogy and petrology of the diamondiferous Madonna Dyke, Marathon, ON; unpublished HBSc. thesis, Lakehead University, Thunder Bay, ON, 72p.

Mitchell, R.H. 1986. Kimberlites: Mineralogy, Geochemistry, and Petrology: New York, Plenum Press, 442 p.

Mitchell, R.H. 1995. The role of petrography and lithogeochemistry in exploration for diamondiferous rocks. Journal of Geochemical Exploration, 53: 339-350.

Mitchell, R.H. 2015. Primary and secondary niobium mineral deposits associated with carbonatites. Ore Geology Reviews 64:626-641.

Puumala, M.A., Campbell, D.A., Tims, A., Debicki, R.L., Pettigrew, T.K., and Brunelle, M.R. 2015. Report of Activities 2014. Resident Geologist Program, Thunder Bay South Regional Resident Geologist Report: Thunder Bay South District; Ontario Geological Survey, Open File Report 6303, 75p.

Puumala, M.A., Campbell, D.A., Tuomi, R.D., Pettigrew, T.K. and Hinz, S.L.K. 2018. Report of Activities

2017, Resident Geologist Program, Thunder Bay South Regional Resident Geologist Report: Thunder Bay South District; Ontario Geological Survey, Open File Report 6338, 101p.

Potter, E.G. and Mitchell, R.H. 2005. Mineralogy of the Dead Horse creek volcaniclastic breccia complex, Northwestern Ontario, Canada. Contributions to Mineralogy and Petrology, 150: 212-229.

Quist, B. 2011. Dead Horse Creek Rare Earth property, Walsh and Grain Townships, Thunder Bay Mining Division; Thunder Bay District, Assessment Report, AFRO 2.52396, 174p.

Rukhlov, A.S. and Bell, K. 2010. Geochronology of carbonatites from the Canadian and Baltic Shields, and the Canadian Cordillera: clues to mantle evolution. Mineralogy and Petrology 98: 11-54.

Sage, R.P. 1982. Mineralization in diatreme structures north of Lake Superior, Ontario Geological Survey Study, vol. 27, Ontario Ministry of Natural Resources, Toronto, p79.

Sage, R.P. 1987. Geology of Carbonatite - Alkalic Rock Complexes in Ontario: Prairie Lake Carbonatite Complex, District of Thunder Bay; Ontario Geological Survey, Study 46, 9Ip

Sage, R.P. and Watkinson, R.H. 1995. Alkalic rocks of the Midcontinent rift, Institute of Lake Superior Geology, 41st Annual Meeting, Proceedings Vol. 41, Part 2a, Marathon, Ontario.

Selway, J. 2017. Assessment report for geological mapping program, Good Hope Niobium Property, Marathon, ON, Canada. Plato Gold Corp. 116p.

Smyk, M.C., Taylor, R.P., Jones, P.C., and Kingston, D.M. 1993. Geology and geochemistry of the West Dead Horse Creek rare metal occurrence, Northwestern Ontario. Exploration and Mining Geology, 2:245-251.

Wahl, R. Wahl's prospecting website. http://users.renegadeisp.com/~rwahl/

Wu, F.Y., Mitchell, R.H., Li, Q-L., Zhang, C., and Yang, Y-H. 2017. Emplacement age and isotopic composition of the Prairie Lake Carbonatite complex, Northwestern Ontario, Canada. Geological Magazine 154(2): 217-236.

Zurevinski, S.E. and Mitchell, R.H. 2015. Petrogenesis of orbicular ijolites from the Prairie Lake complex, Marathon, Ontario: Textural evidence from rare processes of carbonatitic magmatism. Lithos 239: 234-244.

Field trip 3 - Geology of the Western Schreiber-Hemlo Greenstone Belt

Seamus Magnus

Ontario Geological Survey, 933 Ramsey Lake Road Sudbury, ON, P3E 6B5 Canada

Preface

This field trip guidebook was prepared for a 1-day pre-meeting field trip held in conjunction with the Institute on Lake Superior Geology (ILSG) Annual Meeting hosted in Terrace Bay, Ontario from May 7 to 10, 2019. This geological guidebook was written to showcase the preliminary results of four years of bedrock mapping conducted by the author for the Ontario Geological Survey from 2015 to 2018 in the Schreiber–Hemlo greenstone belt (Magnus and Walker, 2015; Magnus and Arnold, 2016; Arnold et al., 2017; Magnus, 2017a,b; Magnus and Hastie, 2018). The coincidence of this meeting being held in Terrace Bay (within the mapping area) as the project was wrapping up provided the perfect opportunity to showcase these preliminary results to a broad audience. The ILSG meeting has never been hosted in Terrace Bay, however the meeting was hosted in the nearby towns of Nipigon in 2005 and Marathon in 1995. A field guide, "Geology of the Schreiber Greenstone Assemblage and its Gold and Base Metal Mineralization" was prepared for the 1995 meeting in Marathon (Smyk and Schnieders 1995); two of the five stops from that field guide are revisited in this field guide, but with updated information.

The tectonically diverse geological history of the Lake Superior region has made it a playground for geologists of every discipline. The north shore of Lake Superior has over a century of mining and exploration history, including precious metals, base metals rare earth metals, and unique industrial minerals such as the colourful marbles at Ruby Lake. The location of Paleoindian sites along the north shore of Lake Superior, which was likely settled during glacial retreat at about 10,000 years before present, tend to be located in close proximity to the cherty rocks of the Gunflint formation, a source for tooling material (Norris, 2012). In fact there is evidence to show that ancient peoples south of the lake were mining, using and trading native copper as early as 4,000 years before present (Pleger, 2000). Furthermore, the Ojibway story of Nanabush and Waub-Ameek (the Giant Beaver) describes the glacial history of the Great Lakes (Snake et al., 1991), albeit it in a mythological way. Indeed, the geology of the Lake Superior area has been of interest to humans for a long time, and the author is thankful for the opportunity to learn a little more about the geological history of the area, and even more thankful to be able to share this knowledge.

Safety

Some of the field trip stops are located on the Trans Canada Highway 17 which is busy year-round and especially during the summer months. This highway is the major transportation route between western and eastern Canada, and as such much of the traffic along this highway includes transport trucks and logging trucks which have great momentum, especially when fully loaded. The terrane along the north shore of Lake Superior is rugged, thus the highway in this area has many hills and blind curves and the road is mostly restricted to two lanes with narrow shoulders. To maximize the safety of the field trip participants and that of the drivers on the highway, and to minimize the effect that our presence has on the flow of traffic, the author has selected field trip stops that provide ample parking space away from the shoulders of the highway and have suitable sight-lines with the traffic. The area along the north shore of Lake Superior is prone to inclement weather conditions, with dense fog possible at any time of year, causing additional risk for drivers and pedestrians; please use extreme caution during foggy periods.

Care should always be exercised when parking, exiting vehicles and crossing the roads. Use of safety vests and/or bright clothing is recommended to improve your visibility to motorists.

Stop 3 involves some driving along a railway

This field trip guide is also available as Ontario Geological Survey, Open File Report 6357, and can be downloaded from:

http://www.geologyontario.mndm.gov.on.ca/mndmaccess/mndm_dir.asp?type=pub&id=OFR6357

maintenance path underlain by sand, gravel and rough ground. Two-wheel drive vehicles are capable of driving on this path, but vehicles with higher clearance and all-wheel or four-wheel-drive are preferred. This stop also involves a short hike away from the parking spot, across a railroad track and up and down a steeply-graded slope. Participants should be aware of the potential for railroad traffic and "slips, trips and falls" hazards. It is recommended that anyone following this field guide individually should bring first aid supplies, food and water. Cell phone service coverage at Stop 3 is not 100% for all providers, especially in areas with more rugged terrain; participants should ensure that their cell phones have adequate connection to their networks before driving down the railroad access path, and again before hiking to the outcrop.

Most of the trip routes and sites are on Crown land or public roadways, but access is on or near private property for some routes. As in all such situations, please respect the property rights of others to maintain good relationships with the landowners so that future access for geologists is not adversely affected.

Terminology

A number of terms used in this report are outlined below.

For the sake of simplicity, the name "Wabigoon Terrane" is used in figures and in the text to refer to the collective granite and greenstone domains between the Quetico and English River metasedimentary terranes. As used in this report, "Wabigoon Terrane" includes several subdivisions included in Stott et al. (2010).

Terminology for clastic sedimentary rocks, such as wacke and mudstone, follows Pettijohn (1975). Terminology for volcaniclastic rocks, such as tuffaceous conglomerates, follows Schmid (1981).

All whole rock chemical analyses that appear in this report were done at the Geoscience Laboratories, Ontario Geological Survey, Ministry of Northern Development and Mines, Sudbury. All chondrite- and primitive mantle-normalized data or diagrams referred to or shown in this report use the normalizing values of Sun and McDonough (1989).

Rock type names based on major element analyses are based on the Total Alkalis versus Silica diagram (TAS; LeMaitre, 1989), except for more ultramafic rocks such as basaltic komatiites, which have been named according to Jensen (1976).

Regional Geology

The bedrock along the north shore of Lake Superior hosts rocks spanning roughly 1.9 billion years of Earth's history, from the beginning of the Mesoarchean era to the end of the Mesoproterozoic era, and include a diverse range of rocks formed in a variety of tectonic settings.

Neoarchean Geological Setting

The Superior Province is an Archean Craton that forms part of the North American continental shield. Rocks of the Superior Province, which range in age from circa 3.4 Ga to 2.6 Ga, are arranged in greenstone belts and plutonic domains. The Superior Province has been subdivided into terranes in which the rocks share similar lithological, geochemical, age and isotopic characteristics and structural and metamorphic histories (Stott et al., 2010). The relationship between these terranes during the early stages of their formation is unclear, however the histories of their evolution converge at circa 2700 Ma, when the terranes were amalgamated to form the Superior Craton (Stott et al., 2010).

Three major terranes are present near the north shore of Lake Superior; the Wawa–Abitibi Terrane to the south, the Wabigoon Terrane to the north, and the Quetico Terrane between them (Fig. 1). The Wawa–Abitibi granite-greenstone terrane contains Neoarchean volcanic rocks erupted through juvenile oceanic crust and is interpreted to represent an oceanic arc depositional environment (Williams, 1989). The Wabigoon granite-greenstone terrane contains Neoarchean volcanic rocks erupted through and deposited upon Mesoarchean crust, is interpreted to represent a continental arc depositional environment, and is considered to have been a "proto-continent" (Williams 1989). The Quetico terrane is composed mainly of turbiditic siliciclastic rocks with sparse slivers of oceanic crust and is interpreted to represent an accretionary wedge deposited offshore of the Wabigoon "proto-continent" (Williams, 1989; Fralick et al., 2006). A preliminary compilation of geochronological data for these terranes (Fig. 2) helps to visualize the timing of events.

Sedimentary rocks in the Manitouwadge greenstone belt and in the western Schreiber–Hemlo greenstone belt, both along the northern margin of the Wawa-Abitibi Terrane (see Fig. 1), contain detrital zircon

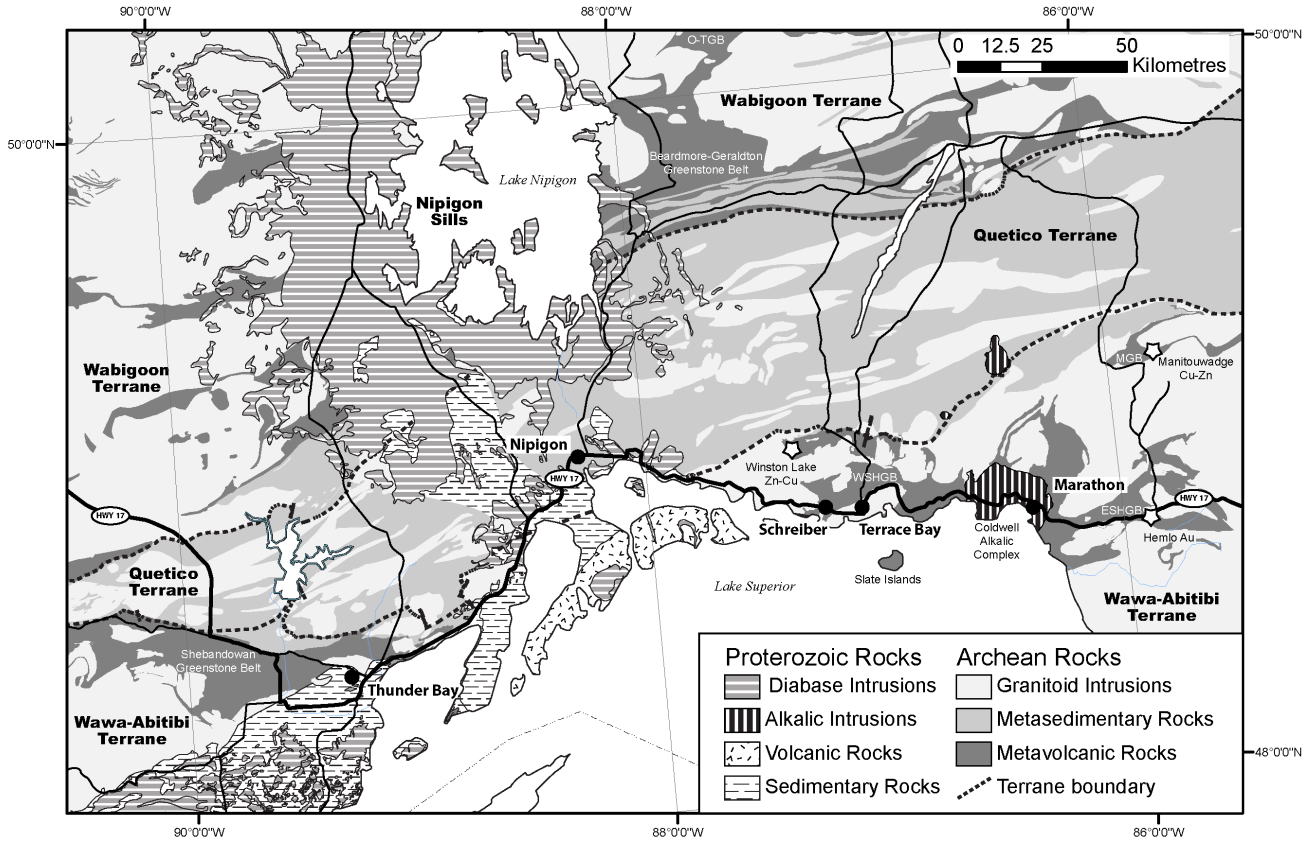


Figure 1. Regional map of the north shore of Lake Superior, displaying Archean and Proterozoic geology. White stars indicate local past-producing and currently producing mines. Abbreviations: O-TGB = Onaman–Tashota Greenstone Belt, MGB = Manitouwadge Greenstone Belt, ESHGB = Eastern Schreiber–Hemlo Greenstone Belt, WSHGB = Western Schreiber–Hemlo Greenstone Belt, HWY 17 = Trans-Canada Highway 17. Geology from Ontario Geological Survey 2011; Terrane and domain boundaries from Stott et al. (2010).

populations that are correlative with those in the Quetico Terrane and in the Beardmore–Geraldton greenstone belt (Zaleski et al., 1999; Fralick et al., 2006; Tóth, 2018; Tóth et al., 2015; Fig. 2). This suggests that during deposition of the sedimentary sequences, the Wabigoon, Quetico and Wawa–Abitibi terranes were a contiguous depositional environment.

In this interpreted environment, detrital material from both the ongoing Wabigoon continental arc volcanism and from erosion of Mesoarchean crust of the Wabigoon "proto-continent" was deposited into a fore-arc accretionary wedge. As the Wawa–Abitibi oceanic arc approached the proto-continent, sediments from the continent began to fill the basin between them, eventually spilling over onto the still-active Wawa-Abitibi volcanic arc (Fralick et al., 2006).

The end of supracrustal rock formation in the northern Lake Superior region is marked at circa 2690 Ma by crosscutting felsic plutons (Figs. 1, 2); plutonism in the region was accompanied by regional deformation and metamorphism from circa 2690 to circa 2670 Ma (Fig. 2). The three terranes were deformed synchronously during three main events; 1) early thrusting during collision of the terranes (D1), 2) upright folding during continued compression (D2), and 3) late transpressional shearing (D3; Williams, 1989). These deformational events likely represent a succession of different styles of deformation during a single protracted event; not three distinct events (Williams, 1989).

The structural histories for the Shebandowan (Corfu and Stott, 1998) and Manitouwadge greenstone belts (Zaleski et al., 1999) and the eastern part of the Schreiber–Hemlo greenstone belt (Muir, 2003) are similar to Williams' (1989) broad interpretation for the region, however the timing and development of deformation is slightly different for each greenstone belt and within each terrane. These differences are likely caused by uncertainties in the geochronological data, inconsistencies in interpretations of all of the geological and related data, and the diachronous nature of regional deformation itself (Corfu and Stott, 1998).

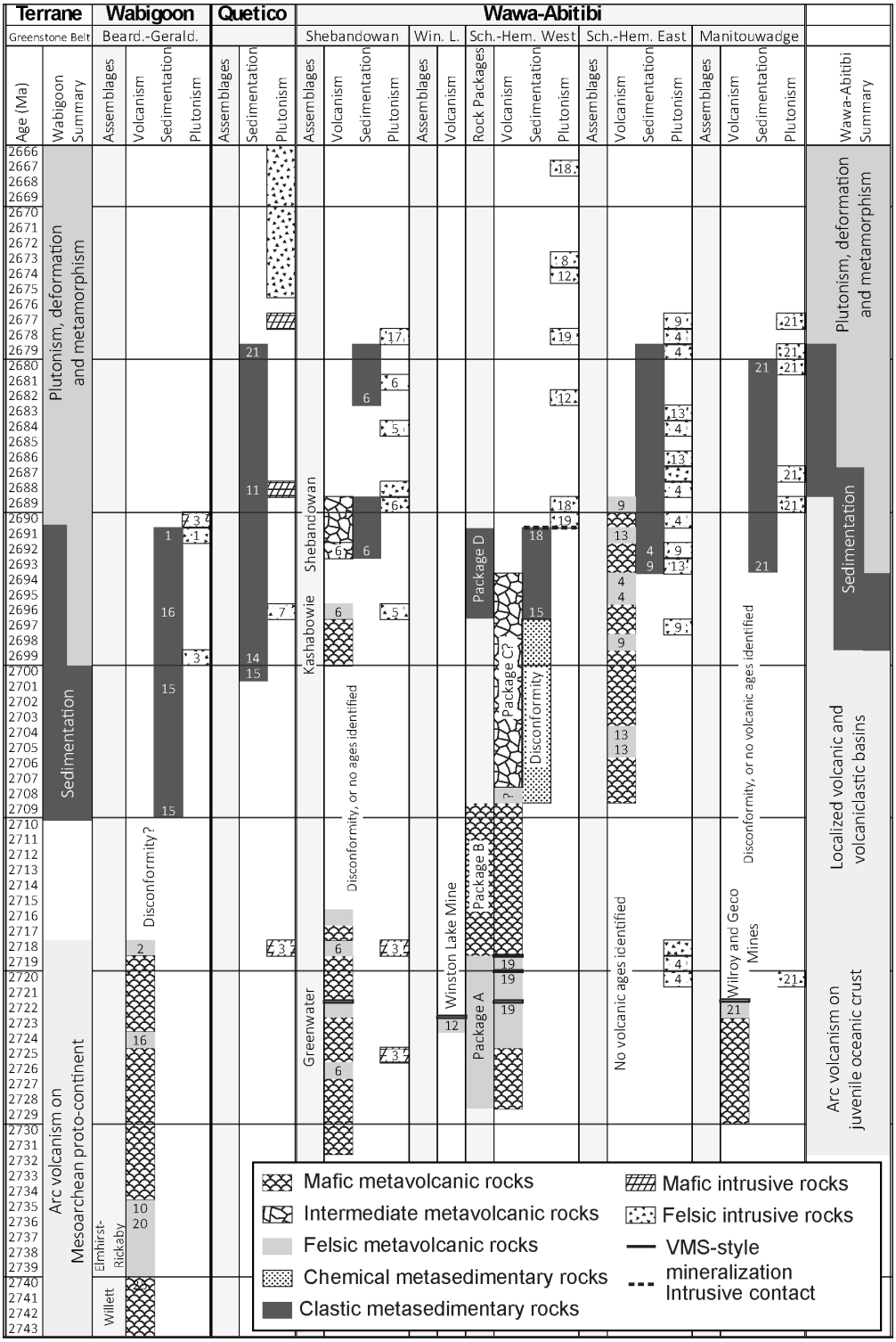


Figure 2. A preliminary compilation of geochronological data for the Wabigoon, Quetico and Wawa–Abitibi Terranes. Error bars have not been illustrated, for the sake of visual simplicity. Abbreviations: Beard.–Gerald. = Beardmore–Geraldton, Win. L. = Winston Lake, Sch.–Hem. = Schreiber–Hemlo. Numbers correspond to sources for geochronology data: 1 = Anglin et al. (1988), 2 = Blackburn et al. (1985), 3 = Corfu (2000), 4 = Corfu and Muir (1989), 5 = Corfu and Stott (1986), 6 = Corfu and Stott (1998), 7 = Davis (1996), 8 = Davis and Sutcliffe (2017), 9 = Davis, Beakhouse and Jackson (1998), 10 = Davis et al. 1985, 11 = Davis, Pezzutto and Ojakangas (1990), 12 = Davis et al. (1994), 13 = Fage (2011), 14 = Fralick and Davis (1999), 15 = Fralick et al. (2006), 16 = Hart et al. (2002), 17 = Kamo (2015), 18 = Kamo (2016), 19 = Kamo and Hamilton (2017), 20 = Tóth and Lafrance (2018) and references therein, and 21 = Zaleski et al. (1999).

Paleoproterozoic Geological Setting

Several Paleoproterozoic mafic dike swarms are present in the area north of Lake Superior, including dikes from the Matachewan (2480-2445 Ma; Heaman, 1997; Bleeker et al., 2012), Biscotasing (2175-2166 Ma; Buchan et al., 1993; Davis and Stott, 2003; Halls and Davis, 2004; Hamilton and Stott, 2008) and Marathon (2122-2100 Ma; Halls et al., 2008) dike swarms (Fig. 3).

Sedimentary rocks of the Animikie Group unconformably overly the Superior Craton and the Paleoproterozoic dike swarms (Fig. 1). The base of the Animikie Group is defined by a thin, locally developed Kakabeka Conglomerate, which hosts carbonaceous microfossils (Gunflintia and Huronosporia) preserved in cherty stromatolites, interpreted to have formed in near-shore and shallow water environments (e.g., Wacey et al., 2013). These rocks are overlain by iron formation, carbonate rocks and siliciclastic rocks of the Gunflint Formation, which is interpreted to have been deposited during multiple marine transgressions in an extensional basin between the Penokean volcanic arc and the Superior Craton prior to their collision at circa 1.86 Ga (Fralick et al., 2002) or, alternatively, in a foreland basin north of the Penokean fold-thrust belt (Ojakangas et al., 2001). The Gunflint Formation is overlain by fine-grained argillites and slates of the Rove Formation, which contain a mixture of Archean zircons and circa 1.83-1.77 Ga zircons (Heaman and Easton, 2006) and are interpreted to have been deposited in a deep marine setting between the assembled Laurentian Craton and the circa 1.8-1.7 Ga Yavapai volcanic arc (Whitmeyer and Karlstrom, 2007). The boundary between the Gunflint Formation and the Rove Formation, and their lithostratigraphic equivalents in the USA, is marked by an unusual rock unit thought to represent distal ejecta from the circa 1.85 Ga Sudbury impact (Addison et al., 2005; Cannon et al., 2010).

Mesoproterozoic Geological Setting

The circa 1.4 Ga Sibley Group, a sequence of sediments deposited in alluvial-fluvial, lacustrine and eolian settings unconformably overlies the Paleoproterozoic Animikie Group (Rogala et al., 2005).

The circa 1.1 Ga Keweenawan Midcontinent Rift event caused widespread magmatic activity in the Lake

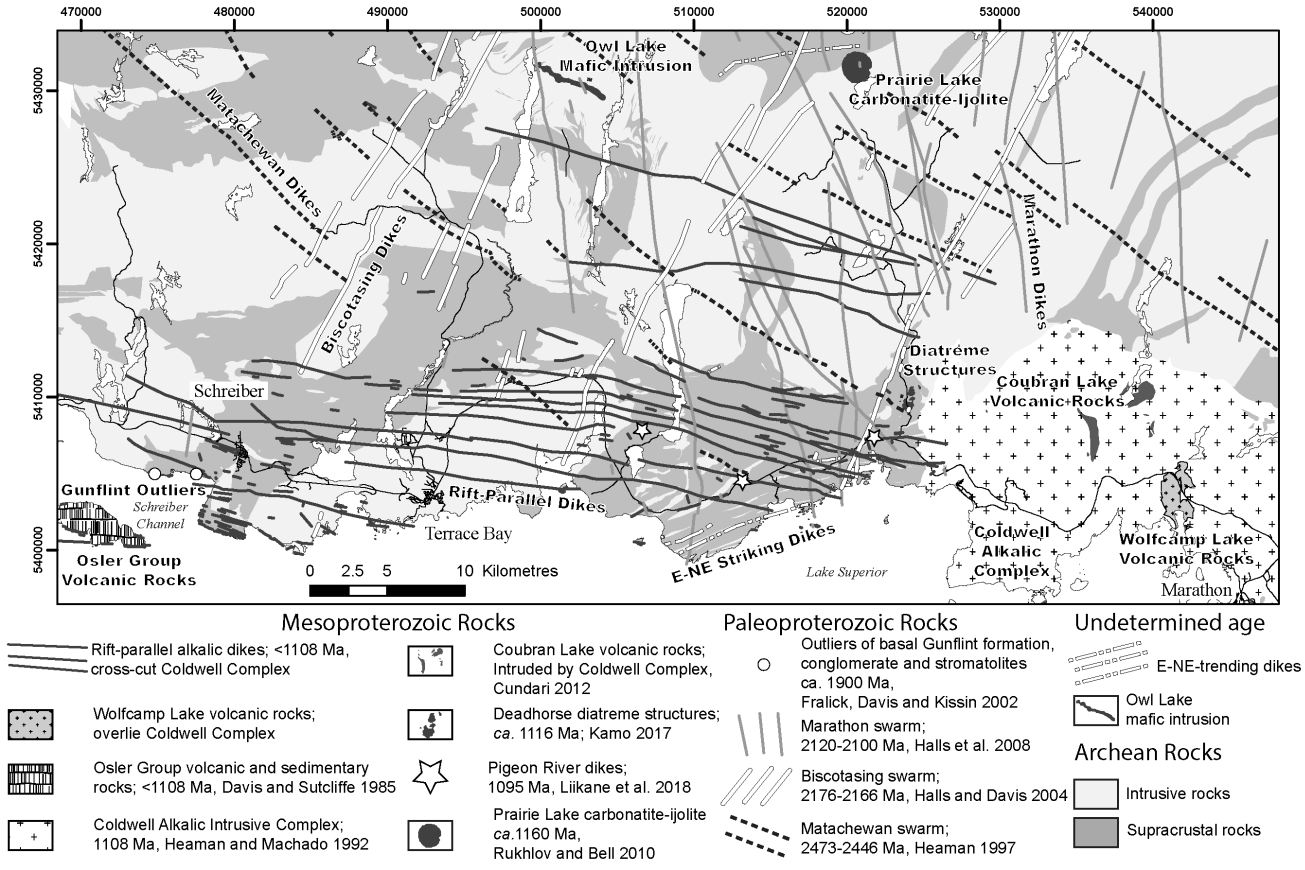


Figure 3. Simplified geological map of the Schreiber–Marathon area highlighting the Proterozoic formations in the area. All UTM coordinates provided using NAD83 in Zone 16.

Superior area. Pre-rift intrusive rocks are preserved north of Lake Superior, including the circa 1157-1164 Ma Prairie Lake carbonatite-ijolite complex (Rukhlov and Bell, 2010; Wu et al., 2017). Early-rift rocks north of Lake Superior include 1120-1110 Ma mafic to ultramafic intrusions such as the Thunder Bay North intrusive complex, Kitto and Seagull intrusions and the Logan diabase sills (Bleeker et al., 2018 and references therein). Most of the preserved rift-related rocks were emplaced between 1109 and 1093 Ma and include both intrusive and supracrustal rocks, including the Osler Volcanic Group, the Nipigon and Inspiration diabase sills and the circa 1108 Ma Coldwell alkalic intrusive complex (Bleeker et al., 2018 and Liikane et al., 2018, and references therein). Younger dike rocks include the circa 1099-1095 Ma Pigeon River and Cloud river dike swarms (Liikane et al., 2018). The supracrustal rocks include several packages of mafic and felsic volcanic rocks and sedimentary rocks, which are overlain by late-rift volcanic and sedimentary rocks as young as circa 1083 Ma (Miller and Nicholson, 2013 and references therein). These supracrustal rocks crop out primarily south of Lake Superior in Minnesota, Wisconsin and Michigan, and occur sporadically along the northern and eastern shores of Lake Superior. In the Terrace Bay area, mafic volcanic rocks of the <1108 Ma Osler Group unconformably overlie the circa 1400 Ma Sibley Group (Davis and Sutcliffe, 1985; Heaman and Easton, 2006), and two groups of volcanic rocks of unknown age unconformably overlie the circa 1108 Ma Coldwell Alkalic Intrusive Complex (Heaman and Machado, 1987, 1992) the Coubran Lake and Wolfcamp Lake volcanic rocks (Fig. 3; Cundari, 2012; Davis, 2016; Davis et al., 2017).

Archean Geology of the Western Schreiber-Hemlo Greenstone Belt

The western Schreiber–Hemlo greenstone belt is a roughly 50km long belt of supracrustal and intrusive rocks bounded on its north and west sides by Archean granitoid plutonic rocks. It extends southward under Lake Superior and is separated from the eastern Schreiber–Hemlo greenstone belt by the Mesoproterozoic Coldwell Alkalic Intrusive Complex (Fig. 1). The greenstone belt is apparently connected to a greenstone belt in the Winston Lake–Big Duck Lake area to the north by a north-trending sliver of greenstone, but the relationship between the belt and the Archean volcanic rocks on the Slate Islands, 10km to the south, is unknown (Fig. 1).

Stratigraphy of the Schreiber–Hemlo Greenstone Belt

Based on stratigraphic way-up indicators such as flow contacts, pillow cusps and graded bedding, the supracrustal rocks of the western Schreiber–Hemlo greenstone belt are arranged in upright, generally open folds that are locally intensified to tight and isoclinal folds proximal to pluton boundaries and in shear zones (Figs. 4 and 5). The supracrustal rocks have been subdivided into several stratigraphic packages based on common volcanic and sedimentary facies as well as geochemical characteristics and geochronological constraints (Fig. 4, inset). At the time of the ILSG field trip, geochemical and geochronological data for the rocks north and west of the Terrace Bay pluton is pending, thus the stratigraphic arrangement presented herein is tentative.

East of the Terrace Bay pluton, three packages of supracrustal rocks are present: Package A, dominated by felsic metavolcaniclastic rocks; Package B, dominated by mafic metavolcanic rocks and Package D, a sequence of turbiditic wackes equivalent to the McKellar Harbour formation of Fralick et al. (2006); Package C is not present (Magnus and Walker, 2015; Magnus and Arnold, 2016; Magnus, 2017a,b). North and west of the Terrace Bay pluton, Packages A and B are present, however Package B is disconformably overlain by Package C, another sequence of distinct mafic metavolcanic rocks, and package D is not present (Magnus and Hastie, 2018). The highly strained and structurally complex area between the Terrace Bay and Santoy Lake plutons appears to mark the boundary between these two stratigraphic sections.

Package A

Package A is composed mainly of felsic volcaniclastic rocks, including tuffs, crystal tuffs, tuffaceous conglomerates and minor coherent flows. The crystal tuffs contain plagioclase phenocrysts and, in many cases, contain blue quartz phenocrysts. The tuffaceous conglomerates are generally clast-supported and contain pebble to cobble-sized clasts of coherent felsic rocks with similar plagioclase and blue quartz phenocrysts in a felsic tuffaceous matrix (Magnus, 2017b). This package contains minor mafic to intermediate massive to pillowed flows, including some massive flows with a high concentration of quartz and/or calcite-filled amygdules. Chert and sulphide-

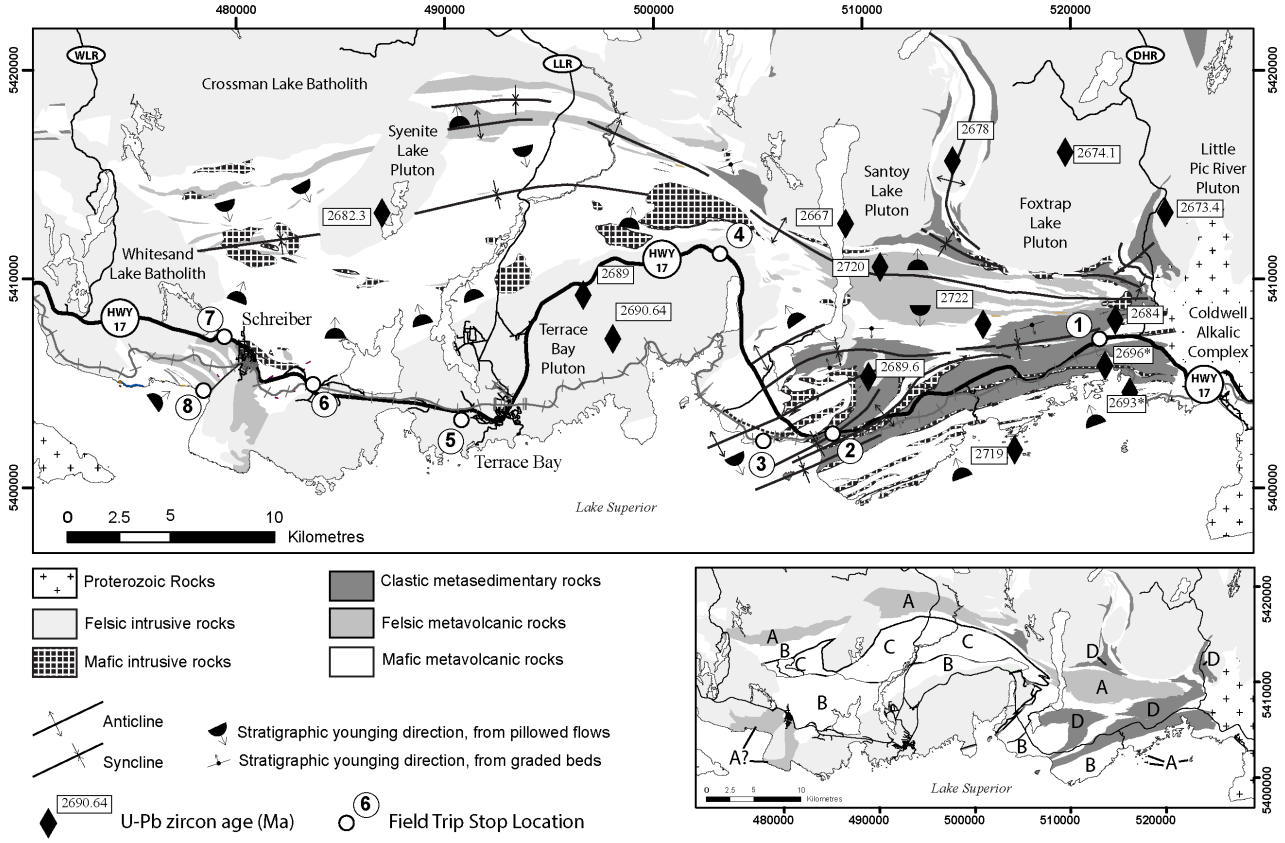


Figure 4. Simplified geological map of the western Schreiber–Hemlo greenstone belt, highlighting the major Archean rock types, some of the stratigraphic younging indicators observed during this study, all of the U-Pb zircon geochronological data in the area, and the inferred fold axial traces. An inset figure outlines the inferred depositional packages A, B, C and D. All UTM coordinates provided using NAD83 in Zone 16.

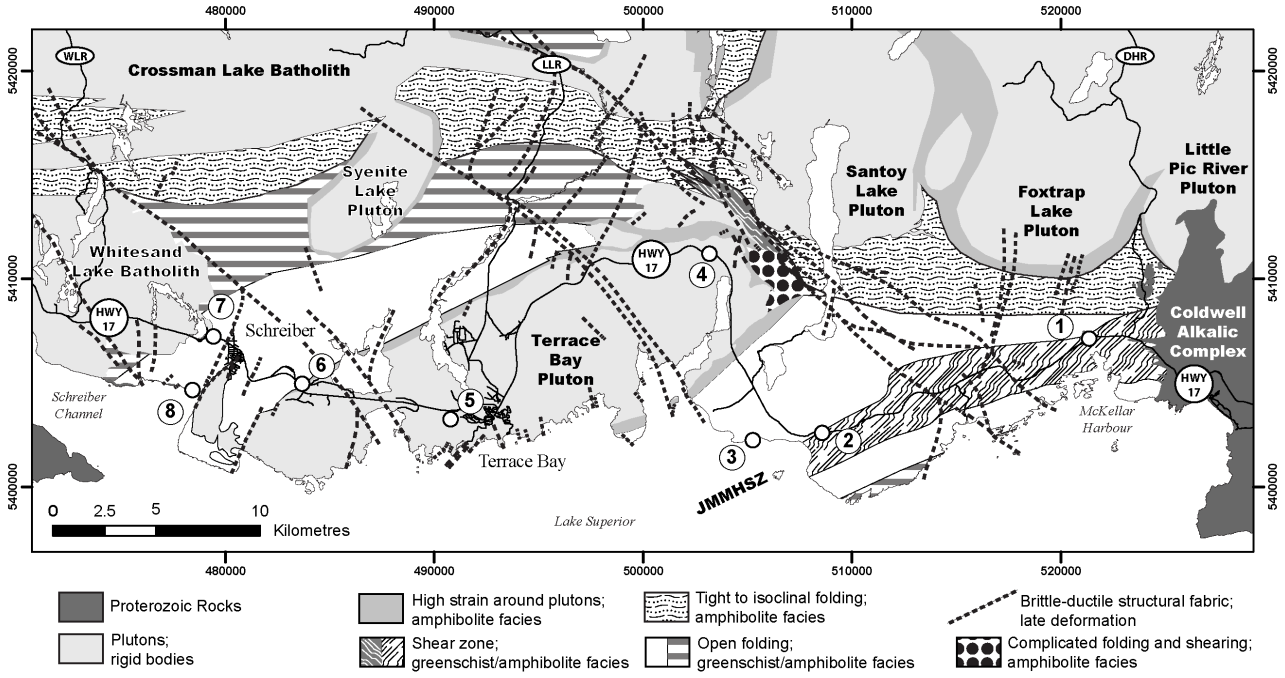


Figure 5. Map of the Western Schreiber–Hemlo greenstone belt outlining domains with distinct structural and metamorphic characteristics. Abbreviations: JMMHSZ = Jackfish-Middleton-McKellar Harbour Shear Zone, HWY 17 = Trans-Canada Highway 17. All UTM coordinates provided using NAD83 in Zone 16.

bearing chemical metasedimentary rocks are present in this package, most commonly near and along the contact between this package and Package B.

An incredibly well-preserved package of felsic, intermediate and mafic metavolcanic rocks southwest of the town of Schreiber is stratigraphically correlative with Package A (i.e. below Package B, from younging directions), however the volcanic facies are different than those present in the majority of Package A as described in the previous paragraph (Magnus and Hastie, 2018). The most notable difference is the absence of the blue quartz phenocrysts present throughout the remainder of Package A. There are also fewer tuffs and crystal tuffs; the felsic rocks present are predominantly massive, plagioclase porphyritic flows and breccias with angular clasts of similar plagioclase porphyritic material. Several intermediate, plagioclase and amphibole porphyritic massive to brecciated flows are also present, as well as massive to pillowed mafic flows up to 200m thick. Interflow formations in this sequence include chert and magnetite-bearing chemical metasedimentary rocks and tuffaceous wackes and conglomerates.

Package A contains the oldest known rocks in the western Schreiber–Hemlo greenstone belt; three samples from the top of the package have ages of circa 2720 Ma, which is correlative with similar felsic volcanism in the Winston Lake area, in the Manitouwadge greenstone belt and with the Greenwater assemblage in the Shebandowan greenstone belt (Davis et al., 1994; Davis and Sutcliffe, 2017). Volcanic rocks of this age have not yet been identified in the eastern Schreiber–Hemlo Greenstone Belt, however there are numerous felsic volcanic formations on that portion of the Schreiber–Hemlo belt that do not have any age information. Older phases of both the Pukaskwa and Black Pic batholiths from the eastern Schreiber–Hemlo belt, however, have yielded similar circa 2720 Ma ages (Corfu and Muir, 1989; Beakhouse and Davis, 2005).

The mafic to intermediate rocks in this package contain trace element concentrations consistent with both arc volcanic and oceanic plateau volcanic settings.

A-B Disconformity

In the Schreiber area, a substantial sequence of interbedded graphitic argillite, chert, sulphide facies iron formation and felsic tuffaceous breccias represents a disconformity between packages A and B. The Elwood and Morley base metal sulphide occurrences occur along this horizon.

Above this disconformity, there are several massive to pillowed flows which are overlain by a chemical metasedimentary sequence that includes graphitic argillite, sulphide facies iron formation and marble. So far two exposures of this horizon have been observed. In one, the marble is composed mainly of calcite with minor silicate and sulphide components; the other is a breccia, with mafic volcanic, argillite and sulphide clasts supported by a matrix of calcite. The significance of these marbles is unknown and requires further study. Is the carbonate derived from a primary sedimentary source? Could the breccia have been formed in a karst-like environment? Or was the carbonate introduced during later hydrothermal alteration?

Elsewhere in the belt, similar chert and sulphide facies iron formation are concentrated along the A-B disconformity, including one occurrence of marble south of the Foxtrap Lake pluton. However, the occurrence of these rocks is more sporadic, which may be a consequence of their location in areas that are more highly strained and metamorphosed than the well-preserved occurrence in the Schreiber area.

A unique feature of the A-B disconformity, which crops out along Highway 17 in Schreiber, is a sequence of interbedded turbiditic wacke and siltstone with basaltic andesitic composition that was deposited either synchronously or directly on top of the chemical metasedimentary rocks. The mafic composition of these rocks indicates they were derived primarily from a mafic volcanic source. No zircons have been found in these rocks, which precludes detrital geochronology, but a whole rock Sm-Nd isotopic study may help identify possible sources for this mafic sediment.

Package B

Package B is dominated by massive to pillowed mafic flows with two distinct geochemical populations based on trace elements that are consistent with both oceanic plateau volcanism and back-arc basin volcanism, respectively. Flows with trace elements consistent with an oceanic plateau volcanic setting are typical green to grey-green massive to pillowed flows, with lath-shaped plagioclase microphenocrysts visible in thin section and small vesicles concentrated around the edges of the pillows. Some massive flows with this chemistry also contain abundant calcite-filled amygdules. Flows with trace elements consistent with a back-arc volcanic setting have distinct variolitic

textures as well as irregular-shaped cavities that likely served as conduits for volatile fluids and gases rather than typical vesicles, which are not present in these rocks (Magnus, 2017b).

One occurrence of a coherent felsic flow, with a perlitic texture and possible flow banding, has been observed near the top of this package near the Steel River (Magnus, 2017b).

B-C Disconformity

North and west of the Terrace Bay pluton, the top of Package B is marked by a horizon of felsic volcaniclastic rocks including tuffs, tuffaceous wackes and tuffaceous conglomerates, locally interbedded with chert and sulphide facies iron formation. This horizon is located between the Terrace Bay pluton and the Lunch Lake pluton (an area known locally as the Empress Structure) and wraps around the southeastern edge of the Terrace Bay pluton (Fig. 4, inset).

Package C

Package C is dominated by massive to pillowed mafic to intermediate flows with trace element concentrations that are predominantly consistent with oceanic plateau volcanism, including a more thorium-enriched variety of that chemical signature and some calc-alkalic arc volcanism. The rocks in this package commonly contain medium grained equant plagioclase phenocrysts, which are uncommon in the other metavolcanic packages. This package lacks the variolitic back-arc volcanic rocks that are a distinctive feature of Package B. Apart from the felsic volcaniclastic rocks that mark the lower contact between this package and Package B, several other isolated lenses of felsic volcaniclastic material have been observed in this package.

A sequence of tuffaceous metasedimentary rocks along the western edge of the Santoy Lake pluton may represent the top of Package C. This sequence includes tuffaceous wackes with abundant plagioclase phenocrysts which locally display graded bedding interbedded with tuffaceous conglomerates. The tuffaceous conglomerates are clast-supported and polymictic, with a variety of felsic and mafic metavolcanic rocks, including clasts of mafic rocks with equant plagioclase phenocrysts like those in the mafic rocks of Package C (Magnus, 2017b).

B-D Disconformity

East of the Terrace Bay pluton, packages B and D are in disconformable contact. This disconformity is marked by a sequence of chert, graphitic argillite and sulphide facies iron formation that is continuous along the entire contact.

Package D – McKellar Harbour Formation

Package D, also known as the McKellar Harbour Formation (Fralick et al., 2006), represents the youngest known supracrustal rocks in the western Schreiber–Hemlo greenstone belt. This package is composed of a sequence of interbedded turbiditic wacke, sandstone and mudstone with normal graded bedding and sharp bedding contacts.

The youngest detrital zircon at the base of the package is 2696±3 Ma, which marks the maximum age of deposition for the package, and the youngest detrital zircon from the top of the package is 2693±4 Ma, which suggests that the basin had a source for young zircons during deposition (Fralick et al., 2006) 2006). The sedimentary rocks are crosscut by the 2689.6±2 Ma Steel River pluton (Kamo and Hamilton, 2017), which places a minimum age of deposition for the package, suggesting deposition occurred between 2690 and 2696 Ma. There is volcanism recorded during the 2696-2689 Ma interval in both the eastern Schreiber–Hemlo greenstone belt (Corfu and Muir, 1989; Davis and Lin, 2003) and in the nearby Shebandowan greenstone belt which could have provided young detrital material during deposition of the package.

Older detrital zircons are present in this package, including several Mesoarchean zircons at circa 2900 Ma (Fralick et al., 2006) and a single concordant Paleoarchean grain at 3423±10 Ma (Davis and Sutcliffe, 2017). This implicates a continental component for the source of the sediments, which is interpreted to have been the Wabigoon proto-continent (Fralick et al., 2006) and/or the Minnesota River Valley terrane.

Mafic to Intermediate Intrusive Rocks

A series of sill-like gabbroic rocks that intrude Package B are parallel to stratigraphy and have chemistry similar to the nearby variolitic mafic metavolcanic rocks. These have been interpreted as syn-volcanic intrusions and may in some cases represent medium to coarse grained massive flows. In several of these bodies, rocks with basaltic chemistry display spinifex-like textures composed of abundant elongate amphibole crystals; invariably these rocks are associated with massive rocks of basaltic komatiitic chemistry, which may represent cumulate phases within an ultramafic flow or sill.

Mafic intrusive rocks that occur locally along the contact between packages B and D east of the Terrace Bay pluton, as well as near the contact between packages B and C northwest of the Terrace Bay pluton, typically have elongate, "plumose" amphibole crystals with interstitial plagioclase feldspar. These intrusions have chemistry similar to arc basalts, which helps distinguish them from the rocks with the spinifex-like texture described above.

The Lunch Lake and Longworth Lake plutons are both composed mainly of diorite and have generally equigranular hypidiomorphic textures. The Lunch Lake pluton also includes porphyritic diorite with distinct blue quartz phenocrysts, which have not been observed in any other mafic or intermediate intrusive rock in the belt, but which are common in the felsic volcanic and volcaniclastic rocks.

Felsic Intrusive Rocks

Felsic intrusive rocks that surround and crosscut the greenstone belt were emplaced over a period of at least 20 million years (Figs. 1, 2).

The Terrace Bay, Steel River and Syenite Lake plutons have ages between 2690-2680 Ma (Kamo, 2016; Kamo and Hamilton, 2017, 2018). These plutons are generally oblate and irregular in shape and have well-developed foliations along their contacts that penetrate up to 500m into the surrounding rocks. The Terrace Bay and Steel River plutons are both composed mainly of grey, equigranular to quartz and/or alkali feldspar porphyritic granodiorite with minor dioritic components. The Syenite Lake pluton is composed mainly of pink alkali feldspar porphyritic quartz monzonite and quartz monzodiorite.

The Foxtrap Lake and Little Pic River plutons, as well as the small pluton between them, have ages between 2680-2670 Ma (Kamo and Hamilton, 2017, 2018). These plutons are round in plan view, have well-developed foliations along their margins, which continue up to 1 km into the surrounding rocks. These plutons are composed mainly of grey, equigranular to alkali-feldspar porphyritic granodiorite.

The Santoy Lake pluton, with a zircon age of 2667±4 Ma (Kamo, 2016), is round to irregular in shape and has a weakly developed foliation along its contacts. This pluton is composed of pink quartz monzonite to monzonite, with local alkali feldspar porphyritic varieties, and contains a distinctly low abundance of mafic minerals.

The Crossman Lake batholith (age unknown) is elongate and has a very well-developed foliation along its southern contact that penetrates up to 3km into the supracrustal rocks to the south. The intrusion is composed of equigranular white to grey trondhjemite, tonalite and granodiorite.

A small pluton south of the town of Schreiber (age unknown) is irregular in shape and does not have foliations developed along its contacts. This intrusion is mostly composed of grey to pink quartz porphyritic granite with more intermediate varieties towards its southern contact.

Quartz and/or feldspar porphyritic felsic dikes (age unknown) are abundant around Schreiber and northwest of the Terrace Bay pluton but are uncommon elsewhere in the greenstone belt.

The "Whitesand Lake Batholith" (age unknown) is heterogeneous and appears to include more than one distinct intrusion; further mapping is required to better delineate the granitoid rocks of this batholith.

Archean Structural Geology

The degree of metamorphism and the nature of structural fabrics varies throughout the western Schreiber–Hemlo greenstone belt. Distinct domains containing common metamorphic mineral assemblages and structural fabrics are illustrated in Figure 5. Few crosscutting relationships have been observed between these different fabrics, thus, the structural features displayed on the map have been separated into two structural events; the early penetrative ductile fabrics, and the later more discrete brittle-ductile fabrics (Fig. 5). Observations of stratigraphic younging indicators, bedding-cleavage relationships and fold closures as well as stratigraphic correlation using geochronology have provided evidence for the upright folded Archean stratigraphy in the Schreiber–Hemlo greenstone belt (Fig. 4).

The intensity of deformation and metamorphism tends to increase towards the granitoid plutons (Fig. 5). The supracrustal rocks in a 1 to 1.5 km wide zone along the northern margin of the greenstone belt have amphibolite facies mineral assemblages and display strong penetrative foliations which define tight to isoclinal fold axial planes that are parallel to the margin. South of this zone, the rocks are generally less deformed, have greenschist to amphibolite facies mineral assemblages and have east to northeast trending foliations and fold axial traces. These fold

axial traces indicate that the rocks were deformed under northwest-directed compression during regional ductile deformation (Fig. 4). Discrete, outcrop-scale shear zones within the "Open Folding" domains (Fig. 5) are also east to northeast striking and have kinematic indicators that indicate reverse, south-side up vertical displacement with a dextral horizontal component, which is consistent with northwest-directed compression.

A thin zone of high strain up to 200 m wide is present along the margins of the circa 2690 Ma Terrace Bay pluton (Kamo and Hamilton, 2018). Kinematic indicators along the strained margins of the pluton indicate reverse, south-side up vertical displacement with a dextral horizontal component. In plan view, this pluton and the 2682.3 ± 1.1 Ma Syenite Lake pluton (Kamo and Hamilton, 2018), which are both hosted within the greenstone belt, strike northeast and resemble large-scale dextral sigma clasts. This suggests that the bulk of horizontal displacement in the greenstone belt during regional ductile deformation was dextral. The Terrace Bay pluton is the oldest known pluton in this part of the Schreiber–Hemlo greenstone belt; there has been no evidence to determine whether regional ductile deformation had commenced prior to emplacement of this pluton.

The 2674.1 ± 1.3 Ma Foxtrap Lake pluton (Kamo and Hamilton, 2018) truncates several east-trending fold axial traces, which are overprinted by fold axial traces that are parallel to the pluton margins. This indicates that regional ductile deformation had commenced prior to 2674 and continued after emplacement of the pluton.

The 2667 ± 4 Ma Santoy Lake pluton (Kamo, 2016) truncates several east-trending fold axial traces and has very thin zones of strain along its margins. This suggests that the pluton was emplaced during the later stages of regional ductile deformation.

There are two highly strained zones to note in the greenstone belt (Fig. 5). 1) The Jackfish–Middleton–McKellar Harbour shear zone is a 1-2 km wide zone of greenschist-facies rocks which are isoclinally folded and heavily sheared along lithological contacts. 2) The Empress Structure, located in a narrow band between the Terrace Bay and Lunch Lake plutons, hosts amphibolite facies rocks which are isoclinally folded and sheared with a moderate penetrative foliation throughout the zone. Throughout the greenstone belt, other thinner, unnamed ductile shear zones occur that are generally parallel with the regional ductile fabric.

Conjugate northwest-striking and north to northeast striking brittle-ductile shear zones and faults crosscut the greenstone belt and offset lithological contacts and the ductile fabrics.

Proterozoic Geology

Gunflint Formation

Several occurrences of polymictic, clast-supported conglomerate with pebble to cobble-sized clasts and interspersed lenses of stromatolitic chert unconformably overly the Archean basement along the shore of Lake Superior southwest of Schreiber. This conglomerate represents the base of the Gunflint Formation, and hosts the famous microfossils Gunflintia and Huronosporia (e.g., Wacey et al., 2013).

Diabase Dikes

A multitude of diabase dikes are present throughout the Schreiber-Terrace Bay area. Where possible, these dikes have been assigned to dike swarms that have been previously recognized in the area based on their orientation and chemistry.

Dikes from three Paleoproterozoic dikes swarms have been recognized, including the circa 2460 Ma Matachewan Swarm, the circa 2170 Ma Biscotasing Swarm and the circa 2120 Ma Marathon Swarm (Bleeker et al., 2012; Halls and Davis, 2004; Halls et al., 2008, respectively).

Three northeast-striking dikes with chemistry similar to dikes of the circa 1096 Ma Pigeon River Swarm (Liikane et al., 2018) have been observed. Previously the Pigeon River Swarm has only been recognized in the Thunder Bay area, however the dikes in the Schreiber–Hemlo greenstone belt are approximately along strike from those dikes (180 km). These dikes do not present a distinctive geophysical signature in the aeromagnetic dataset, thus tracing their extent is difficult.

A series of east to northeast striking subalkalic dikes is present east of Terrace Bay which have not yet been correlated with other regional events. The author believes these to be related to the circa 1.1 Ga Keweenawan Midcontinent Rift.

The most abundant dikes in the area are a series of west to northwest striking alkalic, olivine tholeiitic diabase dikes that are similar in chemistry to, and

appear to point directly to, the Wolfcamp Lake volcanic rocks that unconformably overly the Coldwell Alkalic Intrusive Complex. If this interpretation is correct, then it is likely that the alkalic dikes are related to an episode of Keweenawan volcanism younger than 1108 Ma (the age of the Coldwell Complex which they crosscut).

Mineral Potential

The Western Schreiber–Hemlo greenstone belt has a long history of mineral exploration and has potential for a variety of styles of base and precious metal mineralization.

Base metal sulphide and precious metal occurrences are associated with supracrustal rocks throughout the greenstone belt. Sulphide mineralized rocks occur near and along the upper contact of the circa 2720 Ma metavolcanic rocks of Package A. The host rocks are sulphide facies iron formation and chert, interbedded with felsic volcaniclastic rocks and garnetiferous mafic metavolcanic rocks. These rocks are lithologically similar and chronologically correlative with circa 2720 Ma metavolcanic rocks in the Winston Lake and Manitouwadge areas, which both host past-producing Zn-Cu-Ag base metal mines (see Fig. 1; Davis et al., 1994; Zaleski et al., 1999).

Gold and base metal sulphide occurrences are associated with highly strained supracrustal rocks, including the JMMHSZ, the Empress Structure, strained rocks surrounding plutons and other discrete shear zones throughout the greenstone belt. Mineralization in these shear zones typically occurs in quartz and carbonate veins in the shear zones and in silicate and carbonate altered haloes adjacent to the veins. The Hemlo gold deposit, located in the eastern part of the Schreiber–Hemlo greenstone belt, is hosted in highly strained and altered supracrustal rocks (Fig. 1; e.g. Muir, 2003).

Gold occurrences, with minor silver, molybdenum and copper mineralization, are associated with the Terrace Bay pluton and other granitoid rocks in the map area. Mineralization occurs in sulphide-bearing quartz veins and in altered granitoid rock adjacent to the veins. The veins are typically straight, with sharp contacts, and occur in parallel sets and in "stockwork" arrangements (Arnold et al., 2017; Marmont, 1984).

Zinc, silver and lead mineralization (with minor copper and gold) is associated with north to northeast striking faults near Schreiber. Mineralization occurs as massive sulphide in irregularly-shaped veins, and in sulphide-bearing quartz veins. Where these structures crosscut felsic metavolcanic rocks, the rocks are typically altered from grey to beige, and feldspar phenocrysts are altered to a distinct bright green colour (Magnus and Hastie, 2018).

Proterozoic rocks near the north shore of Lake Superior host a variety of commodities, including nickel, copper and platinum group elements associated with mafic to ultramafic intrusions; other transitional metals, such as niobium, tantalum and titanium and rare earth elements associated with carbonatitic (e.g., the Prairie Lake carbonatite-ijolite complex) and alkalic rocks (e.g., the Coldwell Alkalic Intrusive Complex); and diamond, associated with lamprophyric and kimberlitic dikes.

Road Log

Note: Caution should be taken when parking vehicles on the shoulder of the highway and when examining outcrops located along Highway 17. All UTM coordinates are provided in NAD83, Zone 16. Figures 3 and 4 show the location of the field trip stops.

The primary focus of this trip is on the Archean rocks of the Schreiber–Hemlo Greenstone Belt, however because of the abundance of Proterozoic diabase dikes in the area, some of the stops will also feature Proterozoic rocks. Note the mileages in the road log are not cumulative, rather each number is the distance from one stop to another.

41.7 km - Starting in Terrace Bay, drive east along Highway 17 for roughly 42km (25 minutes). About 1.5km (1 minute) before the parking spot, you will pass under two power transmission lines and Ripple Lake on the southeast side of the road; begin to slow down at this point, to make sure vehicles behind you have time to react, as you will be pulling off the road shortly. As you approach the parking spot, you will drive downhill across the McKellar Creek bridge. The parking spot is on the right (south) side of the road at the east end of this bridge just past the guardrail. Reset odometer to zero as subsequent mileages to stops are based on starting here.

If you pass the stop, turn at the junction between Highway 17 and Dead Horse Road and find a suitable location to turn around, and retrace your route back to the stop.

40.3 km - If starting in Marathon, drive west along Highway 17 for 40.3 km (29 minutes). After crossing the Little Pic River Bridge, then passing Dead Horse Road, Stop 1 will be on the south (left) side of the highway. Beware of oncoming traffic prior to turning into the parking area; east-bound vehicles will be driving speedily downhill at this location.

Stop 1. Sheared rocks, diabase and lamprophyre

UTM coordinates 521355E 5407099N

There are outcrops on the north and south sides of the highway at this location. The highway marks a contact between metasedimentary rocks to the north and mafic metavolcanic and intrusive rocks to the south.

The metasedimentary rocks north of the highway are wacke and siltstone with local sulphide mineralization. Box folds are observed throughout these rocks, which indicate that the rocks have been subjected to bedding-parallel shearing. Several biotite porphyritic ultramafic lamprophyre dikes, up to 8cm wide, crosscut the metasedimentary rocks, which exhibit iron carbonate alteration haloes adjacent to the dikes.

A single 240m long, near vertically-faced outcrop is present south of the highway. In this large outcrop, the mafic rocks display varied degrees of strain. In more highly strained areas, fractures and quartz veins tend to be parallel to the strong foliation, and where the outcrop surface is parallel to the foliation plane, geometric shapes appear in the outcrop. In less strained areas, fractures are more irregular, and parallel sets of quartz veins dip shallowly to the south, nearly perpendicular to the foliation in the outcrop. These areas are most easily observed by viewing the entire outcrop from the north side of the highway.

All primary textures have been obliterated in the highly strained areas, where a strong steeply dipping foliation hosts folded and boudinaged quartz veins and box folds and local sulphide mineralization. Quartz vein boudins with both sigma and delta asymmetries indicate the latest displacement was vertical; reverse motion with the northern side moving up towards the south. Two lineations are present in the outcrop; one shallowly plunging lineation which is interpreted to be a crenulation lineation, and a steeply-plunging lineation which is interpreted to be a stretching lineation, both formed during the reverse shearing event. The trend and plunge of these lineations vary throughout the outcrop as the foliations that host them waver.

The two areas of more competent rock are composed of massive medium-grained equigranular aphyric mafic rock, which may represent either massive metavolcanic flows or intrusive rocks. In the western zone, a dike of granodioritic rock crosscuts the mafic rock.

Near the west end of the outcrop, two adjacent alkalic diabase dikes crosscut the Archean rocks, striking west and dipping to the north. Together, these dikes are about 10m wide. These dikes are generally equigranular with fine-grained chilled margins and fractures orthogonal to the contacts. A 5cm wide feldspar porphyritic diabase dike is present at the very west end of the outcrop. Several north-striking biotite porphyritic ultramafic lamprophyre dikes are present near the middle and at the east end of the outcrop, similar to those on the north side of the highway. The mineralogy and texture of these dikes, including their associated iron carbonate alteration, are typical of lamprophyre dikes in this area.

Return to vehicles and turn left to drive west on Highway 17.

12.9 km - Drive west on Highway 17 for 12.9 km (8 minutes). Two minutes before the stop, you will pass Black Fox Lake on the right (north) side. The parking location for Stop 2 will be on the left (south) side of the highway in a turn-around location, on the east side of the Steel River Bridge (Fig. 6). If you miss the stop, there is a suitable turn-around location on the west side of the bridge.

Stop 2. Turbiditic Wacke

UTM coordinates 508700E 5402577N

There are outcrops on both the north and south sides of the highway at this location. The outcrop on the north side of the highway is shorter in length, and has cleaner outcrop surfaces, so it will be the focus of this stop. Stop 2 is the same locality as Stop 1 in Smyk and Schnieders (1995).

This outcrop is composed of southward-younging normally graded wacke interbedded with mudstone (Photo 1). On the south side of the road, and in outcrops along Santoy Bay and on Lawson Island, the younging direction of graded beds switches from south to north repetitively within tens of metres. These tight younging reversals are the main evidence for isoclinal folding in the area (Fig. 6).

A pervasive schistosity throughout the outcrop,

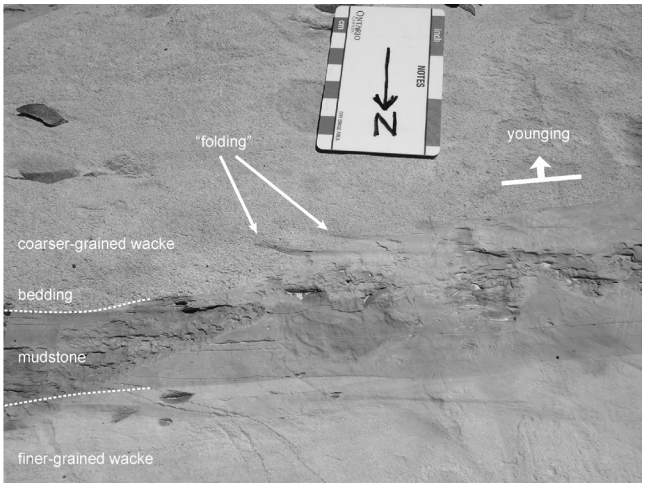


Photo 1. This photograph displays normally graded wacke interbedded with mudstone. Arrows point to enigmatic features which may be related to primary loading structures, folding or both. The outcrop surface is horizontal and a scale card is pointing north.

axial planar to local isoclinal folding, is at a low angle to bedding. Along this schistosity, the bedding planes display a strange pattern in which the more fissile mudstone layers form tabular projections into the sandstone, whereas the sandstone layers form more lobate projections into the mudstone. This may be interpreted as a primary loading structure that has been sheared during folding.

Return to the vehicles and turn left to drive west on Highway 17.

4.6 km - Drive west on Highway 17 for 4.6 km (3 minutes). You will be driving uphill on a moderate to steep grade, and any westbound transport trucks on this stretch of road will be driving below the speed limit with their 4-way flashers on. Do not pass these trucks; stay well behind them to ensure they do not decide to pull over and stop. After cresting the hill, the next turn will be about 1 minute away. Look for a "road intersection" sign and prepare to turn left (south).

2.2 km - Drive down this gravel road south towards Lake Superior, always keeping to the left at any junction. Eventually you will turn east and pass a gravel pit and a railway crossing. Slow down considerably and continue onward.

~2.0 km - The road turns from gravelly to sandy and narrows to a single lane. Continue driving eastward with caution. There are several branches of this trail that quickly lead to dead ends; if you reach a dead end, turn around and try another path. If at any time you feel unsafe or are unsure whether your vehicle is

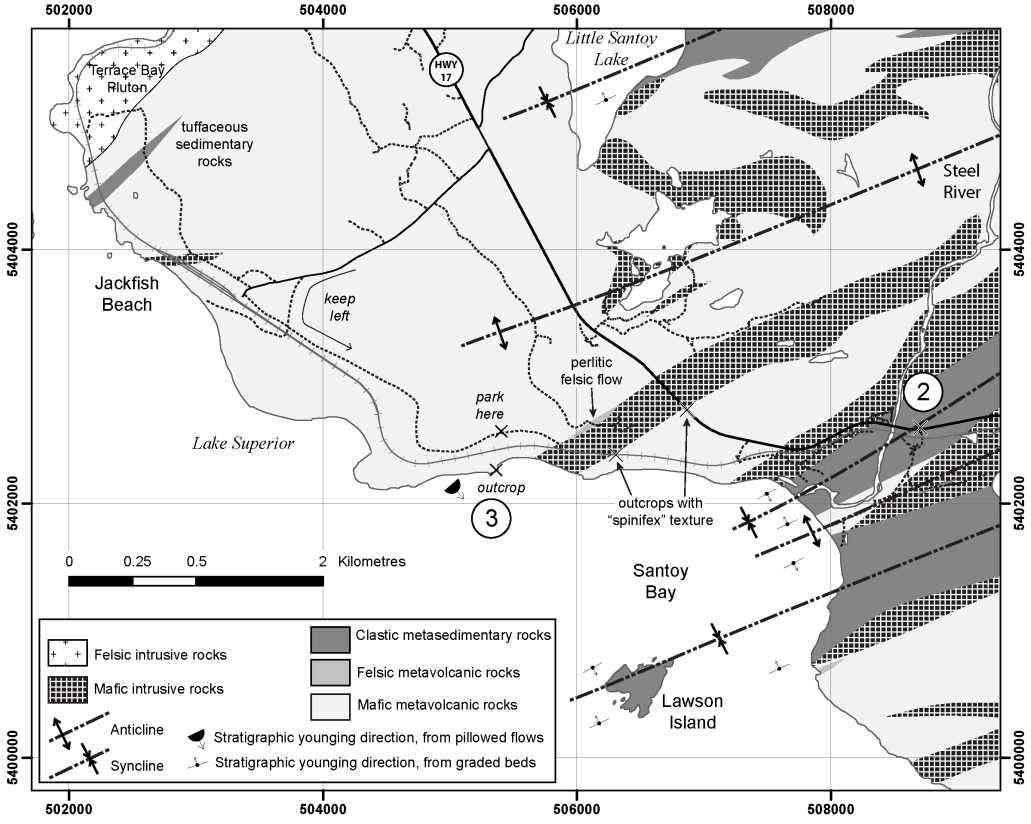


Figure 6. Simplified geological map of the Santoy Bay area, which includes stops 2 and 3. Several rocks of interest near Stop 3 are also indicated but will not be visited during this field trip. All UTM coordinates provided using NAD83 in Zone 16.

capable of driving in this terrain, turn back and skip ahead to Stop 4. The parking spot for Stop 3 is located at UTM 505400E, 5402555N, in a location where the path widens and there is a clearing through the trees on the south side of the path.

250-300 m - Unpack your hiking gear, including food, water and first aid equipment. Walk south along a footpath towards the railway; there is good line-of-sight along the rails at this location to see any oncoming trains. For the 2019 ILSG trip, there will be a flagged trail through the bush towards the lakeshore outcrop (Stop 3). For future users of this guidebook, you will have to navigate directly southward to the lake.

Safety Note: the hill between the railway and Lake Superior is steeply sloping and built out of cobbles. This is a health and safety risk to those with reduced mobility. If at any time you feel unsafe to continue, turn back and skip ahead to Stop 4.

Stop 3. Variolitic Mafic Flows

UTM coordinates 505366E 5402266N

This lakeshore outcrop, which has been kept lichen free by winter ice in Lake Superior is the best exposure of variolitic mafic flows in the western Schreiber–Hemlo Greenstone Belt (Fig. 6). Exposure here is good enough to trace flow contacts and to observe various macrotextures present in at least four consecutive flows (Fig. 7).

Pillows are generally 3m across, with single rinds up to 3 cm thick, and selvages filled with glassy material and hydrothermal minerals like quartz, calcite and epidote. These pillows lack vesicles or amygdules, but some pillows situated at or near the top of flow sequences contain elongate, discontinuous, quartz- and carbonate-filled cavities, which the author interprets to represent large, formerly gas-filled cavities.

The most conspicuous feature of these pillows is the variolitic texture (Fig. 7). Inward from the chilled margins, the pillows are dark green and very fine-grained, with only a few small varioles (up to 2 mm). Varioles become larger (up to 8 mm) and more abundant toward the core of the pillow, where they appear to have amalgamated to produce a more massive, leucocratic pillow core (Fig. 7). The interiors of the varioles are concentrically zoned with bands of calc-silicate minerals. The distribution of varioles in the pillows is not always perfectly concentric; their distribution seems to be more erratic at the tops of the pillows. Very few pillows display multiple concentric variolitic and non-variolitic bands. In pillows that contain both the gas cavities and varioles, the gas cavities are always located in the dark green, non-variolitic upper portions of the pillows.

The massive flows, which may be traced in this

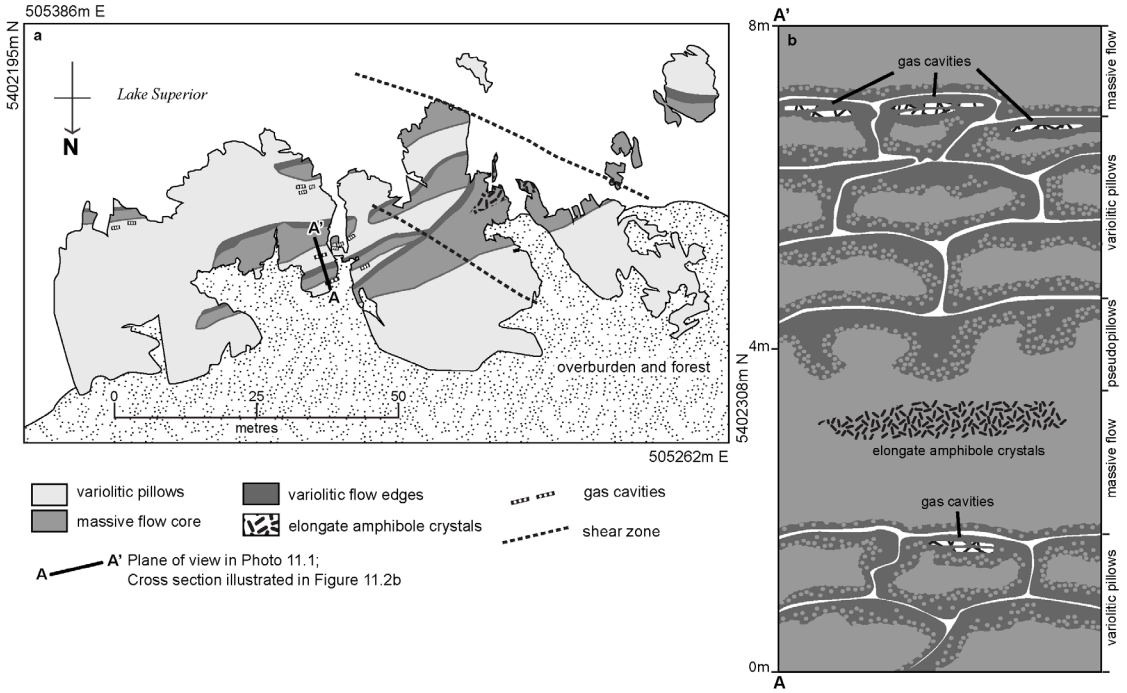


Figure 7. A) Simplified bedrock geology map of the shoreline outcrop at Stop 3, and B) illustration of the macrotextures observed in outcrop along A–A'. All UTM coordinates provided using NAD83 in Zone 16.

outcrop for up to 50 m in length, have widths that vary in proportion to their lengths (i.e., thinner flows are less laterally extensive). The internal structure of the flows is similar to that observed in the pillows, with non-variolitic, dark green material inside the rinds that grades into massive variolitic cores. The transition from rind to variolitic core at the base of the flows occurs over approximately 5 cm, whereas, at the top of the flows, the varioles have coalesced into lobes and pods that appear pillow-like, without the necessary rinds (i.e., pseudopillows). Randomly oriented, elongate crystals of amphibole are present in the massive, medium-grained core of the thickest flow in this outcrop.

These flows and all other variolitic mafic flows in the greenstone belt have trace element contents consistent with mafic rocks erupted in "back-arc basin" volcanic environments. This is the defining characteristic of Depositional Package B, which is dominated by rocks of this chemistry intercalated with mafic rocks of "oceanic plateau" volcanic affinity.

Nearby outcrops of a perlitic felsic flow (accessible along a footpath) and outcrops of spinifex-textured mafic to ultramafic rocks (accessible along Highway 17 or along the railway) are indicated in Figure 6. These rocks will not be visited during this field trip. Please use caution, especially along the highway and the railway, if you decide to visit these rocks.

Return to vehicles by the same path you took to the outcrop. Turn the vehicles around and drive west along the path.

~2.0 km - Drive back along the sandy path the way you entered, until you reach the gravel pit.

2.2 km - Keep to the right and drive north until the gravel road intersects with Highway 17.

7.3 km - Turn left and drive west on Highway 17 for 7.3km (4 minutes). Along the way, you will get an excellent view over Jackfish Lake and the terraced hills to the north. Those hills are the location of the historic Empress gold mine, which produced 112 oz Au at 0.10 oz/ton from 1896-1897. After passing the lake and beginning to drive uphill, prepare to slow down for Stop 4.

The parking spot for Spot 4 is a turn-around spot on the left (south side) of the highway, on the west end of a large granite and diabase outcrop.

Stop 4. Granite, sheared mafic rocks and diabase dikes

UTM coodinates 503233E 5411222N

There are outcrops on the north and south sides of the highway at this location. On the south side of the highway, grey to pink granodiorite of the Terrace Bay pluton is crosscut by a 50 m wide plagioclase porphyritic diabase dike. This dike trends generally northward and is aligned with a north-northeast trending geophysical anomaly consistent with dikes of the Biscotasing dike swarm. There are smaller plagioclase porphyritic dikes with chill margins that crosscut the large dike.

On the north side of the road, there are two outcrops composed of a series of southward dipping panels of granite, mica schist, mafic intrusive rocks and massive felsic rocks.

The bottom of the western outcrop is massive grey to pink granodiorite of the Terrace Bay pluton, the top of the outcrop is a dike or sill of weakly foliated massive, fine grained aphyric felsic rock and a panel of mica schist lies between them. The mica schist is composed of biotite and chlorite with abundant quartz and calcite veins. The dominant foliation in the mica schist dips more steeply to the south than the contacts between the schist and the felsic rocks between which it is sandwiched. This looks like a C-S structural fabric; the contacts between units represent the "C" plane, and the strong foliation in the schistose rock represents the "S" plane. Quartz veins in the schist are boudinaged; asymmetric boudins (mostly sigma clasts) and the orientation of the C-S fabric both indicate south-side up reverse displacement northward. Box folds in this schist post-date the sigmoidal quartz boudins. A biotite porphyritic ultramafic lamprophyre dike crosscuts the rocks at the west end of the outcrop.

The eastern outcrop is a massive sheared mafic rock composed mainly of amphibole and biotite with minor quartz, feldspar and carbonate minerals, cut by a small granitoid dike at the west end of the outcrop. Southward dipping shear zones crosscut this rock with C-S fabrics similar to those observed in the western outcrop, indicating the same south-side up reverse displacement. The trace element composition of this mafic rock is similar to that of the granitoid rocks in the Terrace Bay pluton, with higher concentrations of transitional elements such as iron, magnesium, chromium, vanadium, nickel and copper. This rock is interpreted to represent mafic country rock that was

altered during emplacement of the Terrace Bay pluton.

Return to the vehicles and turn left to drive west on Highway 17.

17.4 km - Drive west on Highway 17 for 17.4km (12 minutes). You will pass through the town of Terrace Bay. On the west side of town, just west of the Aguasabon River, turn left at the intersection between the highway and Aguasabon Gorge Road.

Note the outcrops of grey granodiorite, locally altered to pink granodiorite, along the highway towards Terrace Bay. Most of the rocks in the Terrace Bay pluton look like this.

750 m - Drive to the end of the road. There will be a large parking area with outhouses and picnic tables. There is a boardwalk with railings at the south end of this parking lot that leads towards a vista with a view of the Aguasabon Falls and Lake Superior.

Safety Note: Although there are small foot-paths off of the main boardwalk, do not hop over the railing to walk on these paths. Falling into the gorge would lead to death.

Stop 5. Aguasabon Falls Gorge; structures and alteration

UTM coordinates 490833E 5403233N

This vista overlooks granitoid rocks of the Terrace Bay pluton (Photo 2). Granodiorite in the pluton is normally grey; locally, the granodiorite is altered pink, caused by hydrothermal alteration around regional-scale shear-zones and faults. North, northwest and northeast-striking faults, which correlate with similar shear zones that crosscut the supracrustal rocks of the greenstone belt, control the vertical cliff faces in the Aguasabon River Gorge.

Return to vehicles, drive back along Aguasabon Gorge Road and turn left to drive west on Highway 17.

8.1 km - Drive west on Highway 17 for 8.1 km (5 minutes). Along the way you will get an excellent view of Lake Superior (Terrace Bay). One minute before the next turn, you will pass an intersection between the highway and Worthington Bay Road. You will then cross a train bridge; turn right onto Hays Lake Road 200m north of the bridge (Fig. 8).

Note the large outcrop of sulphide-bearing chert and graphitic argillite at the beginning of Hays Lake Road.

Drive for 800 metres along Hays Lake Road; there will be a clearing in the trees on the north side of the road. Pull your vehicle safely to the shoulder of the road and park.



Photo 2. View of the Aguasabon Falls Gorge, with Lake Superior and the Slate Islands in the background. Photo taken from a vista at the end of Aguasabon Gorge Road.

Stop 6. Harkness Hays and Gold Range

UTM coordinates 483711E 5404933N

North of the road, there is a northeast-trending ridge of outcrops that have been the subject of gold exploration for more than a century, with the earliest staking recorded in 1917. Over the following several decades, numerous adits and shafts were used to sample the bedrock in this ridge, which hosts the Harkness-Hays property to the west and the Gold Range property to the east. The Harkness-Hays property produced 200 oz Au at 2.58 oz/t during intermittent mining activities between 1920 and 1936; the Gold Range property produced 36.35 oz Au at 0.91 oz/t during intermittent mining activities from 1921 to 1941 (Schnieders et al.,

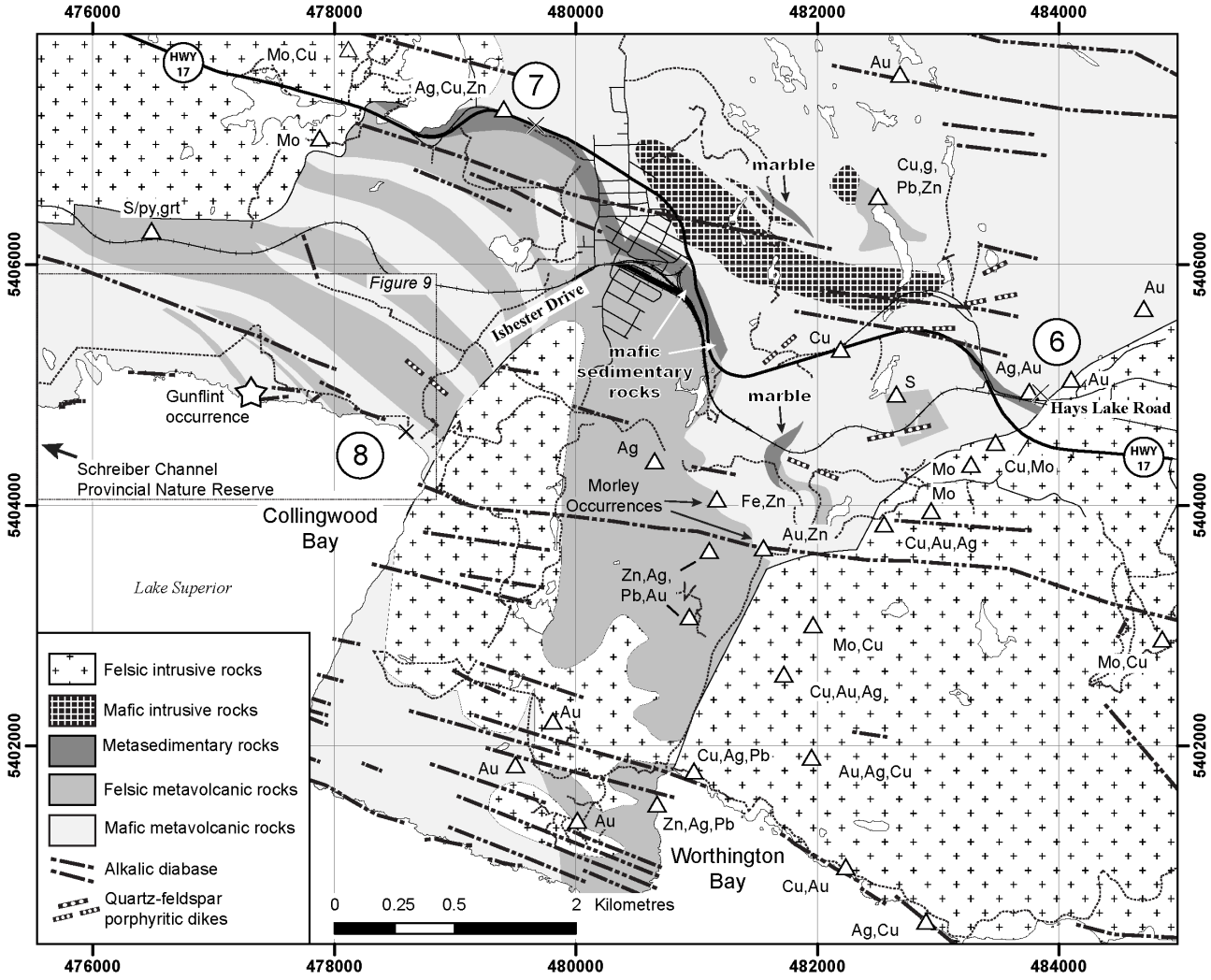


Figure 8. Simplified geological map of the Schreiber area, which includes field trip stops 6, 7 and 8. The mafic metasedimentary rocks and the Morley occurrences, which are correlative with the rocks at Stop 7, are indicated, as well as nearby occurrences of marble associated with other chemical metasedimentary rocks. A box outlines the area covered in Figure 9. Abbreviations: Ag = silver, Au = gold, Cu = copper, Fe = iron, g = graphite, grt = garnet, Mo = molybdenum, Pb = lead, py = pyrite, S = sulphur, Zn = zinc. All UTM coordinates provided using NAD83 in Zone 16.

1996). The focus for this stop will be on the Harkness-Hays property, which is the most easily accessible (and has the better historic gold grade).

These outcrops are composed mainly of massive to pillowed mafic metavolcanic rocks, crosscut by quartz feldspar porphyritic felsic dikes and biotite porphyritic lamprophyre dikes. These rocks are located in a moderately strained zone along the northwest edge of the Terrace Bay pluton and contain amphibolite facies mineral assemblages (Figs. 5 and 8). Quartz veins in the northeast-striking foliation, parallel to the contact with the pluton, host gold-bearing sulphides and occurrences of native gold.

Native gold at this site is found most commonly in white, vuggy quartz veins. Much of the bedrock has been blasted, and quartz vein bearing rocks are dispersed throughout the resultant pile of rocks. It is recommended that visitors search through this pile of rock, rather than scale the pile to access the steep, cliffy outcrops.

Return to vehicles, turn the vehicles around and drive back towards Highway 17.

5.3 km - Turn right and drive westward on Highway 17 for 5.3 km (4 minutes). Along the way you will pass through the town of Schreiber. After passing the Villa Blanca Inn, on the west side of town you will begin driving uphill. The parking spot for Stop 7 will be on the right (north) side of the road at the top of this hill; prepare to stop.

Note as you drive through Schreiber, on the right (northeast) side of the road are several outcrops of turbiditic mafic-derived metasedimentary rocks.

Stop 7. Elwood Occurrence

UTM coordinates 479511E 5407266N

There are outcrops on the north and south sides of the highway at this location (Fig. 8). On both sides of the highway, the outcrops are an upright north-dipping sequence of interbedded chert and graphitic argillite with minor beds of felsic tuffaceous conglomerate. Sulphide mineralization is disseminated throughout the outcrop and occurs in calcite-sulphide veins and as conformable lenses of massive sulphide. The sulphide minerals are dominantly pyrrhotite and pyrite with minor chalcopyrite.

On the north side of the highway, a massive mafic flow marks the top of this sequence and forms an erosion-resistant cap on the outcrop. At the base of this flow, the rock contains abundant siliceous xenoliths of chert ripped up from the underlying cherty units, as well as abundant quartz and calcite amygdules, likely caused by the release of volatile fluids from the underlying sediments as the mafic flow was deposited. One 15cm wide dike of similar composition crosscuts the underlying rocks and is interpreted to be a feeder dike to the flow.

The sequence of sedimentary rocks is roughly 80 m thick and represents a significant disconformity between the arc volcanic rocks of Package A and the back-arc basin volcanic rocks of Package B (Fig. 4). These rocks have a strong electromagnetic signature which is traceable along strike; eastward, the anomaly coincides with the mafic metasedimentary rocks along the highway in Schreiber and with chemical metasedimentary rocks at the Morley occurrence southeast of town (Fig. 8). Several other chemical sedimentary rocks occur east of town, including two occurrences of marble interbedded with argillite and sulphide facies iron formation and the outcrop of sulphide-bearing chert and argillite observed earlier at the intersection of Highway 17 and Hays Lake Road (Fig. 8). Whether these nearby rocks represent separate sequences or are part of the same depositional sequence but separated by cryptic folding requires further, more detailed mapping.

The strata in this area are arranged in open, upright folds, which is apparent in this outcrop. However, the more fissile argillite-rich zones have developed C-S fabrics, kink folds and kinematic indicators like sigma and delta clasts that all indicate a significant amount of dextral shearing has affected these rocks. Because the only place locally that this deformation has been observed is in these argillitic rocks, the timing and cause of this shearing is unknown.

Return to vehicles and turn left to drive east on Highway 17.

1.2 km - Drive 1.2 km into the town of Schreiber and take the third right onto Winnipeg Street. This is the street immediately east of the Golden Rail chip truck.

600 m - Drive to the end of Winnipeg Street, where you will see a railroad museum, and turn right onto Scotia Street.

70 m - Drive 1 block west on Scotia Street, then turn left on Subway Street.

210 m - Driving south on Subway Street, you will pass beneath the railway. Take the first right onto Isbester Drive.

2.3 km - Drive south to the end of Isbester Drive. There is a parking lot at the end of the road, and an outhouse and a gazebo down near the beach.

Walk down the footpath to the beach, then turn right (west) and walk towards the first outcrop. This is Stop 8.

Stop 8. Schreiber Beach Outcrops

UTM coordinates 478600E 5404600N

The outcrops at Schreiber Beach (Photo 3) are the best exposure of a conformable sequence of Archean metavolcanic and metasedimentary rocks in the Schreiber–Hemlo greenstone belt and perhaps throughout Ontario (Fig. 9). From the eastern-most outcrop to the Schreiber Channel Provincial Nature Reserve, where exposures of Proterozoic



Photo 3. View of Schreiber Beach and the rocky shoreline westward, taken from a vista along the Casque-Isles Trail.

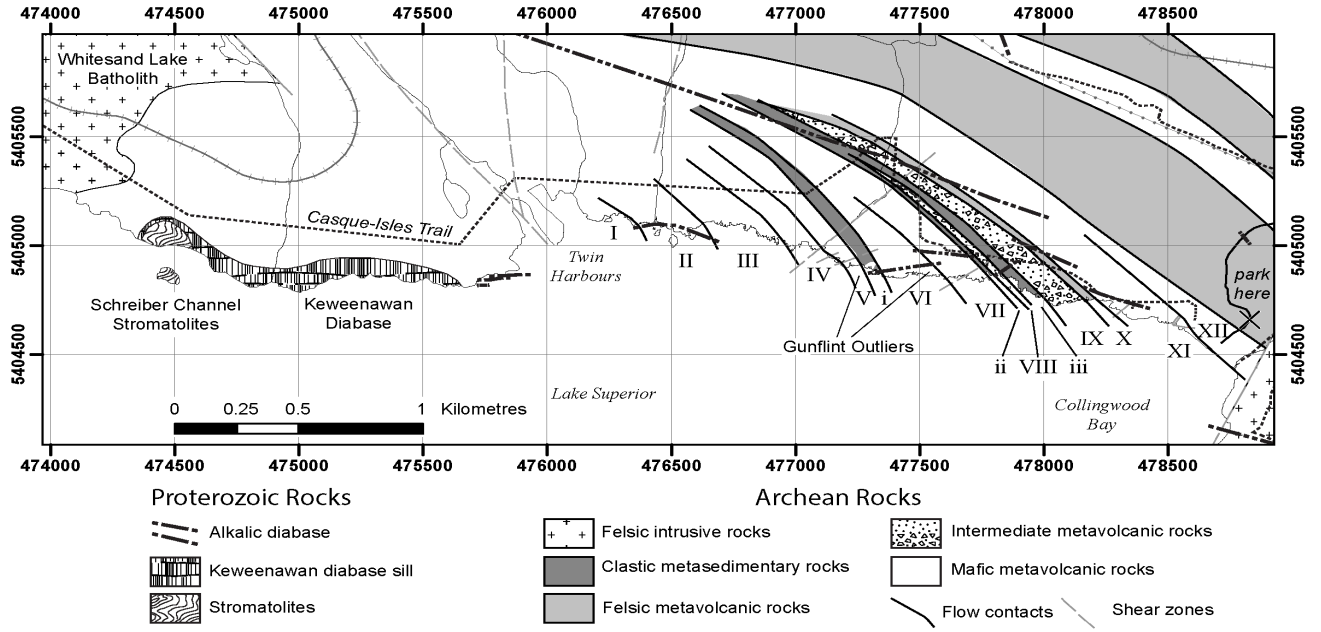


Figure 9. Simplified geological map of the shoreline west of Schreiber Beach on Lake Superior. Metavolcanic flows and metasedimentary sequences are labelled I-XII and i-iii respectively. Proterozoic rocks of interest are labelled. Note that the Casque-Isles trail is well constrained for two km west of the Schreiber Beach, but the author was not able to get better a resolution trace of the trail further west. All UTM co-ordinates provided using NAD83 in Zone 16.

rocks interrupt the Archean exposure, there are three kilometers (as the crow flies) of near-continuous rocky shoreline, with less than 5% of the shoreline covered by cobble beaches. Winter ice scraping against the rocky shoreline keeps the rocks up to several metres inland lichen-free, displaying beautiful mineral, volcanic and sedimentary textures. The rocks are not pervasively deformed; only crosscut by discrete fractures with minimal displacement and up to metre-wide shear zones. There are only a few altered areas in which the primary textures of the rocks are preserved. The upright stratigraphy strikes northwest and dips shallowly to the northeast, such that the straight, east-west trending shoreline provides for us a perfect cross-section; walking west along the shoreline guides us down through stratigraphy.

The lead author only had the opportunity to map the shoreline between Schreiber Beach and Twin Harbours, and so that stretch will be the focus of this description.

From compiled data, the Archean rock between Twin Harbours and the granite-greenstone contact to the west is composed mainly of mafic metavolcanic rock. The world-famous Schreiber Channel Stromatolite outcrop and associated Gunflint conglomeratic rocks occurs along this stretch of shoreline, and a Keweenawan diabase sill occupies the Archean-Proterozoic unconformity.

Eastward from Twin Harbours, higher in the stratigraphy, are five consecutive mafic metavolcanic flows up to 200 m in apparent thickness (roughly 175 m in true thickness, with an estimated 30 degree dip; Fig. 9). These flows are massive at the base, with medium to coarse-grained equigranular textures that could easily be mistaken for mafic intrusive rocks. Thin beds of sulphide-bearing chert are present along the flow contacts. Flow II is crosscut by an alkalic diabase dike, flow III is crosscut by two north-trending, carbonate altered mafic dikes up to 25 m wide, and flow V is crosscut by a series of north-trending dikes that display unique Liesegang textures.

A 50 m thick sequence (i) of tuffaceous conglomerates with pebble to cobble-sized mafic and felsic volcanic clasts lies atop flow V (Fig. 9). Minor graded beds of sandy to gravelly material are present within these conglomerates. These rocks are crosscut by alkalic diabase dikes, and unconformably overlain by an outlier of the Gunflint Formation basal conglomerate, including cherty stromatolite domes similar to those observed at the Schreiber Channel Provincial Nature Reserve. The conglomerate is massive, polymictic and clast-supported, with dominantly pebble to cobble-sized clasts. The conglomerates are interpreted to have been deposited in a shallow water environment akin to the cobble beaches present along the shores of Lake Superior today.

Eastward from metasedimentary sequence i are two consecutive massive to pillowed mafic flows similar to flows I-V. Another outlier of the Gunflint basal conglomerates and stromatolites, crosscut by an alkalic diabase dike, unconformably overlies pillows near the top of flow VI (Fig. 9).

A thin sequence of tuffaceous wacke (ii) marks the top of flow VII. This is overlain by an intermediate volcanic flow (VIII) with plagioclase and amphibole phenocrysts. This flow is generally massive, with an agglomerate of similar composition at its top. This agglomerate grades into the polymictic tuffaceous conglomerate (iii) similar to the conglomerates in sequence i.

Another massive intermediate flow (IX) with plagioclase and amphibole phenocrysts overlies the conglomerates of sequence iii roughly 100 m wide, with agglomerate at its top similar to that of flow VIII. This agglomerate is overlain by a 3 m sequence of normally graded tuffaceous wacke, which is then overlain by a massive to brecciated felsic flow with feldspar phenocrysts (Flow X).

Two consecutive massive to pillowed mafic flows (XI and XII) overlie Flow X with a 1 m wide sequence of banded chert and magnetite between them. Outcrop exposure ends just above the base of Flow XII, which is then covered by the sands of Schreiber Beach. This eastern-most outcrop will be the subject of our last stop on the field trip (Fig. 9).

To access the shoreline to the west, one could either walk along the rocky shoreline, which is quite rugged and slippery when wet, or follow the Casque-Isles Trail, which intermittently jogs down towards the shoreline (Fig. 9). There is a stream with steep-sided banks roughly halfway between Schreiber Beach and Twin Harbours, at the contact between flows IV and V. At the mouth of this stream, there are cobbles and boulders along the shoreline that may be crossed if there are no waves on Lake Superior and the outflow from the stream is minimal. A small wooden footbridge, wide enough for one person, crosses this stream about 500 metres to the north along the Casque-Isles Trail. Neither of these choices are particularly safe, so exercise extreme caution whichever path you choose to follow. Note that aside from the Schreiber Channel stromatolites, most of the rocks observed between here and Twin Harbours are massive to pillowed mafic flows (Fig. 9). To reach the Schreiber Channel stromatolites, it is recommended to start at the west end of the trail in Rossport or to approach the location by boat.

End of road log.

Acknowledgments

The author would like to thank the field crews from the summers of 2015 (Joseph Walker, Andrea Nywening, Matthew Hanewich and Lauren Madronich), 2016 (Kira Arnold, Mallory Metcalf, Lucas Wolfe and Haley Aldred), 2017(Kira Arnold, Joshua Nguyen, Maddison Hodder and Gabrielle Klemt) and 2018 (Evelyn Moorhouse, Cassandra Powell, Mateo Dorado-Troughton, Jessica Verschoor, Shadman Islam and Rachel Bourassa) for their hard work and perseverance through the particularly rough terrain. The author would like to thank Evan Hastie for co-leading the 2018 field season. The author would also like to thank the Richards family of Terrace Bay, who hosted the crew at their Jackfish Lake cottages on Highway 17 during the 2015-2018 field seasons, with special thanks to local prospector Wayne Richards, for all of his logistical aid and for sharing his abundance of local mineral exploration knowledge. Thanks to the people of Pic River and Pic Mobert First Nations communities for their gracious blessing and for allowing us to work on their traditional lands. The author would also like to thank local prospector Rudy Wahl, Mike Koziol of Alto Ventures Ltd. And Troy Gill of Sanatana Resources for tours of their properties and allowing us access to their properties over the last several field seasons. Thanks also to Mark Smyk, Dorothy Campbell and Mark Puumala of the Resident Geologist Program Thunder Bay office for their help during this project. Thanks to Michael Easton and Riku Metsaranta for their careful edits, and to Laura Ratcliffe for help with the figures.

References

Addison W.D., Brumpton, G.R., Vallini, D.A., McNaughton, N.J., Davis, D.W., Kissin, S.A., Fralick, P.W. and Hammond, A.L. 2005. Discovery of distal ejecta from the 1850 Ma Sudbury impact event; Geology, v.33, p.193-196.

Anglin, C.D., Franklin, J.M., Loveridge, W.D., Hunt, P.A. and Osterberg, S.A. 1988. Use of zircon U-Pb ages of felsic intrusive and extrusive rocks in eastern Wabigoon Subprovince, Ontario, to place constraints on base metal and gold mineralization; in Radiogenic age and isotopic studies: report 2, Geological Survey of Canada, Paper 88-2, p.109-115.

Arnold, K.A., Hollings, P. and Magnus, S.J. 2017. Geology and mineral potential of the Terrace Bay pluton, western Schreiber–Hemlo greenstone belt; in Summary of Field Work and Other Activities, 2017, Ontario Geological Survey, Open File Report 6333, p.12-1 to 12-6.

Beakhouse, G.P. and Davis, D.W. 2005. Evolution and tectonic significance of intermediate to felsic plutonism associated with the Hemlo greenstone belt, Superior Province, Canada; Precambrian Research, v.137, p.61-92.

Blackburn, C.E., Bond, W.D., Breaks, F.W., Davis, D.W., Edwards, G.R., Poulsen, K.H., Trowell, N.F. and Wood, J. 1985. Evolution of Archean volcanic-sedimentary sequences of the western Wabigoon Subprovince and its margins: a review; in Evolution of Archean Supracrustal Sequences, Geological Association of Canada, Special Paper 28, p.89-116.

Bleeker, W., Hamilton, M.A., Ernst, R.E. and Soderlund, U. 2012. Resolving the age structure of the Matachewan event: magmatic pulses at c. 2445-2452 Ma, 245802461 Ma and 2475-2480 Ma; unpublished CAMIRO Reports A96, A97, and A98, 17p. available from www.supercontinent.org

Bleeker, W., Liikane, D.A., Smith, J., Hamilton, M., Kamo, S.L., Cundari, R., Easton, M., and Hollings, P. 2018. Controls on the localization and timing of mineralized intrusions in intra-continental rift systems, with a specific focus on the ca. 1.1 Ga Mid-continent Rift system; in Targeted Geoscience Initiative: 2017 report of activities, volume 2; Geological Survey of Canada, Open File 8373, p. 15–27. https://doi.org/10.4095/306594

Buchan, K.L., Mortensen, J.K. and Card, K.D. 1993. Northeast-trending Early Proterozoic dykes of southern Superior Province: multiple episodes of emplacement recognized from integrated paleomagnetism and U-Pb geochronology; Canadian Journal of Earth Sciences, v.30, p.1286-1296.

Cabanis, B. and Lecolle, M. 1989. The La/10-Y/15-Nb/8 diagram: A tool for distinguishing volcanic series and discovering crustal mixing and/or contamination; Comptes Rendus de Academie des Sciences, Série IIA, v.309, p.2023-2029.

Cannon, W.F., Schulz, K.J., Horton, J.W. and Kring, D.A. 2010. The Sudbury impact layer in the Paleoproterozoic iron ranges of northern Michigan, USA; Geological Society of America Bulletin, v.122, p.50-75.

Corfu, F. 2000. Extraction of Pb with artificially too-old ages during stepwise dissolution experiments on Archean zircon, Lithos, v.53, p.279-291.

Corfu, F. and Muir, T.L. 1989. The Hemlo–Heron Bay greenstone belt and Hemlo Au–Mo deposit, Superior Province, Ontario, Canada, Chemical Geology (Isotope Geoscience Section), v.79, p.183-200.

Corfu, F. and Stott, G.M. 1986. U-Pb ages for late magmatism and regional deformation in the Shebandowan Belt, Superior Province, Canada; Canadian Journal of Earth Sciences, v.23, p.1075-1082.

Corfu, F. and Stott, G.M. 1998. Shebandowan greenstone belt, western Superior Province: U-Pb ages, tectonic implications, and correlations; Geological Society of America Bulletin, v.110, p.1467-1484.

Cundari, R. 2012. Geology and geochemistry of Midcontinent Rift-related igneous rocks; unpublished MSc thesis, Lakehead University, Thunder Bay, Ontario, 142p.

Davis, D.W. 1996. Provenance and depositional age constraints on sedimentation in the western Superior transect area from U-Pb ages of zircons; in Western Superior Transect Second Annual Workshop, Lithoprobe Secretariat, University of British Columbia, Vancouver, British Columbia, Lithoprobe Report No. 53, p.18-23.

Davis, D.W., Beakhouse, G.P. and Jackson, S.L. 1998. U-Pb zircon and titanite geochronology; Part 3, p.1-8, in S.L. Jackson, G.P. Beakhouse and D.W. Davis, Geological Setting of the Hemlo GoldDeposit; an Interim Progress Report, Ontario Geological Survey, Open File Report 5977, 121p.

Davis, D.W., Krogh, T.E., Hinzer, J. and Nakamura, E. 1985. Zircon dating of polycyclic volcanism at Sturgeon Lake and implications for base metal mineralization; Economic Geology, v.80, p.1942-1952.

Davis, D.W. and Lin, S. 2003. Unravelling the geologic history of the Hemlo Archean gold deposit, Superior Province, Canada: A U-Pb geochronological study; Economic Geology, v.98, p.51-67.

Davis, D.W., Pezzutto, F. and Ojakangas, R.W. 1990. The age and provenance of metasedimentary rocks in the Quetico Subprovince, Ontario, from single zircon analyses: implications for Archean sedimentation and tectonics in the Superior Province; Earth and Planetary Science Letters, v.99, p.195-205.

Davis, D.W., Schandl, E.S. and Wasteneys, H.A. 1994. U-Pb dating of minerals in alteration halos of Superior Province massive sulphide deposits: Syngenesis versus metamorphism; Contributions to Mineralogy and Petrology, v.115, p.427-437.

Davis, D.W. and Stott, G.M. 2003. Geochronology of two Proterozoic mafic dike swarms in northwestern Ontario; in Summary of Field Work and Other Activities 2003, Ontario Geological Survey, Open File Report 6120, p.12-1 to 12-7.

Davis, D.W. and Sutcliffe, C.N. 2017. U-Pb geochronology by LA-ICPMS in samples from northern Ontario, internal report for the Ontario Geological Survey;

Jack Satterly Geochronology Laboratory, University of Toronto, Toronto, Ontario, 131p.

Davis, D.W. and Sutcliffe, R.H. 1985. U-Pb ages from the Nipigon Plate and Northern Lake Superior; Geological Society of America, Bulletin, v.96, p.1572-1579.

Davis, S. 2016. Petrology and geochemistry of the Wolfcamp Lake basalts; unpublished HBSc thesis, Lakehead University, Thunder Bay, Ontario, 68p.

Davis, S., Hollings, P. and Cundari, R.M. 2017. Geochemistry of the Mesoproterozoic Wolfcamp Lake basalts, northwestern Ontario; Ontario Geological Survey, Miscellaneous Release—Data 345.

Fage, A. 2011. Geology, geochemistry and geochronology of the Hemlo East property, Schreiber–Hemlo greenstone belt, Ontario; unpublished MSc thesis, Lakehead University, Thunder Bay, Ontario, 155p.

Fralick, P. and Davis, D. 1999. The Seine-Couchiching problem revisited: Sedimentology, geochronology, and geochemistry of sedimentary units in the Rainy Lake and Sioux Lookout areas; in 1999 Western Superior Transect 5th Annual Workshop, Lithoprobe Secretariat, The University of British Columbia, Vancouver, British Columbia, Lithoprobe Report No. 70, p.66-75.

Fralick, P., Davis, D.W. and Kissin, S.A. 2002. The age of the Gunflint Formation, Ontario, Canada: single zircon U-Pb age determinations from reworked volcanic ash; Canadian Journal of Earth Sciences, v. 39, p.1085-1091.

Fralick, P., Purdon, R.H. and Davis, D.W. 2006. Neo-Archean trans-subprovince sediment transport in southwestern Superior Province: sedimentological, geochemical and geochronological evidence; Canadian Journal of Earth Sciences, v.43, p.1055-1070.

Halls, H.C. and Davis, D.W. 2004. Paleomagnetism and U-Pb geochronology of the 2.17 Ga Biscotasing dyke swarm, Ontario, Canada: evidence for vertical-axis crustal rotation across the Kapuskasing Zone; Canadian Journal of Earth Sciences, v.41, p.255-269.

Halls, H.C., Davis, D.W., Stott, G.M., Ernst, R.E. and Hamilton, M.A. 2008. The Paleoproterozoic Marathon Large Igneous Province: New evidence for a 2.1 Ga long-lived mantle plume event along the southern margin of the North American Superior Province; Precambrian Research, v.162, p.327-353.

Hamilton, M.A. and Stott, G.M. 2008. The significance of new U/Pb baddeleyite ages from two Paleoproterozoic diabase dikes in northern Ontario; in Summary of Field Work and Other Activities 2008, Ontario Geological Survey, Open File Report 6226, p.17-1 to 17-10.

Hart, T.R., Termer, M. and Jolette, C. 2002. Precambrian geology of Kitto, Eva, Summers, Dorothea and Sandra townships, northwestern Ontario: Phoenix bedrock mapping project; Ontario Geological Survey, Open File Report 6095, 206p.

Heaman, L.M. 1997. Global mafic magmatism at 2.45 Ga: Remnants of an ancient large igneous province?; Geology, v.25, p.299-302.

Heaman, L.M. and Easton, R.M. 2006. Preliminary U-Pb geochronology results from the Lake Nipigon Region Geoscience Initiative; Ontario Geological Survey, Miscellaneous Release—Data 191, 1 CD-ROM.

Heaman, L.M., Easton, R.M., Hart, T.R., Hollings, P., MacDonald, C.A. and Smyk, M. 2007. Further refinement to the timing of Mesoproterozoic magmatism, Lake Nipigon region, Ontario; Canadian Journal of Earth Science, v.44, p.1055-1086.

Heaman, L.M. and Machado, H. 1987. Isotope geochemistry of the Coldwell alkaline complex I—U-Pb studies on accessory minerals; in Program with Abstracts, Geological Association of Canada-Mineralogical Association of Canada, v.12, p.54.

Heaman, L.M. and Machado, H. 1992. Timing and origin of Midcontinent Rift alkaline magmatism, North America: evidence from the Coldwell complex; Contributions to Mineralogy and Petrology, v.110, p.289-303.

Jensen, L.S. 1976. A new cation plot for classifying subalkalic volcanic rocks; Ontario Department of Mines, Miscellaneous Paper 66, 22p.

Kamo, S.L. 2015. Part A: Report on U-Pb ID-TIMS geochronology for the Ontario Geological Survey: bedrock mapping projects, Ontario, Year 1: 2015-2016; internal report prepared for the Ontario Geological Survey, Jack Satterly Geochronology Laboratory, University of Toronto, Toronto, Ontario, 48p.

Kamo, S.L. 2016. Part A: Report on U-Pb ID-TIMS geochronology for the Ontario Geological Survey: Bedrock Mapping Projects, Ontario, Year 1: 2015-2016, internal report prepared for the Ontario Geological Survey; Jack Satterly Geochronology Laboratory, University of Toronto, Toronto, Ontario, 48p.

Kamo, S.L. and Hamilton, M.A. 2017. Part A: Report on U-Pb ID-TIMS geochronology for the Ontario Geological Survey: bedrock mapping projects, Ontario, Year 2: 2016-2017; internal report prepared for the Ontario Geological Survey, Jack Satterly Geochronology Laboratory, University of Toronto, Toronto, Ontario, 72p.

Kamo, S.L. and Hamilton, M.A. 2018. Part A: Report on U-Pb ID-TIMS geochronology for the Ontario Geological Survey: Bedrock Mapping Projects, Ontario, Year 3: 2017-2018, internal report for the Ontario Geological

Survey; Jack Satterly Geochronology Laboratory, University of Toronto, Toronto, Ontario, 44p.

Le Maitre, R.W. 1989. A classification of igneous rocks and glossary of terms; Blackwell Scientific Publications, Oxford, United Kingdom, 193p.

Liikane, D.A., Bleeker, W., Hamilton, M., Kamo, S., Smith, J., Hollings, P., Cundari, R. and Easton, M. 2018. Controls on the localization and timing of mineralized intrusions within the ca. 1.1 Ga Midcontinent Rift system; 64th Institute on Lake Superior Geology, Proceedings, v.64, pt.1, p.65-66.

Magnus, S.J. 2017a. Precambrian geology of Tuuri and Walsh townships, northwestern Ontario; Ontario Geological Survey, Preliminary Map P.3812, scale 1:20 000.

Magnus, S.J. 2017b. Geology and mineral potential of Syine Township, western Schreiber–Hemlo greenstone belt; in Summary of Field Work and Other Activities, 2017, Ontario Geological Survey, Open File Report 6333, p.11-1 to 11-8.

Magnus, S.J. 2019. Precambrian geology, Syine township; Ontario Geological Survey, Preliminary Map P.3826, scale 1:20 000.

Magnus, S.J. and Arnold, K.A. 2016. Geology and mineral potential of the western Schreiber–Hemlo greenstone belt; in Summary of Field Work and Other Activities, 2016, Ontario Geological Survey, Open File Report 6323, p.11-1 to 11-7.

Magnus, S.J. and Walker, J. 2015. Geology and mineral potential of Walsh, Tuuri and Syine townships, Schreiber–Hemlo greenstone belt; in Summary of Field Work and Other Activities, 2015, Ontario Geological Survey, Open File Report 6313, p.14-1 to 14-12.

Magnus, S.J. and Hastie, E.C.G. 2018. Geology and Mineral Potential of Priske and Strey Townships, western Schreiber–Hemlo greenstone belt; in Summary of Field Work and Other Activities, 2018, Ontario Geological Survey, Open File Report 6350, p.10-1 to 10-10.

Marmont, S. 1984. The Terrace Bay Batholith and associated mineralization; Ontario Geological Survey, Open File Report 5514, 95p.

Miller, J.D., and Nicholson, S.W., 2013, Geology and mineral deposits of the Midcontinent Rift—An overview, in Field Guide to the Cu-Ni-PGE Deposits of the Lake Superior Region; Precambrian Research Center Guidebook Series 13-1, University of Minnesota Press.

Muir, T.L. 2003. Structural evolution of the Hemlo greenstone belt in the vicinity of the world-class Hemlo gold deposit; Canadian Journal of Earth Sciences, v.40, p.395-430.

Norris, D. 2012. Current archaeological investigations in Ontario: The discovery of and preliminary information regarding several Paleoindian sites east of Thunder Bay; The Minnesota Archaeologist, v.71, p.45-59.

Ojakangas, R.W., Morey, G.B. and Southwick, D.L. 2001. Paleoproterozoic basin development and sedimentation in the Lake Superior region, North America; Sedimentary Geology, v.141-142, p.319-341.

Ontario Geological Survey 2011. 1:250 000 scale bedrock geology of Ontario; Ontario Geological Survey, Miscellaneous Release---Data 126-Revision 1. ISBN 978-1-4435-5704-7 (CD) ISBN 978- 1-4435-5705-4 [zip file]

Osmani, I.A. and Stott, G.M. 1988. Regional-scale shear zones in Sachigo Subprovince and their economic significance; in Summary of Field Work and Other Activities 1988, Ontario Geological Survey, Miscellaneous Paper 141, p.53-67.

Pettijohn, F.J. 1975. Sedimentary Rocks, 2nd ed.; Harper and Row Publishers, New York, 628 p.

Pleger, T.C. 2000. Old copper and red ocher social complexity; Midcontinental Journal of Archaeology, v.25, p.169-190.

Rogala, B., Fralick, P.W. and Metsaranta, R. 2005. Stratigraphy and sedimentology of the Mesoproterozoic Sibley Group and related igneous intrusions, northwestern Ontario: Lake Nipigon Region Geoscience Initiative; Ontario Geological Survey, Open File Report 6174, 128p.

Rukhlov, A.S. and Bell, L. 2010. Geochronology of carbonatites from the Canadian and Baltic shields, and the Canadian Cordillera: clues to mantle evolution; Mineralogy and Petrology, v.98, p.11-54.

Schmid, R. 1981. Descriptive nomenclature and classification of pyroclastic deposits and fragments: recommendations of the IUGS Subcommission on the systematics of igneous rocks; Geology, v.9, p.41-43.

Schnieders, B.R., Smyk, M.C., Speed, A.A. and McKay, D.B. 1996. Mineral occurrences in the Nipigon-Marathon Area, Volumes 1 and 2; Ontario Geological Survey, Open File Report 5951, 912p.

Smyk, M.C. and Schnieders, B.R. 1995. Geology of the Schreiber greenstone assemblage and its gold and base metal mineralization; 41st Institute on Lake Superior Geology, Proceedings, Part 2c, field trip guidebook, 77p.

Snake, S., Coatsworth, E.S., Coatsworth, D. and Kaggie, F. 1991, The adventures of Nanabush, Ojibway Indian stories; 2nd edition, Doubleday Canada, Toronto, Ontario.

Stott, G.M., Corkery, M.T., Percival, J.A., Simard, M. and Goutier, J. 2010. A revised terrane subdivision of the Superior Province; in Summary of Field Work and Other Activities, 2010, Ontario Geological Survey, Open File Report 6260, p.20-1 to 20-10.

Sun, S-S. and McDonough, W F. 1989. Chemical and isotopic systematics of oceanic basalts: Implications for mantle compositions and processes; in Magmatism in ocean basins: Geological Society of London, Special Publication 42, p.313-345.

Tóth, Z. 2018. The geology of the Beardmore-Geraldton belt, Ontario, Canada: geochronology, tectonic evolution and gold mineralization; unpublished PhD thesis, Laurentian University, Sudbury, Ontario, 276p.

Tóth, Z. and Lafrance, B. 2018. Preliminary results from the assessment of the structural evolution of the southern Geraldton–Onaman transect; in Summary of Field Work and Other Activities, 2018, Ontario Geological Survey, Open File Report 6350, p.32-1 to 32-8.

Toth, Z., Lafrance, B., Dube, B., McNicoll, V.J., Mercier-Langevin, P., and Creaser, R.A. 2015. Banded iron formation-hosted gold mineralization in the Geraldton area, northwestern Ontario: Structural setting, mineralogical characteristics, and geochronology, In: Targeted Geoscience Initiative 4: Contributions to the Understanding of Precambrian Lode Gold Deposits and Implications for Exploration; Geological Survey of Canada, Open File 7852, p. 85–97.

Wacey, D., McLoughlin, N., Kilburn, M.R., Saunders, M., Cliff, J.B., Kong, C., Barley, M.E. and Brasier, M.D. 2013. Nanoscale analysis of pyritized microfossils reveals differential heterotrophic consumption in the ~1.9-Ga Gunflint chert; Proceedings of the National Academy of Sciences of the United States of America, v.110, no.20, p.8020-8024.

Whitmeyer, S.J. and Karlstrom, K.E. 2007. Tectonic model for the Proterozoic growth of North America; Geosphere, v.3, no.4, p.220-259.

Williams, H.R. 1989. Geological studies of the Wabigoon, Quetico and Abitibi–Wawa subprovinces, Superior Province of Ontario, with emphasis on the structural development of the Beardmore–Geraldton belt; Ontario Geological Survey, Open File Report 5724, 189p.

Wu, F-Y, Mitchell, R.H., Li, Q-L, Zhang, C. and Yang, Y-H. 2017. Emplacement age and isotopic composition of the Prairie Lake carbonatite complex, northwestern Ontario, Canada; Geological Magazine, v.154, no.2, p.217-236.

Zaleski, E., van Breemen, O. and Peterson, V.L. 1999. Geological evolution of the Manitouwadge greenstone belt and Wawa-Quetico subprovince boundary, Superior Province, Ontario, constrained by U-Pb zircon dates of supracrustal and plutonic rocks; Canadian Journal of Earth Sciences, v.36, p.945-966.

Appendix 1. Geochemical data for typical samples of the major rock types in the western Schreiber–Hemlo greenstone belt. All analyses were performed at the OGS Geoscience Laboratories, Sudbury. Complete data are available in Magnus (2017) (Tuuri and Walsh townships), Magnus (2019) (Syine township) and in upcoming Miscellaneous Release—Data reports for Priske and Strey townships.

Sample Number	**17SJM013C**	**17SJM013C**	**17SJM013C**	**15SJM068A**	**15SJM068A**	**16SJM157A**	**17SJM082C**	**15SJM204B**
Related Stop	Stop 2	Stop 2	Stop 2	S&S Stop 2A	S&S Stop 2A	near Stop 2	none	S&S Stop 2B
Rock Name	mafic volcanic rock	mafic volcanic rock	mafic volcanic rock	mafic volcanic rock	mafic volcanic rock	melanogabbro	mafic volcanic rock	mafic volcanic rock
Formation	Package B	Package B	Package B	Package B	Package B	Package B	Package C	Package B
Volcanic Setting	back arc volcanic	back arc volcanic	back arc volcanic	back arc volcanic	back arc volcanic	back arc volcanic	plateau volcanic	plateau volcanic
Easting (m)	505364	505364	505364	506861	506861	506123	501620	506190
Northing (m)	5402267	5402267	5402267	5402734	5402734	5402406	5412183	5403315
Notes	base of flow	middle of flow	top of flow	"spinifex" texture	base of flow	n/a	thorium-enriched	trachytic texture
TAS rock name	basalt	basalt	basaltic andesite	basalt	basalt	picro-basalt	basalt	basalt
Tectonic Setting	back arc basin	back arc basin	back arc basin	back arc basin	back arc basin	back arc basin	continental arc	continental arc
SiO_2 (wt %)	48.67	50.07	52.7	49.56	46.17	36.97	47.89	45.45
TiO_2	0.9	1.02	1.05	0.66	0.34	0.22	2.18	1.93
Al_2O_3	12.32	14.05	14.21	12.08	6.2	4.43	15.36	14.76
Cr_2O_3	0.078	0.044	0.054	0.08	0.31	0.58	0.008	0.02
$Fe_2O_3^{total}$	12.99	12.44	11.28	12.07	11.66	10.62	14.57	13.13
MnO	0.194	0.199	0.213	0.173	0.137	0.175	0.242	0.339
MgO	11.08	8.11	6.01	11.06	24.23	26.37	2.54	3.08
CaO	10.036	8.439	9.481	9.384	5.055	6.66	12.959	8.382
Na_2O	0.93	1.02	2.37	1.93	0.02	<0.02	0.42	2.9
K_2O	0.23	2.59	0.27	0.08	0.01	0.03	1.19	0.73
P_2O_5	0.099	0.109	0.118	0.047	0.027	0.018	0.356	0.372
LOI	3.41	2.99	2.98	2.99	6.02	14.12	1.73	9.1
Total	100.95	101.11	100.75	100.12	100.18	100.19	99.47	100.2
Mg Number	0.82	0.78	0.74	0.83	0.92	0.93	0.49	0.56
Th (ppm)	0.382	0.424	0.436	0.212	0.097	0.062	1.151	0.765
Nb	3.098	3.47	3.706	1.29	0.597	0.478	8.719	9.274
Ta	0.205	0.23	0.236	0.071	0.033	0.024	0.562	0.528
Ti	5267	5972	6139	4028	1952	1326	12625	11341
Zr	73	80	85	42	22	14	172	142
La/Lu_{CI}	1.08	1.07	1.07	1.05	1.08	0.98	2.53	3.65
Total REE	44.06	49.17	52.90	25.42	10.89	8.57	112.25	108.66

Notes: *"Formation" refers to the depositional package, pluton or dike swarm that the sample is related to;*
"Volcanic Setting" refers to the volcanic environment inferred using different geochemical and geological parameters;
"Tectonic Setting" refers to the inferred tectonic setting of mafic rocks, based on Cabanis and Lecolle (1989);
"TAS Rock Name" refers to the rock name based on the Total Alkalis versus Silica diagram from Le Maitre (1989);
Major element oxides are in weight %; trace element data are in parts per million;
Mg number = atomic Mg/Mg + Fe, where Fe = total Fe expressed as ferrous iron; this value is dimensionless
La/Lu_{CI} includes elements normalized using values from Sun & McDonough (1995); this value is dimensionless
Abbreviations: LOI = loss-on-ignition; n/a = not applicable; REE = rare earth elements; S&S = Smyk and Schnieders (1995); TAS = Total Alkalis versus Silica;

Appendix 1, *continued*

Sample Number	**17SJM016B**	**17SJM016A**	**16SJM213A**	**16WM043A**	**17SJM129C**	**17SJM168B**	**16WM027A**
Related Stop	Stop 8	Stop 8	none	none	none	none	like Stop 2
Rock Name	mafic volcanic rock	mafic volcanic rock	lapilli tuff	crystal tuff	tuffaceous conglomerate	tuff	wacke
Formation	Package A	Package A	Package A	Package A	B-C Disconformity	B-C Disconformity	Package D
Volcanic Setting	arc volcanic	arc volcanic	arc volcanic	arc volcanic	arc volcanic	arc volcanic	n/a
Easting (m)	478600	478600	512241	514731	498541	499867	513955
Northing (m)	5404609	5404609	5409187	5408709	5402882	5412118	5411351
Notes	pillow core, Flow XI	base of flow, Flow XII		quartz and feldspar phenocrysts	clasts up to 5cm	with interbedded chert	n/a
TAS Rock Name	basaltic andesite	andesite	dacite	rhyolite	dacite	dacite	dacite
Tectonic Setting	transitional arc	calc-alkaline	calc-alkaline	calc-alkaline	calc-alkaline	calc-alkaline	calc-alkaline
SiO_2 (wt %)	54.7	58.89	70.26	76.1	69.22	64.6	63.96
TiO_2	1.32	0.74	0.47	0.1	0.56	0.49	0.57
Al_2O_3	15.92	15.16	14.66	12.05	13.14	12.35	15.92
Cr_2O_3	0.027	0.022	<0.002	0.01	0.009	0.024	0.03
$Fe_2O_3^{total}$	11.85	6.44	3.75	1.35	3.61	5.66	5.99
MnO	0.11	0.084	0.052	0.047	0.034	0.17	0.094
MgO	3.31	4.53	1	0.11	4.04	3.55	3.14
CaO	2.651	5.437	3.518	0.502	2.99	6.886	3.511
Na_2O	2.38	3.63	4.27	0.45	2.82	2.19	4.03
K_2O	1.84	0.51	1.35	8.99	0.61	1.09	1.79
P_2O_5	0.12	0.174	0.113	0.017	0.145	0.108	0.179
LOI	5.62	5.33	1.28	0.85	2.23	2.35	1.04
Total	99.86	100.98	100.76	100.64	99.42	99.5	100.28
Mg Number	0.60	0.79	0.59	0.31	0.86	0.77	0.74
Th (ppm)	0.559	2.941	3.728	5.249	1.816	1.764	9.035
Nb	3.969	6.999	6.471	9.436	4.74	3.572	7.056
Ta	0.251	0.468	0.603	0.918	0.335	0.275	0.471
Ti	6481	5823	2781	563	3209	2842	3462
Zr	86	175	187	167	133	86	158
La/Lu_{CI}	3.29	13.81	6.25	5.12	6.33	9.55	19.71
Total REE	61.83	163.67	101.45	124.07	80.13	58.96	181.12

Notes: *"Formation" refers to the depositional package, pluton or dike swarm that the sample is related to;*
"Volcanic Setting" refers to the volcanic environment inferred using different geochemical and geological parameters;
"Tectonic Setting" refers to the inferred tectonic setting of mafic rocks, based on Cabanis and Lecolle (1989);
"TAS Rock Name" refers to the rock name based on the Total Alkalis versus Silica diagram from Le Maitre (1989);
Major element oxides are in weight %; trace element data are in parts per million;
Mg number = atomic Mg/Mg + Fe, where Fe = total Fe expressed as ferrous iron; this value is dimensionless
La/Lu_{CI} includes elements normalized using values from Sun & McDonough (1995); this value is dimensionless
Abbreviations: LOI = loss-on-ignition; n/a = not applicable; REE = rare earth elements; S&S = Smyk and Schnieders (1995); TAS = Total Alkalis versus Silica;

Appendix 1, *continued*

Sample Number	**17SJM147A**	**17SJM038A**	**15JW094A**	**17KA040A**	**15JW006A**	**16SJM171A**	**17SJM200A**	**17SJM033B**
Related Stop	Stops 4 and 5	none	none	none	none	none	none	none
Rock Name	granodiorite	granodiorite	granite	monzogranite	quartz monzodiorite	tonalite	quartz syenite	porphyritic dike
Formation	Terrace Bay pluton	Crossman Lake batholith	Foxtrap Lake pluton	Santoy Lake pluton	Little Pic River pluton	Steel River pluton	Syenite Lake pluton	porphyritic dikes
Easting (m)	506412	488795	522826	507404	524180	511259	487180	482667
Northing (m)	5410351	5423075	5412786	5412210	5413445	5405636	5415617	5405457
TAS rocktype	dacite	dacite	rhyolite	rhyolite	trachy-andesite	dacite	trachy-dacite	dacite
SiO_2 (wt %)	64.15	69.74	71.6	70.18	61.77	64.34	67.92	67.67
TiO_2	0.44	0.36	0.18	0.28	0.58	0.53	0.25	0.25
Al_2O_3	15.19	15.19	16.04	14.99	17.36	14.05	15.82	14.87
Cr_2O_3	0.017	0.006	<0.002	0.004	<0.002	0.02	0.006	0.022
$Fe_2O_3^{total}$	4.04	3.56	1.37	2	5.1	6.1	2.21	2.73
MnO	0.078	0.062	0.024	0.025	0.086	0.082	0.04	0.042
MgO	3.03	0.98	0.5	0.55	2.17	2.91	1.03	2.49
CaO	3.89	3.282	1.122	1.129	4.113	2.713	2.067	2.937
Na_2O	4.57	4.09	6.31	5.23	4.67	2.84	4.95	5.58
K_2O	2.45	1.52	2.95	4.66	2.86	2.42	4.17	0.89
P_2O_5	0.256	0.13	0.085	0.127	0.292	0.138	0.136	0.099
LOI	1.46	1.19	0.81	0.81	0.72	3.81		3.39
Total	99.7	100.14	101.14	100.08	99.84	100.04	99.3	101.02
Mg Number	0.80	0.60	0.67	0.60	0.70	0.72	0.72	0.83
Th (ppm)	9.668	3.212	5.215	32.841	6.723	7.388	13.741	1.795
Nb	5.497	7.076	3.251	11.59	6.843	5.554	7.084	2.326
Ta	0.378	0.726	0.194	0.683	0.385	0.42	0.612	0.193
Ti	2551	2046	1106	1661	3396	3278	1477	1438
Zr	190	160	94	287	191	144	174	87
La/Lu_{CI}	24.83	5.45	19.80	52.14	23.09	17.57	31.85	17.62
Total REE	244.97	77.55	84.17	270.77	230.87	137.44	185.46	66.37

Notes: *"Formation" refers to the depositional package, pluton or dike swarm that the sample is related to;*
"TAS Rock Name" refers to the rock name based on the Total Alkalis versus Silica diagram from Le Maitre (1989);
Major element oxides are in weight %; trace element data are in parts per million;
Mg number = atomic Mg/Mg + Fe, where Fe = total Fe expressed as ferrous iron; this value is dimensionless
La/Lu_{CI} includes elements normalized using values from Sun & McDonough (1995); this value is dimensionless
Abbreviations: LOI = loss-on-ignition; n/a = not applicable; REE = rare earth elements; S&S = Smyk and Schnieders (1995); TAS = Total Alkalis versus Silica;

Appendix 1, *continued*

Sample Number	**16SJM178D**	**15SJM019B**	**15JW072E**	**16SJM119C**	**15SJM068B**	**17SJM006B**	**16SJM139A**
Related Stop	Stop 1	none	Stops 1 and 4	Stop 4	S&S Stop 2A	none	none
Rock Name	alkalic diabase	alkalic diabase	lamprophyre	subalkalic diabase	subalkalic diabase	subalkalic diabase	subalkalic diabase
Formation	rift-parallel alkalic dikes	rift-parallel alkalic dikes	lamprophyre dikes	Biscotasing	Marathon	Matachewan	Pigeon River
Easting (m)	515772	523556	512213	517970	506861	498906	506570
Northing (m)	5408307	5407664	5405453	5406078	5402734	5412471	5407803
Notes	n/a	trachytic texture	n/a	n/a	n/a	n/a	n/a
TAS rocktype	basalt	trachy-dacite	foidite	basalt	basalt	basalt	basalt
Tectonic Setting	continental arc	continental arc	intercontinental rift	continental arc	calc-alkaline	calc-alkaline	continental arc
SiO_2 (wt %)	46.11	60.78	29.55	49.74	47.65	50.08	48.02
TiO_2	1.19	0.49	4.35	1.22	0.74	1.45	1.93
Al_2O_3	14.54	15.66	3.97	14.77	13.35	13.68	16.04
Cr_2O_3	0.02	<0.002	0.1	0.02	0.11	0.02	0.02
$Fe_2O_3^{total}$	12.77	8.63	15.76	14.04	10.82	14.92	13.86
MnO	0.217	0.234	0.269	0.206	0.171	0.19	0.193
MgO	5.51	0.34	15.94	6.4	10.47	6.9	6.04
CaO	10.656	1.814	13.069	10.428	11.079	8.774	9.742
Na_2O	3.22	6.41	0.1	2.27	1.71	2.81	2.75
K_2O	1.53	4.82	2.35	0.4	0.31	0.39	0.48
P_2O_5	1.099	0.077	0.876	0.118	0.117	0.098	0.214
LOI	2.89	0.82	12.61	0.7	3.33	1.5	0.54
Total	99.92	100.08	99.04	100.32	99.87	100.83	99.86
Mg Number	0.70	0.18	0.85	0.71	0.84	0.72	0.70
Th (ppm)	9.282	56.416	8.508	1.138	0.496	3.17	1.669
Nb	63.339	>277	124.706	4.426	2.866	6.18	11.382
Ta	2.739	14.976	7.901	0.28	0.129	0.435	0.774
Ti	7279	2967	>25000	6976	4623	3630	11126
Zr	180	1041	375	80	62	148	160
La/Lu_{CI}	26.63	19.55	53.01	2.16	4.20	11.19	3.50
Total REE	468.09	923.53	418.37	56.87	62.82	144.04	103.50

Notes: *"Formation" refers to the depositional package, pluton or dike swarm that the sample is related to;*
"Tectonic Setting" refers to the inferred tectonic setting of mafic rocks, based on Cabanis and Lecolle (1989);
"TAS Rock Name" refers to the rock name based on the Total Alkalis versus Silica diagram from Le Maitre (1989);
Major element oxides are in weight %; trace element data are in parts per million;
Mg number = atomic Mg/Mg + Fe, where Fe = total Fe expressed as ferrous iron; this value is dimensionless
La/Lu_{CI} includes elements normalized using values from Sun & McDonough (1995); this value is dimensionless
Abbreviations: LOI = loss-on-ignition; n/a = not applicable; REE = rare earth elements; S&S = Smyk and Schnieders (1995); TAS = Total Alkalis versus Silica;

Field trip 4 - Geology of the Nipigon Area

Philip Fralick

Department of Geology, Lakehead University, Thunder Bay, Ontario, P7B 5E1, Canada

and

Robert Cundari

Resident Geologist Program, Ontario Geological Survey, Ministry of Northern Development and Mines, Thunder Bay, Ontario, P7E 6S7, Canada

Introduction

The Nipigon area, west of Terrace Bay, hosts Neoarchean, amphibolite-facies metamorphic and intrusive rocks of the Quetico Subprovince, as well as overlying Mesoproterozoic Sibley Group sedimentary rocks and Midcontinent Rift-related mafic intrusive rocks. This trip buids upon previous ILSG trips, namely Fralick et al. (2000) and Smyk and Kissin (2005). A lot of this guide is taken from them. The field trip begins on Highway 17 just north of Lake Helen focusing on metamorphosed clastic sedimentary rocks, their high-grade metamorphic equivalents and derived granitic rocks of the Quetico Subprovince (Stops 1-6; Fig. 1). The trip continues east of Nipigon highlighting Proterozoic sedimentary rocks of the Sibley Group and intrusive mafic rocks related to the Midcontinent Rift (Stops 7-10; Fig. 1). Many stops, especially Stop 1 through 6, are on road cuts along a narrow section of highway. Please use extreme caution when viewing road side outcrops.

Regional Geology - Quetico Subprovince

The Quetico Subprovince of the Superior Province is situated between the Wabigoon and Wawa volcano-plutonic subprovinces that bound the Quetico on its northern and southern margins, respectively. This east-



Figure 1: Geology of the Nipigon area field trip stop locations.

trending subprovince has a fairly consistent width of 70 km and is composed predominantly of metasedimentary rocks and their migmatitic and anatectic derivatives (Fig. 2; Williams, 1991). In general, the boundaries of the Quetico, whether or not they may be primary and/or tectonic, have been mapped as steeply dipping surfaces across which there is commonly a distinct contrast in lithology. However, LITHOPROBE deep seismic has shown that the Quetico and Beardmore-Geraldton volcanic and sedimentary belts of the Wabigoon Subprovince are thrust over the volcanic rocks of the Onaman-Tashota terrane of the Wabigoon Subprovince at an angle of 12 degrees (Geller, 2012). This agrees well with prior interpretations of the Quetico as an accretionary prism (Devaney and Williams, 1989) and the Beardmore-Geraldton area as its associated forearc basin (Barrett and Fralick, 1989; Fralick et al., 1992) that were thrust northward onto the Wabigoon arc during Wawa arc collision.

An overview of the lithologic, metamorphic, structural and tectonic characteristics of the Quetico Subprovince has most recently been provided by Easton (2000):

"The intensity of metamorphism varies within the subprovince, such that rocks marginal to the subprovince tend to be at lower grade than in the interior. The lowest metamorphic grade is found along the northern boundary with the Wabigoon subprovince (Pirie and Mackasey, 1978). Locally, subgreenschist- to greenschist-facies rocks occur along the southern boundary (Borradaile, 1982), but typically, there is a rapid rise in metamorphic grade north of the Wawa subprovince, especially north of Manitouwadge, where a belt of metasedimentary granulites occurs within the Quetico subprovince close to, and parallel with, the northern margin of the Wawa Subprovince (Coates, 1968; Williams and Breaks, 1989, 1990; Pan et al., 1994). As a result, grade distribution is asymmetrical, with the maximum in temperature and pressure occurring south of the central Quetico, locally coincident with the southern margin."

In contrast, Seemayer (1992) also described an asymmetric metamorphic grade distribution that had metamorphic grade increasing from south to north across the Quetico, southwest of Lake Nipigon. The southern margin was characterized by greenschist-facies rocks, the central portions were at amphibolite facies and the northern margin displayed an abrupt decrease in grade

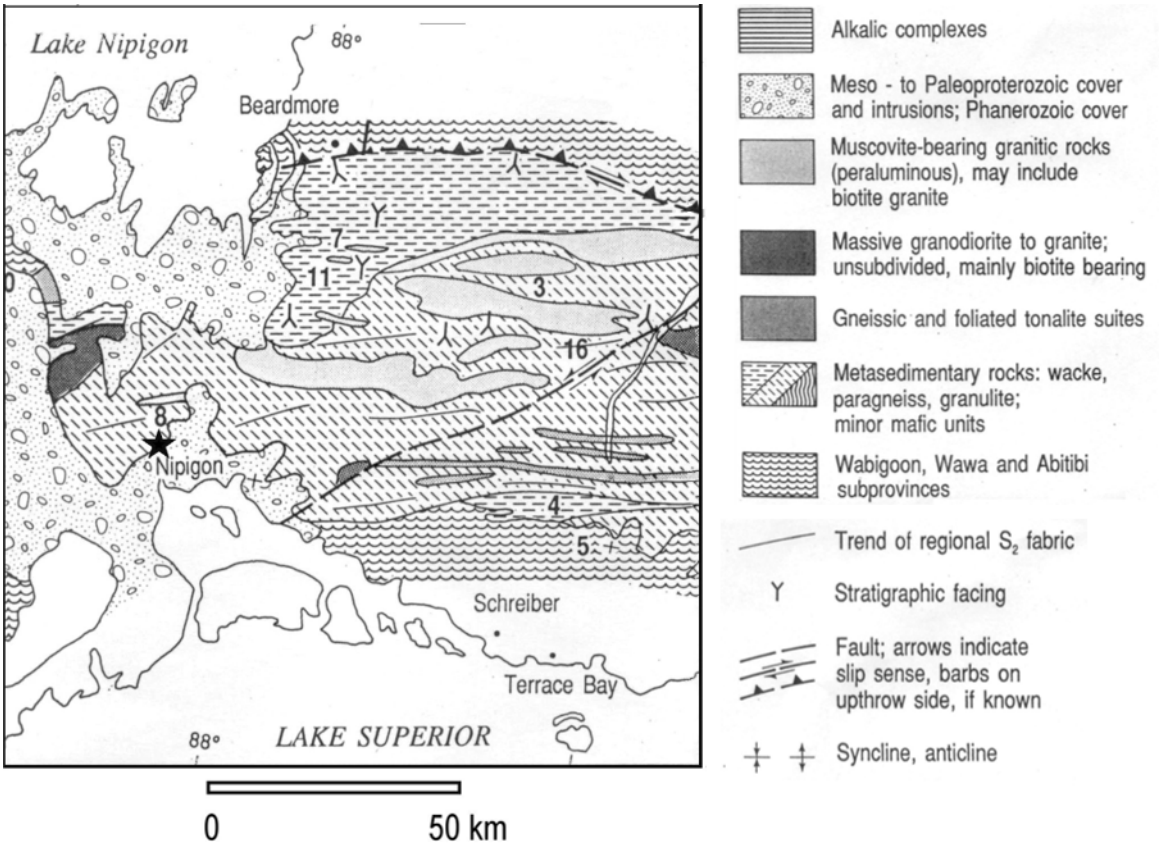


Figure 2. Generalized regional geology of the Quetico Subprovince (after Williams, 1991).

adjacent to the Wabigoon Subprovince to the north. The Quetico Fault, which is normally situated at the northern margin of the Quetico in this western area, lies well within the Quetico southwest of Lake Nipigon (Seemayer, 1992). Seemayer (1992) determined temperatures based on garnet-biotite thermometry ranging from 526°C at the southern margin of the Quetico Subprovince, increasing asymmetrically to a maximum of 714°C, then falling sharply at the northern margin to 517°C. Pressure calculated at near peak temperature was 5 ± 1.5 kbar.

Easton (2000) described the regional metamorphic conditions and metamorphic history:

"P–T conditions increase from west to east, for example, 500ºC and 2.5 kbar at the Minnesota border west of Thunder Bay (Percival, 1989), to 700–780ºC and 5.4–6.1 kbar adjacent to the Kapuskasing structural zone (Percival and McGrath, 1986; Percival, 1989). Typical conditions in the central region are on the order of 620ºC and 3.3 kbar (Percival, 1989). Granulites north of Manitouwadge yield 680–770ºC and 4.4–6.4 kbar (Pan et al., 1994; Percival, 1989). The regional variation in P–T can be ascribed to a relatively shallow level of erosion in the west (<10 km) and a deeper level in the east (>12 km) (Percival et al., 1985). Rocks located east of the Kapuskasing structural zone are believed to be generally at upper-amphibolite-facies conditions (Williams, 1991)."

"Evidence for an earlier, medium-pressure, low-temperature, pre-tectonic or early syntectonic metamorphism comes from four areas within the subprovince. In the Atikokan region, and in northern Minnesota, both at the northern margin of the Quetico subprovince, an early M1 metamorphic peak between D1 and D2 produced Ky–St–Bt assemblages (Ayres, 1978; Tabor et al., 1989). Kyanite inclusions in plagioclase within Grt–Sil–Bt–Pl–Qtz schist near Raith, north of Thunder Bay, have been reported by Percival et al. (1985). Kehlenbeck (1976) also presented textural evidence for a polymetamorphic history along the northern margin of the Quetico subprovince north of Thunder Bay. Again, along the northern margin of the subprovince, in the Beardmore–Geraldton area (Williams, 1989), amphibolite-facies conditions were attained prior to D2 deformation, with the distribution of facies being structurally controlled within thrust-bounded panels (Williams, 1991)."

"In contrast, the main phase of regional metamorphism (M2), which produced the observed map-pattern (Fig. 2), occurred late syntectonically (Sawyer, 1983; Williams, 1991). The general sequence of isograds, based on the appearance of diagnostic assemblages in pelites, is Chl–Ms–Bt, Grt+And+Sil, Grt+Crd+Sil, in situ granitic leucosome, and Opx (Pirie and Mackasey,1978; Percival and Stern, 1984). The common occurrence of Grt–And in metapelites in the western Quetico subprovince is diagnostic of bathozone 2 (<3.4 kbar; Carmichael, 1978), whereas the presence of Sil–St in the eastern Quetico is diagnostic of bathozones 3 and 4 (3.4–5.5 kbar)."

"As noted by Williams (1991), tectonic thickening of the sedimentary pile and intrusion of minor I-type granitic rocks occurred prior to the thermal acme. Most of the large pre- to syntectonic granitic bodies are peraluminous and have sedimentary sources but display little evidence of thermal contact metamorphism; one exception is the South Beatty Lake pluton in the northern Quetico subprovince (Pirie & Mackasey, 1978). Steeply dipping thermal gradients, local increases in temperature around large plutons, and the general association of the highest-grade rocks with abundant generation of leucosome, indicate that the source of heat was a combination of burial, upward magmatic transport, and tectonism."

"In the northern Quetico, M1 metamorphism is estimated to have occurred between 2698 Ma, the maximum age of sedimentation (Davis et al., 1990) and 2688+4 Ma, the age of emplacement of the late syntectonic Blalock pluton (ibid). In the southern Quetico, M1 occurred after 2690 Ma, the maximum age of sedimentation (Zaleski et al., 1999). The timing of M2 metamorphism is less well constrained and may have been protracted. In the Manitouwadge area, (ibid) constrained regional D2 deformation to 2680–2677 Ma and suggested that migmatization in both the northern Wawa and southern Quetico subprovinces occurred after 2679 Ma, broadly coincident with D3 deformation. This inference is consistent with observations elsewhere in

the Quetico that contact aureoles around late plutons, dated at 2671±2 to 2665±2 Ma, as well as late granitic pegmatites dated at 2653±4 Ma, overprint regional metamorphic fabrics (Percival and Sullivan, 1988; Percival, 1989). North of Manitouwadge, Pan et al. (1998) reported a U–Pb zircon age of 2666±1 Ma from a granitic pegmatite concordant with respect to the D3 fabric, and suggested that the regional amphibolite-facies metamorphism occurred between 2671 and 2665 Ma, consistent with the ages cited above. The timing of peak granulite-facies metamorphism north of Manitouwadge appears to be some 15 Ma younger, on the basis of U–Pb zircon ages of 2650± and 2651±3 Ma from a mafic granulite and a tonalitic leucosome, respectively (ibid). Zaleski & van Breemen (1997) reported that titanite ages young with increasing metamorphic grade, ranging from ~2686 Ma in the southern Manitouwadge greenstone belt to ~2640 Ma in the southern Quetico, suggesting that the thermal effects of regional metamorphism may have lasted over ~30 million years, from 2677 to 2640 Ma, in the higher-grade parts of the Wawa and Quetico subprovinces. On the basis of their regional geological and geochronological studies, Zaleski et al. (1999) concluded that "M2 metamorphism occurred after the tectonic juxtaposition of the Quetico and Wawa subprovinces."

This field trip will cover the southern half of the Quetico Subprovince, from south of Beardmore to Nipigon (Fig. 1). As mentioned above, there is an asymmetric distribution in metamorphic grade, with a gradual progression from greenschist-facies, clastic metasedimentary rocks near the northern contact with the Wabigoon Subprovince; to lower amphibolite-facies schists and gneisses; through to upper amphibolite-facies migmatites and derived granitic rocks near the southern contact with the Wawa Subprovince near Nipigon. Thermal and pressure maximum occurs south of the center of the Quetico. The metamorphic character is of high-temperature/low-pressure (Abukuma-type) metamorphism, associated with the abundant intrusion of granitoid rocks and the regional distribution of migmatites derived from the metasedimentary rocks (Kamineni et al., 1988; Percival and McGrath, 1986; Percival, 1989; Williams, 1989). Peak metamorphic assemblages in the field trip area suggest conditions >650ºC and 5 kbar, corresponding to bathozones 4 to 5 (14 to 15 km deep in the crust; Easton, 2000; Percival, 1989).

The nomenclature of Mehnert (1968) has been used in describing migmatites in this field guide.

Regional Geology - Sibley Group

The Mesoproterozoic, 1.4 Ga, Sibley Group crops out in a ~175 km wide by 400 km long ovoid under Lake Superior extending north to the south and west of Lake Nipigon with a minimum thickness of 950 m inferred from drill core (Rogala et al., 2007). The group is a predominantly flat-lying red-bed sequence which can be broken up into five lithological units; Pass Lake Formation, Rossport Formation, Kama Hill Formation, Outan Island Formation and Nipigon Bay Formation (Fig. 3).

The following is mainly based on research conducted and published on by Becky Rogala and Riku Metsaranta:

The Pass Lake Formation consists of two members; the basal Loon Lake Member conglomerates and the overlying Fork Bay Member sandstones. The basal conglomerates are typically only a few metres thick with a maximum 15 m thickness in topographic lows within the basement rock. Conglomerates of the Loon Lake Member begin the large-scale, thinning-upward succession of the lower portion of the group and are dominantly composed of associated basement material (Rogala et al., 2007). They were deposited in channels eroded into the basement below braided streams in a semi-arid environment as highlighted by dolocrete horizons in floodplain sediment. Lower energy streams deposited trough cross-stratified sandstone. In places these materials were reworked into cobble-pebble beach deposits as a lacustrine system to the south expanded northward. With transgression fining- and thinning-upwards successions of sheet sandstone were deposited offshore from river mouths, while in areas with higher sediment supply deltaic forced regression occurred.

With time the location of the lacustrine system in an area of internal drainage resulted in saline conditions developing. Alternating dolomitic red and light grey thin layers of the Channel Island member, Rossport Formation, attest to cyclic changes in organic productivity leading to more organic material in the bottom sediment reducing the oxidized iron. Higher hematitic clay contents in the red layers may be the

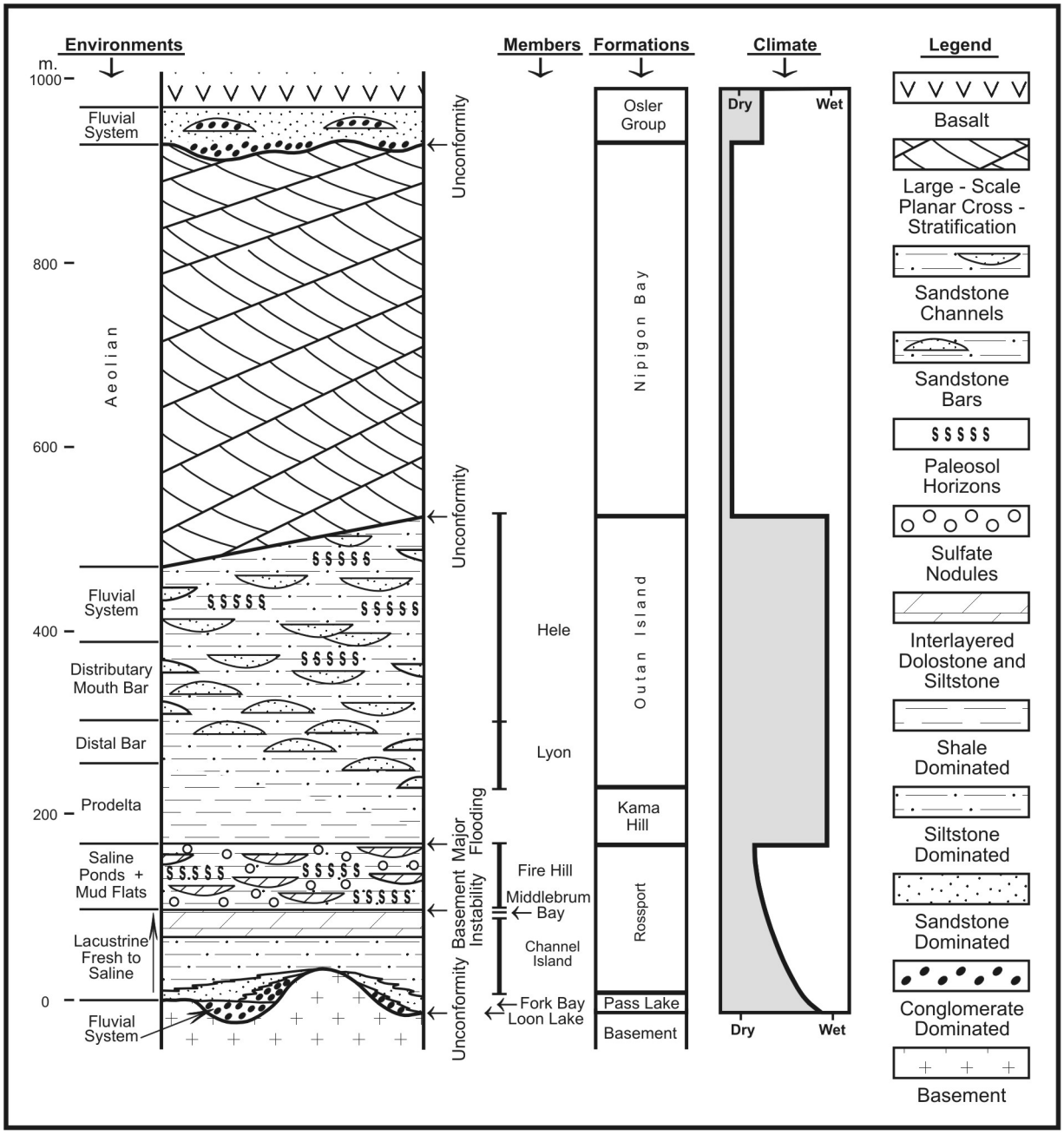


Figure 3. Lithostratigraphy, depositional environments and climate during Sibley Group Sedimentation (from Rogala et al., 2007).

result of sediment water influx leading to more rapid deposition and therefore less organic sediment. Tectonic instability brought this phase of sedimentation to an end by flooding the lacustrine system with sheet sandstone probably derived from the south because of north down-tilting of the terrain (Rogala et al., 2007). Strandline stromatolitic dolomite of the Middlebrun Bay Member was laid down as the lake shrunk. Subaerial exposure caused the development of karst topography, terra rosa and other types of soil horizons on the dolomite. Intrabasin mass flows composed of clasts from underlying Sibley lithologies commonly developed during this time period.

With the end of widespread lacustrine conditions the water table remained close to the surface resulting in the precipitation of gypsum and carbonate in extensive mudflats of the Fire Hill Member, Rossport Formation. Saline ponds with gypsiferous stromatolites and teepee structures developed in lower areas. Higher mudflats were too dry for evaporates to form. This is the end of continuous sedimentation in the lower Sibley Group.

A time gap of unknown extent separates the underlying playa system from overlying deltaic

deposits of the Kama Hill and Outen Island Formations (Rogala et al., 2007). The Kama Hill Formation represents a ~50 m thick wave-rippled and hummocky cross-stratified sandstone and mudstone package which abruptly overlies the upper Fire Hill Member of the Rossport Formation (Rogala et al., 2007). Paleocurrent indicators suggest material comprising the Kama Hill Formation was derived from the south to southeast with the unit being thickest in the central portion and thinning toward the east (Cheadle, 1986). The Kama Hill Formation is dominated by horizontally laminated siltstone and fine-grained sandstones with interbeds of mudstone and ripple-laminated, fine-grained sandstone (Rogala et al., 2007).

It represents prodelta and distal bar deposits. The Outan Island Formation consists of two members; the lower Lyon Member including coarsening- and thickening-upward sandstone successions overlain by siltstone and ripple laminated sandstone and the Hele Member consisting of a fining-and thinning-upward sandstone succession overlain by mud-cracked siltstone (Rogala et al., 2007). The Lyon Member represents coarsening- and thickening-upwards, sandy distributary mouth bars overlain by the Hele Member fluvial system with extensive floodplains deposited in a non-arid climate (Fralick and Zaniewski, 2012; Ielpi et al., 2018). The coarsening upwards delta lobes are on the same scale as the modern Mississippi giving the impression that this was a substantive drainage system.

A slight angular unconformity exists at the top of the Outan Island Formation with the overlying Nipigon Bay Formation. Four hundred and fifty meters of Nipigon Bay sandstones make up half of the Sibley Group. They were deposited sometime between 1.4Ga and 1.1 Ga. This Formation represents large Aeolian dunes developed in an arid setting.

Franklin et al. (1980) originally inferred the Sibley Basin to be a result of subsidence caused from the ~1.1 Ga Midcontinent Rift system. This was called into question with age constraints on the Sibley Group, based on U-Pb geochronology of detrital zircons and stratigraphy, less than 1440 Ma for the entire Sibley Group (Rogala et al., 2007). The basal conglomerate of the Osler Group, erosively overlying the Nipigon Bay Formation, gives a lower age constraint of 1109 Ma (Davis and Sutcliffe, 1985) for the Nipigon Bay, whereas the other formations have a tighter lower limit of 1339±33 Ma derived from diagenetic Sr geochronology (Franklin et al., 1980). Cheadle (1986) noted intercalation of English Bay Complex rhyolites with Sibley sandstones, which together with geochronology, debunks the Sibley Group as being of MCR affinity and lends the notion that the succession was in fact 250-350 m.y. older than the MCR. The current model holds that the Sibley Group was deposited in a half graben-controlled basin (Rogala et al., 2007) inferred to be a product of large-scale thermal subsidence following the ~1550 Ma thermal plume event which produced the English Bay Complex (Hollings et al., 2004).

Regional Geology - Midcontinent Rift

Mesoproterozoic intrusive, volcanic and minor sedimentary rocks associated with the MCR collectively constitute the Keweenawan Supergroup. On the northern margin of the MCR, Keweenawan rocks include a variety of intrusive rocks and Osler Group volcanic rocks, which represent some of the earliest magmatism in the MCR. Ages range from ca. 1140 Ma (Heaman et al., 2007) to ages younger than the magnetic polarity reversal that occurred between 1105 and 1102 Ma (Davis and Green, 1997).

The majority of mafic and ultramafic rocks in the Lake Nipigon and northern Lake Superior areas, including the Nipigon and Logan sills, appear to have been emplaced in a short, magnetically reversed, interval between ca. 1115 and 1100 Ma (Heaman et al., 2007). Emplacement of alkalic intrusions, such as the 1108 Ma Coldwell Complex (Heaman and Machado, 1992), and filling of much of the submerged part of the rift in Lake Superior, also occurred in this period. This was followed by a period of magnetically normal, waning mafic and felsic magmatism, between 1096 and 1085 Ma, that is preserved mainly along the Lake Superior shore by units such as the Crystal Lake (1099±1 Ma), Moss Lake (1095±2 Ma) and Blake (1095±2 Ma) gabbros, and a Pigeon River dyke near Arrow River (1093±3 Ma; Heaman et al., 2007).

Hypabyssal Mafic Rocks

Diabase sills, extending from the vicinity of Thunder Bay to east of Lake Nipigon, represent the northern remnants of the Midcontinent Rift, and have previously been referred to as the Logan sills (Stockwell et al., 1972). However, a geochemical difference has been noted between the sills to the north and south of the City of Thunder Bay (Hart, 2003; Hart et al., 2005). Hollings et al. (2007a) proposed that the

term Logan Igneous Suite, which would fall within the Midcontinent Rift Intrusive Supersuite (Miller et al., 2002), should be applied to all the diabase sills in the area north of Lake Superior, with subdivision into the informal terms, Nipigon sills for the sills north of Thunder Bay, and Logan sills to the south.

Nipigon Sills

Nipigon sills are commonly massive, medium- to coarse-grained, olivine-tholeiitic diabase/gabbros (Sutcliffe, 1989; Hart and MacDonald, 2007). Nipigon sills are dominantly present throughout the Lake Nipigon area but have also been recognized in the Thunder Bay area (Hollings et al., 2007b). Nipigon sills are characterized by a massive, subophitic to ophitic, plagioclase and clinopyroxene texture with trace to 3% olivine and 1-2% modal magnetite (Hart et al., 2005).

Nipigon sills display a reverse magnetic polarity and generally form thick, columnar jointed sheets. Sills commonly intrude Sibley group sedimentary rocks but also can be found in contact with Archean rocks of the Quetico subprovince and the Marmion and Winnipeg River terranes. Sills often intrude earlier emplaced ultramafic units of the Nipigon Embayment as well as the 1129.0 ± 2.3 Ma Pillar lake Volcanic rocks and the 1546.5 ± 3.9 Ma English Bay Complex (Heaman et al., 2007) providing evidence for their emplacement during the second main phase of magmatism (Hart and MacDonald, 2007). The shallow dipping Nipigon diabase sills are estimated to cover an area in excess of 20,000 km^2 (Sutcliffe 1991) ranging in thickness from <5 m to >180 m (Hart and Macdonald, 2007).

Stops

Stop 1 – Glacier Lake Batholith Leucogranite

UTM coordinates 0409911E 5445897N

Large road cuts on both sides of Highway 11 provide excellent exposures of the Glacier Lake Batholith (GLB). At this location, it consists of white, massive to locally foliated, muscovite < biotite, medium- to coarse-grained granite. Localized pods of tourmaline-biotite-muscovite- potassium feldspar pegmatite occur within the granite. These pods may reach 1 m in diameter and locally contain tourmaline-quartz intergrowths. Numerous, curvate, fibrolite-muscovite+tourmaline veins up to 1 cm thick also occur in the host granite. Purple fluorite is exposed on a fractured outcrop face on the west side of the highway (Fig. 4).

Field Trip Road Log

Stop	Locality	km
	Terrace Bay to Nipigon	105 km
Lake Helen stops		
	Intersection of Hwy.'s 11 &17 in the Town of Nipigon	0
	Take Hwy 11 north	
1	Glacier Lake Batholith	17.1
2	Biotite leucogranite	10.8
3	Migmatite - roadside rest area	7.4
	Pull-off area	5.9
4	Pegmatitic granite	5.2
5	Pegmatitic granite	4.85
6	Pegmatites in migmatite	4.6
Nipigon Stops		
	Intersection of Hwy.'s 11 &17 in the Town of Nipigon	0
	Take Hwy 17 east	
7	Stendlund Barite-Amethyst	
8	Ruby Lake	6.8 (4.1 km into site)
O1	Polygonal Diabase	
O2	Migmatites	18.4
9	Kama Hill	21.4
10	Unconformity at Gurney	39.9
O3	Sunrise-Sunset Fluorite	

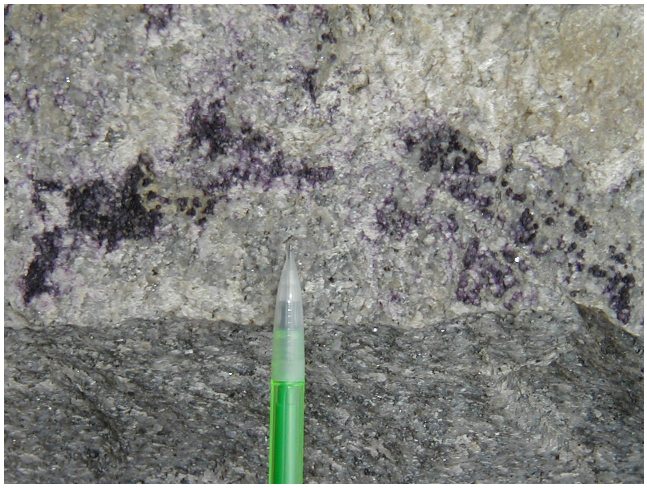


Figure 4. Fluorite on fracture surface in sericite- and fibrolite-bearing Leucogranite (Stop 1).

Stop 2 – Glacier Lake Batholith Leucogranite/ Migmatite

UTM coordinates 0407163E 5440408N

This is another example of the southern margin of the Glacier Lake Batholith where it is in contact with metasedimentary migmatite (Fig. 5). White, biotite-muscovite leucogranite contains rare, blue-green apatite. Foliation is developed in feldspathic segregations and biotitic seams. Leucogranite dykes and migmatite locally exhibit a lit-par-lit structure. Tight to isoclinal folds have developed in the quartz-biotite-feldspar schist (Fig. 6). All rocks display boudinage and folding. Folded leucosome suggests an early and protracted deformation history (Fig. 7). Metasedimentary migmatite enclaves are common in the white, S-type pegmatitic granites along the highway. Note that less evolved S-type granite may contain biotite as the only mica. Narrow diabase dykes cut the country rocks on the western side of the highway.



Figure 5. Contact between folded metasedimentary migmatite and Leucogranite (Stop 2).



Figure 6. Folded metasedimentary migmatite (Stop 2).



Figure 7. Folded metasedimentary schist, incipient leucosome development (Stop 2).

Stop 3 – Migmatite

UTM coordinates 0406986E 5437331N (Rest Area; Coffee)

Migmatites are exposed on the shore and islands of Lake Helen and on a large, glacially streamlined, whaleback outcrop behind the highway rest stop/ pull-off area. There is quite a bit of variation in the relative amounts of leucosome and restite (Fig. 8). Boudinaged and pytgmatically folded leucosome pods and veins occur in a quartzo-feldspathic matrix with narrow, biotitic restite septa.



Figure 8. Lit-par-lit migmatites with large metasedimentary inclusions (schollen) (Stop 3 area).

Stop 4 – Pegmatitic Granite

UTM coordinates - 0407272E 5435208N

This outcrop shows a transition in magmatism from S-type (i.e. Glacier Lake Batholith) to I-type granitoids. Pink, coarse-grained, biotite granite here consists of pink, coarse-grained, perthitic K-feldspar, quartz, coarse-grained biotite, and brown, altered plagioclase (up to 4 cm long). These weakly peraluminous, pegmatitic, biotite granites are relatively primitive and are younger than the white, two mica leucogranites. Such rocks are probably of I-type origin and typically are metasedimentary enclave free. Bulk rock levels of rare-elements are very low: 128 ppm Rb, 2.63 ppm Cs, 1.8 ppm Nb, 0.39 ppm Ta (F. Breaks, OGS, personal communication, 2004). A K-feldspar-megacrystic, pink biotite granite (Fig. 9) with a shallowly east-dipping foliation and metasedimentary xenoliths is intruded by a more massive granite at this locality. The intrusive contact is embayed and scalloped, suggestive of co-mingling magmatic textures (Fig. 10). The megacrystic, foliated granite may represent an earlier, xenolith-bearing phase that was intruded by the massive granite while still relatively warm and plastic.



Figure 9. Pegmatitic K-spar - quartz – biotite granite (Stop 4).

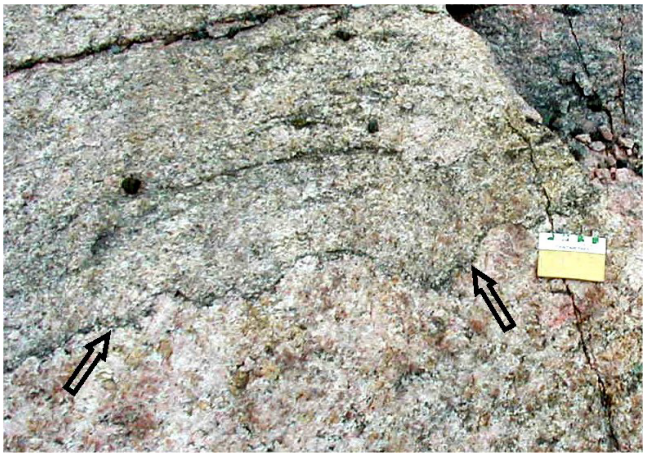


Figure 10. Scalloped contact (arrow) between foliated biotite granite (top) and pegmatitic granite (bottom) (Stop 4).

Stop 5 – Pegmatitic Granite

UTM coordinates - 0407458E 5434906N

A large, bare, whaleback outcrop on the east side of the highway consists of coarse-grained to pegmatitic, massive, homogeneous pink granite (i.e. the younger granitic unit at Stop 4; Fig. 11). Crystals or interstitial patches of quartz, biotite and locally sericitized K-feldspar average 2 to 3 cm in size (Fig. 12). Individual feldspar megacrysts may attain lengths of over 60 cm.

Stop 6 – Pegmatite Dykes in Migmatite

UTM coordinates 0407587E 5434690N

Approximately 200 m south of the massive pink granite, white pegmatite dykes intrude fine-grained



Figure 11. "Whaleback" outcrop of coarse-grained to pegmatitic granite; note large (>60 cm) feldspar megacryst (circled) (Stop 5).

metasedimentary schist. This dark, fine-grained, feldspathic, biotite schist displays a well-developed foliation and minor folds, indicative of a long, protracted ductile deformation history, perhaps coeval with dyke emplacement. Note the sub-horizontal mineral lineation. Flattening of feldspars, producing small-scale, augen structures, is also indicative of high-temperature (>500º C) deformation. The boudinaged and annealed, sericite- and biotite-bearing dykes range from a few centimetres (lit-par-lit structured) to several metres in thickness. They are mineralogically and texturally interesting, containing both cordierite and quartz-tourmaline intergrowths with alkali (locally sericitized) feldspar. Garnet is conspicuous by its absence. Breaks et al. (2003) described potassic, biotite pegmatite that grades into a medium-grained, biotite granite near this stop (UTM: Easting 408339; Northing 5433016). The pegmatite contains coarse, euhedral



Figure 13. Quartz-tourmaline intergrowth in pegmatite dyke (Stop 6).



Figure 12. Coarse-grained to pegmatitic granite (Stop 5).

K-spar; quartz; prismatic, medium- to coarse-grained, black tourmaline (schorl-dravite; Fig. 13); and fine grained, green and blue fluor-apatite (0.3 to 0.9 weight % MnO). A biotite-rich, metasomatic contact occurs between the biotite granite and diabase. Graphic, coarse-grained cordierite (<2 cm) and tourmaline occur in the granite near a diabase contact.

Lunch Stop – Nipigon Marina

UTM coordinates 0408076E 5429202N (Rest Area)

Stop 7 – Stenlund Amethyst- Barite Occurrence

UTM coordinates 0413918E 5429779N

The property is underlain by flat-lying Sibley Group sedimentary rocks of the Lower Rossport Formation. Brick-red to orange muddy dolomite are interbedded with buff-coloured units. Small beige reduction spots occur in the red, hematite-rich dolomites. In contrast to this early reduction of hematite by flecks of organic matter late alteration (reduction of the ferric iron) occurs along the joints. Veins are exposed in two locations, 60 m and 170 m north of Highway 17. At the occurrence nearer the highway, 0.5 to 6.0 cm wide quartz-barite+/-amethyst veins occupy a parallel fracture set apparently controlled by a dominant set at 070°-085° SE. Vein breccias up to 20 cm wide and larger cavities and vugs appear to have developed preferentially in a sandier unit which locally overlies the red dolostone. Brecciated rock fragments are grey and green in some cases, possibly due to the vein alteration. Small, parallel quartz-barite filled fractures and veinlets, also striking 070°, occur 110 m north of the occurrence. Pieces of barite, baritic vein and breccia float are abundant in the vicinity. However, their source was not found. The

flat relief and lack of outcrop necessitates extensive overburden stripping.

Colorless, smoky and amethystine quartz and rare citrine occur with white and pink, bladed to massive barite (Fig. 14). Drusy quartz is commonly associated with barite seams. Lavender to deep purple amethyst crystals with pyramidal terminations are 0.2 to 15 mm across at their bases. Hematite has been reduced to an unspecified mineral.



Figure 14. Drusy white quartz and amethyst with barite (Stop 7).

Stop 8 – Ruby Lake Marble Quarry

UTM coordinates 0414973E 5426071N

Variegated, multicoloured, banded marble has been quarried here for landscaping stone (Fig. 15). Approximately 175 tonnes of marble were quarried and shipped in 1998 (D. MacAlpine, personal communication, 1999). The dimensions of the largest, transported block was 1.8 by 0.75 by 0.50 m (1.8 tonnes; *ibid*). Approximately 398 tonnes of marble were quarried and shipped in 1999 (D. MacAlpine, pers. comm., 2000).

This marble consists of contact metamorphosed, Mesoproterozoic, Rossport Formation dolostone and other, calcareous sedimentary rocks in the contact metamorphic aureole of Midcontinent Rift-related Nipigon diabase sills. It has previously been termed Nipigon River marble and was quarried from 1883 to ca. 1910 at a site on the eastern side of the Nipigon River, approximately 6 km west of the Ruby Lake



Figure 15. Extracted blocks of multicoloured and banded Ruby Lake marble (Stop 8).

quarry (Hinz et al., 1994).

Calcite, dolomite, epidote and opaque minerals were noted in thin section by Hinz et al. (1994) from the Nipigon River quarry. A number of chemical analyses for Nipigon River marble (wt.%) were also provided (Table 1).

Shallow exploration trenches on the side of the road leading to the top of Ruby Mountain (i.e. top of the upper sill) have exposed copper-mineralized marble. Fine-grained, disseminated blebs of native copper (0.1 to 1.0 mm) occur along calcite-coated, hairline fractures parallel to bedding planes. Mineralized fractures are most easily recognized where secondary (supergene) malachite has formed. The top of the adjacent (middle?) sill is exposed farther along the road (optional stop 2).

Similar, copper-mineralized, calcareous units have been noted near a diabase sill contact at Hughes Point, 2.5 km to the south-southwest by Schnieders et al. (1996). At this location, 2 to 5 cm wide calcite veins contain disseminated covellite (after chalcocite?) and malachite. The orientation of the veins are roughly parallel to joints developed in the adjacent sill. Grab samples have returned up to 3.065% Cu, nil Au and nil Ag (*ibid*).

Franklin (1970) described copper-mineralized stromatolitic units near Disraeli Lake. A variety of copper minerals, including digenite, cuprite, covellite,

Table 1. Chemical analyses from the Nipigon River Marble. From Hinz et al. (1994).

Sample	SiO_2	TiO_2	Al_2O_3	Fe_2O_3	FeO	MnO	MgO	CaO	Na_2O	K_2O	P_2O_5
89MCK-09	35.21	0.20	8.20	2.04	1.53	0.05	23.56	26.74	0.00	2.38	0.09
89MCK-10	29.19	0.10	5.20	2.04	0.00	0.03	27.63	35.32	0.00	0.41	0.07

chalcopyrite, native copper and malachite, were identified as open-space fillings in the vuggy host rock (ibid) suggested that the copper was introduced epigenetically from a gabbro to peridotite plug that intruded these Sibley Group rocks. The close spatial association of copper mineralized rocks with diabase sill contacts in the vicinity of Ruby Lake supports this theory. Alternatively these deposits are very similar to those in the Zambian copper belt where organic matter in the stromatolitic mats reduced copper travelling in groundwater forming large syngenetic ores.

The marble is stromatolitic, though this is difficult to ascertain in most places due to the lack of pinnacles. The stromatolites are best seen on the tops of beds where they protrude, causing the contact to become wavy. Hints of the presence of stromatolites are visible, giving the impression that a large amount of the horizontal layering is stromatolitic S-mat (smooth mat that has a crinkly appearance). Non-crinkly, commonly lighter coloured layers interlaminated with the S-mat are storm layers of dolomitic silt washed in by wave activity. This sequence was deposited in a strandline proximal position in the playa, as denoted by the presence of teepee structures in this horizon at other locations and lacustrine deposits below the stromatolites and sub-aerial deposits above. This infers that lake size had stabilized during this interval, eliminating the large-scale fluctuations in shoreline positioning.

Optional Stop 1 – Polygonal Jointed Diabase Sill

UTM coordinates 0414746E 5426684 N

This optional stop is accessed via a steep, rough trail ~500 m northwest from the turnoff to the Ruby Lake Marble quarry to the top of Ruby Mountain. Exposed here is an excellent exposure of the chilled, upper margin of a Nipigon diabase sill. The diabase is massive, homogeneous, fine- to medium-grained and locally feldspar-phyric. The large pavement outcrop displays polygonal cooling joints (seen in plan view) also referred to as "tortoise-shell" texture (Fig. 16).

Optional Stop 2 –Migmatites

UTM coordinates 0425006E 5429614N

This optional stop displays schollen (raft)-structured migmatites in which folded and schlieric, mafic, paleosome xenoliths have been highly deformed and



Figure 16. Polygonal jointed ("Tortoise-shell" texture) diabase (Optional Stop 1).

disrupted (Fig. 17). There is a relatively high proportion of quartzo-feldspathic neosome matrix to the xenoliths, suggesting high(er) degrees of partial melting. Patches and dykelets of coarse-grained, biotite-quartz-feldspar neosome contain garnet, cordierite and large (>10 cm), euhedral green apatite crystals.

Stop 9 – Kama Hill

UTM coordinates 0425272E 5428131N

Diabase-capped Kama Hill provides an excellent roadside exposure of the Rossport Formation (Fig. 18).

The sequence is dominated by interlaminated shaley dolostone and dolomitic red shale with layer thicknesses ranging from millimeters to ten centimeters. There is some cyclicity in layer thickness variation up through the sequence, but it is not a strong trend. Some carbonate-dominated layers contain



Figure 17. Schollen structure in migmatite (Optional Stop 2).

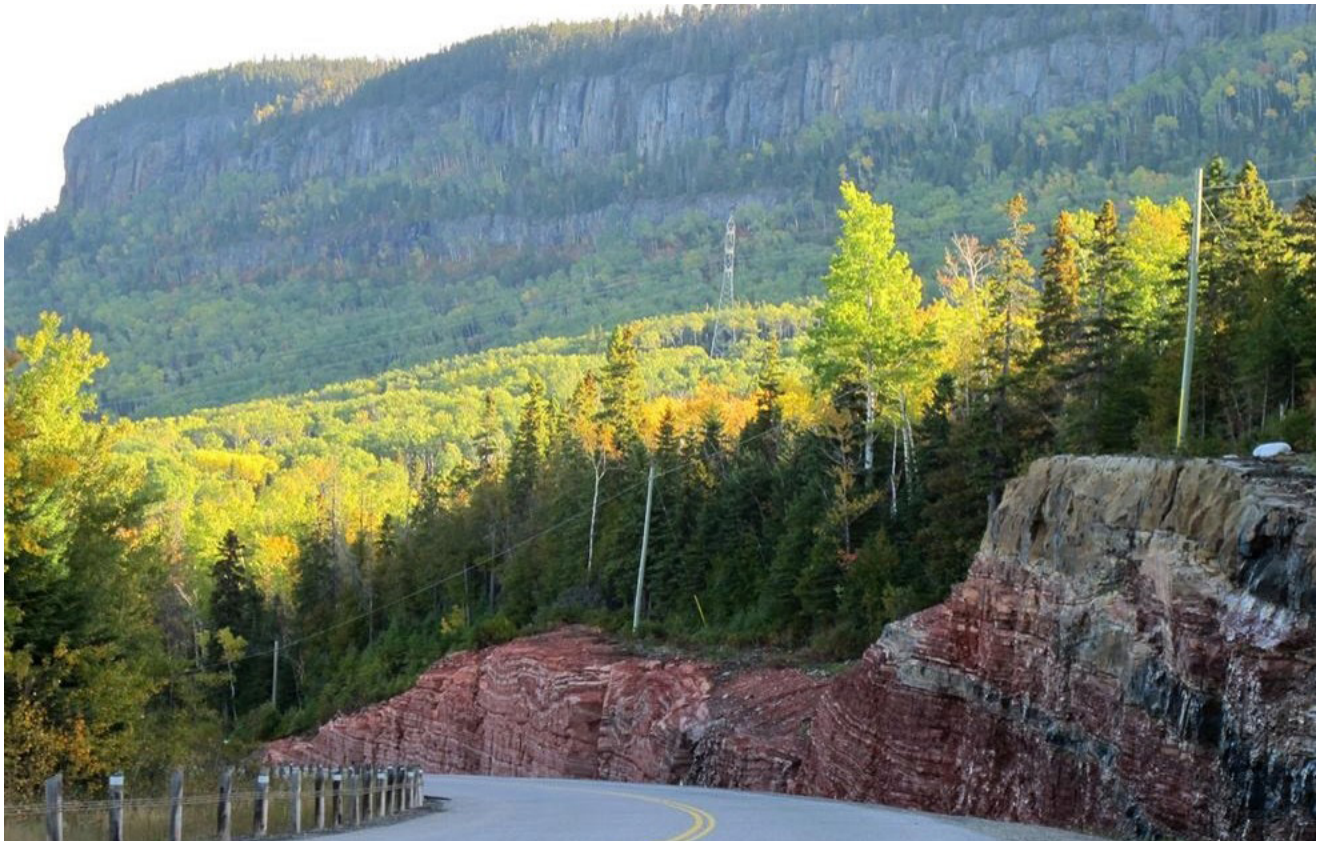


Figure 18. View looking northwest at Kama Hill. Lower outcrop is Rossport Formation. Upper cliff is a Nipigon diabase sill (Stop 9).

coarse- to medium-grained sand grains. Desiccation cracks are present, but not common. The central areas of some thicker more dolomitic (lighter-coloured) layers contain molds where gypsum crystals have weathered out. The alternation between red, more clay-rich layers, and gray, more dolomitic layers, represents climatic fluctuations over large time periods, as secular paleomagnetic trends measured in core of this facies indicates that the average meter of sediment took thousands of years to be deposited (Rogala, 2003). This compares well with modern playa systems and is reasonable as most of the sediment is dolomite formed from precipitation of HCO^{3-}, Ca^{+2} and Mg^{+2} from solution in inflowing water. The lake was not totally drying up so there was always a standing body of saline water for the new fresh water to mix with. This lowering of salinity should have caused dissolution prior to evaporation over time causing more precipitation. See if you can see evidence of this.

During rainy periods, water influx into the lake brought and deposited hematite-rich clays. In dry periods, evaporation from the internal drainage system resulted in lake contraction, hypersalinity and the precipitation of dolomite. This requires a high Mg/Ca ratio in the lake water and may have been the result of the precipitation of gypsum in the central lake. However, this is unlikely as higher salinities are expected in the shallower, marginal areas than the lake center, and thus, gypsum precipitation should be initiated in the shallows, producing shale-gypsum-dolomite triplets. The lack of these means that gypsum precipitation was not necessary to increase the Mg/Ca ratio. The ambient ratio in the lake water itself must have been high enough for the precipitation of dolomite

Synsedimentary deformation manifests itself as small to large slump folds and brecciation of units in places. The sequence is intruded by diabase dykes which bake immediately adjacent sediments. Some evidence has been put forward that the diabase intruded watery sediment, but we have not seen clear indications of this. Structural controls on the emplacement of local sills were suggested by Antonellini and Cambray (1992).

Towards the top of the alternating layers (cyclic facies) thick sandstone sheets start appearing. These are the harbingers of tectonic rotation of the basin causing the basin to switch from northern drainage to southern drainage. Tension is recorded in sandstone

layers developing vertical joints along which they rotate as they extend. The sandstones also represent the dying phases of the lake. Overlying this succession is a chert-carbonate unit (Middlebrun Bay Member; Cheadle, 1986), which locally hosts stromatolites and hydrocarbons. It represents a shoreline microbialite similar to those present in some modern lakes. It is mostly composed of S-mat (crinkly layers) with extensive brecciation and silicification. The silicification is early, probably driven by rotting organic matter creating acidic conditions that favours carbonate replacement by silica. The brecciation is also quite early likely resulting from both dewatering of underlying muds having upward progress impeded by the impermeable microbialites and rainwater causing weakening of the layer through dissolution. A freshwater altered zone can be seen at the top of the dolostone. The siltstones and fine-grained sandstones immediately above the dolostone also contain stromatolites; one of the few places siliciclastic stromatolites can be seen in the rock record.

As the lake shrank sub-aerial mudflats of the upper Rossport Formation were deposited on top of the dolostone. Pieces accessible in a pile of excavated talus display ripple marks, mudcracks and rare raindrop impressions. In many areas these siltstones and mudstones contain abundant gypsum, but it is only present in core as it readily weathers out of outcrops.

Stop 10 – Unconformity at Gurney

UTM coordinates 0440046 E 5419045 N

The basal unconformity between the Sibley Group and underlying granitoids is exposed at this location (Fig. 19). A channel is visible, eroded into basement, and containing matrix-supported conglomerates overlain by cross-stratified sandstones. It represents episodes of subaerial debris flow activity interspersed with normal flash flood runoff.

Archean granitic rocks are altered at the unconformity and likely represent a pre-Sibley weathered regolith. This weathered paleosol, noted by Gill (1926) and Moorhouse (1960), was locally described by Scott (1987). Friable, blotchy, red and green granite hosts quartz-carbonate veins between exfoliation blocks. Feldspars have been hematitized and/or destroyed; ferromagnesian minerals have been chloritized (ibid). Limited sampling of drill core from the Black Sturgeon Lake area cited by Scott (1987) suggests that this



Figure 19. Unconformity between weathered Archean granite and Pass Lake Formation debris flows and sandstones, Highway 17 at Gurney (Stop 10).

alteration may typically involve marked increases in Fe_2O_3, MgO, H_2O) and decreases in Na_2O, CaO and perhaps K_2O. Paleomagnetic data suggest that this weathering was equatorial (G. Borradaille, unpublished data, 1999).

As noted by Franklin (1978), Scott (1987) and Tanton (1948), a number of uranium occurrences are associated with altered Archean granitoids and overlying sedimentary rocks within the Sibley basin, prompting comparisons with the Athabasca basin in Saskatchewan. Favourable local parameters for supergene uranium deposits include: (i) uranium-enriched basement rocks (quartz monzonites, pegmatites); (ii) onlaps of basal Sibley sandstones on Archean paleotopographic "highs"; and (iii) Keweenawan(?) faults that extend to the basement (*ibid*).

Optional Stop 3 – Sunrise-Midday Veins

UTM coordinates 0454557E 5415513N

The Sunrise vein is 18 m wide in the Highway 17 roadcut. It strikes approximately northeast and dips vertically with sharp contacts. Detailed mapping has not been successful in tracing this fluorite-bearing zone along strike. To the northeast, it is covered by alder swamp and glacial till. To the southwest, there is no outcrop along the strike of the vein.

The Midday vein is about 5.8 m wide, strikes 74° and dips 68° northwest. It is located to the west of the Sunrise vein in the same roadcut. It extends into a swampy area to the west and pinches out 61 m east of the road-cut. It has a possible maximum strike length of 305 m.

Both the Sunrise and Midday veins contain barite and fluorite, but very little amethyst. Brecciation in the

Midday vein is not as apparent as in the Sunset vein, although epidotization is very strong, giving the zones a greenish-yellow colour on fresh surfaces. The fluorite and barite occur as narrow veinlets along irregular fractures within these zones. Assay values are erratic due to the irregular nature of the mineralization. One section across the Sunrise vein assays up to 23.11% CaF_2 over 3 m.

References

Antonellini, M.A. and Cambray, F.W. 1992. Relations between sill intrusions and bedding parallel extensional shear zones in the Mid-continent rift system of the Lake Superior region; Tectonophysics, v.212, p.33 1-349

Ayres, L.D. 1978. Metamorphism in the Superior Province of northwestern Ontario and its relationship to crustal development; in Metamorphism in the Canadian Shield, Geological Survey of Canada, Paper 78-10, p.25-36.

Barrett, T.J. and Fralick, P.W., 1989. Turbidites and iron formation, Beardmore-Geraldton Ontario: application of a combined ramp/fan model to Archean clastic and chemical sedimentation. Sedimentology, v. 36, p. 221-234.

Borradaile, G.J. 1982. Comparison of Archean structural styles in two belts of the Canadian Superior Province; Precambrian Research 19, p.179-189.

Breaks, F.W., Selway, J.B. and Tindle, A.G., 2003. Fertile peraluminous granites and related rare-element mineralization in pegmatites, Superior Province, northwest and northeast Ontario: Operation Treasure Hunt; Ontario Geological Survey, Open File Report 6099, 179p.

Carmichael, D.M., 1978. Metamorphic bathozones and bathograds: a measure of the depth of postmetamorphic uplift and erosion on the regional scale; American Journal of Science, 278, p.769-797.

Cheadle, B.A.1986. Alluvial-playa sedimentation in the lower Keweenawan Sibley Group, Thunder Bay District, Ontario; Canadian Journal of Earth Sciences, v.23, p.527-542.

Coates, M.E., 1968. Stevens–Kagiano Lake area; Ontario Department of Mines, Geological Report 68, p.

Davis, D.W. and Sutcliffe, R.M., 1985. U-Pb ages from the Nipigon plate and northern Lake Superior; Geological Society of America Bulletin, v.96, p.1572-1579.

Davis, D.W. and Green, J.C., 1997. Geochronology of the North American Midcontinent rift in western Lake Superior and implications for its geodynamic evolution. Canadian Journal of Earth Sciences, 34: 476-488.

Davis, D.W., Pezzutto, F., & Ojakangas, R.W., 1990. The age and provenance of metasedimentary rocks in the Quetico Subprovince, Ontario, from single zircon analyses: implications for Archean sedimentation and tectonics in the Superior Province; Earth and Planetary Science Letters, v.99, p.195-205.

Devaney, J.R. and Williams, H.R., 1989. Evolution of an Archean subprovince boundary: a sedimentological and structural study of part of the Wabigoon-Quetico boundary in northern Ontario. Canadian Journal of Earth Sciences, v. 26, p. 1013-1026.

Fralick, P. W., Wu, J., and Williams, H.R., 1992. Trench and slope basin deposits in an Archean metasedimentary belt, Superior Province, Canada. Canadian Journal of Earth Sciences, v. 29, p. 2551-2557.

Fralick, P., Smyk, M. and Mailman, M. 2000. Geology and stratigraphy of the Mesoproterozoic Sibley Group; Institute on Lake Superior Geology, 46th Annual Meeting, Thunder Bay, Ontario, Proceedings Volume 46, part 2, Field Trip Guidebook, p.1-41.

Fralick, P.W. and Zaniewski, K., 2012. Sedimentology of a wet pre-vegetation floodplain assemblage. Sedimentology, v. 59, p. 1030-1049.

Hart, T.R. 2003. Keweenawan mafic and ultramafic intrusive rocks of the Lake Nipigon and Crystal Lake areas, northwestern Ontario; 49th Institute on Lake Superior Geology, Proceedings volume 49, Part 1, Programs and abstracts, p.21-22.

Hart, T.R., MacDonald, C.A., Hollings, P., and Richardson, A., 2005. Proterozoic intrusive rocks of the Nipigon Embayment and Midcontinent Rift. In, T.O. Tormanen and T.T Alapieti, 10th International platinum Symposium Extended Abstracts, Geology Survey of Finland, 365-368.

Hart, T.R. and MacDonald, C.A., 2007. Proterozoic and Archean Geology of the Nipigon Embayment: implications for emplacement of the Mesoproterozoic Nipigon diabase sills and mafic to ultramafic intrusions. Canadian Journal of Earth Sciences 44: 1021-1040.

Heaman, L.M., Easton, M., Hart, T.R., Hollings, P., Macdonald, C.A., and Smyk, M., 2007. Further refinement to the timing of Mesoproterozoic magmatism, Lake Nipigon region, Ontario. Canadian Journal of earth Sciences 44: 1055-1086.

Heaman, L.M. and Machado, N., 1992. Timing and origin of midcontinent rift alkaline magmatism, North America: evidence from the Coldwell Complex; Contributions to Mineralogy and Petrology, v. 110, p. 289-303.

Hollings, P.N., Fralick, P.W., and Kissin S.A., 2004. Geochemistry and geodynamic implications of the Mesoproterozoic English Bay granite-rhyolite complex, northwestern Ontario. Canadian Journal of

Earth Sciences, v. 44, p. 389-412.

Hollings, P., Hart, T., Richardson, A., and MacDonald, C.A., 2007a. Geochemistry of the mid-Proterozoic intrusive rocks of the Nipigon Embayement, northwestern Ontario. Canadian Journal of Earth Sciences 44: 1087-1110.

Hollings, P.N., Smyk, M.C., and Hart, T., 2007b. Geochemistry of Midcontinent Rift-related mafic dikes and sills near Thunder Bay: New insights into geographic distribution and the geochemical affinities of Nipigon and Logan sills and Pigeon River and other dikes. 53rd Institute on Lake Superior Geology, Annual Meeting, Proceedings volume 53, Part 1. Lutsen, Minnesota, May 2007, pp. 40–41.

Ielpi, A., Fralick, P.W., Ventra, D., Ghinassi, M., Lebeau, L., Marconato, A., Meek, R., and Rainbird, R.H., 2018. Fluvial floodplains prior to greening of the continents: Stratigraphic record, geodynamic setting, and modern analogs. Sedimentary Geology, v. 372, p. 140-172.

Easton, R.M. 2000. Metamorphism of the Canadian Shield, Ontario, Canada I: The Superior Province; The Canadian Mineralogist, v.38, p.287-317.

Franklin, J.M. 1970. Metallogeny of the Proterozoic rocks of the Thunder Bay District, Ontario; unpublished Ph.D. thesis, The University of Western Ontario, London, 304p

Franklin, J.M. 1978. Uranium mineralization in the Nipigon area, Thunder Bay District, Ontario; in Current Research, Part A, Geological Survey of Canada, Paper 78-lA, p.275-282.

Franklin, J.M., McIlwaine, W., Poulsen, K., and Wanless, R. 1980 Stratigraphy and depositional setting of the Sibley Group, Thunder Bay District, Ontario, Canada. Canadian Journal of Earth Sciences, v. 17, p. 633-650.

Geller, P., 2012. A review of the western Superior Lithoprobe Line 3. Unpublished Honours Thesis, Lakehead University, 45 pp.

Gill, J.E. 1926. Gunflint iron-bearing formation, Ontario; Geological Survey of Canada, Summary Report, 27C, p.28c-88c.

Hinz, P., Landry, R.M., and Gerow, M.C. 1994. Dimension stone occurrences and deposits in northwestern Ontario; Ontario Geological Survey, Open File Report 5890, 191p.

Kamineni, D.C., Stone, D., and Johnston, P.J. 1988. Metamorphism of Quetico sedimentary rocks near Atikokan, Ontario; in Program with abstracts, Geological Association of Canada-Mineralogical Association of Canada-Canadian Society of Petroleum Geologists Annual Meeting, v.13, p.A63.

Kehlenbeck, M.M., 1976. Nature of the Quetico–Wabigoon boundary in the De Courcey – Smiley Lakes area, northwestern Ontario; Canadian Journal of Earth Sciences, v.13, p.737-748.

Mehnert, K.R., 1968. Migmatites and the origin of granitic rocks. Elsevier. 405p.

Miller, J.D., Smyk, M.C., Severson, M.J., Lavigne, M.J., and Middleton, R.S. 2002. PGE occurrences in mafic intrusions around western Lake Superior, USA and Canada; 9th International Platinum Symposium, Field Trip Guidebook, 135p.

Moorhouse, W.W. 1960. The Gunflint iron range in the vicinity of Port Arthur; Ontario Department of Mines, Annual Report, v.69, pt.7, p.1-40.

Pan, Y., Fleet, M.E., and Williams, H.R., 1994. Granulite facies metamorphism in the Quetico subprovince, north of Manitouwadge, Ontario; Canadian Journal of Earth Sciences, v.31, p.1427-1439.

Pan, Y., Fleet, M.E., and Heaman, L.M., 1998. Thermotectonic evolution of an Archean accretionary complex: U–Pb geochronological constraints on granulites from the Quetico subprovince, Ontario, Canada; Precambrian Research, v.92, p.117-128.

Percival, J.A and Stern, R.A., 1984. Geological synthesis in the western Superior Province, Ontario; in Current Research, Part A, Geological Survey of Canada, Paper 84-1A, p.397-407.

Percival, J.A and Sullivan, R.W., 1988. Age constraints on the evolution of the Quetico belt, Superior Province, Ontario; in Radiogenic Age and Isotopic Studies: Report 2, Geological Survey of Canada, Paper 88-2, p.97-108.

Percival, J.A., 1989. A regional perspective of the Quetico metasedimentary belt, Superior Province, Canada; Canadian Journal of Earth Sciences, v.26, p.677-693. Percival, J.A. and McGrath, P.H., 1986. Deep crustal structure and tectonic history of the northern Kapuskasing uplift of Ontario: an integrated petrological-geophysical study; Tectonics, v.5, p.553-572.

Percival, J.A. and McGrath, P.H., 1986. Deep crustal structure and tectonic history of the northern Kapuskasing uplift of Ontario: an integrated petrological-geophysical study; Tectonics, v.5, p.553-572.

Percival, J.A., Stern, R.A., and Digel, M.R., 1985. Regional geological synthesis of western Superior Province, Ontario; in Current Research, Part A, Geological Survey of Canada, Paper 85-1A, p.385-397.

Pirie, J. and Mackasey, W.O., 1978. Preliminary examination of regional metamorphism in parts of the Quetico metasedimentary belt, Superior Province, Ontario; Geological Survey of Canada, Paper 78-10, p.37-48.

Rogala, B., 2003. The Sibley Group: A lithostratigraphic,

geochemical, and paleomagnetic study. Unpublished MSc thesis, Lakehead University, Thunder Bay, 254 pp.

Rogala, B., Fralick, P.W., Heaman, L.M., and Metsaranta, R., 2007. Lithostratigraphy and chemostratigraphy of the Mesoproterozoic Sibley Group, northwestern Ontario, Canada. Canadian Journal of Earth Science 44, 1131-1149.

Sawyer, E.W., 1983. The structural history of a part of the Archean Quetico metasedimentary belt, Superior Province, Canada; Precambrian Research, v.22, p.271-294.

Schnieders, B.R., Smyk, M.C., Speed, A.A., and McKay, D.B. 1996. Mineral occurrences in the Nipigon-Marathon area, Volumes 1 and 2, Ontario Geological Survey, Open File Reports 5951, 912 p.

Scott, J.F. 1987. Uranium occurrences of the Thunder Bay-Nipigon-Marathon area; Ontario Geological Survey, Open File Report 5634, l58p.

Seemayer, B.E., 1992. Variations in metamorphic grade in metapelites in transects across the Quetico Subprovince north of Thunder Bay, Ontario; unpublished M.Sc. thesis, Lakehead University, Thunder Bay, 163p.

Smyk, M.C. and Kissin, S.A. 2005. Geology and rare element pegmatites of the Quetico Subprovince near Nipigon, 51st Institute on Lake Superior Geology, Proceedings volume 51, pt.2d,14p.

Stockwell, C.H., McGlynn, J.C., Emslie, R F., Sanford, B.V., Norris, A.W., Donaldson, J.A., Fahrig, W.F., and Currie K L. 1972. Geology of the Canadian Shield, in Geology and Economic Minerals of Canada, edited by R.J.W. Douglas, Geological Survey of Canada, Economic Geology Report 1, 838 p.

Sutcliffe, R.H. 1989. Mineral variation in Proterozoic diabase sills and dykes at Lake Nipigon, Ontario; Canadian Mineralogist, v.27, p.67-79

Sutcliffe, R.H., 1991. Proterozoic geology of the Lake Superior area. In: Geology of Ontario. Edited by P.C. Thurston, H.R. Williams, R.H. Sutcliffe, and G.M. Stott. Ontario Geological Survey, Special Vol. 4, Part 1, pp. 405–484.

Tabor, J.R., Hudleston, P.J., and Mcloughlin, J., 1989. Metamorphism of the Quetico supracrustals north of the Vermillion granitic complex, northern Minnesota; Geological Association of Canada – Mineralogical Association of Canada, Program with Abstracts, v.14, p.A38.

Tanton, T.L. 1948. Radioactive nodules in sediments of the Sibley series, Nipigon, Ontario; Transactions of the Royal Society of Canada, v. XLII, series III, section IV, p.69-75.

Williams, H.R., 1989. Geological studies in the Wabigoon, Quetico, and Abitibi–Wawa subprovinces, Superior Province of Ontario, with emphasis on the structural development of the Beardmore–Geraldton belt; Ontario Geological Survey, Open File Report 5724p.

Williams, H.R., 1991. Quetico subprovince; in Geology of Ontario, Ontario Geological Survey, Special Volume 4, v.1, p.383-403.

Williams, H.R. and Breaks, F.W., 1989. Geological studies in the Manitouwadge–Hornepayne area; Summary of Field Work and Other Activities 1989, Ontario Geological Survey, Miscellaneous Paper 146, p.79-91.

Williams, H.R. and Breaks, F.W., 1990. Geological studies in the Manitouwadge–Hornepayne area; Summary of Field Work and Other Activities 1990, Ontario Geological Survey, Miscellaneous Paper 151, p.47-51.

Zaleski, E. and van Breemen, O., 1997. Age constraints on plutonism, metamorphism and deformation across the Wawa–Quetico subprovince boundary near the Manitouwadge greenstone belt, northeastern Ontario; Institute on Lake Superior Geology, Program with Abstracts, v.43, p.67-68.

Zaleski, E., van Breemen, O., and Peterson, V.L., 1999. Geological evolution of the Manitouwadge greenstone belt and Wawa–Quetico subprovince boundary, Superior Province, Ontario, constrained by U–Pb zircon dates of supracrustal and plutonic rocks; Canadian Journal of Earth Sciences, v.36, p.945-966.

Field trip 5 - A stratigraphic transect across the Northern flank of the Midcontinent Rift near Rossport

Pete Hollings and Philip Fralick

Department of Geology, Lakehead University, Thunder Bay, Ontario, P7B 5E1, Canada

Safety

As this trip will be taking place on Lake Superior it will be weather dependent and could be cancelled or curtailed at very short notice. Please exercise caution when getting in and out of the boats as the outcrops are often extremely slippery. Life jackets must be worn in the boats at all times. It will probably be very cold out on the lake so please dress warmly.

Introduction

This field guide has been updated from Hollings and Fralick (2005) that was published as part of the 51st ILSG meeting in Nipigon, Ontario. We have updated the regional geology to include some more recent work and modified some stop descriptions to reflect changing lake levels.

Regional geology

Archean granites, outcropping along the shoreline near Rossport, are unconformably overlain by strata of the Gunflint Formation (Fig. 1). These sediments were deposited on a south facing shelf at approximately 1878 Ma (Fralick et al., 2002). The Formation consists of a Lower Member composed of basal stromatolitic bioherms overlain by ankeritic, interclastic grainstones. A regressive, karstified surface caps the northern portion of this assemblage (Fralick and Barrett, 1995) and is succeeded by the Upper Member. It begins with a repetition of the underlying lithologies to which, higher in the succession, are added carbonaceous shales, tuffs and rarely mafic volcanic rocks. These chemical and fine-grained siliciclastic sediments record parasequence development on a storm-dominated shelf (Pufahl and Fralick, 2004) forming the relatively stable portion of a back-arc basin (Kissin and Fralick, 1994; Hemming et al., 1995) prior to compressive northward thrusting of the arc at approximately 1860 to 1835 Ma. As the compression of the Penokean Orogeny waned the sea again transgressed over the area depositing Rove Formation black, carbonaceous shales gradually transitioning upward into turbidites (Morey, 1967). The turbitite fan fed off of a delta prograding to the SSE, with sediment sourced from the rising TransHudson Mountains (Maric and Fralick, 2005). This depositional cycle occurred at 1832 Ma (Kissin et al., 2003; Addison et al., 2005).

The lower portion of the Gunflint Formation in the Rossport area is poorly exposed. Lithologies present in the limited outcrop of the Lower Gunflint are similar to those in the succession comprising the thin, basal Kakabeka Conglomerate and overlying interclastic grainstones present in exposures to the west near Thunder Bay. Good exposure of the Upper Gunflint exists on Quarry Island and consists of possible basaltic flow rocks with associated stromatolites, overlain by a succession of medium- to coarse-grained, graded, sandstone beds. The geochemistry of the sandstones is similar to Archean rocks to the north indicating probable derivation from this source. Black shales, lithically correlative with the Rove Formation, outcrop on an island approximately 5 km to the west. The shales do not overlie the turbidite succession on Quarry Island where arenites of the Sibley Group disconformably rest on an erosion surface at the top of the Gunflint sandstones.

The basal unit of the Sibley Group is the Pass Lake Formation. It is composed of the conglomeratic Loon Lake Member and the overlying sandstones of the Fork Bay Member (Cheadle, 1986). Where the basal conglomerates are present they either represent: 1) large channel fills cutting down into sandstones to shales with abundant caliche zones, or; 2) more laterally continuous conglomerates interbedded and overlain by parallel laminated, medium-grained sandstones. The former represent channel gravels in braided fluvial systems and the latter coarse-grained strandline deposits. The overlying Fork Bay sandstones likewise

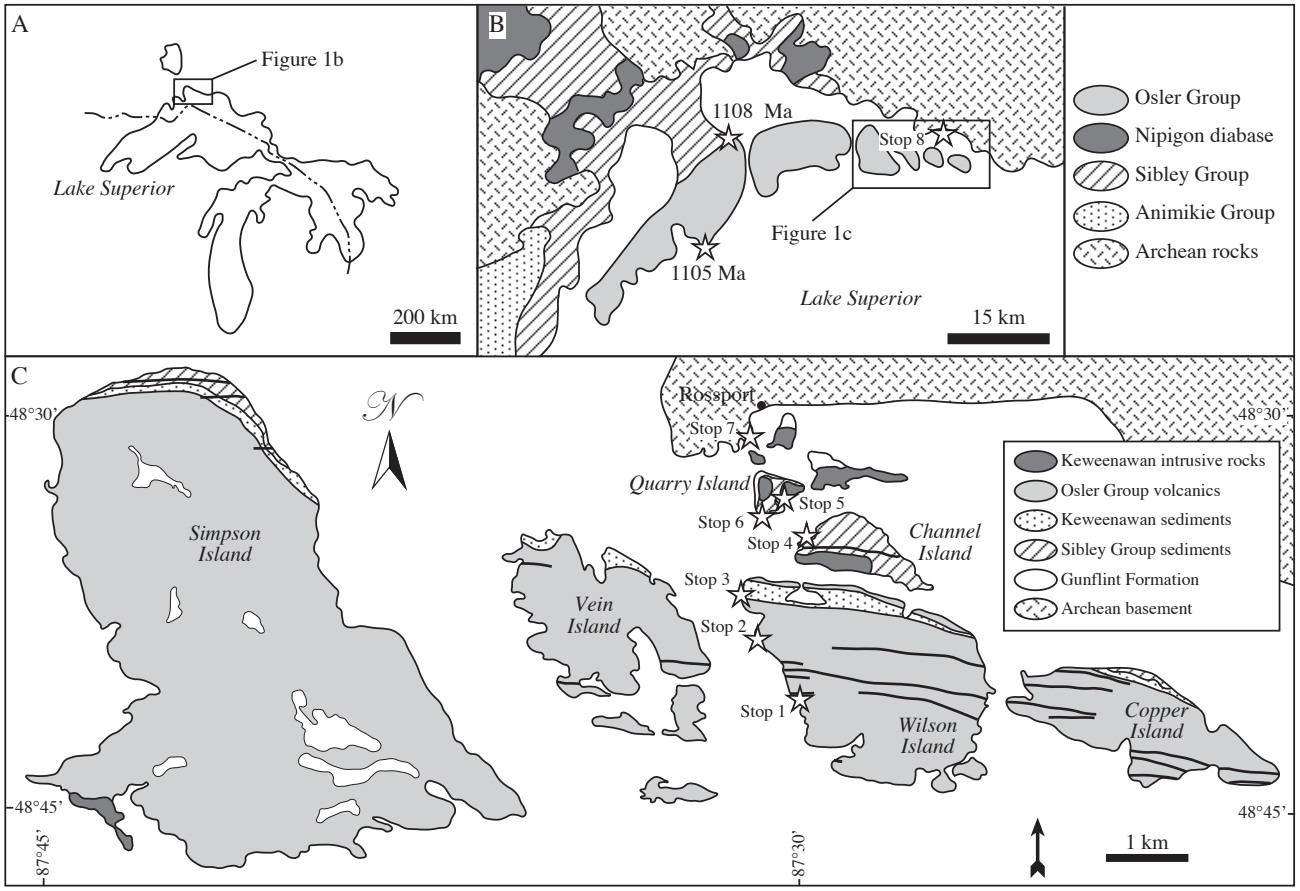


Figure. 1. Map showing the location of the field trip area. B) Regional geology map showing the extent of the Osler Volcanic Group. Age data from Davis and Sutcliffe (1985) and Davis and Green (1997). Modified after Sutcliffe (1986). C) Geological map of the Osler Volcanic Group showing sample locations. Modified after Giguerre (1975).

record both braided fluvial deposition and subaqueous, strand proximal sand-sheet development. In addition to upward thinning and fining successions developed during transgressive systems tract formation, other sandstone assemblages thicken and coarsen upwards representing progradational, delta lobe outbuilding. The delta prograded into a lacustrine setting that isotopes (C, O, S and Sr) indicate became more saline with time (Metsaranta, 2006). This is consistent with Cheadle's (1986) findings and those of Rogala et al. (2007) based on regional paleogeography. The increasing salinity of the water resulted in dolomite, minor gypsum and rarer barite and celestite precipitation mixed with mud deposition. A red and green banding developed in this assemblage due to periodic anoxia of the bottom sediments. The final desiccation of the lacustrine basin is recorded by the development of strandline microbial bioherms (stromatolites) which are overlain by either a terra rosa (red, wind-delivered soil) or subareal, intraformational, mass-flow conglomerates. This is succeeded upwards by mudstones with abundant gypsum nodules representing mudflats formed in an arid climatic setting where hypersaline groundwaters precipitated gypsum. Together all these fine-grained sediments comprise the Rossport Formation. It is overlain by the Kama Hill Formation; a coarsening upwards deltaic succession recording flooding of the basin and development of a more humid climate. The age of the Pass Lake and Rossport Formations can be bracketed between laser ablation MS youngest ages on detrital zircons of 1600 Ma and a Rb-Sr isochron of 1339 Ma (Franklin, 1978). The youngest detrital zircons in the deltaic succession of the Outan Island Formation is 1443±31 Ma.

The Sibley Group is very well exposed along the shorelines of the islands off Rossport. The basal disconformity can be seen about two thirds of the way up the cliff face on the western side of Quarry Island where it overlies graded sandstone beds of the Gunflint Formation. Blocks of medium-grained sandstone were extracted from the cliff face on the island for use in the construction of buildings in Thunder Bay. These

sandstones are medium- and large-scale planar cross-stratified and may represent a sandflat composed of transverse bars in a braided stream or small barchan, eolian dunes. Rare pebbles indicate the former may be the case but this evidence is not conclusive. Channel and Copper Islands contain excellent exposures of the lacustrine rocks with outbuilding of channel systems along the paleolake margins. One of the best outcrops of the strandline stromatolitic carbonates occurs on Channel Island and will be visited during this field trip. On Copper Island the Rossport Formation is overlain disconformably by pebbly, fluvial conglomerates of the basal Osler. Thirty kilometers to the west the uppermost unit of the Sibley, the Nipigon Bay Formation, underlies the same disconformity. This highlights the fact that approximately 600 m of erosive downcutting occurred in the Rossport area before the basal Osler was deposited.

The oldest rift-related rocks on which U-Pb age determinations have been performed lie along the northwestern portion of the rift. These include, from NE to SW, the alkaline intrusive rocks of the Coldwell Complex (1108±1 Ma, Heaman and Machado, 1992), the lower Osler Group volcanic rocks (1108+4/-2 to 1105±2 Ma, Davis and Sutcliffe, 1985; Davis and Green, 1997), the Logan Sills (1109+4/-2 Ma, Davis and Sutcliffe, 1985), the lower portion of the North Shore Volcanics (1108±2 Ma, Davis and Green, 1997), the

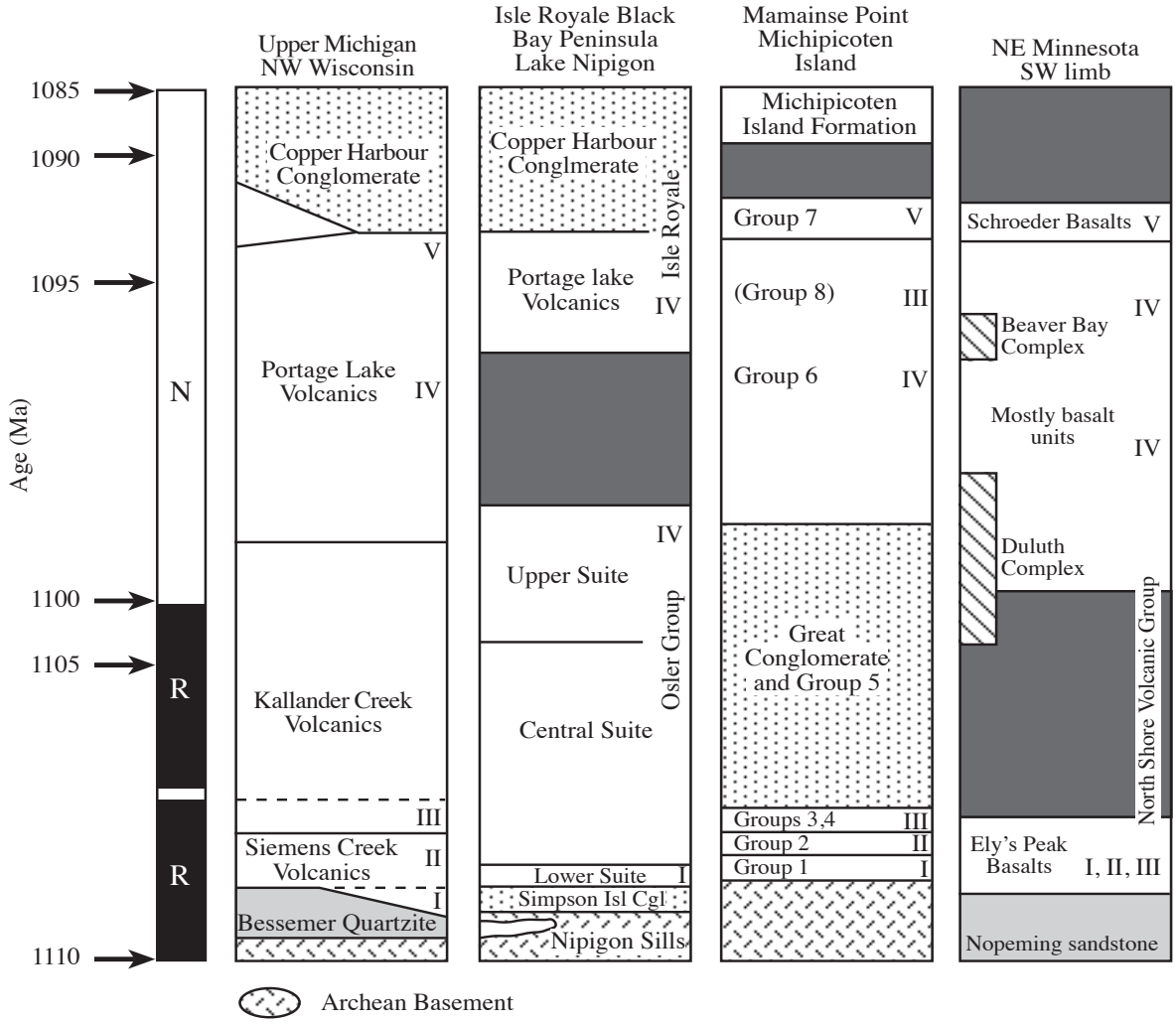


Figure 2. Schematic correlations of volcanic rocks of the Midcontinent Rift based on the stratigraphic position of distinctive basalt sequences, magnetic polarity and absolute age where possible. Modified after Nicholson et al. (1997). Dashed lines in Upper Michigan section separate lower and upper members of Kallander Creek and Siemens Creek volcanics. Left hand column shows magnetic polarity. Roman numerals I-IV refer to five distinctive laterally extensive basalt compositions identified on the south shore of western Lake Superior. Where equivalent basalt compositions occur in other stratigraphic successions, the appropriate Roman numeral is noted (see Nicholson et al., 1997 for data sources). Shaded regions represent intervals in which contacts are covered or obscured by plutonic rocks.

Swamper Lake Gabbro and Nathan's Series intrusive rocks (1107 Ma, Paces and Miller, 1993) and the lower portion of the Powder Mill Group (1107±2 Ma, Davis and Green, 1997). These older units outcrop on the rift flanks where erosion has removed the younger rift sequence or, in the case of the Coldwell and Logan Sills, are intruded into older rocks immediately north of the rift. More recently a number of older sill complexes have also been identified in the vicinity of the Nipigon Embayment (Heaman et al., 2007).

The Osler Volcanic Group comprise a ~3km thick sequence (Cannon et al., 1989) lying unconformably above Sibley Group metasedimentary rocks (Fig. 2). The volcanic sequence is overlain and intruded by the St. Ignace Island Volcanic-Plutonic Complex an intercalated sequence of basaltic rocks and rhyolitic flows (Sutcliffe and Smith, 1988). Detailed descriptions of the Osler Group have been provided by McIlwaine and Wallace (1976), Lightfoot et al. (1991) and Keays and Lightfoot (2015). Generally the mafic flows of the Osler Group consist of massive to amygdaloidal flows, with locally developed ropey tops and pahoehoe textures (Sutcliffe and Smith, 1988). The flows range in thickness from 5cm to 30m (Lightfoot et al., 1991) with a regional dip of ~6-15° S (Giguerre, 1975; Lightfoot et al. 1991; Hollings et al., 2007). The majority of the exposed section is magnetically reversed with only the upper 100m displaying a normal polarity (Halls, 1974). Recent work by Swanson-Hysell et al., (2014) has shown that there is a progressive change in the paleomagnetic sequence of the Osler volcanic rocks that is consistent with a ca. 25° of latitudinal motion of Laurentia. The contact between the two units is marked by the presence of the Puff Island conglomerate and a discordance between the basalt flows above and below the contact. This has been interpreted as representing a significant break in the eruption history. A felsic porphyry near the base of the Osler Group has yielded an age of 1107.5+4/-2 Ma (Davis and Sutcliffe, 1985) whereas zircons from the Agate Point rhyolite towards the top of the reversely magnetized sequence have yielded an age of 1105±2 Ma (Fig. 1b; Davis and Green, 1997).

Within the Osler Group interflow sediments are typically thin and of limited extent. Field descriptions of the sedimentary successions appear in Giguere (1975) and McIlwaine and Wallace (1976). They show that there are two main zones of sedimentary rocks within the Osler Group. One occurs near the base of the volcanic pile. The other is present approximately 2700 meters higher in the succession marking the paleomagnetic reversal.

Lightfoot et al. (1991) in a study of the Osler Volcanic Group exposed along the shores of the Black Bay Peninsula to the west of the field trip location proposed that the major and trace element geochemical data could be used to subdivide the flows into an Upper, Central and Lower Suite although the boundaries between the suites were not clear cut. While the geochemical compositions of the Central (750-900m) and Upper suites (1900-3000m) overlap their Lower Suite (0-750m) is distinguished by elevated Mg numbers (0.55-0.7 versus 0.3-0.6), lower Al_2O_3 (8-12 wt% versus 13-17wt%), lower Th/Nb ratios (0.09-0.70 versus 0.3-0.6) but higher Gd/Yb_n ratios (3.5-4.5 versus 1.6-2.6). Nicholson et al. (1997) concluded that there were five geochemically distinct flood-basalt compositions within the Mid-continent rift that are common to most sections and appear in approximately the same stratigraphic order (Fig. 2) They recognized a lower suite in the Siemens Creek Volcanics (Basalt Type 1; Fig. 2), which they suggest is analogous to the Lower Suite of Lightfoot et al. (1991). In the United States this unit is less than 100m thick whereas the Lower Suite of Lightfoot et al. (1991) is ~750m thick. They report a narrow range of $\varepsilon_{Nd(1100)}$ values for the Siemens Creek Volcanics of -0.7 to +0.7. Nicholson et al. (1997) further suggest that there is a broadly recognizable suite of basalts above this (Basalt type II) which includes the upper Siemens Creek Volcanics and in the upper part of the Grand Portage lavas (Fig. 2). The suite is characterized by slight negative Nb anomalies and a range of $\varepsilon_{Nd(1100)}$ values of -1.4 to -6.9. They suggest that this may be analogous to the most primitive members of the Central Suite of Lightfoot et al. (1991).

The volcanic flows of the Osler Group on Wilson Island are all basalts or basaltic andesites (SiO_2 = 47-56 wt%; MgO = 5-16 wt%; Hollings et al., 2007). The basalts are characterized by LREE enrichment (La/Sm_n = 1.5-3.9) in conjunction with moderately fractionated HREE (Gd/Yb_n = 1.5-3.7) and slight positive to moderately negative Nb anomalies (Nb/Nb* = 0.56-1.13; Hollings et al., 2007; Fig. 3). Major and trace element data show trends of increasing SiO_2 and decreasing MgO and display strong positive correlations between La/Sm_n, Th/La and Th/Nb with height (Fig. 4). This correlation is most pronounced

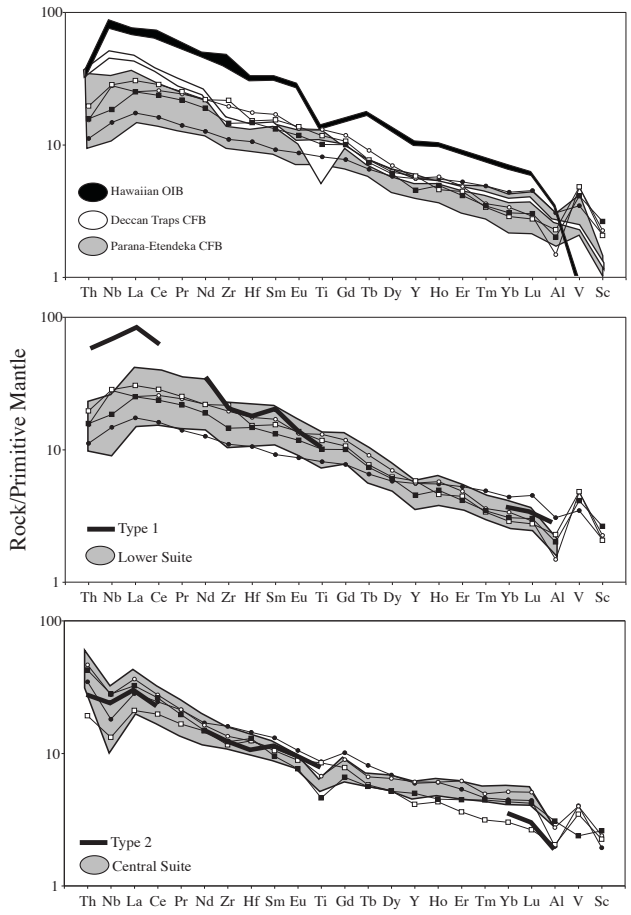


Figure 3. Comparison of primitive mantle normalized plots from the Osler Group with A) Phanerozoic OIB and Continental Flood Basalts (CFB) and B & C) the Lower and Central suites of Lightfoot et al. (1991). From Hollings et al. (2005).

above 400m with samples from the base of the stratigraphy displaying more or less constant values of these ratios (Fig. 4). Measured $^{143}Nd/^{144}Nd$ ratios for the seven Osler basalts analysed range from 0.511857-0.512286 with $\varepsilon_{Nd(t=1106Ma)}$ of +0.3 to -5.3 (Hollings et al., 2007). The high incompatible element abundances, in conjunction with LREE enrichment and strongly fractionated HREE are comparable to modern OIB, albeit at lower absolute abundances (Fig. 3). When compared to other flood basalt sequences the more primitive basalts from this study closely resemble basalts from the Parana-Etendeka flood basalt sequence (Fig. 4; Gibson et al., 2000). The ε_{Nd} data from the most primitive members of the Osler Group is consistent with an enriched mantle plume rather than a contaminated depleted mantle source, given the lack of trace element evidence for contamination in these samples. Depleted mantle at 1100 Ma would have had a positive ε_{Nd} perhaps as high as +6 whereas an enriched plume source would have ε_{Nd} ~0 (Nicholson and Shirey, 1990; Shirey et al., 1994). Up sequence the basalts are characterized by higher SiO_2, Th and La/Sm_n abundances in conjunction with increasingly negative Nb and Ti anomalies and $\varepsilon_{Nd(1106)}$ values of -4 to -5. This is consistent with contamination of these basalts by an older lithospheric component characterized by pronounced LREE enrichment, high Th abundances but generally unfractionated HREE (Hollings et al., 2007).

The sedimentary successions near the base of the Osler Group constitute the Simpson Island Formation and have recently been described in detail by Hollings et al. (2007). They are composed of a Lower Member dominated by trough cross-stratified, medium-grained sandstones directly overlying basement and an Upper Member with a greater variety of siliclastic units. The Lower Member sits on an irregular, erosional surface cut into the underlying quartz arenites of the Nipigon Bay Formation, Sibley Group. A massive pebble-cobble conglomerate overlies the unconformable surface and is in turn overlain by decameter-scale layers of coarse-grained and pebbly sandstone (Fig. 5, Section

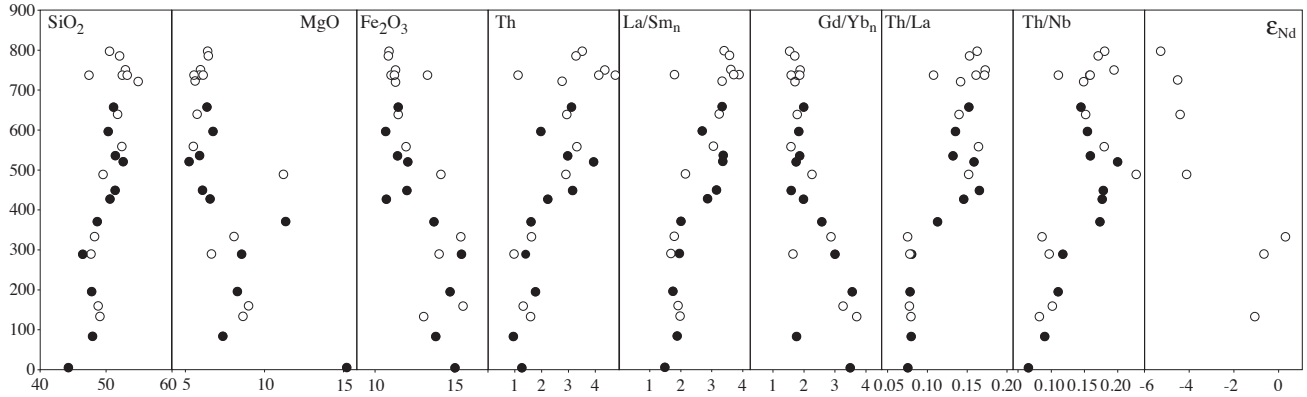


Figure 4. Geochemical stratigraphy of the Osler Group on Vein and Wilson Islands. The stratigraphic position of the samples has been calculated assuming a dip of 10° parallel to the section. From Hollings et al. (2005).

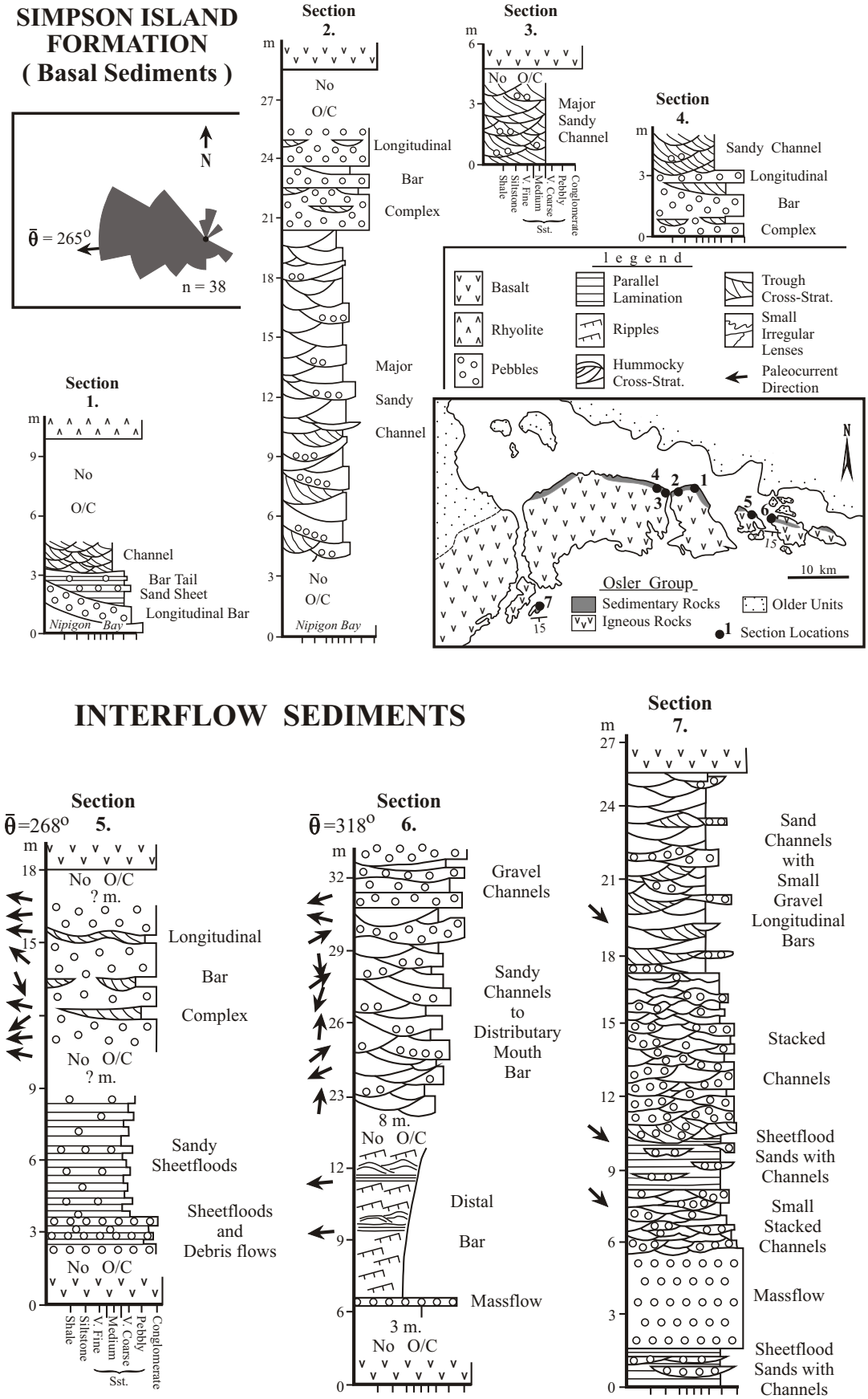


Figure 5. Sections of sedimentary rocks in the Osler Group. Sections 1 through 4 are the basal sedimentary succession of the Lower Member, Simpson Island Formation, at different locations (see inset map). Sections 5 and 6 are of the Upper Member, Simpson Island Formation, interlayered with basal basalt flows. Section 7 is the sedimentary assemblage near the top of the Osler Group on Puff Island. From Hollings et al. (2005).

1). Sandstones are parallel laminated, commonly have cross-stratified tops, more rarely contain pebbly transverse ribs and chute and pool-like structures. The central portion of the succession is composed of trough cross-stratified, medium-grained sandstone organized into a stacked assemblage of lenses. Pebble stringers and pebbly sandstones commonly occur on the deeper portions of curving set boundaries (Fig. 5, Section 2). Massive pebble-cobble conglomerates sharply overly the sandstone succession (Fig. 5, Sections 2 and 4). The conglomerates contain trough cross-stratified, medium-grained sandstone lenses; decameter- to meter-scale wedges of planar cross-stratified sandstone and are interbedded with assemblages of trough cross-stratified sandstones up to one meter thick. Another assemblage of trough cross-stratified sandstone, similar to the one in the central portion of the succession, caps the basal sedimentary assemblage (Fig. 5, Sections 3 and 4). Clast lithologies in the pebble-cobble population are dominated by quartz, chert, various types of volcanic rocks, red siltstone, metamorphosed granite and at the east end of the outcrop belt, on Copper Island, a higher proportion of unmetamorphosed red granite. Current indicators show flow was to the west, averaging 265°.

A sedimentary assemblage also occurs near the upper limit of outcrop of the Osler Formation, at the top of the magnetically reversed interval (Fig. 5, Section 7). These interflow sediments are located on Puff Island and overly a felsic porphyry with a U-Pb age of 1105 Ma (Davis and Green, 1997). They contain: sharp sided assemblages of laterally continuous, pebbly, coarse-grained sandstone beds with caliche horizons which are scoured into by small lenses of conglomerate; large scours filled with trough cross-sets over a meter thick; stacked assemblages of irregular lenses filled by trough cross-stratified, coarse-grained, pebbly sandstone; and, poorly sorted, disorganized, massive boulder-cobble conglomerate. Clasts are all volcanic, ranging from quartz-feldspar porphyries to mafic compositions. Paleocurrents on large-scale sedimentary structures consistently show flow to the southeast.

The Simpson Island Formation is composed of a laterally continuous sedimentary succession up to 25 meters thick and discontinuous sedimentary units up to 30 meters thick interlayered with the basal basalt flows. The lowest sedimentary beds fill channelways cut into the underlying sandstones of the Nipigon Bay Formation. The channel fills and overlying sedimentary assemblage represent a braided stream system, similar to the South Saskatchawan model (Miall, 1978), where dunes composed of coarse-grained sand migrated down the channels and gravelly longitudinal bars with chute channels and bar edge sand wedges form the higher relief areas (Fig. 5). The fluvial interpretation is consistent with Tanton (1931) and McIlwaine and Wallace (1976). Clast lithologies indicate debris was mainly derived from erosion of local lithologies.

Stops

The trip will depart from the public dock at Rossport and will undertake a traverse through the stratigraphy of the Midcontinent Rift, starting with the youngest rocks of the Osler Volcanic Group, proceeding through the Sibley and Gunflint Formations and finishing with a look at the granites of the Archean basement (Fig. 1). In order to make the most of the calmer weather typical of early mornings we will first travel for approximately 30 minutes to the most southerly outcrop on Wilson Island.

Stop 1 – Osler volcanics, Wilson Island

UTM coordinates 0462794E 5402095N

Flows of the Osler Group on Wilson Island are typically >1m thick, frequently amygdaloidal towards the top and bottom of the flow with a massive core and rarely displayed a pahoehoe texture on the flow surface. The basalts are characterized by clinopyroxene and



Figure 6. Well-developed vesicle column in basaltic flows, Stop 1 on Wilson Island.



Figure 7. Approximately 2m thick mafic flow cut by sediment filled cooling crack. Stop 1, Wilson Island.

plagioclase phenocrysts in a groundmass of plagioclase, augite and Fe-Ti oxides. Rarely, basalts from the base of the sequence contained pseudomorphed olivine phenocrysts. The basalts have all been subjected to low-grade metamorphism ranging from zeolite to prehnite-pumpellyite facies (McIlwaine and Wallace, 1976). At this stop, approximately 500m above the basal conglomerates, are exposed a sequence of thin rubbly basalt flows ~50cm thick with rare massive flows ~2-4m thick and thin interflow sediments. These thick flows host well-developed vesicle columns (Fig. 6). Geochemically basalts at this outcrop are similar to the Central Suite of Lightfoot et al. (1991). Sedimentary units are predominantly quartz sandstones with thin shale partings. These are best interpreted as sands washing into small hollows on the surface of the flow units with a mud drape settling out towards the top of the layer. In places units that appear to have been deposited on the surface of basalt flows connect into sub-vertical cooling cracks in the flows. Sediment filled cooling cracks can be up to 2m deep (Fig. 7).

Stop 2 – Osler Volcanics, North end of Wilson Island

UTM coordinates 0461810E 5403438N

Exposed at this outcrop, are the lower flows of the Osler Volcanic Group ~300m above the conglomerates of the Upper Simpson Island Formation. The basaltic



Figure 8. Pahoehoe texture at Stop 2, Wilson Island.



Figure 9. Toe lobe in pahoehoe basalt flow at Stop 2, Wilson Island.

flows are generally massive, ranging in thickness from 1-3m. Flow tops vary from rubbly to well-developed pahoehoe textures (Fig. 8). The basalts are vesicular and amygdaloidal and in places the vesicles are elongated giving them almost a pipe-like appearance. Geochemically basalts at this outcrop are similar to the Central Suite of Lightfoot et al. (1991). In some well-developed flow lobes are preserved (Fig. 9). At the north end of the outcrop the flows are cut by a 2-3m wide mafic dyke. This dyke is geochemically distinct from the flows but comparable to the older diabase intrusions in the vicinity of Lake Nipigon.

Stop 3 – Upper Simpson Island Formation, Daylight Point, Wilson Island

UTM coordinates 0461450E 5404650N

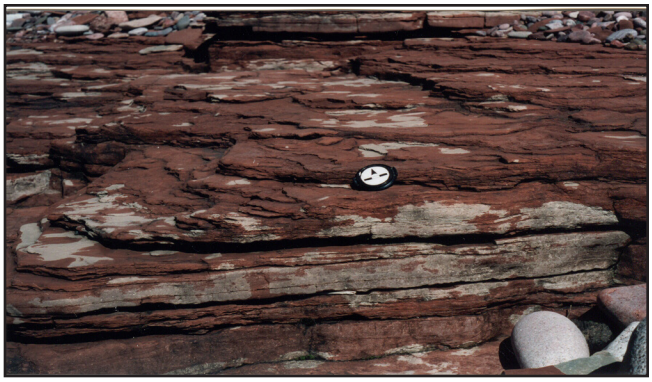


Figure 10. Fine-grained red sandstones with thin shale partings forming the base of the deltaic deposits at Stop 3.

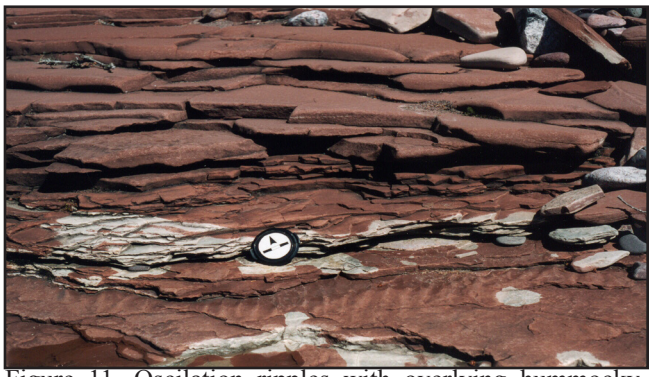


Figure 11. Oscilation ripples with overlying hummocky, medium-grained sandstone showing the effects of wave reworking on the sediments forming the delta front at Stop 3.

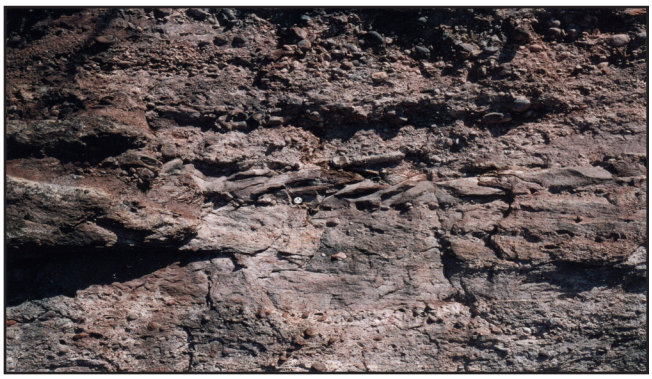


Figure 12. Cross-stratified sandstone and massive conglomerate forming the upper portion of the prograding deltaic succession present in the Upper Member of the Simpson Island Formation present at Stop 3. These sediments represent a longitudinal bar-channel complex of a braided stream.

A sedimentary assemblage of the Upper Member occurs on Wilson Island, overlying approximately 50 meters of basal basalt. This coarsening upwards succession has oscillation rippled, very fine-grained sandstones at its base (Fig. 5, Section 6). These coarsen upwards by the addition of increasing amounts of medium-grained, parallel laminated to hummocky cross-stratified to oscillation rippled, decimeter-scale sandstone beds (Figs. 10, 11). A covered interval separates this assemblage from overlying medium- to large-scale, trough cross-stratified, coarse-grained sandstones to conglomerates (Fig. 12). Paleocurrent indicators show flow to the west, though with a higher variance than other sections. Clast lithologies are probably locally derived from both Archean and Proterozoic sources. The fine-grained sandstone near the base of the section represents a wave modified delta-front (i.e., a distributary mouth bar of a small delta). The presence of small, dish-shaped scours suggests a shallow water environment with no large channels. The upper part of the sequence represents badly organized river deposits with gravelly, longitudinal bar forms and channels filled with sand. The planar cross sets at the base of the cliff were formed by transverse bars, while the trough cross beds represent migrating dunes.



Figure 13. Interlayered red siltstones and dolostones (lower unit underlying the more massive strandline carbonate with overlying mass-flow deposits) were deposited in a saline lake away either temporally or spatially from areas of coarse sand influx. The colour banding reflects the position of the redox boundary as the sediments accumulated. The grey layers commonly have slightly higher dolomite contents possibly reflecting higher organic productivity leading to more photosynthetically mitigated carbonate precipitation (higher dolomite content) and heavier organic loading to the sediment (redox boundary moving upward to at or above sediment water interface). Stop 4, Mary Ann Bay.



Figure 14. Stromatolitic layering (smooth mat with small pinnacles) with interbedded coarse silt to very fine-grained sand storm layers (white). This is typical of strandline to sabkha environments and especially open water ponds on the sabkha. Some of the storm layers were remobilized in the form of clastic dykes and sills.

Stop 4 – Sibley Group, Mary Ann Bay, Channel Island

UTM coordinates 0462769E 5405999N

A succession of grey dolomites interbedded with red siltstones outcrop on the shoreline here (Fig. 13). These are interpreted to be part of the cyclic facies (Channel Island Member) of the Rossport Formation as exposed at Kama Hill. The dolomite and minor gypsum indicate a hypersaline environment interpreted to be lacustrine because of the multiple deltas and sand sheets building in from a variety of directions. The cyclic facies is overlain by stromatolites and interbedded thin, sandy, carbonate storm layers (Fig. 14) of the Middlebrun Bay Member. This meter thick assemblage is similar to recent sabkha deposits on the south shore of the Persian Gulf, and in particular the open water ponds on this sabkha where sandy storm layers are well preserved. The upper few centimeters of the stromatolitic unit is altered to a grey-green layer that represents a weathered horizon interpreted to have formed as the sequence became subaerial and the stromatolites weathered in situ. This weathered zone is traceable throughout the basin with the strandline deposits below it commonly containing well developed tepee structures. The carbonates are overlain by a mass-flow unit with intraformational clasts of red siltstone, sandstone and dolostone up to boulder size. Although the contact between the carbonates and the mass flow units is locally obscured by the intrusion of a sill, the transition is interpreted to represent a minor time gap based on the weathered zone which expands to thick terra rosa (soil) deposits at other locations.



Figure 15. Odd shaped structures of probable stromatolitic origin. within the Gunflint Formation. Stop 5, Quarry Island

Stop 5 – Gunflint Formation, Quarry Island

UTM coordinates 0462371E 5406786N

A succession of sandstones and mafic volcanic rocks outcrop on the south shore of Quarry Island. On the northeastern end of the outcrop area a gabbro, probably related to the Midcontinental Rift, is exposed. Next to this is a small outcrop of stromatolites with a box-like appearance (Fig. 15). The rectangular to square outline of the mounds contrasts with the round to oval appearance of classic stromatolites, though their organic origin is exemplified by the high angle layering, which, when projected into the area now eroded, can be seen to form mounded structures. Areas between the stromatolites are infilled with coarser siliciclastic sandstones and cherty clasts. The next outcrop of Gunflint volcanic rocks is problematic. Mafic volcanic flow rocks occur interbedded with Upper Gunflint lithologies southwest of Thunder Bay. These are also associated with stromatolites that developed on the firm substrate of the flow tops. Thus, the igneous rocks in the Gunflint assemblage on Quarry Island could be correlative to the other flow rocks, but



Figure 16. Well graded sandstone layers. Though these are probably turbidites they were not deposited in excessively deep water and may, in fact, represent distal tempestites. Stratigraphic position is problematic as these beds may belong to either the Upper Gunflint or Rove Formations. Stop 5, Quarry Island.

it is difficult to conclusively show that these rocks are extrusive. Possible flow banding is present, as are areas of finer and coarser material in individual units. The igneous rocks are overlain by medium- to coarse-grained sandstones with bed thicknesses averaging approximately 30 cm. The sandstones are dark in appearance giving the impression they were derived

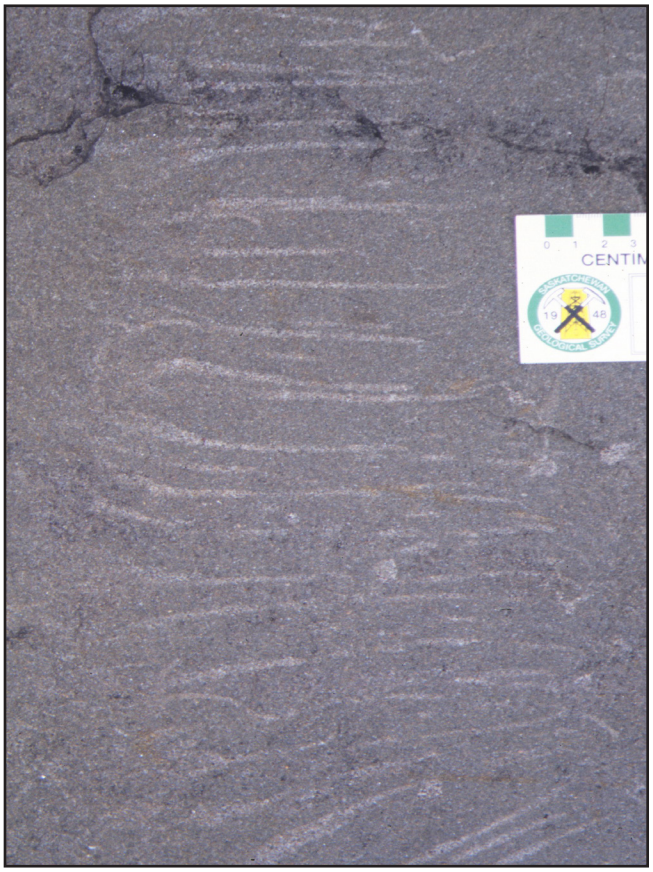


Figure 17. Unusual markings on the bedding planes of the graded sandstones. Stop 5, Quarry Island.



Figure 18. A second example of unusual marking observed at Stop 6. The origin of these markings is unclear. Stop 5, Quarry Island

from mafic detritus, but their geochemistry indicates an intermediate source similar in composition to the Archean crust to the north. The layers are excellently graded (Fig. 16) with the only sedimentary structure being sporadically developed parallel lamination. Beds such as these are commonly thought of as typical turbidites and the deposits ascribed to reasonably deep water. However, it must be remembered that graded bedding simply means a decelerating flow deposited the bed, which can occur in any water depth. These beds may be tempestites, ie. beds formed by storm events, in this case in water deeper than storm wave base but certainly not anything approaching abyssal depths. Or they may have formed from inter- or overflow sediment-water plumes off river mouths, though lack of current reworking of bed tops makes this unlikely. Alternatively they may represent prodelta deposits formed by slumping of the delta front. All of these environments are relatively shallow which agrees with the presence of stromatolites not far stratigraphically below the graded beds. Another interesting point concerning these clastic units is that although such sandstones are common in the upper Rove Formation they are not present in the Gunflint at any other location. Thus, their stratigraphic position is debatable. The third unusual attribute is the presence of difficult to interpret structures on some bedding planes. Series of enechelon small crack-fill like features cut across bedding planes (Fig. 17). In addition a jellyfish-like impression was found on a bedding plane (Fig. 18). This feature had five-fold symmetry, similar to echinoderms, but the age of the rocks and its presence in sandstone leads to the distinct possibility that it was manufactured.



Figure 19. Silicified alteration envelopes adjacent to quartz veins in basal Gunflint carbonates, near Rossport. Photo courtesy of Mark Smyk.

Stop 6 – Pass Lake Formation, Quarry Island

UTM coordinates 0461720E 5406798N - this stop will be time dependant.

This outcrop consists of a cliff-face in sandstones, which were quarried, and the blocks produced used in the construction of buildings in Thunder Bay (Fralick et al., 2000). Here we see the basal sediments of the Sibley Group, the Pass Lake Formation. The Pass Lake forms a diverse group of basal coarse clastic deposits representing environments ranging from braided fluvial through to subaqueous sand sheets. The medium-grained sandstones present in this cliff are organized into a series of large-scale planar cross-stratified sets with normal to low dip angles. Sorting is fairly good and only one pebble has been found in the succession. Assemblages such as this pose a dilemma in formulating an interpretation of their depositional environment. Both aeolian sand dunes and sandflats composed of transverse bars in braided rivers are



Figure 20. Matrix supported basal conglomerate of the Gunflint Formation containing rounded pebbles of quartz, chert and lithic fragments. Photo courtesy of Mark Smyk.



Figure 21. Black chert with gossan within the basal conglomerate of the Gunflint Formation at Gut Point. Photo courtesy of Mark Smyk.

capable of creating such an organization of lithofacies. The presence of the pebble is significant as only freak wind-storms, such as tornadoes, can move material of this weight, and these do not form sand dunes. So, it is more likely that these deposits are subaqueous but this rests only on a slim piece of evidence.

Stop 7 – Basal conglomerate of the Gunflint, Gut Point

UTM coordinates 0461610E 5408587N

The unconformity and basal Gunflint are exposed at Gut Point as a thin, discontinuous veneer along the lakeshore on top of Archean basement (Fig. 19). The basement is a medium-grained, equigranular granite, which has been altered (sausseritized/chloritized) beneath the basal Gunflint. The basal conglomerate is up to 30 cm thick and occupies depressions in the paleo-erosion surface in the basement. The conglomerate is matrix-supported, with subangular to rounded pebbles of white, sugary quartz, lesser cherty and lithic fragments and minor jasper in a medium-grained, sandy matrix (Fig. 20). A black, pyritiferous chert breccia is marked by a conspicuous gossan (Fig. 21). Sulphide mineralization may be related to a persistent, parallel fracture set at 115°. Fractures may host quartz-calcite-barite veins ranging from < 1 to 20 cm wide as well as vein breccia. A conjugate fracture set at right angles to the first is locally developed. Silicification adjacent to the veins has preserved a thin (1 to 5 cm) veneer of Gunflint from being eroded (especially the carbonate units). A 2m wide diabase dyke strikes at 115° through the outcrop.



Figure 22. Porphyritic Archean granite, Selim Point.



Figure 23. Feldspar phenocrysts in Archean porphyritic granite at Selim Point.

Stop 8 – Archean basement, Selim Point

UTM coordinates 0469219E 5409146N

From the dock in Rossport return to Highway 17 and head east for ~5 km. Turn right on to Lakeshore Drive just west of Whitesand Provincial Park. Follow the dirt road to a parking spot opposite a small tombola (Fig. 22). The porpyritic granite exposed here is Archean in age and part of the Wawa Subprovince. The area was mapped by Carter (1988) who described the rocks as porphyritic pink, hornblende + biotite alkali feldspar granite, a phase of the Whitesand Lake Batholith. The porphyritic "facies" is surrounded by massive pink and grey phases of alkali feldspar granite that is not exposed at this locality. The batholith is about 8 x 16 km in size and intrudes the Schreiber greenstone belt; no radiometric date has been generated. Feldspar phenocrysts are typically 3-4 cm across (Fig. 23), subhedral to euhedral and in places appear to display localized alignment suggestive of flow banding.

Acknowledgements

We would like to thank Mark Smyk and John Scott for their help and advice in the preparation of this field guide. In particular Mark Smyk provided text and photographs for Stop 7.

References

Addison, W.D., Brumpton, G.R., Vallini, D.A., Davis, D.W., Kissin, S., Fralick, P.W., McNaughton, N.J., and Hammond, A., 2005. Discovery of distal ejecta from the 1850 Ma Sudbury impact event. Geology, 33, 193-196.

Cannon, W., Green, A., Hutchinson, D., Lee, M., Milkereit, B., Behrendt, J., Halls, H., Green, J., Dickas, A., Morey, G., Sutcliffe, R., and Spencer, C., 1989. The North American Midcontinent Rift beneath lake Superior from GLIMPCE seismic reflection profiling. Tectonics, 8, 305-332.

Carter, M.W. 1988. Geology of the Schreiber-Terrace Bay area, District of Thunder Bay; Ontario Geological Survey, Open File Report 5692, 287p.

Cheadle, B.A., 1986. alluvial-playa sedimentation in the lower Keweenawan Sibley Group, Thunder Bay District, Ontario. Canadian Journal of Earth Sciences, v. 23, p. 527-542.

Davis, D.W., and Green, J.C., 1997. Geochronology of the North American Midcontinent rift in western Lake Superior and implications for its geodynamic evolution. Canadian Journal of Earth Sciences, 34, 476-488.

Davis, D.W. and Sutcliffe, R., H., 1985. U-Pb ages from the Nipigon plate and northern Lake Superior. Geological Society of America Bulletin, 96, 1572-1579.Davis, D.W., and Green, J.C., 1997. Geochronology of the North American Midcontinent rift in western Lake Superior and implications for its geodynamic evolution. Canadian Journal of Earth Sciences, 34, 476-488.

Fralick, P.W. and Barrett, T.J., 1995. Depositional controls on iron formation associations in Canada. In, ed by A.G. Plint, Sedimentary Facies Analysis, Special Publication of the International Association of Sedimentologists, v. 22, p. 137-156.

Fralick, P.W., Kissin, S.A. and Davis , D.W., 2002. The age of the Gunflint Formation, Ontario, Canada: single zircon U-Pb age determinations from reworked

volcanic ash. Canadian Journal of Earth Sciences, v. 39, p. 1085-1091.

Fralick, P.W., Smyk, M. and Mailman, M., 2000. Geology and stratigraphy of the Mesoproterozoic Sibley Group. In, ed. by P. Fralick, Field trip Guide Books, Forty-Sixth Annual Meeting, Institute of Lake Superior Geology. p. 7-42.

Franklin, J.M., 1978. The Sibley Group, Ontario. In, Rubidium-strontium isochron age studies, Report 2, Geological Survey of Canada, Paper 77-14, p. 31-34.

Giguere, J.F., 1975. Geology of St. Ignace Island and adjacent islands, District of Thunder Bay. Ontario Ministry of natural Resources, Geological Report 118, 35p.

Halls, H.C., 1974. A paleomagnetic reversal in the Osler Volcanic Group, Northern Lake Superior. Canadian Journal of Earth Sciences, 11, 1200-1207/

Heaman, L.M., and Machado, N., 1992. Timing and origin of the Midcontinent Rift alkaline magmatism, North America: evidence from the Coldwell Complex. Contributions to Mineralogy and Petrology, 110, 289-303.

Hemming, S.R., McLennan, S.M. and Hanson, G.N., 1995. Geochemical and Nd/Pb isotopic evinence for the provinance of the early Proterozoic verginia Formation, Minnisota. Implications for the tectonic setting of the Animikie Basin. Journal of Geology, v. 103, p. 147-168.

Heaman, L.M., Easton, M., Hart, T.R., Hollings, P., MacDonald, C.A., and Smyk, M., 2007. Further refinement to the timing of Mesoproterozoic magmatism, Lake Nipigon Region, Ontario. Canadian Journal of Earth Sciences, 44, 1055-1086.

Hollings, P., and Fralick, P., 2005. A stratigraphic transect across the northern flank of the Midcontinent Rift near Rossport. In; Hollings, P. (Ed.), Institute on Lake Superior Geology Proceedings, 51st Annual Meeting, Nipigon, Ontario, Part 2 - Field trip guidebook, v.51, part 2, 57-70.

Hollings, P., Fralick, P. and Cousens, B., 2007. Geochemistry and sedimentology of the Osler Formation: Evaluating rifting in the Proterozoic. Canadian Journal of Earth Sciences, 44, 389-412.

Keays, R. and Lightfoot, P., 2015. Geochemical Stratigraphy of the Keweenawan Midcontinent Rift Volcanic Rocks with Regional Implications for the Genesis of Associated Ni, Cu, Co, and Platinum Group Element Sulfide Mineralization. Economic Geology, 110, 1235–1267.

Kissin, S.A. and Fralick, P.W., 1994. Early Proterozoic volcanics of the Animikie Group, Ontario and Michigan, and their tectonic significance. Proceedings Institute of Lake Superior Geology, v. 40, p. 18-19.

Kissin, S.A., Vallina, D.A., Addison,W,D. and Brumpton, G.R., 2003. New zircon ages from the Gunflint and Rove Formations, northwestern Ontario. Proceedings Institute of lake Superior Geology,

Lightfoot, P., Sutcliffe, R., and Doherty, W., 1991. Crustal contamination identified in Keweenawan Osler Group tholeiites, Ontario: A trace element perspective. Journal of Geology, 99, 739-760.

McIlwaine, W.H., and Wallace, H., 1976. Geology of the Black Bay Peninsula Area, District of Thunder Bay, Accompanied by Map 2304, scale 1 inch to 1 mile. Ontario Division of Mines, GR133, 54p.

Maric, M. and Fralick, P.W., 2005. Sedimentology of the Rove and Virginia formations and their tectonic significance. Institute of Lake Superior Geology, v. 51, p. 41-42.

Metsaranta, R.T., 2006. Sedimentology and geochemistry of the Mesoproterozoic Pass Lake and Rosport Formations. Sibley Group. Unpublished MSc. Thesis, Lakehead University, 217 pp.

Morey, G.B., 1967. Stratigraphy and sedimentology of the Middle Precambrian Rove Formation in northeastern Minnesota. Journal of Sedimentary Petrology, v. 37, p. 1154-1162.

Miall, A.D., 1978. Lithofacies types and vertical profile models in braided river deposits: A summary. In ed. A.D. Miall, Fluvial Sedimentology, Canadian Society of Petroleum Geologists Memoir 5, 597-604.

Nicholson, S.W., Shirey, S., Schulz, K., Green. J., 1997. Rift-wide correlation of 1.1 Ga Midcontinent rift system basalts: implications for multiple mantle sources during rift development. Canadian Journal of Earth Sciences, 34, 504-520.

Paces, J.B., and Miller, J.D, Jr., 1993. Precise U-Pb ages of Duluth Complex and related mafic intrusions, northeastern Minnesota; geochronological insights to physical, petrogenetic, paleomagnetic, and tectonomagnetic processes associated with the 1.1 Ga Midcontinent Rift System. Journal of Geophysical Research, B, Solid Earth and Planets, vol.98, no.8, pp.13,997-14,013.

Pufahl, P.K. and Fralick, P.W., 2004. Depositional controls on paleoproterozoic shallow-water iron formation accumulation, Gogebic Range, Wisconsin, U.S.A. Sedimentology, v. 54, p. 791-808.

Rogala, B., Fralick, P.W., Heaman, L.M. and Metsaranta, R., 2007. Lithostratigraphy and chemostratigraphy of the Mesoproterozoic Sibley Group, northwestern Ontario, Canada. Canadian Journal of Earth Sciences, v. 44, p. 1131-1149.

Shirey, S., Lewin, K., Berg, J., and Carlson, R., 1994. Temporal changes in the sources of flood basalts: Isotopic and trace element evidence from the 1100 Ma old Keweenawan Mamainse Point Formation,

Ontario, Canada. Geochimica et Cosmochimica Acta, 58, 4475-4490.

Sutcliffe, R. H., 1986. The petrology, mineral chemistry and tectonics of Proterozoic rift-related igneous rocks at Lake Nipigon, Ontario. Unpublished Ph.D. thesis, University of Western Ontario, London, 325p.

Sutcliffe, R.H., and Smith, A.R., 1988. Project number 87-17. Geology of the St. Ignace Island volcanic-plutonic complex. Summary of Fieldwork and Other Activities 1988. Ontario Geological Survey Miscellaneous Paper 141, 368-371.

Swanson-Hysell, N. L., Vaughan, A. A., Mustain, M. R. and Asp, K. E., 2014. Confirmation of progressive plate motion during the Midcontinent Rift's early magmatic stage from the Osler Volcanic Group, Ontario, Canada. Geochem. Geophys. Geosyst., 15, 2039–2047, doi:10.1002/2013GC005180

Tanton, T.L., 1931. Fort William and Port Arthur, and Thunder Cape map areas, Thunder Bay District, Ontario. Geological survey of Canada Memoir 167, 222p.

Field trip 6 - Geology of the Coldwell alkaline complex

Allan MacTavish

Panoramic PGMs (Canada) Limited, Thunder Bay, ON, Canada

Mark Smyk

Resident Geologist Program, Ontario Geological Survey, Ministry of Energy, Northern Development and Mines, Thunder Bay, Ontario, P7E 6S7, Canada

David Good

Earth Sciences Dept., Western University, London, Ontario, Canada

and

John McBride

Stillwater Canada Inc., Marathon, Ontario, Canada

The Coldwell Alkaline Complex Trip will consist of two parts comprising 1) a west to east transect through southern part of the complex and 2) a visit to the Marathon Cu-PGE Deposit. This guide is modified from the 2017 ILSG Field Guide.

Part 1: Transect Through the Coldwell Alkaline Complex

Allan MacTavish and Mark Smyk

A variety of Mesoproterozoic, Midcontinent Rift-related alkalic and carbonatitic rocks occur within several intrusive complexes on or near the northern shore of Lake Superior (Figs. 1 and 2). They include the Coldwell and Killala Lake alkaline complexes, the Prairie Lake and Chipman Lake carbonatites, and numerous diatremes and related dikes in the vicinity of Dead Horse Creek (Sage, 1982, 1985, 1987; Fig. 2). These complexes are spatially localized and structurally controlled by the Trans-Superior Tectonic Zone (TSTZ), a north-northeast-trending structure that extends for over 600km and includes the Thiel Fault in Lake Superior (Klasner et al., 1982). Alkaline magmatism related to Midcontinent rifting occurred along the TSTZ from approximately 1.2 to 1.0 Ga (Table 1).

It has been postulated that the TSTZ may represent

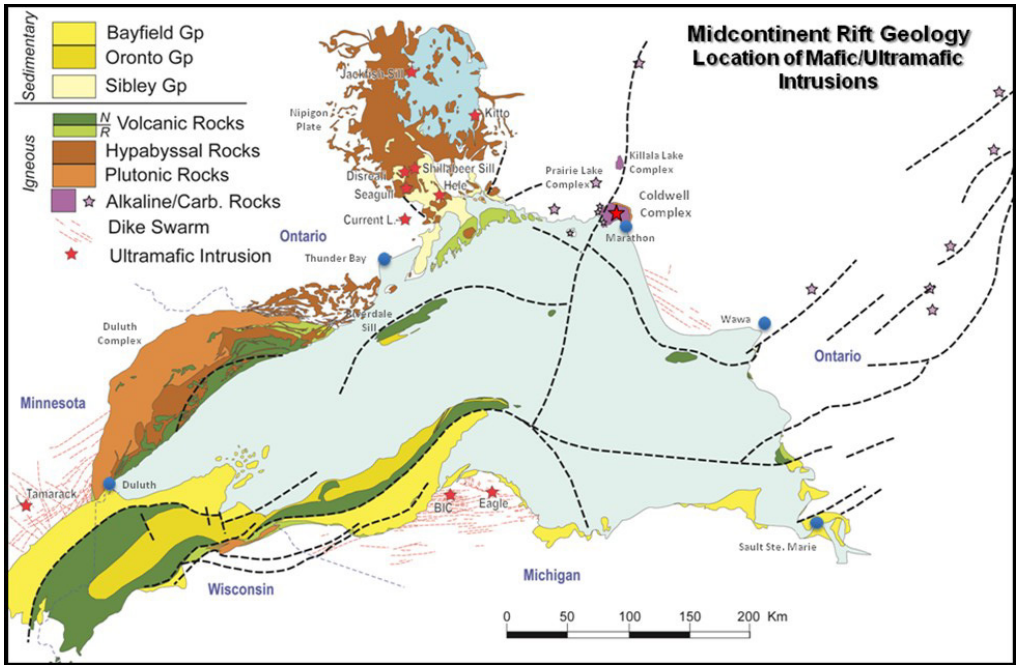


Figure 1. Midcontinent Rift geology and the locations of mafic/ultramafic intrusions (After Miller et al., 1995).

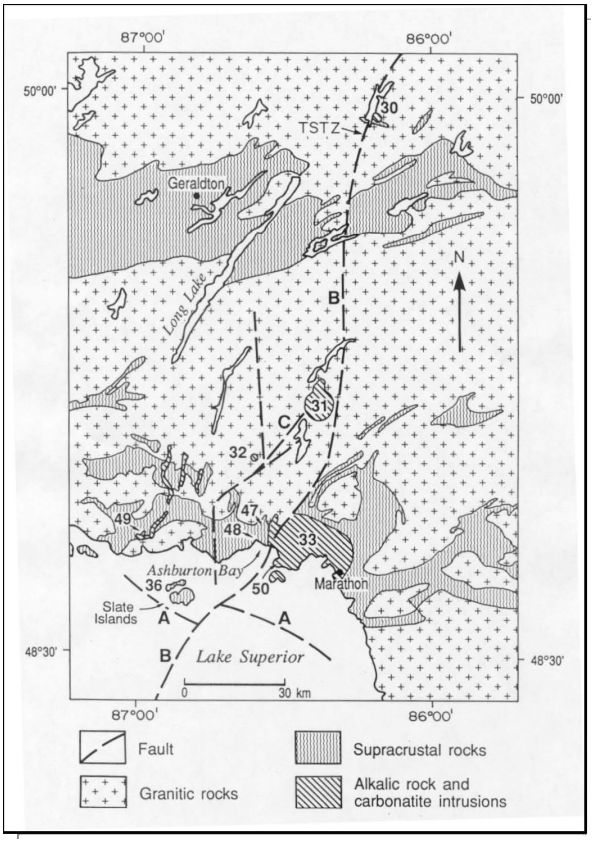


Figure 2. Regional geology (Sage, 1991) in the vicinity of the Trans-Superior Tectonic Zone (TSTZ), extension of the Thiel Fault (B). Key to numbering: 30 – Chipman Lake fenites / carbonatite dikes; 31 – Killala Lake alkaline complex; 32 – Prairie Lake Carbonatite; 33 – Coldwell alkaline complex; 36 – Slate Islands; 47 – Dead Horse Creek diatremes; 48 – McKellar Creek diatreme; 49 – Gold Range Diatreme; 50 – Neys Diatreme; A – Michipicoten Fault; C – Killala Lake Deformation Zone.

part of a failed arm of a Keweenawan-age triple junction (Weiblen, 1982; Mitchell and Platt, 1982b) or the intersection of a late fracture system with the rift (Mitchell et al., 1983). Local alkalic and carbonatite complexes have been emplaced at inflections in the trends of major structural zones, or at sites of cross-faulting (Sage, 1991). The Coldwell and Killala Lake alkaline complexes are both thought by some to have formed as the result of ring fracturing and caldera collapse. The abundance of observed xenolithic blocks and roof pendants suggests that these complexes are presently exposed at relatively high structural levels.

Similar ages for numerous mafic intrusions in the Nipigon Embayment (cf. Heaman et al., 2007) and the alkalic rocks of the Coldwell Complex (1108 ± 1 Ma; Heaman and Machado, 1992) indicate the contemporaneous production of tholeiitic and alkalic magmas during Midcontinent rifting. The oldest magnetization, found in the gabbros and augite syenites on the eastern side of the complex, records a concordant pole position with reversed polarity at about 1109 ± 5 Ma on the Keweenawan segment of the Precambrian apparent polar wander path (Lewchuk and Symons, 1990). The localization of the alkalic magmatism off-axis, dominantly northeast of the central rift, prompted Heaman and Machado (1992) to suggest that this may have been a region of maximum lithospheric extension during rifting. U/Pb data (Heaman and Machado, 1992) demonstrate that most rock units in the Coldwell Complex were emplaced within a relatively short time span (<3 million years) ca. 1108 Ma, and support the contention that the complex experienced relatively rapid cooling from initial emplacement temperatures to at least ~500º C.

Strontium-, neodymium- and lead-isotopic compositions of selected minerals from different phases of the complex (Heaman and Machado, 1992) display considerable scatter, suggesting that their magmas had different isotopic compositions. The initial strontium- and neodymium-isotopic compositions of clinopyroxene and plagioclase from one of the earliest gabbroic phases are identical to data derived from primitive olivine tholeiites from the Midcontinent Rift and indicate that the majority of magmas, both

Table 1 MCR-related Alkaline Magmatism Occurring Along the TSTZ

Lithologic Unit/Complex	Age(s) (Method)	Reference
Coldwell Alkaline Complex	1108 ± 1 Ma (U/Pb)	Heaman and Michado (1987)
Be-Zr Zone crosscutting Dead Horse Creek diatreme	1112.7 ± 4 Ma (U/Pb)[1] 1128.7 ± 6 Ma (U/Pb)[2]	Krogh and Wilkinson (M. Smyk pers. Comm., 1995)
Prairie Lake Carbonatite Lamprophyre Dyke, McKellar Harbour	1130 ± 10Ma (Rb/Sr) 1145 + 15/10 Ma (U/Pb) ~1160 Ma (U/Pb)	Pollock (1987) Queen et al. (1996) Wu et al. (2016)
Gabbro (biotite), Killala Lake Complex	1185 ± 90 Ma (K/Ar)	Coats (1970)
Syenite, Killala Lake Complex	1050 ± 35 Ma (Rb/Sr)	Bell and Blenkinsop (1980)

([1]-2.49% discordant; [2] 1.82% discordant)

tholeiitic and alkaline, have a uniform, nearly chondritic isotopic composition (ibid). Samarium- neodymium data, supported by oxygen-isotopic and whole-rock geochemical data, indicate that crustal contamination played a small, varied role in the generation of the Coldwell magmas (Bohay, 1997). In addition to small, variable amounts of assimilation of upper and lower crust, the parental plume magmas also interacted with the lithospheric upper mantle to a small degree (ibid).

Local alkalic and carbonatitic intrusive rocks host a variety of characteristic base, precious, titaniferous, phosphate, and rare metal occurrences (cf. Smyk and Sage, 1995). They include the following:

1. Magmatic Cu-Ni-PGE (± Au, Ag) in gabbros of the Killala Lake and Coldwell complexes;
2. Magmatic Ti-V±apatite deposits in the Eastern Border Gabbros of the Coldwell Complex;
3. Magmatic U, Nb (+ wollastonite, apatite) in the Prairie Lake carbonatite (Sage, 1987);
4. Late-stage magmatic Nb-Y-F-family rare earth elements in syenite pegmatites (Alexander, 2007);
5. A Be-Zr-U-Th-Y mineralized zone crosscutting the Dead Horse Creek diatreme (Smyk et al., 1993; Potter, 2004); and
6. Pb-Zn-Ag-mineralized quartz-carbonate veins (Kissin and McCuaig, 1988).

The Coldwell Alkaline Complex (Fig. 3) covers an area of ~580km^2, making it one of the largest alkalic complexes in the world and the largest in North America. It was emplaced during the early stages of the Midcontinent rift system, which includes: early large and small mafic to ultramafic intrusions (i.e. Seagull Lake Complex, Thunder Bay North Intrusive Complex); Keweenawan flood basalts, the Duluth Complex, the Nipigon and Logan sills, and a variety of non-diabase mafic to ultramafic dyke-rocks. The Coldwell Complex was mapped by Kerr (1910a, 1910b), Puskas (1967), and Walker et al. (1993b, 1993c), and comprises three, superimposed ring sub-complexes or magmatic centers (Mitchell and Platt, 1978) that young progressively (Centers 1 to 3) to the southwest (Fig. 4). Walker et al. (1993) and Barrie et al. (2002) dispute the series of ring dykes or sheeted cones interpretation and suggest that the complex is a composite lopolith or sill. The intrusive centres can be generally described as follows:

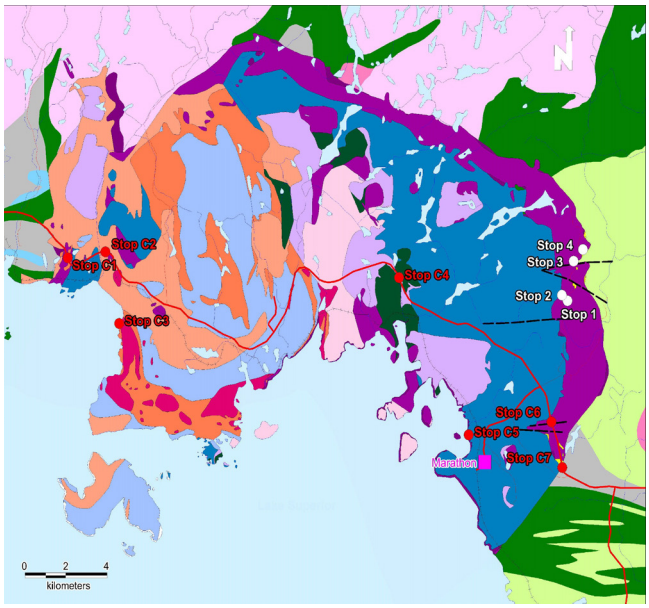


Figure 3. Generalized geology of the Coldwell Alkaline Complex (after Walker et al., 1993) with field trip stops.

Center 1: Generally silica-saturated rocks with oversaturated residue; chiefly consisting of the Eastern and Western border gabbros (the oldest rocks within the complex) and later iron-rich augite syenite and syenite-syenodiorite (Mitchell and Platt, 1978, 1982; Mulja, 1989);

Center 2: Generally silica-undersaturated alkalic rocks with oversaturated residue; consisting of locally nepheline- and hastingsite-bearing miaskitic nepheline syenite, and numerous volumetrically minor alkaline lamprophyre and analcime tinguaite dykes (Mitchell and Platt, 1978, 1982; Laderoute, 1989; and Mulja, 1989); and

Center 3: Silica-oversaturated alkalic rocks with oversaturated residue; consisting of magnesio-hornblende syenites, quartz syenites, and minor granites (Mitchell and Platt, 1994; Lukosius-Sanders, 1988).

The mineralogy of the main lithologic units is listed in Table 2. The superimposition of the three intrusive centres and a complex, protracted magmatic history has produced a myriad of hybrid rocks, igneous breccias, and ambiguous crosscutting relationships.

The wide variety of lamprophyric and other dyke rocks occurring within the complex (as described by Mitchell and Platt, 1994) include (in order of emplacement):

1. Mafic ocellar lamprophyre (camptonitic variety)
2. Quartz-bearing, mafic lamprophyres (camptonitic variety)

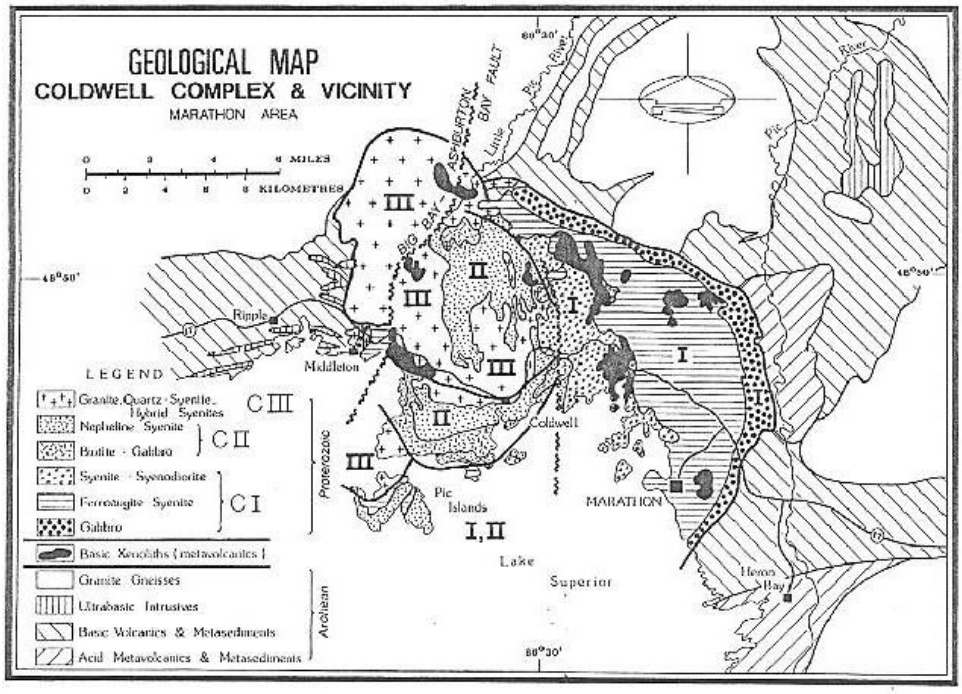


Figure 4. Coldwell Alkaline Complex magmatic centres: CI (Centre 1), CII (Centre 2), and CIII (Centre 3). Generalized geology after Mitchell and Platt (1994).

3. Sannaite-type lamprophyres
4. Monchiquitic-type lamprophyres
5. Feldspar glomeroporphyritic and alkali basalt dikes
6. Analcime tinguaite (heronite)

Abundant large rafts and/or roof pendants of mafic volcanic rocks are mapped throughout the Coldwell Complex and in places exhibit horizontal extensional cooling cracks on a ten to hundreds of metres scale that are thought consistent by some workers with sub-horizontal bedding. For the most part the roof pendants may be the lowermost portions of the Keweenawan flood basalt sequences suggesting that the complex is barely unroofed and is exposed at a very shallow crustal level (Mitchell and Platt, 1994; Sage and Watkinson, 1995; Barrie et al., 2002). It is also highly probably that some, or most of the mafic rafts observed within the complex that could not be roof pendants are detached portions of chilled complex roof or wall rocks (fine-grained gabbros).

The mafic intrusive rocks occurring within Centers

Table 2. Mineralized Zones Associated with the Mafic Intrusive Rocks of Centres 1 and 2.

Intrusion (Centre)	Lithologic Units	Reference(s)
Eastern Gabbro (1)	Layered gabbro cumulates (olivine gabbro, gabbro, troctolite, anorthositic (leuco-) gabbro); Fe-Ti oxide ± apatite cumulates	Shaw (1994, 1997); Lum (1973); Barrie et al. (2002)
Western Gabbro (1)	Massive and layered series gabbro; olivine-bearing	Penczak (1992); Wilkinson (1983)
Two Duck Lake (1)	Gabbronorite, olivine gabbronorite, olivine-bearing gabbro, leucogabbro	Shaw (1994, 1997)
	Hornblende gabbro to monzodiorite; olivine ferrogabbro to ferrodiorite; olivine gabbro to diorite	Dahl et al. (1987)
Malpas Lake (1)	Amphibole-bearing olivine gabbro	Shaw (1994, 1997)
Geordie Lake (2)	Troctolite, olivine gabbro	Mulja (1989); MacTavish et al. (1987); Good, pers. com. (2019)
Alkalic gabbro (2)	Biotite gabbro	Mitchell and Platt (1982b)
	Biotite- and olivine-gabbro	Walker et al. (1993a)

1 and 2 are tabulated, with their associated mineralized zones (Table 2).

Magmatic, gabbro-hosted Cu-Ni-PGE deposits in the Coldwell Complex have been the focus of much exploration and research for the past 60 years. Mineralized zones occur within the border gabbro at the eastern (Marathon deposit; Skipper Lake Zone) and western (Middleton occurrences) margins of the complex, and within its interior at Geordie Lake. The Geordie Lake mineralized zones, hosted by a younger (?) gabbro, are enriched in tellurium and silver and have higher Pd:Pt ratios (~19) (Mulja and Mitchell, 1991) than the border gabbro-hosted deposits (~4; Smyk, 2001). Geochemical variations in mineralized zones in the Coldwell Complex are shown in Figure 5. A table of selected Coldwell Complex deposits and mineralized zones is shown below (Table 3).

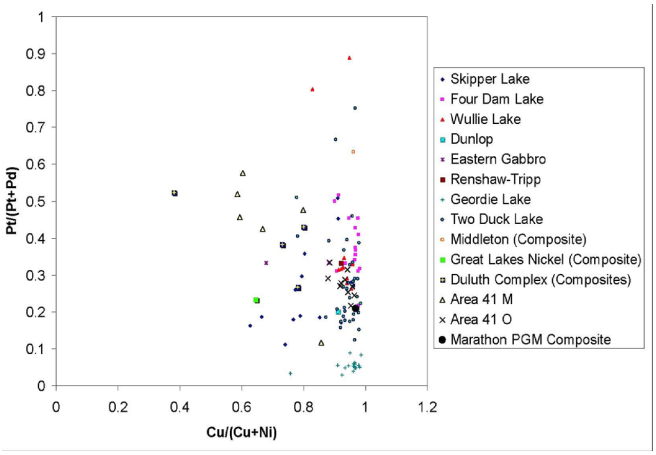


Figure 5. Discrimination plot for PGE-mineralized samples for Coldwell and other Midcontinent Rift-related intrusions. Data from Good (1992), MacTavish (unpublished data, Resident Geologist's Files, Thunder Bay), Watkinson et al. (1983), Wilkinson (1983), and unpublished data, Resident Geologist's Files, Thunder Bay. Duluth Complex composite data from Hauck et al. (1997).

Marked similarities exist between the mineralization style, geochemistry, and host rocks of Coldwell Complex-, Duluth Complex-, and the Crystal Lake gabbro-hosted deposits near Thunder Bay. Similarities include mineral textures, abundance and compositions, crystallization paths for the host gabbros, silicate-sulphide associations, trace-element trends and chalcophile element fractionation trends (Good and Crockett, 1994a).

Research by Watkinson and Ohnenstetter (1992) and Good and Crockett (1994a, 1994b) produced debate between the relative importance of magmatic and hydrothermal processes in local copper-nickel-PGE

Table 3. Selected Coldwell Alkaline Complex Deposits and Mineralized Zones

Mineralized Zone	Grade / Significant Assays	Ore Mineralogy	Reference(s)
Marathon	Measured and Indicated In-Pit Resources: 114.8 Mt @ 0.775 g/t Pd, 0.228 g/t Pt, 0.083 g/t Au, 0.241% Cu, 1.567 g/t Ag; Proven and Probable In-Pit Reserves: 91.447 Mt @ 0.832 g/t Pd, 0.237 g/t Pt, 0.085 g/t Au, 0.247% Cu, 1.440 g/t Ag (January 2010)	Chalcopyrite ≤ pyrrhotite >> pentlandite > cubanite ≤ pyrite; sphalerite, hollingworthite, atokite-zvyaginstevite, sperrylite, Bi-kotulskite, michenerite, merenskyite, monceite, stibiopalladinite, paolovite, merteite II, palladoarsenide, unnamed (Pd_xAs_y), nickeline, majakite, argentian gold	Marathon PGM Corporation Ohnenstetter et al. (1991); Watkinson and Ohnenstetter (1992); Good and Crocket (1994a, 1994b)
Geordie Lake	Measured and Indicated Resources (above $13.00/t cut-off): 32.42 Mt @ 0.61 g/t Pd, 0.04 g/t Pt, 0.05 g/t Au, 0.37% Cu, 2.93 g/t Ag	Chalcopyrite, bornite, pyrite, millerite, siegenite, pentlandite, galena, chalcocite, melonite, hessite, unnamed (Ag_xTe_y), altaite, kotulskite, merenskyite, michenerite, sopcheite, Pd-bismuthotelluride, paolovite, Pd-arsenide, guanglinite, Pd-antimonide, sperrylite, electrum, $Pd_{1.6}As_{1.5}Ni$, $AgSb_x$	news release, Marathon PGM Corporation, May 04, 2010 Mulja (1989); Mulja and Mitchell (1990, 1991)
Middleton		Chalcopyrite, pyrrhotite, pentlandite, sphalerite, pyrite	Penczak (1992)
Skipper Lake	average grade of 1.05 g/t Pd+Pt+Au over 12 m	Chalcopyrite, bornite, pentlandite, cobaltite, galena, chalcocite; telargpalite, polarite, kotulskite, taimyrite, merteite, zvyagintsevite, plumbopalladinite, majakite, tetraferroplatinum	MacTavish (2000)
Area 41	0.48 g/t Pt+Pd+Au over 202 m, incl. 1.23 g/t Pt+Pd+Au over 61 m	n/a	Benton Resources Corp.

mineralization processes. Watkinson and Ohnenstetter (1992) presented field, petrographic and mineral-chemical data that support the interaction of magmatic sulphide mineral assemblages with a chlorine-rich mixture of magmatic (deuteric) fluid and volatile species generated by the breakdown of assimilated xenoliths at low temperatures. However, Good and Crockett (1994a, 1994b) contended that element migration took place over only very short distances and that the original, bulk sulphides were not enriched in copper and PGE by later fluids.

The information within this field trip guide was taken from a variety of sources, including guidebooks from previous field trips to the Coldwell Complex: Puskas (1970); Loubat (1972); Mitchell and Platt (1977, 1982a, 1994); Smyk and Sage (1995), Smyk (2001), Smyk (2010), and unpublished field observations and mapping completed by A. MacTavish (1992). All UTM co-ordinates listed are NAD83 Zone 16 with locations shown on Figure 6.



Photo 1. Pink, natrolite-bearing, pegmatitic augite syenite. Photo credit D. Campbell.

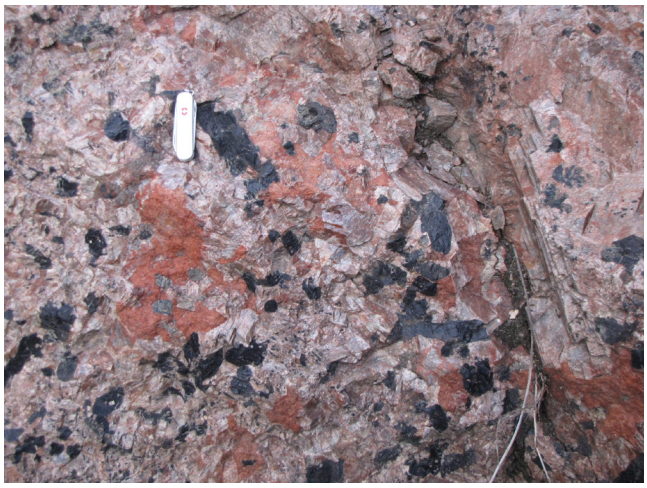


Photo 2. Pegmatitic syenite containing reddish orange patches of natrolite, light pinkish perthitic feldspar, and black amphibole. Photo credit A. MacTavish.

Stop descriptions

Stop C1: Natrolite-Bearing Syenite and Massive Fe-Ti-oxides

UTM coordinates 525528E 5405511N

29.4 to 29.9 km west of the Highway 626 and Highway 17 junction

Description: This exposure displays natrolite-bearing, pegmatitic syenite (Photo 1). Reddish orange natrolite (an acicular or prismatic zeolite mineral replacing nepheline) patches up to 15cm in diameter, crystals of perthitic feldspar up to 30cm in length, and crystals or black amphibole up to 25cm in length comprise the bulk of this syenite (Photo 2). Mitchell and Platt (1994) reported accessory pleochroic clinopyroxene, zircon, titanite, and biotite. Natrolite has locally been ascribed to the hydrothermal alteration of primary nepheline and has also been referred to as "hydronepheline" by local workers. The syenite is intruded by a camptonite lamprophyre dike (Mitchell and Platt, 1994) and also hosts large, medium-grained gabbro xenoliths (Photo 3), up to 1m in thickness and sometimes up to 5m in length (west-side of the highway), that exhibit 1 to 2cm wide, dark reaction rims adjacent to the enclosing syenite. To the east, the pegmatitic syenite gives way to finer grained nepheline syenite in which chalky-weathering nepheline may be



Photo 3. Large gabbro xenolith located on the west side of the highway. Please note that the xenolith has been crosscut by fine-grained syenite veins and that the syenite below the xenolith is varitextured to pegmatitic in texture, whereas the syenite above is medium- to coarse-grained. Photo credit A. MacTavish.

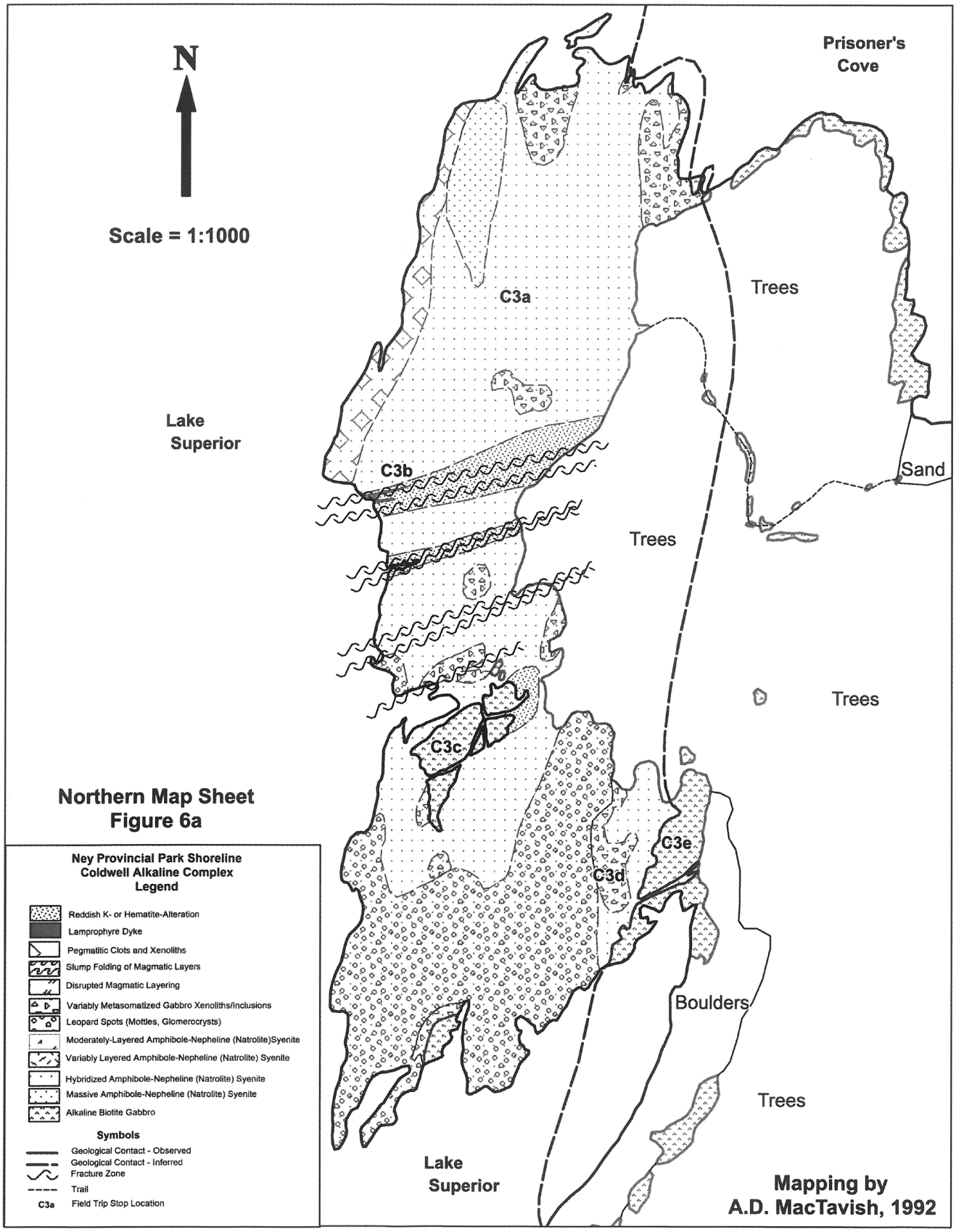


Figure 6a. Northern portion of Neys Shoreline geological map starting at Prisoner's Cove, Neys Provincial Park with Field Stop locations.

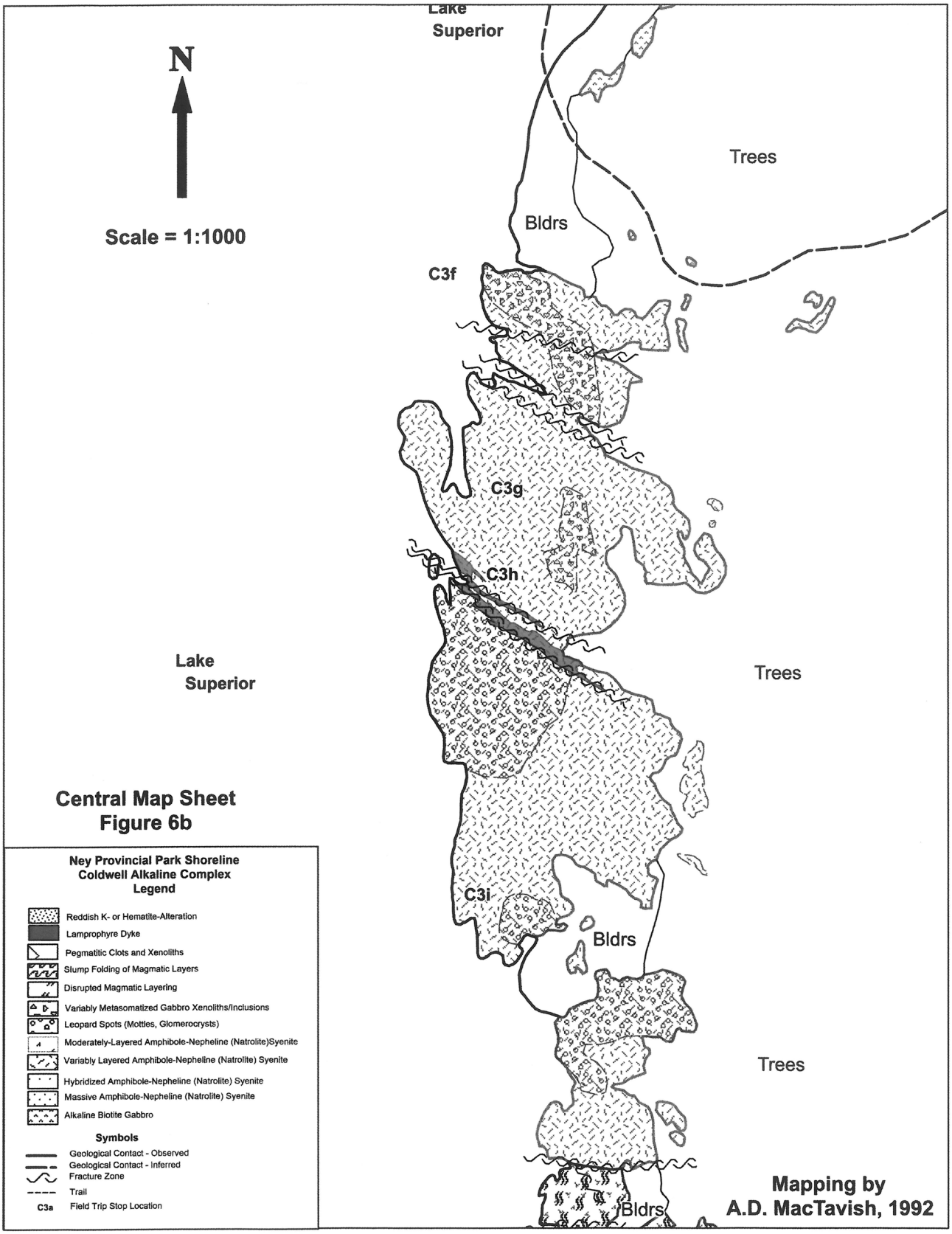


Figure 6b. Central portion of Neys Shoreline geological map, Neys Provincial Park with Field Stop locations.

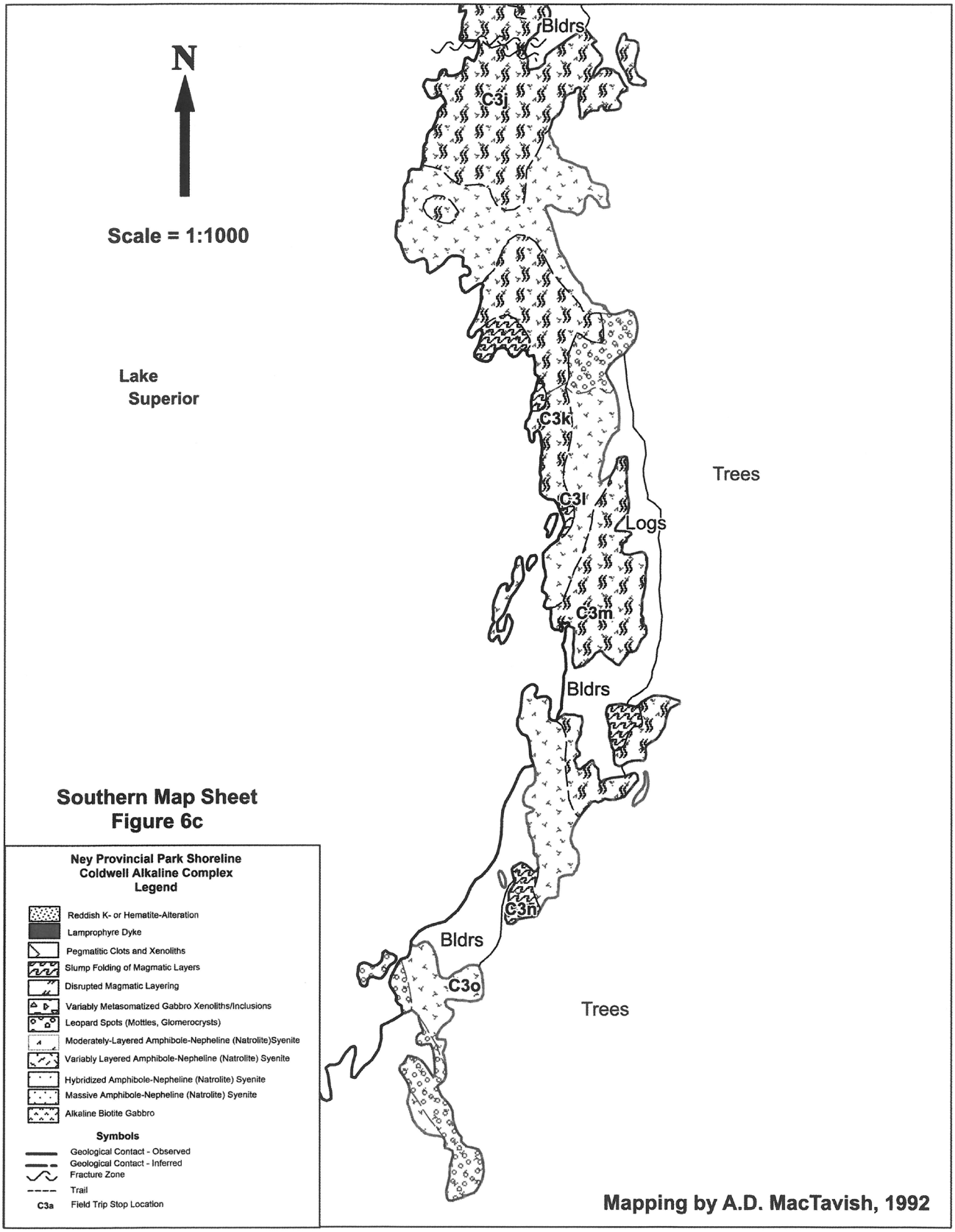


Figure 6c. Southern portion of Neys Shoreline geological map, Neys Provincial Park with Field Stop locations.

observed. Rare natrolite grains are also present. Farther east, a variety of equigranular and pegmatitic syenites are exposed.

Near the eastern end of the outcrop (UTM 525625E, 5404825N), a large xenolith of gabbro-hosted, massive titaniferous magnetite has been exposed. Minor clinopyroxene, plagioclase and apatite occur within the massive oxide unit. Analyses completed in 1951 and reported by Hinz and Landry (1994) indicated total iron and titanium values ranging between 33 and 45%, and 4.5 and 13.5%, respectively; phosphorus contents ranged up to 0.371%.



Photo 4. Syenite outcrop on the south side of the highway containing blocks of mafic xenoliths often occurring in elongated, semi-continuous rafts. Photo credit A. MacTavish.



Photo 5. Elongated, jig-saw-fit xenolithic block exhibiting both angular and lobate/cuspate (amoeboid) margins. Please note the lighter-coloured, pinkish-grey elongated xenolithic block with apparently sharp margins located below the dark grey block. This lower block appears to be coarser-grained and may possibly be different in composition. Photo credit A. MacTavish.

Stop C2: Little Pic River Breccia Zone

UTM coordinates 527478E 5405531N

27.3 km west of the Highway 626 and Highway 17 junction

These road cuts, particularly along the south side of the highway, expose spectacular intrusive breccias within the youngest rocks of the complex, along the east side of the fault zone that the Little Pic River occupies. The breccias often occur as semi-continuous, fragmented, elongate rafts (western end of southern rock cut, Photo 4) that consist of angular to rounded blocks of fine- to medium-grained, equigranular, mafic (gabbroic?) rocks within a groundmass of pink, medium-grained, quartz syenite. In some cases blocks can exhibit both angular and lobate to cuspate (amoeboid) margins (see Photo 5). The mafic rocks comprising the blocks were interpreted as oligoclase-bearing basalt by Mitchell and Platt (1982a). Subsequent discussion and study has led to the suggestion of perhaps 2 texturally discernable types of basic xenoliths, those with: (1) sharp, angular margins, and (2) those with lobate to cuspate margins. In this model, the angular xenoliths represent synplutonic basalts which are now preserved elsewhere as megaxenoliths in younger intrusions. The cuspate-margined xenoliths may represent the effects of mixing between two contemporaneous gabbroic/basaltic and syenite magmas (i.e., magma mixing or co-mingling). Cuspate, possible chilled margins with quench-textured clinopyroxene, plagioclase and skeletal olivine have been noted in similar xenoliths to the south on the Coldwell Peninsula by G. Shore (personal communication with M. Smyk, 1995) and suggest the quenching of the basic magma against the cooler, syenitic magma. These are reasonable hypotheses and there are definitely at least two types and textures of xenoliths; however, they do not completely explain the presence of blocks exhibiting both margin types as observed by the senior author of this guide and shown in Photo 5. Texturally there also seems to be three different types of xenoliths: the most abundant are dark grey to black, very fine-grained xenoliths (Photo 4); medium-grained, greyish pink xenoliths with somewhat less distinct, but still relatively sharp margins (Photo 5), and several unusual zones where there is are subvertical zones of rounded, dark grey, amphibole-phyric xenoliths within a pinkish, mafic groundmass. Are these some sort of breccia dykes or just hybridized zones of xenoliths (Photo 6; what do you think?)? Although isolated xenoliths are



Photo 6. Rounded dark grey, amphibole-phyric xenoliths/ inclusions within a fine- to medium-grained, pinkish mafic groundmass (breccia dyke?). Photo credit M. Puumala.

common, there are many areas within these outcrops where incipient or in-situ brecciation characterized by syenite dykes and "jig-saw puzzle/jig-saw fit" breccias are observed, where brecciated fragments can be fitted back together. Miarolitic cavities, up to several centimetres in width, contain euhedral quartz, feldspar, and calcite crystals.

The breccia zone persists to the east, towards the scenic lookout located 800m to the east. The south side of the highway is underlain by oligoclase gabbro and quartz syenite, while various, xenolithic-bearing syenitic rocks are exposed on the north side. These pyroxene- and amphibole-(ferro-edenite) bearing syenites contain xenoliths of alkali gabbro, alkali diorite and other, equigranular to porphyritic syenites. Near the lookout turnoff, gray, nepheline-bearing syenite intrudes the mafic rocks and contains orange natrolite. Sannaite and ocellar, camptonitic lamprophyre dikes have been reported near this site by Mitchell and Platt (1994) who proposed the following order of local emplacement:

Mg-hornblende syenite → contaminated Fe-edenite syenite → Fe-edenite syenite → quartz syenite (earliest → latest)

Lukosius-Sanders (1988) classified the local rocks as miaskitic, metaluminous syenites enriched in U, Th, REE and Zr. These syenites have affinities to A-type granites and have been interpreted to be the result of fractional crystallization of mantle-derived, basaltic magma (Lukosius-Sanders, 1988; Mitchell et al., 1993).

Stop C3: Prisoners Cove, Neys Provincial Park (Sample Collecting Prohibited!)

UTM coordinates 527984E 5402537N

The descriptions (unpublished mapping/field descriptions, MacTavish, 1992) herein are for 14 sub-stops along the shoreline south of Prisoner's Cove; however, due to time constraints only the northernmost stops will be visited.

23.5km west of the Hwy 626 and Hwy 17 junction; 2.8km south of Hwy 17 to the park headquarters and then south along the shoreline trail

General Description: The wave-washed, glacially polished outcrops along the shoreline of Lake Superior at Prisoner Cove and south for over a kilometre along the western side of the Coldwell Peninsula exhibit a variety of lithologic, textural, and crosscutting features that characterize much of the Center 2 magmatism in the Coldwell Complex. In its simplest sense, this composite stop displays the contact between alkalic biotite gabbro and amphibole-nepheline syenite, but the enigmatic effects of assimilation and hybridization have severely complicated and obscured many of the primary features. In all cases within the nepheline syenitic rocks exposed along the shoreline at this stop the nepheline has been completely altered to the zeolite mineral natrolite which weathers to orange-coloured pits.

Medium- to coarse-grained, olivine- and enclave-bearing, biotite gabbro comprises much of the eastern portion of the outcrops. Gabbro xenoliths occur within the syenite and within hybrid phases along their mutual contact, which trends roughly north-south, parallel to the shoreline. The outcrops often exhibit a pitted surface resulting from the preferential weathering of mafic enclaves consisting of biotite-olivine gabbro to biotite-clinopyroxene gabbro or leucogabbro (Walker et al., 1992) within a more syenitic groundmass. The syenitic groundmass consists of fine- to coarse-grained nepheline (altered to natrolite) syenite with minor acicular amphibole and poikilitic biotite. Mitchell and Platt (1994) have identified the amphibole as hastingsite.

Distinct to diffuse layering, a nebulous to locally distinct igneous foliation, and localized soft-sediment style magmatic deformation exists within the amphibole-nepheline syenite. Identifiable, undisturbed layering may be oriented parallel to the apparent syenite/gabbro contact and dips from very steeply to vertically in the north to shallow to moderate to the east (where measurable) in the south. Observed soft-sediment deformation features consist of flame structures, fluid-escape features, slump folds, and isolated well-layered syenite blocks surrounded by obvious fluid escape textures. Much past discussion has focused on whether the observed structures have resulted simply from igneous process, syn- or post-intrusion shearing, or a combination of these processes. The present author's strongly favour igneous processes since the observed fracturing is very localized, is late and brittle, and does not appear to have affected the foliation or layering within the surrounding rocks in any observable way. It is highly probable that the crystallizing magma chamber was often shocked by MCR tectonic activity. These earthquakes then caused the slumping of unstable crystallizing layers along chamber walls; allowed the isolation of broken, but relatively intact layered blocks; and allowed trapped deuteric fluids formed during the fractionation process to escape upwards through the broken layers. Upon close examination the fracturing presently observed in outcrop obviously took place after the chamber was completely crystallized and was able to deform in a brittle manner.

Sub-Stop C3a (527980E, 5402571N): This area, located on the point to the north and west of the old flat-bottomed boats, mainly consists of foliated, wispy, hybridized amphibole-nepheline syenite with diffuse discontinuous "layers" (Photo 7). The core of this outcrop is flanked to the northeast by a heterogeneous zone containing large numbers of rounded to angular, variably assimilated (metasomatized?) and disaggregated inclusions/xenoliths of biotite gabbro. Reaction rims around these inclusions are readily visible. Also the inclusion-rich zone, as a whole, seems to be enclosed within a diffuse reaction zone when compared to the hybrid syenites adjacent to the west. The western margin of the exposure is a medium- to coarse-grained hybridized syenite with numerous very coarse-grained to pegmatitic inclusions of amphibole-nepheline syenite. At the northwestern tip of the outcrop is an elongate, diffuse zone of apparently non-hybridized, non-foliated syenite (possibly the original parent syenite?).



Photo 7. Wispy, relatively mafic in appearance, hybrid amphibole-nepheline syenite exhibiting diffuse discontinuous layers. Photo credit A. MacTavish.

Sub-Stop C3b (527950E, 5402535N): This stop, located 30m west-southwest of the old boats near the shoreline, consists of a 4 to 5m wide, west-northwest-striking, brittle fracture zone hosting a 70 to 100cm thick, dark greenish-grey, ocellar lamprophyre dyke at its northern margin near the water's edge. The ocellae present within the dyke are composed of reddish, recessive-weathering carbonate (±zeolites?) which are elongated parallel to dyke margins (elongated by flow?). The lamprophyre dyke is also enveloped by a brick-red alteration halo that is not completely within the fracture zone and also extends into the unfractured hybrid syenites to the north for up to 5m. This red halo could be due to either hematization or K-alteration. Similar, subparallel fracture zones can also be observed about 10m and 23m to the south.

Sub-Stop C3c (527966E, 5402475N): This stop is located ~50m east-southeast of Sub-stop C3b, and consists of a zone of large blocks (?) of coarse-grained, natrolite-bearing, biotite gabbro to biotite melagabbro that are surrounded by fine- to medium-grained amphibole-nepheline syenite containing diffuse gabbro xenolith ghosts. It is distinctly possible that this is not a zone of xenoliths/inclusions at all, but the exposed upper contact of an underlying biotite gabbro that is part of the biotite gabbro body located about 40m to the southeast (see Sub-Stop C3e, below) where the syenite is observed to overly the gabbro. These blocks (?) are cross-cut by narrow horizontal and subvertical syenite veins and dykes (Photo 8).



Photo 8. Large biotite gabbro xenolith/inclusion (?) crosscut by veins and dykes of amphibole-nepheline syenite. Photo credit A. MacTavish.



Photo 9. Biotite gabbro xenoliths/inclusions separating from and original larger block and beginning to assimilate (?) into the surrounding syenite melt through a process of metasomatism and disaggregation. Photo credit A. MacTavish.



Photo 10. Disaggregating biotite gabbro xenoliths exhibiting subparallel reaction haloes. Photo credit M. Puumala.

Sub-Stop C3d (528004E, 5402440N): This location (45m southeast of Sub-stop C3c) consists of an irregular zone of gabbro xenoliths/inclusions, surrounded by fine- to medium-grained, weakly foliated syenite (Photos 9 and 10). The xenoliths are in the process of being broken down in stages from originally angular, cohesive blocks to diffuse groupings of amoeboid to wispy mafic remnants within a mafic mineral-rich, hybrid syenite. This process is probably not assimilation in the strictest sense, but is more likely a process of chemical (rather than thermal) invasion through metasomatism that over time breaks down the xenoliths and then eventually disaggregates the mineral constituents of the blocks to the point where they are then assimilated into the syenite melt. The hybridized (?) syenite surrounding the xenoliths exhibit aligned amphibole grains that may indicate flow (?) around and between fragments. There are also places where there are noticeable (up to 15cm thick) halos surrounding zones of xenoliths that consist of aligned amhibole grains that are somewhat separated into diffuse bands.

Sub-Stop C3e (528014E, 5402433N): Located only 12m southeast of Sub-Stop 3d and consists of coarse-grained, knobby-weathering, biotite gabbro that has been cross-cut by numerous hair thin to 5cm thick, very fine- to fine-grained syenite stringers and veins and the occasional, larger, fine-grained to pegmatitic syenite vein (pegmatite is in centre of these veins; Photo 11). There are numerous leucocratic clots (oikocrysts?) of plagioclase (Photo 12) throughout.

Sub-Stop C3f (527982E, 5402324N): This sub-stop (~115m west-southwest of Sub-stop C3e) consists of an irregular, variably assimilated zone of mafic



Photo 11. Biotite gabbro crosscut by fine-grained to pegmatitic syenite dyke (centre) and thinner syenite veins (centre left). Photo credit A. MacTavish.



Photo 12. Leucocratic clots of plagioclase (oikocrysts) within biotite gabbro. Photo credit A. MacTavish.

(gabbroic?) xenoliths of highly variable size ranges. Many blocks are in the last stages of assimilation where the original xenoliths are now merely ghosts infilled with isolated mafic remnants and considerable numbers of hornblende grains.

Sub-Stop C3g (527978E, 5402292N): This location (~30m south of Sub-stop C3f) consists of locally well-developed modal layering within medium- to locally coarse-grained amphibole-nepheline syenite. The magmatic layering dips shallowly to the west and west-southwest at between 20 and 26° and there is a possible weak alignment of K-feldspar laths parallel to layering. The bases of the undulating modal layers are defined by a sharp increase in amphibole content. The best defined layering is near the lake with layering becoming increasingly more diffuse, disrupted, folded (slumping?), and contorted to the east until it becomes unrecognizable.



Photo 13. Ocellar lamprophyre dyke in narrow fracture zone. Photo credit A. MacTavish.

Sub-Stop C3h (527971E, 5402265N): At this location (~27m south of Sub-stop C3g) are two, sub-parallel, aphanitic to fine-grained, ocellar lamprophyre dykes (Photo 13) occupying a narrow southeast-striking fracture zone. The dykes dip to the northeast between 54° and subvertical. The ocellae (immiscible liquid droplets) are usually centralized within the dykes away from the strongly chilled dyke margins and are infilled with several minerals including apple-green and greyish minerals (zeolites?), and possibly white calcite.

Sub-Stop C3i (527987E, 5402198N): At this location (~70m south of Sub-stop C3h) is a zone of leopard mottles in moderately mafic, often grain-size-layered (?) amphibole nepheline syenite.

Sub-Stop C3j (527971E, 5402265N): This location (~80m south of Sub-stop C3i) is, for lack of a better name, a "Layer Breccia Zone" where there has been strong disruption, localized rotation, and folding of original magmatic syenite layers (Fig. 7). Finer-grained syenite containing acicular amphibole grains has flowed around the layer blocks and alignment of those amphibole grains mirrors flow directions. The zone is surrounded by a highly disturbed hybrid mixtite with few measurable features. Thinner blocks consist of a series of thin modal layers of highly variable textures. The thicker layers are usually the coarsest, are sometimes size-graded, and contain glomerocrysts of K-feldspar (with include amphibole and natrolite after nepheline) up to 1.5cm in diameter surrounded by acicular amphibole grains and recessive-weathering altered nepheline.

Sub-Stop C3k (528000E, 5402039N): Located 77m south of Sub-stop C3j. This sub-stop comprises a well-layered block of amphibole-nepheline syenite (~6.5m by 3.5m in size) that is surrounded by a highly distorted zone of fine- to very-coarse-grained (varitextured) syenitic material that appears to have flowed around the block (Photo 14 and Fig. 8). This

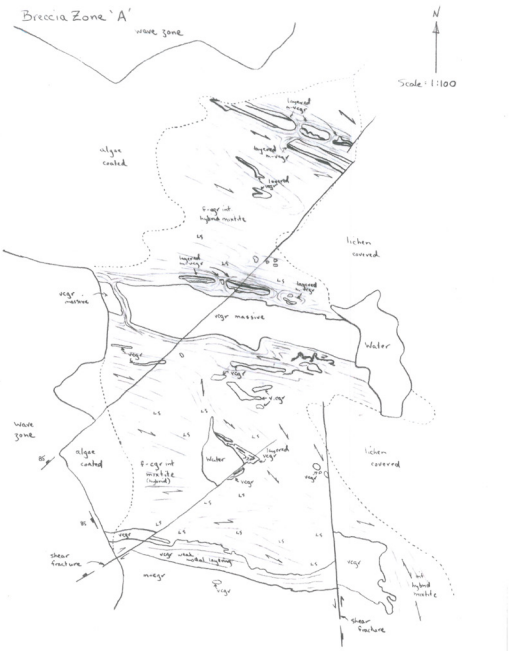


Figure 7. Hand drawn detailed map of Layer Breccia Zone 'A'. Mapping by A. MacTavish (1992). Abbreviation key: vcgr = very coarse-grained; f-cgr = fine- to coarse-grained; m-vcgr = medium-verycoarse-grained; int = intermediate; LS = Leopard spots (mottles).



Photo 14. A well-layered block of amphibole-nepheline syenite that is surrounded by a highly distorted zone of fine- to very-coarse-grained (varitextured) syenitic material that appears to have flowed around the block. Photo credit A. MacTavish. Also refer to Figure 9.

isolated, Spectacular Block 'B', consists of a sequence of three thick layers where amphibole and K-feldspar are aligned subparallel to layer bases. The base of each layer is undulatory on the scale of a single very coarse feldspar crystal.

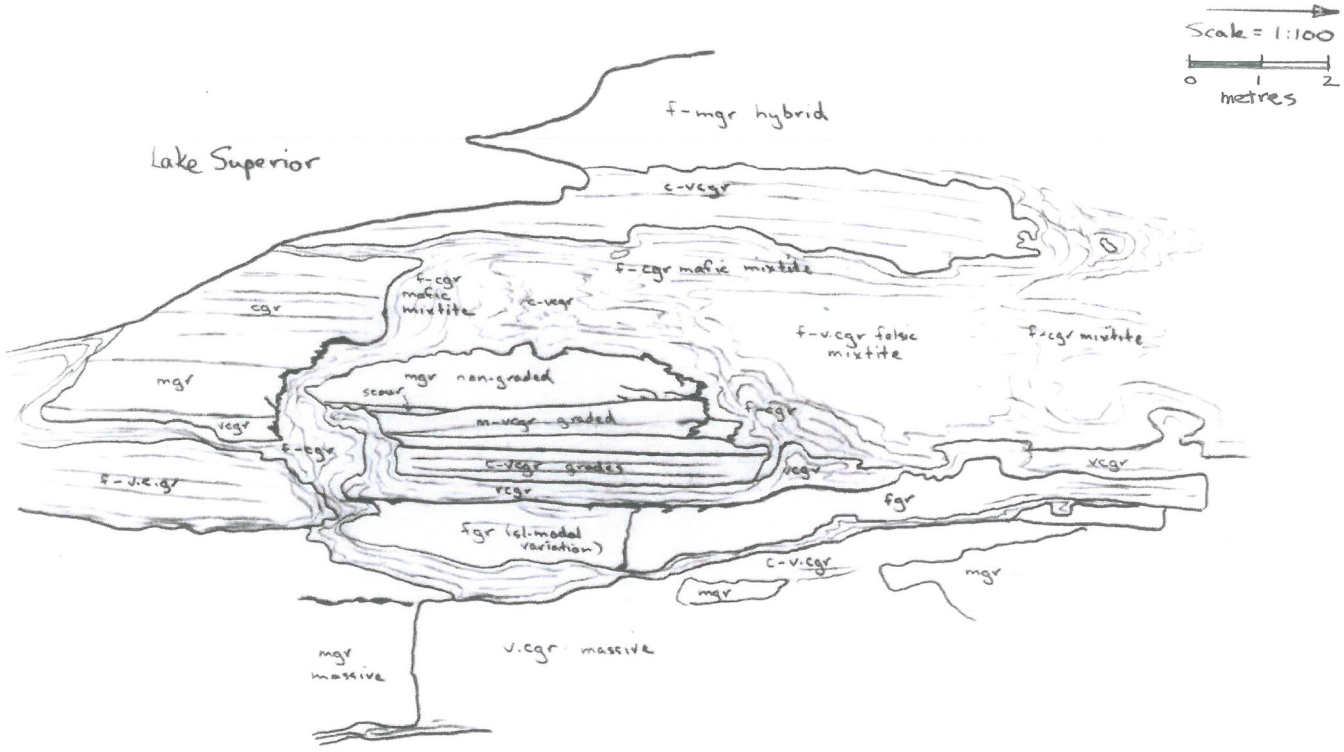


Figure 8. Hand drawn detailed map of Layer Breccia Zone 'A'. Mapping by A. MacTavish (1992). Abbreviation key: fgr = fine-grained; mgr = medium-grained; cgr = coarse-grained; vcgr = very coarse-grained; f-cgr = fine- to coarse-grained; m-vcgr = medium-very coarse-grained; int = intermediate.

Sub-Stop C3l (528004E, 5402016N): A further 23m south of Sub-stop C3k is a zone characterized by well-developed syenite layering (Photo 15), some possible magmatic channel scours, some localized soft-sediment-style deformation, and a few zones of intense, localized layer disruption. Most of the layers within the southern part of the zone are quite flat lying (18°W dip).



Photo 15. Well-developed, relatively flat-lying, magmatic layering within amphibole-nepheline syenite. Photo credit A. MacTavish.

Sub-Stop C3m (528011E, 5402006N): This sub-stop is located 12m southeast of Sub-stop C3l and is directly adjacent to it. It consists of a zone of disturbed and distorted syenite layering similar to that observed north of the isolated block observed at Sub-stop C3k. Contorted and convoluted layering is common and folding is observed locally with the disturbance increasing in intensity to the south. Most noticeable in this area is a deformed, crosscutting, texturally variable, vein-like body (Photo 16) composed of mobile "flow-banded" material. The margins of this "Vein C" (Fig. 9) are often irregular, possibly due to volatile fluid seepage (?) and it is often cored by coarse-grained to pegmatitic veinlets and pods. It is possible that this structure has erupted from the nose of a slump fold.

Sub-Stop C3n (528020E, 5401977N): This final sub-stop is located 30m east-southeast of Sub-stop C3m and consists of a large slump-fold (Fig. 10) composed of medium- to very coarse-grained, modally- and normally grain-size graded syenite layers (Photo 17). This was interpreted as slump folding due to the presence of at least three axial planar directions present within three separate folds all in close proximity to each other. Unfortunately since mapping was completed in 1992 this exposure has become partially obscured by the growth of lichen.



Photo 16. Crosscutting, vein-like body possibly resulting from the movement of volatile-rich magmatic fluids. Photo credit A. MacTavish.

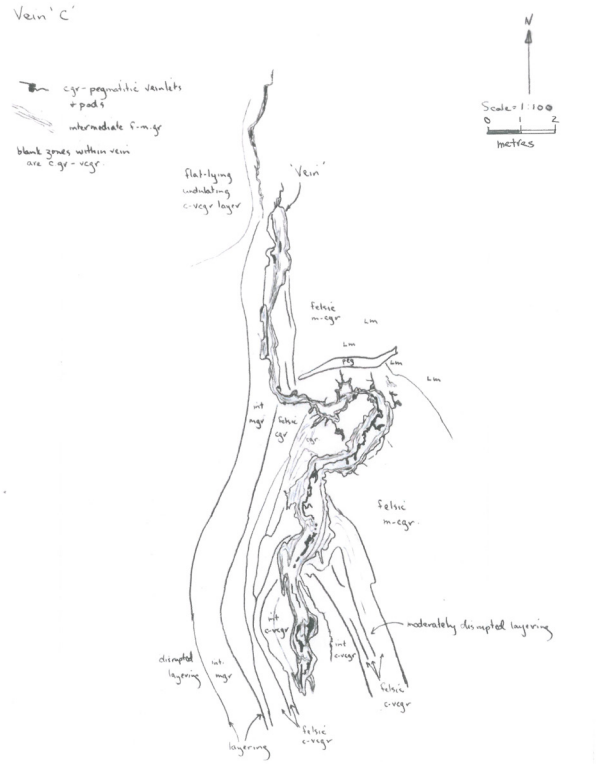


Figure 9. Hand drawn detailed map of Vein 'C'. Mapping by A. MacTavish (1992). Abbreviation key: fgr = fine-grained; mgr = medium-grained; cgr = coarse-grained; vcgr = very coarse-grained; f-mgr = fine to medium-grained; c-vcgr = coarse to very coarse-grained; LM = Leopard mottles; peg = pegmatitic; int = intermediate



Figure 10. Hand drawn detailed map of the Area 'D' slump fold. Mapping by A. MacTavish (1992). Abbreviation key: fgr = fine-grained; cgr = coarse-grained; f-mgr = fine to medium-grained; f-cgr = fine to coarse-grained; int = intermediate

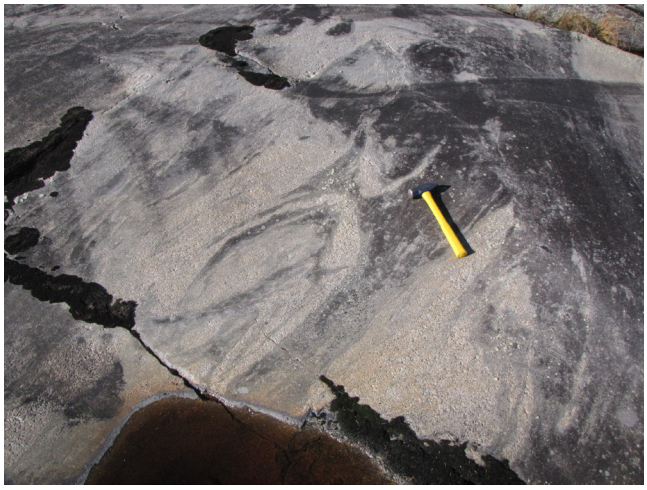


Photo 17. Lichen-obscured slump fold within layered amphibole-nepheline syenite. Photo credit A. MacTavish.

Stop C4: Hornfelsed Basaltic Roof Pendants, Wolf Camp Lake

UTM coordinates 541775E 5404189N

8.6 km west of the Highway 626 and Highway 17 junction

Description: Hornfelsed basaltic rocks overlying the complex were recognized early in its mapping by Tuominen (1967) and Puskas (1970) and likely represent a volcanic edifice that has been subsequently eroded (Sage 1986). Mitchell and Platt (1994) and Nicol (1990) have considered these basalts to have a tholeiitic lineage, contemporaneous with the Coldwell Complex. Fresh, metasomatized and hornfelsed, andesine-oligoclase basalt flows are estimated to attain a thickness of 5 km (Mitchell and Platt, 1994; Nicol, 1990). Assimilation and brecciation of the flows by subsequent gabbroic to syenitic magmatism has resulted in the widespread development of basaltic xenoliths ranging from 1m to over 1 km in size, comprising a roof pendant in the central part of the complex (Walker et al., 1992). Walker et al. (1992) subdivided these basaltic rocks into three main units:

1. Aphanitic to fine-grained, massive, locally amygdaloidal (?) / ocellar basalt;
2. Medium-grained, diabasic (ophitic) basalt; and
3. Aphanitic to medium-grained, feldspar-phyric, diabasic (ophitic) basalt.

At Wolf Camp Lake, aphanitic basalts contain round to amoeboid, epidote- and quartz-filled structures up to 2cm in diameter that have been interpreted as amygdules (Photo 18). Well-defined, amygdule-bearing zones dip 8° to the southwest in this vicinity (Walker et al., 1992). The basaltic roof pendant is locally underlain and enveloped by feldspar-phyric amphibole syenite and Fe-rich augite syenite.



Photo 18. Amygdules within the basaltic roof pendant located near Wolf Camp Lake. Photo credit D. Campbell.

Stop C5: Layered Fe-rich Augite Syenite (Alternate stop if time allows)

UTM coordinates 544782E 5398443N

680 m west along the shoreline of Lake Superior from the end of the James River industrial road along the waterfront in Marathon; OR 150m south of Carden Cove road, 0.3 km past CPR tracks (park at 544864E, 5398750N)

Description: Broad expanses of glacially polished and wave-washed, massive Fe-rich augite syenite occur all along this part of the Lake Superior shoreline near Marathon. Fresh surfaces vary from dark green-brown to black, despite a buff to white weathered surface. Small dimension stone quarries were developed and produced in this area during the 1930's. Much of the stone was shipped to larger centres in the American mid-west and Toronto.

Fe-rich augite syenite (formerly referred to as ferroaugite syenite) comprises a large portion of the exposure in the eastern half of the Coldwell Complex. It appears to be a sheet-like intrusion that dips approximately 15° toward the center of the complex, sandwiched between the underlying Eastern Border Gabbro and an overlying, recrystallized amphibole-quartz syenite; it also intrudes the basaltic roof pendants (Walker et al., 1992; 1993a). Crystallization of the syenite inwards from its upper and lower contacts produced mineralogical and compositional variations across it (Walker et al. 1993a). Constituent minerals include iridescent, lathlike, cryptoperthitic feldspar (up to 30% interstitial), and variable amounts of fayalite, amphibole, aenigmatite, and rare quartz. Coarse-grained to pegmatitic portions of the syenite host a variety of REE-bearing fluoro-carbonates, quartz, chalcedony, and molybdenite. Iridescent feldspar, known locally as "spectrolite", was recently (2010) commercially extracted on a very small-scale from pegmatite at Shack Lake near Marathon.

Although this unit is typically massive, rhythmic to chaotic layering is locally developed and where observed commonly dips shallowly towards the centre of the complex. At this site, layering strikes at 070° and dips 60° north. The layering is unusual in that it is defined by an intercumulus mineral (augite) rather that by cumulus phases (feldspar).

Stop C6: Layered Eastern (Border) Gabbro

UTM coordinates 549199E 5398010N

1.7 km east of the Highway 626 and Highway 17 junction

Description: Layering in the Eastern Border Gabbro shows distinct variations in style, is usually parallel to the eastern contact of the gabbro, and dips 20° to 60° toward the center of the complex (Shaw, 1994, 1997). At this stop, layering strikes approximately north and dips west towards the rest of the complex at ~45°. This thickly layered sequence is underlain by massive gabbro near the contact with the Archean country rocks. The macrorhythmic layering is laterally discontinuous, pinching out over distances of 5 to 10m and contacts are sharp and conformable (Shaw, 1994, 1997). Rhythmic layering is modal and has been related to variation in the respective proportions of plagioclase (An_{60-35}), augite (Fo_{67-43}), minor orthopyroxene (En_{55-66}), and Fe-Ti-oxides by Lum (1973). Modal plagioclase varies from approximately 60 to 80% in the leucocratic layers and 20 to 35% in the meso- to melanocratic layers (Shaw, 1994). A second band of layered gabbro, separated from the first by massive gabbro, is exposed on top of the long rock cut (Photo 19). Here, the macrorhythmic layering (Photo 20) produces relatively thin (1 to 5cm) to medium thick (5 to 100cm) layers that can be traced for over 35m along



Photo 19. Macrorhythmic layering within the Eastern Border Gabbro. Photo credit M. Smyk.



Photo 20. Macrorhythmic modal layering within the Eastern Border Gabbro. Photo credit A. MacTavish.

strike. Layer contacts are sharp, locally scalloped and conformable. Trough cross-bedding has been noted on vertical faces by Shaw (1994). This stop is also close to the contact between the Eastern Border Gabbro and the Fe-rich augite syenite to the west. Pegmatitic syenite dykes intrude the gabbro at this locality and contain miarolitic cavities. McLaughlin (1990) has reported the presence of a variety of REE-bearing fluorocarbonates (bastnaesite, parisite, synchisite), Nb-bearing phases, and zircon in pegmatitic syenite with quartz, feldspar, and sodic amphibole.

Stop C7 (Alternate Stop): Eastern Contact of the Coldwell Complex

UTM coordinates 549656E 5396238N

3.3 to 3.6km east of the Highway 626 and Highway 17 junction

Description: A number of highway rock cuts and outcrops expose the eastern contact of the Coldwell Complex with the enclosing Archean greenstone belt country rocks. Center 1 gabbros, the oldest rocks of the complex, form a ring dyke that forms the eastern and northern margins of the complex where it is in contact with Archean supracrustal and granitoid rocks. The reverse magnetization of these gabbros (Lilley, 1964) produces prominent magnetic "lows" on aeromagnetic maps. The most recent and comprehensive study of the Eastern Border Gabbro was conducted by Shaw (1994, 1997) who noted that more than 90% of the unit consists of layered gabbro.

At this location, varitextured, unlayered Eastern Border Gabbro is in contact with, and contains numerous xenoliths of, Archean metasedimentary rocks. This has produced hybrid and contaminated phases and rheomorphic breccia. Crosscutting Center 1 syenite dikes are commonly pegmatitic. Amethystine quartz, calcite, and molybdenite occur in vugs within this chaotic contact zone.

Disseminated iron- and copper-sulphides occur in biotite-rich, varitextured gabbro (Dunlop Occurrence), which has experienced sporadic exploration since the discovery of copper in the early 1950's. It was last drilled in 1992 by Noranda Inc. with the best assay intervals grading 0.35% Cu/6.0m and 0.42% Cu/4.0m, respectively (Resident Geologist's Files, Thunder Bay). A grab sample of rusty-weathering, moderately magnetic, fine- to medium-grained gabbro with coarse biotite and blebby chalcopyrite graded 5090ppm Cu, 494ppm Ni, 241ppm Zn, 8ppb Pd, 2ppb Pt and 22ppb Au (ibid). Overgrown pits are located just inside the tree line, west of the highway (UTM 549575E, 5396290N).

Shaw (1994; 1997), Walker et al. (1993a, 1993b, 1993c), Currie (1980), and Tucker (1995) have documented a number of occurrences of rheomorphic breccia associated with the Eastern Border Gabbro along its intrusive, basal contact with the Archean supracrustal country rocks. Breccia units are characterized by chaotic flow fabrics that surround flow-oriented clasts situated in a medium-grained, granitic matrix. This unit has been somewhat enigmatic, having been alternatively described by earlier workers as conglomerate and ignimbrite (Resident Geologist's Files, Thunder Bay). Similar exposures of this map unit also occur along the western contact of the complex, north of Middleton (cf. Wilkinson, 1983).

Locally, pods of breccia vary from 20 to 75m in width and are up to 250m long. The breccia exposed along Highway 17 at this site contains mainly hornfelsed Archean clastic metasedimentary and metavolcanic rocks and massive vein quartz. In the vicinity of Two Duck Lake, the breccia contains fine-grained gabbro clasts (Tucker, 1995). The breccia varies from clast- to matrix-supported; the matrix consists of equigranular quartz, feldspar, and minor biotite, clino- and orthopyroxene, and opaque minerals; and tourmaline and prehnite overgrowths have been noted (Tucker, 1995). Rounded to angular clasts range in size from 0.5 to over 100cm and locally have developed 1 to 2cm wide, chlorite-rich reaction rims that are thickest where they are matrix-supported (Shaw, 1994). Magnetite and quartz¬feldspar-tourmaline veins cut both matrix and clasts. Quartzo-feldspathic rinds and crosscutting veinlets have been interpreted to be the result of partial melting of the felsic material during assimilation. The close association between rheomorphic breccia and the Eastern Border Gabbro suggests that the intrusion of the gabbro led to the brecciation and partial melting of the country rocks (Shaw, 1994, 1997; Tucker, 1995).

PART 2: Marathon Cu-PGM Deposit

David Good and John McBride

Introduction to the Marathon Deposit

The Cu-PGM sulphide mineralization of the Marathon deposit is hosted by the Two Duck Lake Gabbro, the latest mafic intrusive event and consequently the most continuous gabbroic body within the Eastern Gabbro Suite at the Marathon deposit.

The Eastern Gabbro Suite, located around the eastern and northern margin of the Coldwell, was composed initially of a thick sequence of tholeiitic basalt that was subsequently intruded by a much larger volume of leucocratic to ultramafic intrusions that caused contact metamorphism of the basalt to pyroxene-hornfels grade (Good et al., 2015). All of these units are represented at the Marathon deposit (Fig. 1).

The topography of the Coldwell is characterized by deep valleys and steep cliffs that form strong surface lineaments. Two lineaments at the Marathon deposit correspond to north dipping normal faults (north side down) with displacement of approximately 50 metres.

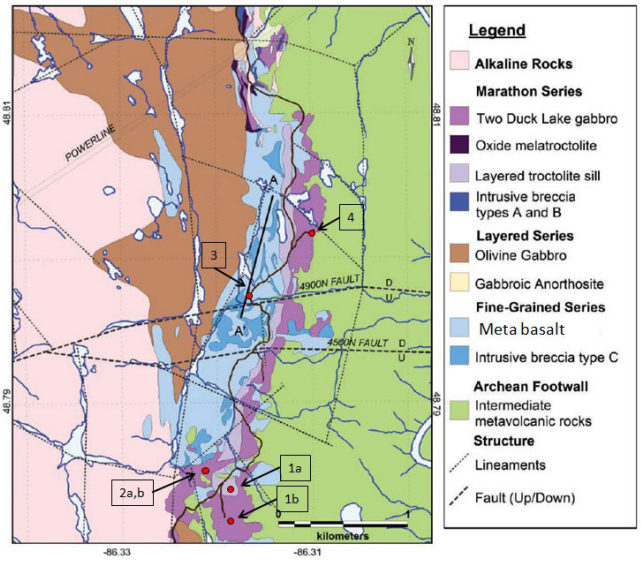


Figure 1. Geology of the Marathon deposit (after Good et al., 2015) highlighting location of field trip stops. Stops are marked with red dot and labelled as stop 1a, etc. Note two normal faults that correspond to strong surface lineaments (dashed lines)

Two Duck Lake Intrusion

The Two Duck Lake intrusion is irregular in shape and elongated north-south (Fig. 2). The dip at the east contact is variable from nearly flat (at the south end) to vertical and locally overturned where the footwall overhangs the intrusion. The intrusion is composed of coarse-grained to pegmatitic olivine gabbro and troctolite. Modal layering is rare.

The TDL gabbro was interpreted to have formed by intrusion of a nearly homogeneous plagioclase crystal mush by Good and Crocket (1994). But recent work suggests the intrusion formed by accumulation of several pulses of magma in a conduit setting (Good,

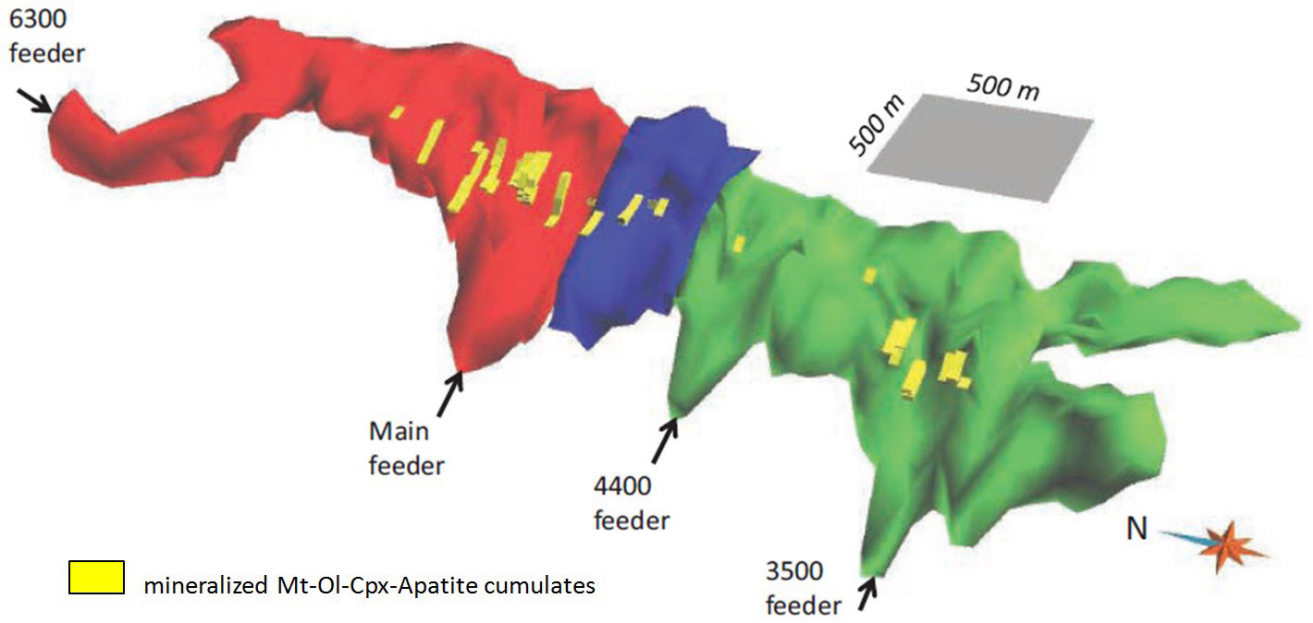


Figure 2. 3d isometric view of the Two Duck Lake intrusion (from Good et al., 2015). Three coloured portions indicate blocks that were offset by normal faults with north side down by up to 60 metres. Note that numerous intrusions of mineralized Mt-Ol-Cpx-Ap rock (yellow) occur in the vicinity of major feeder zones, but those above the 6300 feeder but are not shown.

2010; Ruthart, 2012; Good et al., 2015; and Shahabi Far, 2017).

Multiple feeder channels were inferred by Good et al. (2015) to occur in the vicinity of several coincident features, including: deep V- or U-shaped channels in the footwall contact; topographic lineaments; very thick mineralized intervals; and irregular-shaped intrusions of olivine-magnetite-clinopyroxene-apatite.

Age relationships

Evidence suggests that all units in the Coldwell were emplaced within a short time interval between about 1108 Ma and 1105 Ma (Heaman and Machado, 1992; Good et al. in preparation). Age relationships, based on cross-cutting contacts and U-Pb age dating for the various mafic units are summarized in Figure 3.

The metabasalt is interpreted to correlate with Mamainse Point Volcanic Group 1 (Fig. 4) which was emplaced at approximately 1108 Ma (Keays and Lightfoot, 2015).

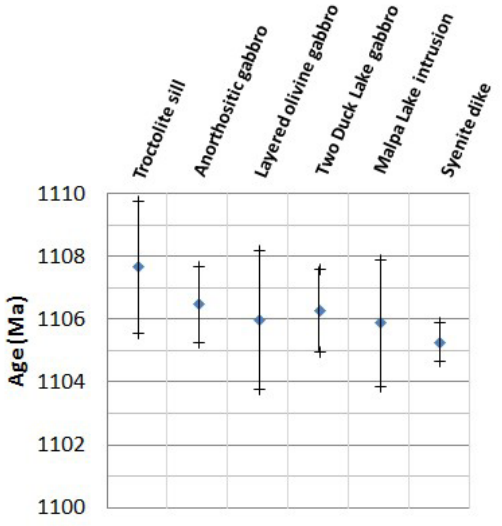
The metabasalt was subsequently intruded by the following units, listed in order from oldest to youngest, layered troctolite sill of the Marathon Series, gabbroic anorthosite and olivine gabbro of the Layered Series, Two Duck Lake gabbro and various ultramafic units composed of magnetite +/- olivine +/- apatite +/- clinopyroxene of the Marathon Series, Malpa Lake intrusion, and syenite.

Mineralization

Disseminated sulfide mineralization is hosted by the Two Duck Lake gabbro and associated breccia (Fig. 5) and occurs within several thick and continuous shallow-dipping lenses that parallel the footwall contact. The disseminated sulphides are concentrated in troughs along the footwall contact that approximately follow topographic lineaments (Fig. 6). The lenses are referred to as the Footwall, Main, and Hangingwall zones and the W Horizon. Sulfides in the Footwall, Main, and Hanging-wall zones consist predominantly of chalcopyrite and pyrrhotite with minor amounts of cubanite, bornite, pentlandite, cobaltite, and pyrite. Sulfides occur interstitial to primary silicates and also in association with hydrous silicates such as amphibole, chlorite, and minor serpentine (Watkinson and Ohnenstetter, 1992; Samson et al., 2008). Chalcopyrite occurs as separate grains or as rims on pyrrhotite grains. Some chalcopyrite is intergrown with highly calcic plagioclase (An_{70}–An_{80}) in replacement zones at the margins of plagioclase crystals (Good and Crocket, 1994; Shahabifar, 2016).

The W horizon is characterised by extreme PGE enrichment relative to Cu with several 2m thick drill hole intersections having 20 to 70 ppm Pd and Cu/Pd as low as 3 (e.g., Fig. 7, top and bottom photos). The best intersection contains 34 ppm Pd and 9.6 ppm Pt over 10 m. Mass balance considerations, assuming initial magma contained 10 ppb Pd, would require a magma column on the order of 34 km to generate the 34 ppm Pd in this interval.

The W Horizon is commonly difficult to identify in drill core because it typically contains only trace sulfides, but if sulfides are present, they consist of



(after Good, Dunning, Epstein and Dunsworth, in preparation)

	unit	age	+/-	grains	note
youngest	Syenite dike	1105.3	0.6	6Z	
	Malpa Lake intrusion	1105.9	2	7Z	
	Two Duck Lake gabbro	1106.3	1.3	2B, 3Z	Cross cuts LS
	Layered olivine gabbro	1106.0	2.2	4B	
	Anorthositic gabbro	1106.5	1.2	2B	
	Troctolite sill	1107.7	2.1	3B	
oldest	Metavolcanic rocks				Correlate with MPVG1

B - represents baddeleyite grain
Z - represents zircon grain

Figure 3. Relative timing of mafic metavolcanic and intrusive events (age dates after Good et. al, in preparation) in the Eastern Gabbro Suite of the Coldwell Alkaline Complex.

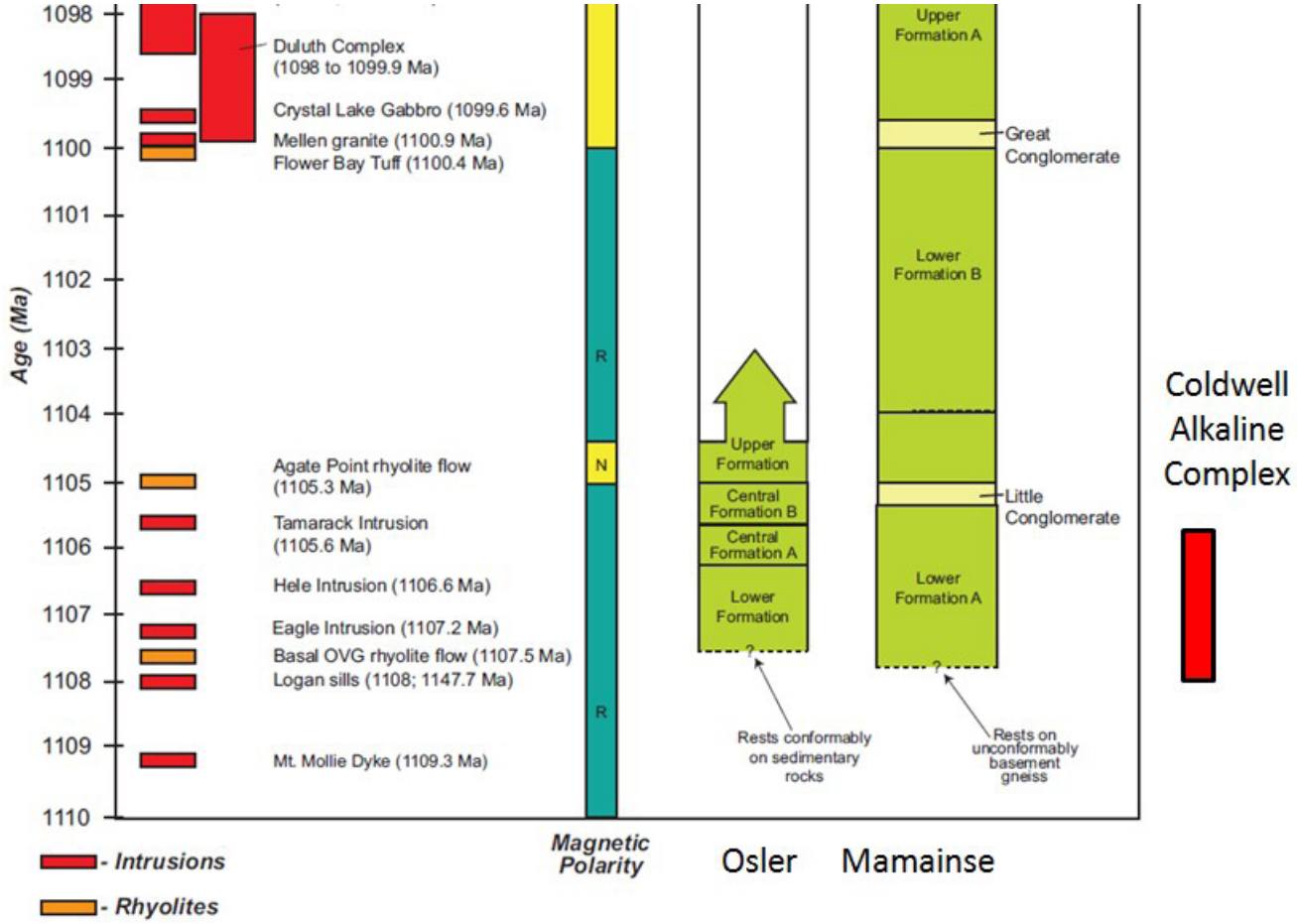


Figure 4. Correlation diagram showing range of ages for the Coldwell units compared to volcanic and intrusive units in the Midcontinent Rift (after Keays and Lightfoot, 2015).

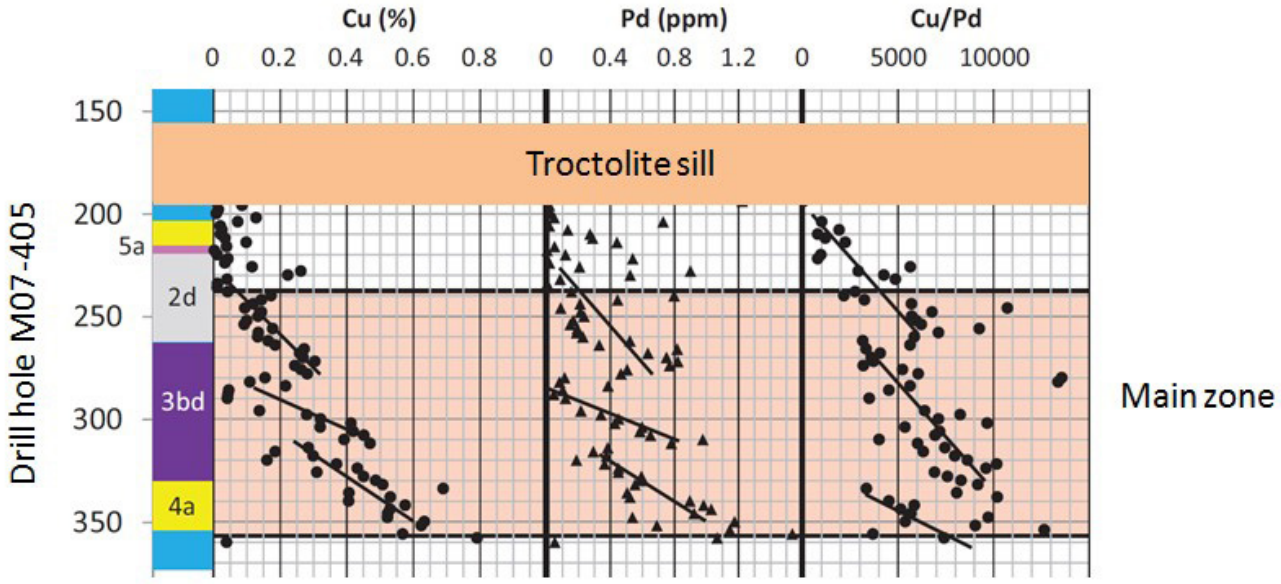


Figure 5. Stratigraphic section through the Main zone and overlying troctolite sill. Note the saw tooth pattern for Cu, Pd and Cu/Pd indicating individual pulses of sulphide-bearing crystal slurry. Unit 2d, breccia of metabasalt blocks and Two Duck Lake gabbro; unit 3bd, coarse grained ophitic and pegmatitic Two Duck Lake gabbro; unit 4a, breccia of footwall blocks and Two Duck Lake gabbro (from Good et al., 2015).

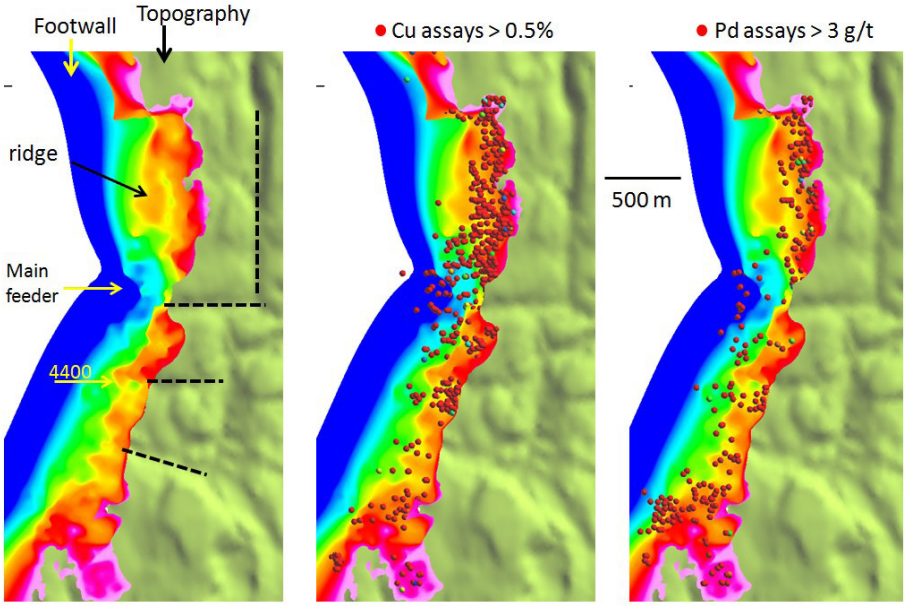


Figure 6. Three versions of top view for the Marathon deposit showing 3d topography (green surface) and contoured footwall surface models. Note the troughs and ridges (left hand image) correspond to surface lineaments. Note the higher-grade assays for Cu (>0.5%) and Pd (>3 ppm) are aligned within zones that parallel troughs within the 3d footwall surface model.

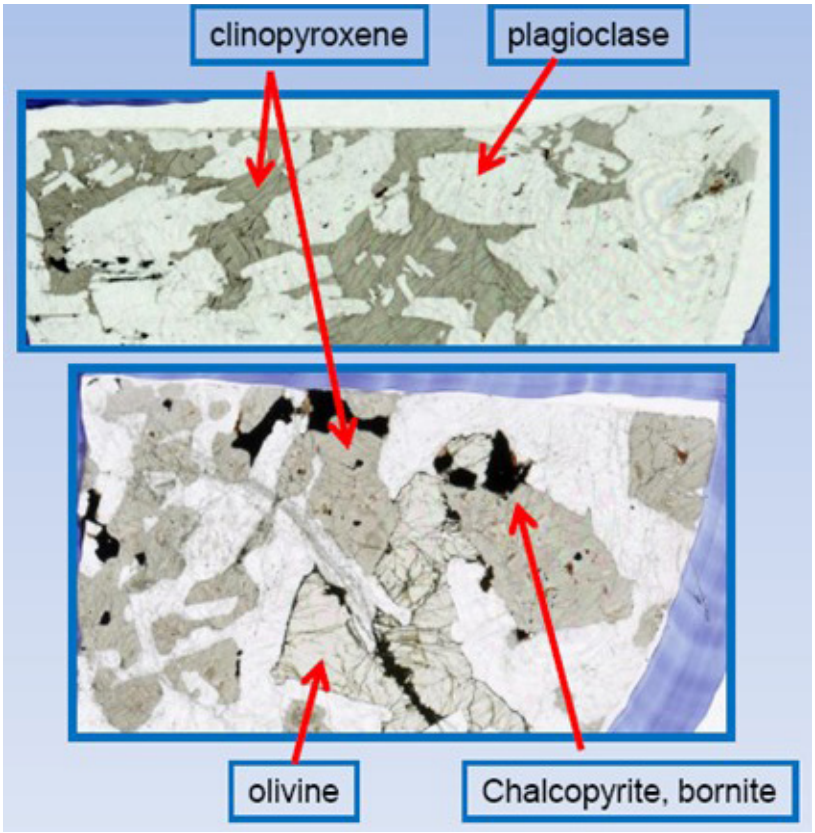


Figure 7. PGE rich samples from the W Horizon contain fresh clinopyroxene, olivine and plagioclase. Top photo sample with 107 ppm Pd+Pt+Au and 203 ppm Cu. Bottom photo sample with 70 ppm Pd+Pt+Au and 0.86 % Cu.

chalcopyrite and bornite with minor pyrrhotite and trace amounts of pentlandite, cobaltite, and pyrite (Ruthart, 2012).

Deposit Model

Exploration strategies in the Coldwell are based on the conduit model and a schematic magmatic plumbing system such as that envisioned by Barnes et al. (2016)

(Fig. 8). Evidence for a magma conduit setting at the Marathon deposit were described by Good et al. (2015), and include:

- association with metavolcanic rocks
- fault control (mineralization parallel to topographic lineaments)
- brecciation and assimilation
- accumulation in trough setting
- flow through PGE upgrading
- tube shaped intrusion
- gravity driven back flow (Mt-Ol-Cpx-Ap cumulates)
- high heat flux (wide zone of pyroxene-hornfels grade metavolcanic rocks)

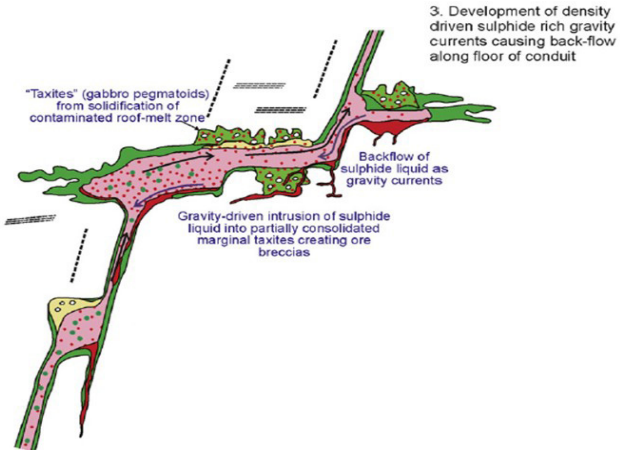


Figure 8. Step 3 of schematic illustration for magmatic plumbing system (after Barnes et al., 2016)

Field Trip Stops

Stop 1a: South end of Troctolite Sill (Figs. 10b)

UTM coordinates 549995E 5403560N

Trench exposure with coarse-grained mottled augite troctolite shows large fresh oikocrysts of olivine (brown), clinopyroxene (black) and magnetite (black) and subhedral plagioclase (white).

The layered troctolite sill is an important marker horizon because it occurs just above the top of the Main Mineralized zone and is an indicator of the relative fault offset that occurred along E-W–trending normal faults at 5404500 and 5404900 North (Fig. 1).

The sill dips moderately west at the north end, but flattens out in the south to sub-horizontal (Fig. 9b). Note layering is approximately east west at Stop 1a, consistent with rotation of sill from west dipping in the north to sub horizontal or north dipping in the south.

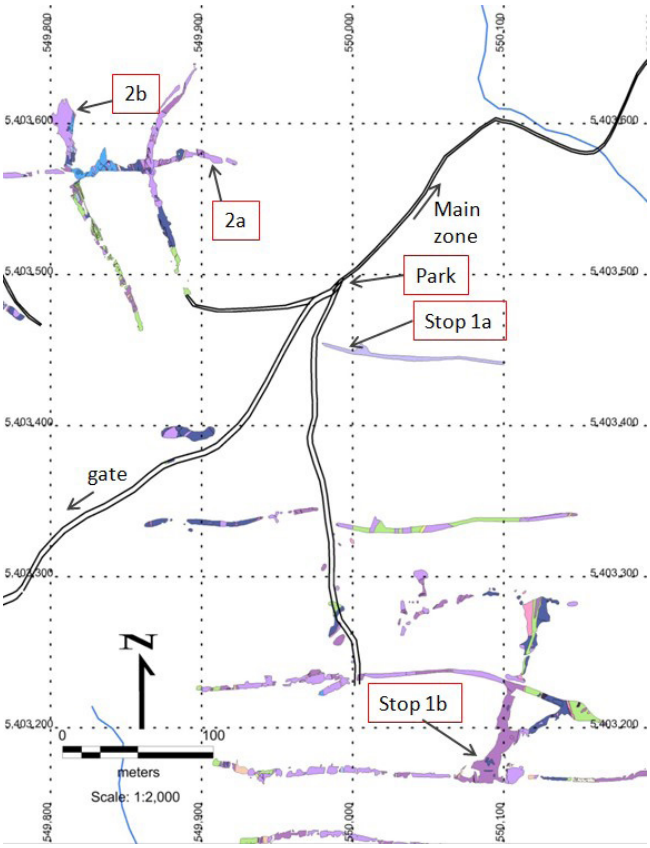


Figure 9. Map at south end of Marathon deposit showing location of stops 1 and 2.

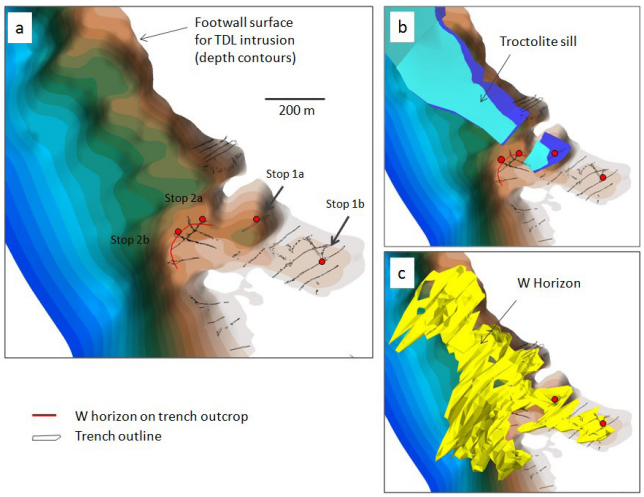
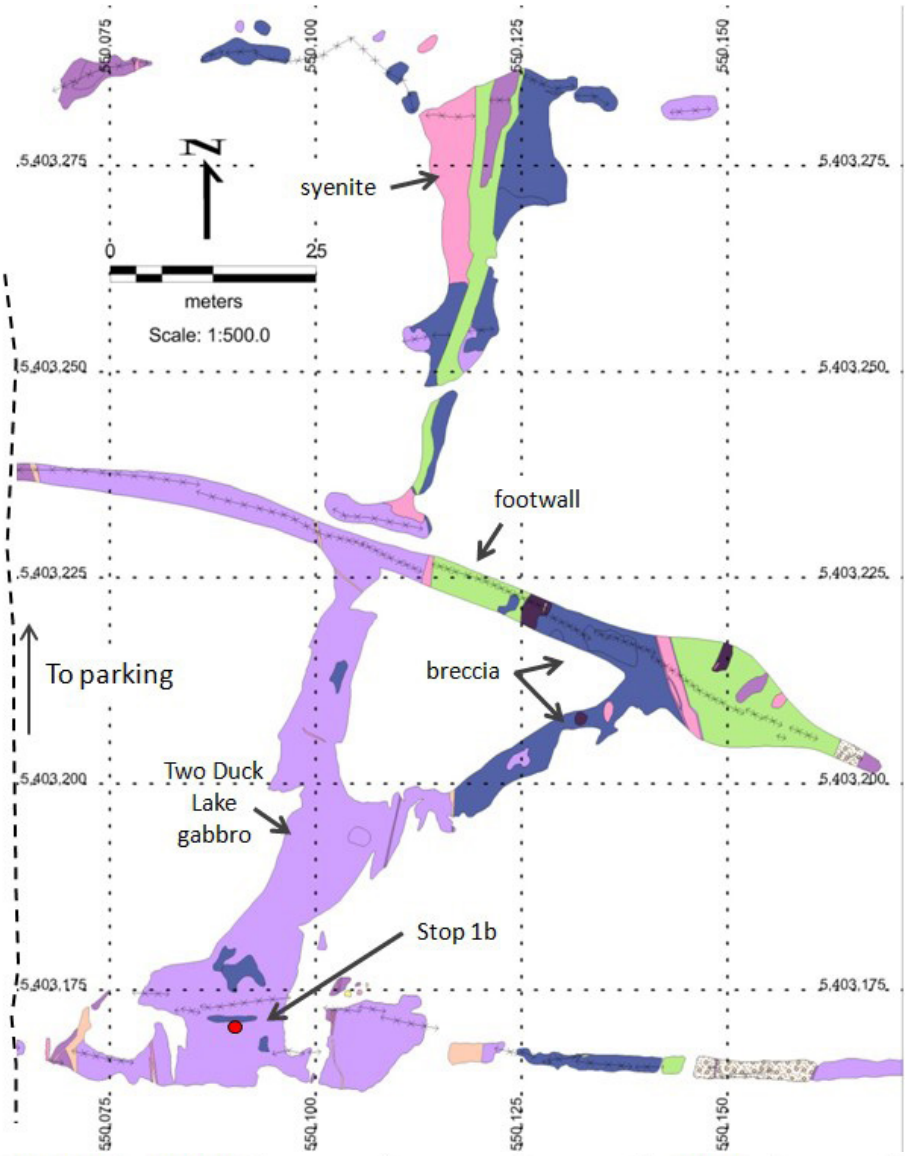


Figure 10. 3d image (iso view) of geology at south end of Marathon deposit showing location of stops 1 and 2 on trenched outcrops (black polygons): (a) shows orientation of footwall surface troughs approximately perpendicular to contact, and the red centre line of the W horizon at surface on the splat trench; (b) top (light blue) and bottom surfaces (dark blue) of the troctolite sill. Gap in the troctolite sill surfaces represents location where W Horizon and TDL gabbro cuts the through the sill; (c) surface model of W Horizon (yellow).

Stop 1b: Southeast corner of Marathon deposit (Figs. 10 and 11)

UTM coordinates 550090E 5403395N

Trench outcrop exposure of Two Duck Lake gabbro within a shallow dipping bowl-shaped depression in the footwall (Fig. 10a) includes W Horizon and Main zone type mineralization.



Sample #	Interval (M)	Pd	Pt	Au	Total PGM	Cu
		g/t	g/t	g/t	g/t	%
44	1.53	5.20	1.44	0.70	7.34	0.86
45	1.45	1.92	0.68	0.17	2.77	0.13
46	1.63	2.15	0.71	0.22	3.08	0.23
47	1.42	3.26	0.69	0.35	4.29	0.50
48	1.15	3.90	1.03	0.56	5.49	0.36
49	1.29	4.48	1.13	0.33	5.95	0.47
50	1.03	2.51	0.56	0.17	3.23	0.50
51	1.1	2.60	0.81	0.26	3.67	0.47
52	1.53	1.11	0.39	0.09	1.58	0.26
53	1.48	2.91	0.74	0.21	3.86	0.50
54	1.51	0.10	0.06	0.02	0.19	0.04
55	1.75	0.25	0.11	0.04	0.40	0.04
56	1.68	1.38	0.42	0.12	1.92	0.24

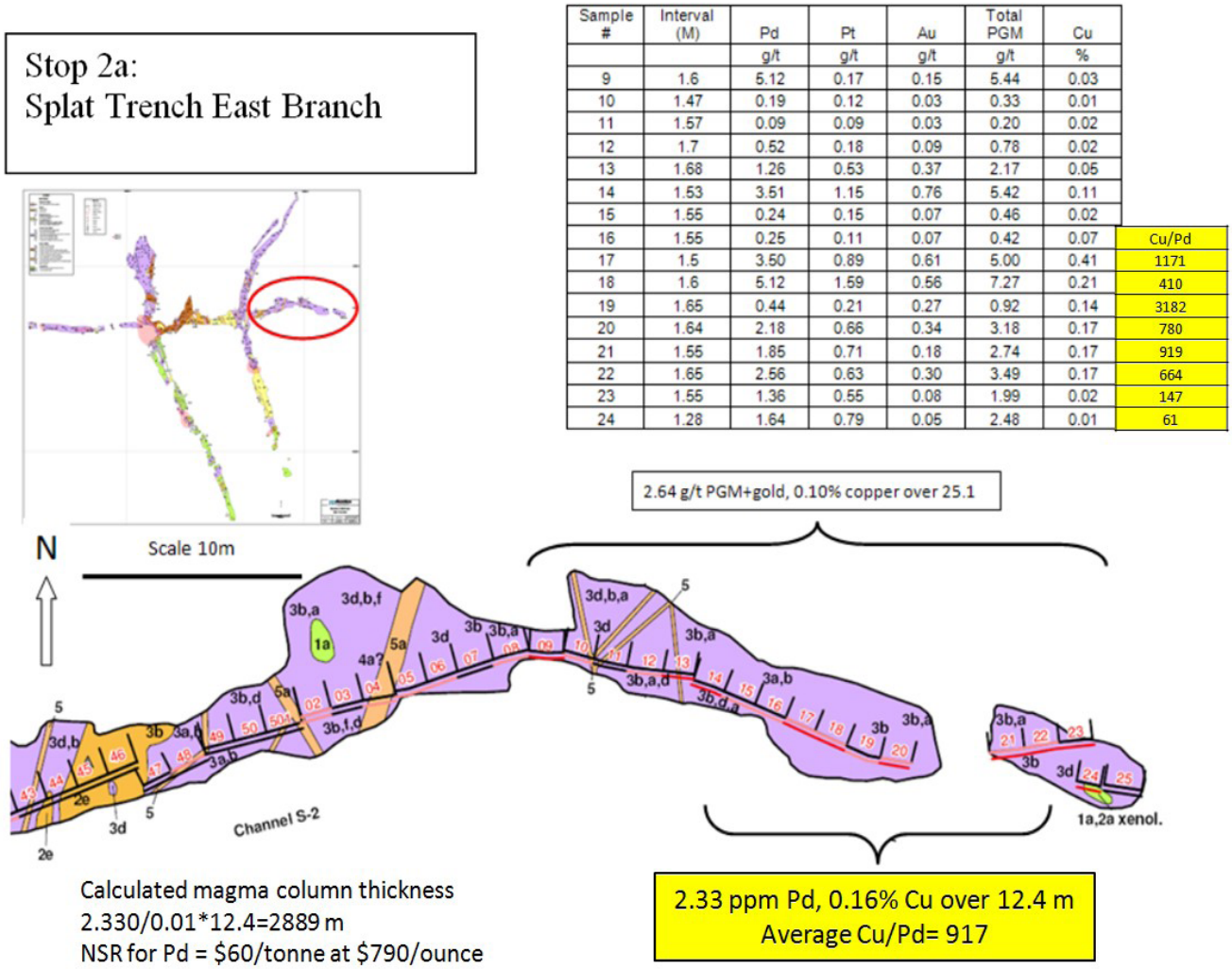
Figure 11. Plan map of trench at the southeastcorner of the Marathon deposit including assay table for samples 44 to 56 located in channel immediately north of the historic trench. Red circle marks location of historic trench (ca. mid 1960's) with high copper mineralization. The unit was not assayed for Pd until 2005.

The channel sample located just north of the red circle returned assays of 3.37 ppm Pd+Pt+Au, and 0.35% Cu over 18.6 m. East-west layering in TDL gabbro is visible just south of trench. Outcrop shows textural evidence for cross cutting intrusions of subophitic olivine gabbro.

Stop 2a: Splat trench and the W Horizon (Fig.12)

UTM coordinates 549900E 5403804N

Stops 2a and 2b are located on the east and northwest branches of the splat trench, respectively, and highlight two locations along the W horizon as it drapes over top of a north plunging ridge in the footwall.

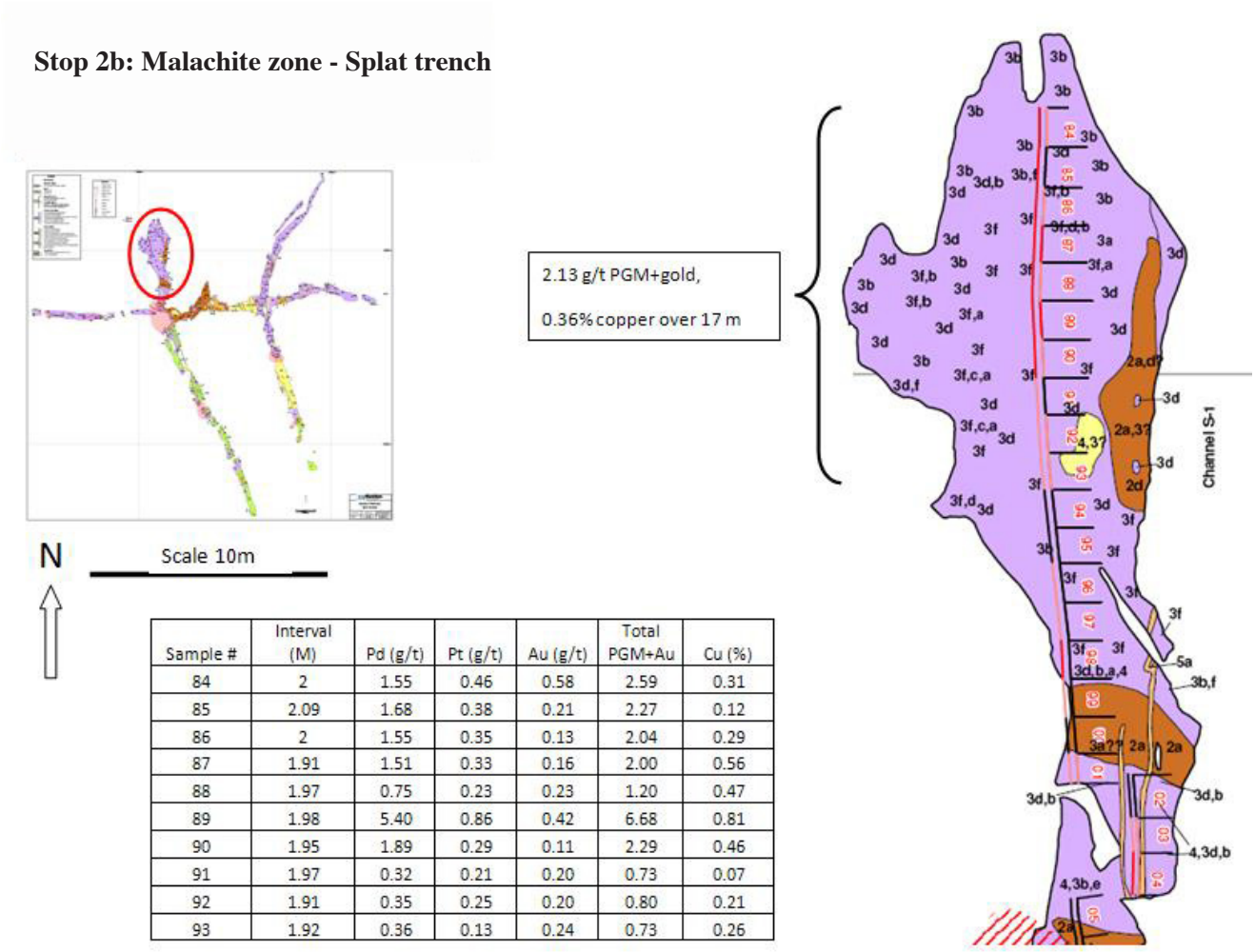


Sample #	Interval (M)	Pd	Pt	Au	Total PGM	Cu	
		g/t	g/t	g/t	g/t	%	
9	1.6	5.12	0.17	0.15	5.44	0.03	
10	1.47	0.19	0.12	0.03	0.33	0.01	
11	1.57	0.09	0.09	0.03	0.20	0.02	
12	1.7	0.52	0.18	0.09	0.78	0.02	
13	1.68	1.26	0.53	0.37	2.17	0.05	
14	1.53	3.51	1.15	0.76	5.42	0.11	
15	1.55	0.24	0.15	0.07	0.46	0.02	
16	1.55	0.25	0.11	0.07	0.42	0.07	Cu/Pd
17	1.5	3.50	0.89	0.61	5.00	0.41	1171
18	1.6	5.12	1.59	0.56	7.27	0.21	410
19	1.65	0.44	0.21	0.27	0.92	0.14	3182
20	1.64	2.18	0.66	0.34	3.18	0.17	780
21	1.55	1.85	0.71	0.18	2.74	0.17	919
22	1.65	2.56	0.63	0.30	3.49	0.17	664
23	1.55	1.36	0.55	0.08	1.99	0.02	147
24	1.28	1.64	0.79	0.05	2.48	0.01	61

Figure 12. Plan map of the stripped outcrop on the east arm of the splat trench highlights the distinct coarse-grained to pegmatitic subophitic olivine gabbro of the Two Duck Lake intrusion. Stratigraphic top of the section is to the northeast (compare to Fig. 9a and 9c). Note the large xenolith/breccia of metavolcanic rock along the east edge of the outcrop. Codes: 3a, medium-grained (1-5 mm) Two Duck Lake gabbro; 3b, coarse-grained (5mm to 1cm); 3d, pegmatitic gabbro; 3f, magnetite and clinopyroxene rich gabbro; 4, breccia; 2a, metavolcanic rock. Mineralization consists of disseminated cpy, bn and minor po. Assay table for samples 9 to 24 within the saw-cut channel on the outcrop have an average grade of 2.64 g/t Pd+Pt+Au and 0.1% Cu over 25.1 m.

Stop 2b: Splat trench and the W Horizon (Fig. 13)

UTM coordinates 549810E 5403825N



Sample #	Interval (M)	Pd (g/t)	Pt (g/t)	Au (g/t)	Total PGM+Au	Cu (%)
84	2	1.55	0.46	0.58	2.59	0.31
85	2.09	1.68	0.38	0.21	2.27	0.12
86	2	1.55	0.35	0.13	2.04	0.29
87	1.91	1.51	0.33	0.16	2.00	0.56
88	1.97	0.75	0.23	0.23	1.20	0.47
89	1.98	5.40	0.86	0.42	6.68	0.81
90	1.95	1.89	0.29	0.11	2.29	0.46
91	1.97	0.32	0.21	0.20	0.73	0.07
92	1.91	0.35	0.25	0.20	0.80	0.21
93	1.92	0.36	0.13	0.24	0.73	0.26

Figure 13. Plan map of the northwest outcrop on the splat trench highlights the distinct coarse-grained to pegmatitic subophitic olivine gabbro of the Two Duck Lake intrusion. Stratigraphic top of the section is to the north (compare to Fig. 9a and 9c). Note the large xenolith/breccia zone of metavolcanic rock along the east edge of the outcrop. Codes: 3a, medium-grained (1-5 mm) Two Duck Lake gabbro; 3b, coarse-grained (5mm to 1cm); 3d, pegmatitic gabbro; 3f, magnetite and clinopyroxene rich gabbro; 4, breccia; 2a, metavolcanic rock. Mineralization consists of disseminated cpy, bn and minor po. Assay table for samples 84 to 93 within the saw-cut channel on the outcrop have an average grade of 2.13 g/t Pd+Pt+Au and 0.36% Cu over 17 m.

References

Alexander, M. 2007. The mineralogy of NYF pegmatites from the Coldwell Alkaline Complex, northwestern Ontario; unpublished MSc thesis, Lakehead University, Thunder Bay, Ontario.

Barnes, S.J., Cruden, A.R., Arndt N., Saumur B.M. 2016. The mineral system approach applied to magmatic Ni–Cu–PGE sulphide deposits, Ore Geology Reviews 76, 296-316.

Barrie, C. Tucker, MacTavish, A.D., Walford, P.C., Chataway, R., and Middaugh, R., 2002. Contact-type and magnetite reef-type Pd-Cu mineralization in ferroan olivine gabbros of the Coldwell Complex, Ontario; in The Geology, Geochemistry, Mineralogy and Mineral Beneficiation of Platinum-Group Elements. Edited by L.J. Cabri; Canadian Institute of Mining and Metallurgy and Petroleum, Special Volume 54, p.321-337.

Bell, K. and Blenkinsop, J. 1980. Grant 42: Ages and initial 87Sr-86Sr ratios from alkaline complexes of Ontario; in Geoscience Research Grant Program, Summary of Research, 1974-1980, Ontario Geological Survey, Miscellaneous Paper 93, p.16-23.

Bohay, T.J. 1997. The Coldwell alkaline complex, Ontario: Magmatic affinity as determined by an isotopic

and geochemical study; unpublished MSc thesis, McMaster University, Hamilton, Ontario, 135p.

Coates, M.E. 1970. Geology of the Killala–Vein lakes area, Ontario; Ontario Department of Mines, Geological Report 81, 35p.

Good, D.J. 1992. Genesis of copper-precious metal sulfide deposits in the Port Coldwell alkalic complex, Ontario; unpublished PhD thesis, McMaster University, Hamilton, Ontario, 203p.

Good, D.J. 1993. Genesis of copper-precious metal sulfide deposits in the Port Coldwell Alkalic Complex, Ontario Geoscience Research Grant Program, Grant No. 341, Ontario Geological Survey, Open File Report 5839, 23.

Good, D.J. and Crockett, J.H. 1994a. Genesis of the Marathon Cu-platinum-group element deposit, Port Coldwell alkaline complex, Ontario: A Midcontinent Rift-related magmatic sulfide deposit; Economic Geology, v.89, p.131-149.

Good, D.J. and Crockett, J.H., 1994b. Origin of albite pods in the Geordie Lake gabbro, Port Coldwell alkaline complex, northwestern Ontario: Evidence for late-stage hydrothermal Cu-Pd mineralization; The Canadian Mineralogist, v.32, p.681-701.

Good, D.J, Epstein, R., McLean, K., Linnen, R.L., & Samson, I.M. 2015. Evolution of the Main Zone at the Marathon Cu-PGE Sulfide Deposit, Midcontinent Rift, Canada: Spatial Relationships in a Magma Conduit Setting, Econ Geol v.110, p.983-1008.

Hauck, S.A., Severson, M.J, Zanko, L., Barnes, S.-J., Morton, P., Alminas, H., Foord, E.E. and Dahlberg, E.H. 1997. An overview of the geology and oxide, sulfide and platinum-group element mineralization along the western and northern contacts of the Duluth Complex; Geological Society of America, Special Paper 312, p.137-185.

Heaman, L.M., Easton, R.M., Hart, T.R., Hollings, P., MacDonald, C.A. and Smyk, M. 2007. Further refinement to the timing of Mesoproterozoic magmatism, Lake Nipigon Region, Ontario; Canadian Journal of Earth Sciences, v.44, no.8, p.1055-1086.

Heaman, L.M. and Machado, N. 1987. Isotope geochemistry of the Coldwell alkaline complex: 1. U-Pb studies on accessory minerals; Geological Association of Canada–Mineralogical Association of Canada, Joint Annual Meeting, Saskatoon, Saskatchewan, Program with abstracts, p.54.

Heaman, L.M. and Machado, N 1992. Timing and origin of the Midcontinent Rift alkaline magmatism, North America: Evidence from the Coldwell complex; Contributions to Mineralogy and Petrology, v.110, p.289-303.

Hinz, P. and Landry, R. 1994. Industrial mineral occurrences and deposits in northwestern Ontario; Ontario Geological Survey, Open File Report 5889, 145p.

Keays, R.R. and Lightfoot, P.C. 2015. Geochemical Stratigraphy of the Keweenawan Midcontinent Rift Volcanic Rocks with Regional Implications for the Genesis of Associated Ni, Cu, Co, and Platinum Group Element Sulfide Mineralization, Econ Geol, 110, 1235-1267.

Kerr, H.L. 1910a. Geological map of part of the north shore of Lake Superior, District of Thunder Bay; Ontario Bureau of Mines, Annual Report Map 19B, scale 1:63 360.

Kerr, H.L. 1910b. Nepheline syenites of Port Coldwell; Ontario Bureau of Mines, Annual Report, v.19, p.194-232.

Kissin, S.A. and McCuaig, T.C. 1988. The genesis of silver vein deposits in the Thunder Bay area, northwestern Ontario: Geoscience Research Grant Program, Summary of Research, 1987-1988; Ontario Geological Survey, Miscellaneous Paper 140, p.146-156.

Klasner, J.S., Cannon, W.F. and Van Schmus, E.R. 1982. The Pre-Keweenawan tectonic history of the southern Canadian Shield and its influence on the formation of the Midcontinent Rift; in Geology and Tectonics of the Lake Superior Basin, Geological Society of America, Memoir 156, p.27-46.

Lewchuk, M.T. and Symons, D.T.A. 1990. Paleomagnetism of the late Precambrian Coldwell complex, Ontario, Canada; Tectonophysics, v.184, p.73-86.

Laderoute, D.G. 1987. The petrology, geochemistry, and petrogenesis of alkaline dyke rocks from the Coldwell Alkaline complex; unpublished M.Sc. Thesis, Lakehead University, Thunder Bay, Ontario, 89p. Tectonophysics, v.184, p.73-86.

Lilley, F.E.M. 1964. An analysis of the magnetic features of the Port Coldwell intrusion; unpublished BSc thesis, University of Western Ontario, London, Ontario, 89p.

Lukosius-Sanders, J. 1988. Petrology of the syenites from Center III of the Coldwell alkaline complex, northwestern Ontario; unpublished MSc thesis, Lakehead University, Thunder Bay, Ontario, 141p.

Lum, H.K. 1973. Petrology of the eastern gabbro and associated sulphide mineralization of the Coldwell alkaline complex, Ontario; unpublished BSc thesis, Carleton University, Ottawa, Ontario, 68p.

MacTavish, A. 2000. A new style of PGE mineralization within the Coldwell alkaline complex, northwestern Ontario; Ontario Exploration and Geoscience Symposium, Toronto, December 11-12, 2000, Speaker Abstracts, p.3.

MacTavish, A., Lukosius-Sanders, J. and Jowett, R. 1987. Geological report of the Joa Option (Geordie Lake

property), St. Joe Canada Inc.; unpublished report, Resident Geologist's Files, Thunder Bay, 7p.

MacTavish, A Smyk, M., Good, D., and McBride, J., 2017. Transect Through the Coldwell Alkaline Complex In; MacTavish, A. and Hollings, P. (Eds.), Institute on Lake Superior Geology Proceedings, 63rd Annual Meeting, Wawa, Ontario, Part 2 - Field trip guidebook, v.63, part 2, 1-44.

McLaughlin, R.M. 1990. Accessory rare metal mineralization in the Coldwell alkaline complex, northwest Ontario; unpublished MSc thesis, Lakehead University, Thunder Bay, Ontario, 123p.

Miller, J.D., Jr., Nicholson, S.W., and Cannon, W.F. 1995. The Midcontinent rift in the Lake Superior region, in Miller, J.D., Jr., ed., Field trip guidebook for the geology of ore deposits of the Midcontinent rift in the Lake Superior region; Minnesota Geological Survey Guidebook Series, no. 20, p.1-22.

Mitchell, R.H. and Platt, G. R. 1978. Mafic mineralogy of ferroaugite syenite from the Coldwell alkaline complex, Ontario, Canada; Journal of Petrology, v.19, p.627-651.

Mitchell, R.H. and Platt, G. R. 1982a. The Coldwell alkaline complex; in Field Trip Guidebook, Proterozoic geology of the northern Lake Superior area, Geological Association of Canada–Mineralogical Association of Canada, Joint Annual Meeting, Winnipeg, Manitoba, p.42-61.

Mitchell, R.H. and Platt, G. R. 1982b. Mineralogy and petrology of nepheline syenites from the Coldwell alkaline complex, Ontario, Canada; Journal of Petrology, v.23, p.186-214.

Mitchell, R.H. and Platt, G. R. 1994. Aspects of the geology of the Coldwell alkaline complex: Field trip A2, Geological Association of Canada–Mineralogical Association of Canada, Joint Annual Meeting, Waterloo, Ontario, 36p.

Mitchell, R.H., Platt, G.R., Lukosius-Sanders, J., Artist-Downey, M. and Moogk-Pickard, S. 1993. Petrology of syenites from Center III of the Coldwell alkaline complex, northwestern Ontario, Canada; Canadian Journal of Earth Sciences, v.30, p.145-158.

Mitchell, R.H., Platt, R.G. and Cheadle, S.P. 1983. A gravity study of the Coldwell complex, northwestern Ontario, and its petrological significance; Canadian Journal of Earth Sciences, v.20, p.1631-1638.

Mulja, T. 1989. Petrology, geochemistry, sulphide- and platinum-group element mineralization of the Geordie Lake intrusion; unpublished MSc thesis, Lakehead University, Thunder Bay, Ontario, 234p.

Mulja, T. and Mitchell, R.H. 1990. Platinum-group minerals and tellurides from the Geordie Lake intrusion, Coldwell complex, northwestern Ontario; Canadian Mineralogist, v.28, p.489-501.

Mulja, T. and Mitchell, R.H. 1991. The Geordie Lake intrusion, Coldwell Complex, Ontario: Palladium- and tellurium-rich disseminated sulfide occurrence derived from an evolved tholeiitic magma; Economic Geology, v.86, p.1050-1069.

Nicol, D.N. 1990. Assimilation of basic xenoliths with Center 3 syenites of the Coldwell Complex, Ontario; unpublished MSc thesis, Lakehead University, Thunder Bay, Ontario, 59p.

Ohnenstetter, D., Watkinson, D.H. and Dahl, R. 1991. Zoned hollingworthite from the Two Duck Lake intrusion, Coldwell complex, Ontario; American Mineralogist, v.76, p.1694-1700.

Penczak, R.S. 1992. Petrology and mineral chemistry of the Middleton copper occurrence of the Western gabbro, Coldwell alkaline complex, Ontario; unpublished BSc thesis, University of Waterloo, Ontario.

Pollock, S.J. 1987. The isotopic geochemistry of the Prairie Lake carbonatite complex; unpublished MSc thesis, Carleton University, Ottawa, Ontario, 71p.

Potter, E.G. 2004. The rare and exotic mineralogy of the western subcomplex of the Dead Horse Creek diatreme, northwestern Ontario; unpublished MSc thesis, Lakehead University, Thunder Bay, Ontario.

Puskas, F.W. 1967. Port Coldwell area; Ontario Department of Mines, Preliminary Map P.114, scale 1:31 680.

Puskas, F.W. 1970. The Port Coldwell alkali complex; in Proceedings, 16th Institute on Lake Superior Geology, Thunder Bay, Ontario, p.87-100.

Queen, M., Heaman, L.M., Hanes, J.A., Archibald, D.A. and Farrar, E. 1996. 40Ar/39Ar phlogopite and U-Pb perovskite dating of lamprophyre dykes from the eastern Lake Superior region: Evidence for a 1.14 Ga magmatic precursor to Midcontinent Rift volcanism; Canadian Journal of Earth Sciences, v.33, p.958-965.

Ruthart R. 2012. Characterization of high-PGE, low-sulphur mineralization at the Marathon PGE-Cu deposit, Ontario: M.Sc. thesis, Waterloo, ON, University of Waterloo, 145 p.

Sage, R.P. 1982. Mineralization in diatreme structures north of Lake Superior; Ontario Geological Survey, Study 27, 79p.

Sage, R.P. 1985. Geology of carbonatite-alkaline rock complexes in Ontario: Chipman Lake area; Ontario Geological Survey, Study 44, 40p.

Sage, R.P. 1986. Alkalic rock complexes – carbonatites of northern Ontario and their economic potential; unpublished PhD thesis, Carleton University, Ottawa, Ontario, 335p.

Sage, R.P. 1987. Geology of carbonatite-alkaline rock complexes in Ontario: Prairie Lake carbonatite

complex, District of Thunder Bay; Ontario Geological Survey, Study 46, 91p.

Sage, R.P. 1991. Alkaline rock, carbonatite and kimberlite complexes of Ontario, Superior Province; in Geology of Ontario, Ontario Geological Survey, Special Volume 4, Part 1, p. 683-709.

Sage, R.P. and Watkinson, D.H. 1995. Alkalic rocks of the Midcontinent rift; Institute on Lake Superior Geology, Marathon, ON, Proceedings Volume 41:2A, 79p.

Samson, I.M., Fryer, B.J., and Gagnon, J.E. 2008. The Marathon Cu-PGE deposit, Ontario: Insights from sulphide chemistry and textures, in Goldschmidt conference, p. 820.

Shaw, C.S.J. 1994. Petrogenesis of the eastern gabbro, Coldwell alkaline complex, Ontario; unpublished PhD thesis, University of Western Ontario, London, Ontario, 292p.

Shahabi Far, M.. 2016. The magmatic and volatile evolution of gabbros hosting the Marathon PGE-Cu deposit: evolution of a conduit system, PhD thesis, University of Windsor, Ontario.

Shaw, C.S.J.1997. The petrology of the layered gabbro intrusion, eastern gabbro, Coldwell alkaline complex, northwestern Ontario, Canada: Evidence for multiple phases of intrusion in a ring dyke; Lithos, v.40. p.243-259.

Smyk, M.C., Taylor, R.P., Jones, P.C. and Kingston, D.M. 1993. Geology and geochemistry of the West Dead Horse Creek rare-metal occurrence, northwestern Ontario; Exploration and Mining Geology, v.2, no.3, p.245-251.

Smyk, M.C. and Sage, R.P. 1995. Geology and mineralization of intrusive complexes of the Marathon, Ontario area; in Field Trip Guidebook for the Geology and Ore Deposits of the Midcontinent Rift in the Lake Superior region, International Geological Correlation Program, Project 336, Field Conference and Symposium, Duluth, Minnesota, August 19 to September 1, 1995, p.182-193.

Tucker, C. 1995. Origin of breccia associated with the Eastern Gabbro, Coldwell alkaline complex, northwestern Ontario; unpublished BSc thesis, University of Western Ontario, London, 57p.

Tuominen, H.V. 1967. Port Coldwell area; Ontario Department of Mines, Map P.114, scale 1:15 840.

Walker, E.C., Sutcliffe, R.H., Shaw, C.S.J., Shore, G.T. and Penczak, R.S. 1992. Geology of the Port Coldwell alkaline complex; in Summary of Field Work, 1992, Ontario Geological Survey, Miscellaneous Paper 160, p.108-119.

Walker, E.C., Sutcliffe, R.H., Shaw, C.S.J., Shore, G.T. and Penczak, R.S 1993a. Precambrian geology of the Coldwell Alkaline Complex; Ontario Geological Survey, Open File Report 5868, 30p.

Walker, E.C., Sutcliffe, R.H., Shaw, C.S.J., Shore, G.T. and Penczak, R.S 1993b. Precambrian geology, Port Coldwell complex, west half; Ontario Geological Survey, Preliminary Map P.3232, scale 1:20 000.

Walker, E.C., Sutcliffe, R.H., Shaw, C.S.J., Shore, G.T. and Penczak, R.S 1993c. Precambrian geology, Port Coldwell complex, east half; Ontario Geological Survey, Preliminary Map P.3233, scale 1:20 000.

Watkinson, D.H., Whittaker, P.J. and Jones, P.L. 1983. Platinum group elements in the eastern gabbro, Coldwell complex, northwestern Ontario; Ontario Geological Survey, Miscellaneous Paper 113, p.183-191.

Watkinson, D.H. and Ohnenstetter, D. 1992. Hydrothermal origin of platinum-group mineralization in the Two Duck Lake intrusion, Coldwell Complex, Northwestern Ontario: Canadian Mineralogist, v. 30, p. 121-136.

Weiblen, P.W. 1982. Keweenawan intrusive rocks; Geological Society of America Memoir 156, p.57-82.

Wilkinson, S.J. 1983. Geology and sulphide mineralization of the marginal phases of the Coldwell complex, northwestern Ontario; unpublished MSc thesis, Carleton University, Ottawa, Ontario, 129p.

Wu, F.Y., Mitchell, R.H., Li, Q-L., Zhang, C., and Yang, Y-H. 2017. Emplacement age and isotopic composition of the Prairie Lake Carbonatite complex, Northwestern Ontario, Canada. Geological Magazine 154(2): 217-236.

Field trip 7 - Building and ornamental stone sites of the Marathon Area, Ontario

Peter Hinz

Mineral Exploration & Development Section, Ontario Ministry of Energy, Northern Development and Mines, 435 James Street South, Suite B002 Thunder Bay, Ontario, P7E 6S7, Canada

Foreward

This tour will examine two past-producing "granite" quarries, two "granite" exploration sites in the Marathon area, one ornamental stone occurrence and, time permitting, the possible source of the recently popular "yooperlite" cobbles found in the Upper Peninsula of Michigan.

Introduction (taken from Hinz et al., 1994)

The dimension and monument stone industry in northwestern Ontario has a long history and is linked to the development and prosperity of the region. One of the earliest commercial operations was located on Vert Island in Nipigon Bay of Lake Superior. The Mesoproterozoic Sibley Group yielded an attractive red sandstone which was extracted by the Chicago Verte Island Sandstone Company. The stone was used locally for the construction of the Canadian National Railway and shipped to Chicago, Winnipeg, southern Ontario, and other U.S. cities for construction uses.

Development of some of the earliest quarries in the Marathon and Nipigon areas was directly related to the construction of the Canadian Pacific Railway in the late 1880's. Syenites of the Coldwell Alkaline Complex in the vicinity of Marathon and sandstones south of Nipigon were used in the construction of railway trestles to span the Black, Pic, Little Pic, Steel, and Nipigon rivers. Today these trestles show very little wear and are a testament to the long-standing durability of the stones. Although markets for dimension stone decreased in the early 1900's, production continued at the Simpson Island sandstone quarry (1900 to 1910) and at the Bannerman and Horne quarry (1912 to 1915) near Ignace. The next period of quarry development took place during the late 1920's to early 1930's. Five small scale quarries operated northwest of Marathon along the Canadian Pacific Railway. Black and brown granites were extracted and shipped to customers in Toronto, Buffalo, Chicago, and Detroit. In 1932, the last of these quarries closed due to the loss of market.

In 1948, the Vermilion Pink Granite Company opened a quarry approximately 12 km southwest of the town of Vermilion Bay. This highly popular pink granite began production in 1954 and continued sporadically under various names until 1991 when the quarry, now named Granite Quarriers (GQI) Inc., closed. In 1981, Nelson Granite Limited of Sussex, New Brunswick began production of an identical granite from a quarry immediately south of the highway from the Granite Quarriers Inc. site. This quarry has operated year-round since that time and is still in production.

Currently, 2019, Nelson Granite Limited is the only stone producer operating in northwestern Ontario. Nelson Granite produces a range of colours including pink, yellow, green, brown, and white granite from four quarries located north of Kenora and west of Vermilion Bay. Northwestern Ontario stone is shipped around the world for a range of uses including: building stone for interior and exterior uses; monumental stone; and landscape uses including pavers, benches, and accent pieces.

Detailed descriptions of the historic quarries, their operations, geology and geotechnical test results are provided in Hinz et al. (1994). Descriptions of current producers are available in the Kenora portion of the Report of Activities 2018 (Paterson et al., 2019).

Geologic setting

Puumala (2018) provides the following general geological description of the Coldwell Alkaline Complex. *"The geology of this area is dominated by rocks of the Coldwell Alkaline Complex. The Coldwell Complex was emplaced into Neoarchean supracrustal rocks of the Wawa Subprovince of the Superior Province during the Mesoproterozoic Midcontinent Rift event at ca. 1108 +/- 1 Ma (Heaman and Machado, 1992). The complex approximately bisects the Schreiber-Hemlo greenstone belt and is located at the north end of the Thiel fault, a zone of faulting which separates grabens with different subsidence history in the rift (Cannon et al., 1989).*

The Coldwell Complex was mapped by Kerr (1910a,

1910b), Puskas (1967), and Walker et al. (1993), and comprises three, superimposed ring sub-complexes or magmatic centers (Mitchell and Platt, 1978) that young progressively (Centers 1 to 3) to the southwest. The rocks of Center 1 are silica-saturated and include the Eastern and Western border gabbros (the oldest rocks within the complex) and later iron-rich augite syenite and syenite-syenodiorite (Mitchell and Platt, 1978, 1982; Mulja, 1989). Center 2 includes silica-undersaturated alkalic rocks with oversaturated residue. Rock types include nepheline- and hastingsite-bearing miaskitic nepheline syenite, and numerous volumetrically minor alkaline lamprophyre and analcime tinguaite dykes (Mitchell and Platt, 1978, 1982; Laderoute, 1987; and Mulja, 1989). Center 3 includes silica-oversaturated alkalic rocks with oversaturated residue consisting of magnesio-hornblende syenites, quartz syenites, and minor granites (Mitchell and Platt, 1994; Lukosius-Sanders, 1988).

The map area covers much of the Eastern border gabbro, which hosts numerous occurrences of Magmatic Cu-Ni-PGE (± Au, Ag) and Ti-V±apatite mineralization (MacTavish and Smyk, 2017). The Marathon Cu-PGE deposit is the most notable example of the deposits hosted in the Eastern border gabbro. Another gabbroic intrusion within the interior of the Coldwell Complex hosts the Geordie Lake Cu-PGE deposit (MacTavish and Smyk, 2017). Centre 1 augite and amphibole syenite has previously been quarried as dimension stone in Marathon, just to the south of the Coldwell Complex map area (Hinz et al., 1994), and these rocks continue to see periodic exploration interest. Late-stage syenite pegmatites that host occurrences of Nb-Y-F-rare earth elements also occur in the area (Alexander, 2007)."

The current field trip stops will feature rocks of all intrusive centres as shown in Figure 1:

1. Center 1: Stops 1, 2, 3, and 4;
2. Center 2: Stops 5 and 6;
3. Center 3: Stop 7.

MacTavish and Smyk (2017), Walker et. al. (1993) and Hinz et. al. (1994) provide descriptions of the lithologies which will be visited.

From MacTavish and Smyk (2017), "*Fe-rich augite syenite (formerly referred to as ferroaugite syenite) comprises a large portion of the exposure in the eastern half of the Coldwell Complex. It appears*

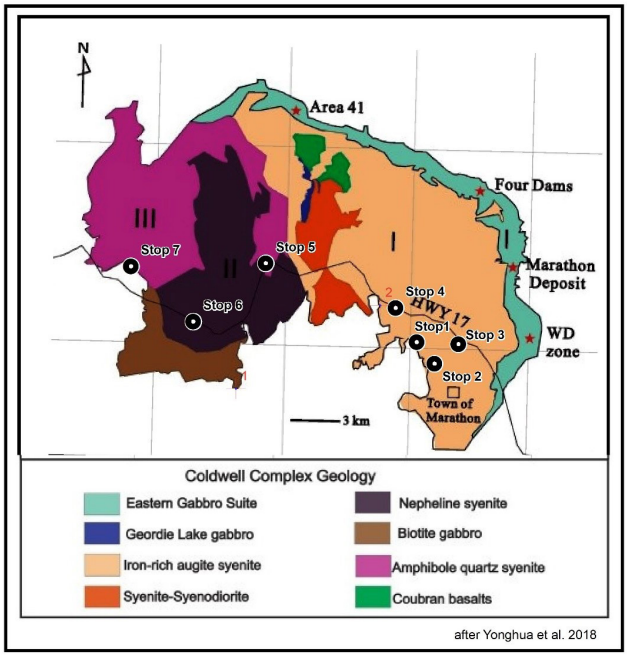


Figure 1. Coldwell Complex maps showing field trip stop locations within the three intrusive centres.

to be a sheet-like intrusion that dips approximately 15° toward the center of the complex, sandwiched between the underlying Eastern Border Gabbro and an overlying, recrystallized amphibole-quartz syenite; it also intrudes the basaltic roof pendants (Walker et al., 1992, 1993a). Crystallization of the syenite inwards from its upper and lower contacts produced mineralogical and compositional variations across it (Walker et al.; 1993a). Constituent minerals include iridescent, lathlike, cryptoperthitic feldspar (up to 30% interstitial), and variable amounts of fayalite, amphibole, aenigmatite, and rare quartz. Coarse-grained to pegmatitic portions of the syenite host a variety of REE-bearing fluoro-carbonates, quartz, chalcedony, and molybdenite. Iridescent feldspar, known locally as "spectrolite", was recently (2010) commercially extracted on a very small-scale from pegmatite at Shack Lake near Marathon. Feldspar-porphyritic amphibole syenite contains two textural variants, a feldspar porphyritic amphibole syenite with an aphanitic to medium-grained groundmass and interstitial amphibole; and a later intrusion of medium-grained amphibole syenite with columnar feldspar and interstitial amphibole."

Walker et al. (1993) stated that "*the amphibole-nepheline syenite (Unit 13) is white to red, mesocratic to leucocratic, medium-grained with variable proportions of feldspar, nepheline, amphibole, biotite, apatite, and zeolites. Locally the nepheline syenite is well-layered*

with melanocratic olivine-nepheline syenite grading into mesocratic syenite. Spectacular orbicular layering occurs on the south shore of Pic Island. An intergranular texture resulting from intergrown feldspar, amphibole, and nepheline is typical of the unit. Near lineaments and lithological contacts the amphibole-nepheline syenite becomes red. Texturally different varieties of amphibole-nepheline syenite occur near the contacts and include mesocratic nepheline-amphibole syenite with near-equant euhedral amphibole prisms and mesocratic amphibole-nepheline syenite with interstitial amphibole and euhedral columnar feldspar.

The amphibole-natrolite-nepheline syenite (Unit 14) is an extremely variable rock unit that intrudes the roof pendant mafic volcanics, gabbro, iron-rich augite syenite, amphibole syenite, and amphibole-nepheline syenite. The main rock type within this unit is a gray to pink, mesocratic, amphibole-natrolite-nepheline syenite with variable amounts of natrolite, lath feldspar and acicular amphibole. The textural complexities of the amphibole-natrolite-nepheline syenite is considered to be a product of assimilation and mixing of a variety of rock compositions in a solid, semi-molten or molten state and synplutonic intrusion of the alkaline gabbro."

From Hinz et al. (1994), "Amphibole-natrolite-nepheline syenite: contains primarily anhedral, "turbid" crystals of perthitic feldspar. The turbid areas are caused by the presence of numerous vacuoles. The reddish colour of the stone may be due to iron-staining of the vacuoles and fractures within the feldspar crystals. Anhedral pyroxene (augite), biotite, amphibole (hornblende), and opaque minerals occur together."

Field Trip Stops

Field trip stops are illustrated in Figure 2.

Stop 1: Peninsula Quarry (1927-1932)

UTM coordinates 544191E 5399826N

In the 1880's, prior to commercial production, several small quarries were operated supplying stone for the construction of river abutments and railway trestles in support of the construction of the Canadian National Railway.

In 1927, "*commercial operations were initiated by Peninsula Granite Quarries Ltd. on 17 claims located on the east shore of Carden Cove" (Hinz et al., 1994).*

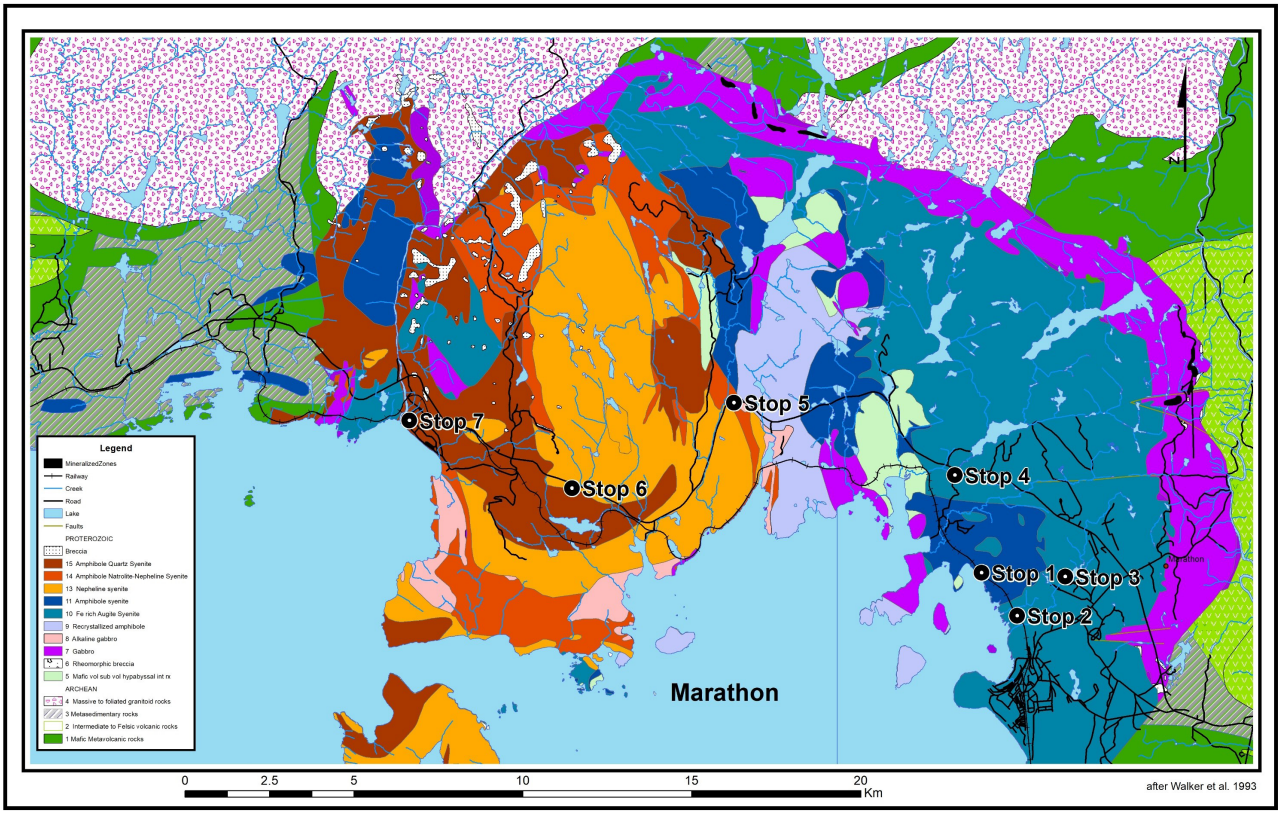


Figure 2. Geology of the Coldwell Alkaline Complex with field trip stop locations.

Peninsula Granite Quarries Ltd. operated four quarries at various points along Carden Cove, north of the town of Marathon. Most of the historic infrastructure related to the operations is lost however remains of the original derrick, grout shovel, and steam engine can still be seen on-site (Figs. 3 and 4).



Figure 3. Remains of the derrick at the Peninsula Quarry.



Figure 4. Remains of the steam winch at the Peninsula Quarry.

The Peninsula Quarry site is underlain by iron-rich augite syenite and amphibole syenite as described above in Walker et al. (1992, 1993a) and MacTavish and Smyk (2017)."

Thomson (1931) described the jointing, "Two sets of joints are seen in the quarry. The most prominent strikes almost due north and varies in dip from vertical to 70°W. The cross-jointing strikes east-west and is nearly vertical. At the quarry the north-south joints are 70ft apart and run parallel for at least 500ft. Rectangular blocks of a size limited only by plant capacity can be quarried. The sheets lie horizontally and exhibit an even and well-defined floor. The first sheet quarried had a maximum thickness of 14ft. Drilling in the next sheet below to a depth of 10ft did not reach another sheeting plane. The rift is roughly parallel to the sheeting planes."

Stop 2: Coldspring Quarry (1931-1938?)

UTM coordinates 545332E 5398469N

From Hinz et al. (1994): *"The ground covering the black granite was purchased by the Cold Spring Granite Company from the Peninsula Granite Quarries Ltd. During the year, a new quarry was opened with a new derrick, drilling equipment and power plant. Twelve men were employed to quarry blocks that weighted up to 35 tons. In 1931, twenty car loads of black granite were sent to Cold Spring, Minnesota for fabrication (Thomson, 1932; The Northern Miner, 1931). In the late 1930s the quarry operations were abandoned due to the lack of market."*

The claims are underlain by Fe-rich augite syenite as described above in Walker et al. (1992, 1993a) and MacTavish and Smyk (2017). The stone is medium- to coarse-grained, dark brown to black in fresh-cut surfaces. Two sets of jointing are documented, the most prominent is 335° with a dip of 50° south and a second is 005° with a vertical dip. Sheeting (horizontal) fractures range from 0.45m to 2.4m and dip 8-10° west (Thomson, 1932).

Stop 3: Shack Lake Spectrolite (1963-present)

UTM coordinates 546698E 5399605N

From Hinz et al. (1994): *"The Shack Lake occurrence was first staked in 1963 by C.S. Downey, sporadic exploration work including diamond drilling and blasting was conducted on the site since then. For a time in the early 1990's the property owners of the time, Jon and Audrey Ferguson considered opening a "pick-your-own"* operation similar to the amethyst operations in the Thunder Bay area, this never came to fruition. At the time the Town of Marathon adopted spectrolite as the "town mineral". Currently the property is held by G. Blakely who has conducted additional diamond drilling and blasting.

Spectrolite is a variation of labradorite, with a deeper and wider range of colours (full spectrum) hence its name. Spectrolite was first identified in Finland.

The spectrolite occurs within the syenite as two phases: large crystals up to 10cm across in pegmatite dikes cross-cutting the syenite; and

smaller crystals within the contact zone between the pegmatite and medium-grained host syenite. In both cases the spectrolite displays bluish to yellow-gold schillerescence. Ribbe (1983) states that'Schiller' may be used to refer to diffuse, often silvery reflections from mutually oriented, platy inclusions, especially common in labradorite parallel to (010) (Rayleigh, 1923).

Portions of ferro-augite syenite (commercially known as "black granite") in the eastern part of the Coldwell Alkalic Complex near Marathon are coarse grained to pegmatitic. Large feldspar crystals may display yellow-orange to blue schillerescence and have been locally termed "spectrolite". Two properties near Shack Lake, 2 km northwest of Marathon, have undergone limited exploration in the past but are being re-examined by owners Don Wilkinson, and Jon and Audrey Ferguson, respectively. The main potential usage of the "spectrolite"-rich syenite is as decorative or ornamental stone for use in cabochons, bookends and perhaps tiles."

From Schnieders et al. (1991): "Pegmatitic zones are commonly deeply weathered and are not amenable to large block quarrying. Hand picking and sorting can be undertaken on a small scale. Prospectors should investigate any coarse-grained to pegmatitic sections of syenite or dikes for feldspars that display this characteristic schiller effect. In deeply weathered outcrops, the feldspars commonly remain intact and retain their schiller colours. Stripping and blasting may be required to obtain "fresher", unfractured material.

X-ray diffraction analysis of the "spectrolite" shows the presence of plagioclase and minor K-feldspar (antiperthite). Examination of the mineral in oils shows that it is oligoclase. The schiller effects may be brought about by diffraction that occurs at the boundary of the exsolution lamellae (H. DeSouza, Ontario Geological Survey, personal communication, 1990)."

Stop 4: Marathon Black Occurrence (1990-1994)

UTM coordinates 543576E 5402637N

The Marathon Black occurrence was staked by D. Petrunka in the early 1990's when interest in building stone was high and the Cold Spring Granite (Canada) Ltd. was active in the area. Mr. Petrunka was able to secure funding to remove test blocks from the site, however further development did not occur.

The stone is a generally coarse-grained black to olive-brown with some greenish sections. Compositionally the stone is an iron-rich augite syenite as described above in Walker et al. (1992, 1993a) and MacTavish and Smyk (2017).

Hinz et al. (1994) reports testing done by Cold Spring Granite (Canada) Ltd. yielded the following physical properties:

Bulk specific gravity: 2.738

Percent absorption (48 hours): 0.560

Compressive strength: 20,130 (psi) dry, 18,420 (psi) wet

Modulus of Rupture: 1,420 (psi) dry, 1,530 (psi) wet

Testing completed by "Twin City Testing Corp., St. Paul, Minnesota (Assessment Files, Thunder Bay).

Stop 5: Yooperlite Source Location

UTM coordinates 536816E 5404785N

In 2018 the US media was a-buzz over the discovery of a new "mineral" with the unofficial name of "yooperlite". In a 2018 paper, Laughlin et al. (2018) reported that yooperlite is a fluorescent sodalite-bearing syenite which occurs in the Upper Peninsula of Michigan as beach pebbles and cobbles. The authors indicate that it is probable the bedrock source is likely the Coldwell Alkaline Complex in Ontario.

Centre 2 of the Coldwell Complex hosts amphibole-natrolite-nepheline syenite (Unit 14) within which, the fluorescent mineral hackmanite, a sulphur-bearing variety of sodalite, has been identified. It can be postulated that the yooperlite pebbles and cobbles found along the Lake Superior shoreline of Michigan originated from this unit and were glacially transported to their current location and subsequently wave-washed and tumbled.

From Sage & Watkinson (1995). "Stop 20: Biotite gabbro intruded by various types of nepheline syenite.

This stop is at a broad curve in Highway 17 and one should be very **CAREFUL OF VEHICLES**.

Starting at approximately 18.8km outcrops on the east side of the highway of grey to buff pyroxene-amphibole syenite contain orange fluorescing hackmanite, a variety of sodalite. This mineral can only readily be seen with a UV lamp. The syenite contains numerous mafic xenoliths up to 25 to 30cm in maximum length. The xenoliths are subangular to

subrounded and the mafic minerals within the syenite tend to occur in clots. The larger xenoliths may have feldspar phenocrysts or porphyroblasts up to 1.0cm. The phenocrysts or porphyroblasts display a seriate size distribution and comprise up to 5 % of the rock.

At the centre of the curve at 19.2km an alkalic biotite gabbro is exposed on the north side of the highway. The medium- to coarse-grained gabbro is extensively cut by medium- to coarse-grained syenite and some of the nepheline has been altered to reddish orange "hydronephelinite". There may be two ages of alkalic gabbro with the older coarser grained gabbro displaying dark selvages up to 7 or 8cm wide and an irregular shape suggesting that it behaved in a more or less ductile manner. The alkalic gabbros have a clotty mafic mineral assemblage. The surface of the coarser grained biotite gabbro is pitted from the weathering of mafic clots.

Dikes of nepheline syenite pegmatite occur on the north side of the highway at the inflection in the curve. At this site, two ages of nepheline syenite pegmatite of essentially identical composition cut each other. The trends of these dikes are approximately 340° dipping 60° south and 090° dipping 50° north. The dike trending 090° cuts the dike trending 340° and both are on the order of 20 to 30 cm in width. The dikes have been sketched by Puskas (1970). Both dikes are zoned from an amphibole-rich margin to a feldspar-natrolite (hydronephelinite)-rich core. The central parts of these dikes are commonly relatively rich in reddish orange "hydronephelinite". West from the two dikes toward the hackmanite-bearing outcrop, coarse-grained alkalic biotite gabbro is intruded by medium- to coarse-grained pyroxene, amphibole syenite with traces of nepheline. Both of these rock types are in turn cut by coarse-grained nepheline syenite dikes. Brecciation is so intensive that the outcrop is an igneous breccia. West toward the hackmanite-bearing outcrop the syenite is pink to grey, fine- to medium-grained, inequigranular seriate with clotty assemblages of mafic minerals.

On the south side of the highway coarse-grained alkalic gabbro appears to be cut by medium-grained alkalic gabbro which is in turn intruded by mottled pink to grey, inequigranular seriate amphibole syenite. There is a slight coarsening in texture next to the medium-grained gabbro and a dike of similar material projects from the contact with the medium-grained gabbro through both phases of alkalic gabbro"

Stop 6: Marathon Red Occurrence (1960-1994)

UTM coordinates 532030E 5402401N

The first attempts to quarry red syenite occurred in the late 1880's near Port Coldwell. From the 1960's to mid-1980's exposures of red granite east of Neys Lunch along the Trans-Canada Highway were staked several times, however no further work was recorded. D. Petrunka staked the claims in 1985 and optioned the ground to Cold Spring Granite (Canada) Ltd. Coldspring removed blocks from the highway exposures to evaluate the colour and market suitability. Diamond drilling conducted by Coldspring determined that the red colour of the syenite was limited to top 9.1m of the unit below which it changed to pink. In 1990 Cold Spring terminated the option agreement.

The stone is an amphibole-natrolite-nepheline syenite described above by Walker et al. (1993). From Hinz et al. (1994): "*In thin section, the stone is composed of primarily anhedral, "turbid" crystals of perthitic feldspar. The turbid areas are caused by the presence of numerous vacuoles. The reddish colour of the stone may be due to iron-staining of the vacuoles and fractures within the feldspar crystals. Anhedral pyroxene (augite), biotite, amphibole (hornblende), and opaque minerals occur together*."

The stone is red-brown on fresh surface and orange-red on the weathered surface, medium- to coarse-grained with some randomly distributed mafic knots.

Hinz et al. (1994) reports samples sent to the Geoscience Laboratories in Sudbury yielded the following physical properties:

Bulk specific gravity: 2.75

Percent absorption (2 hours): 0.22, (48 hours): 0.32

Compressive strength: 22,049 (psi)

Modulus of Rupture: 1,394 (psi)

Stop 7: Little Pic River Quarry (circa. 1884)

UTM coordinates 527367E 5405024N

This optional stop will be dependant on timing and weather.

The construction of the Canadian Pacific Railway (C.P.R.) in the mid 1880's required good stone quality for piers and abutments at river crossings (Fig. 5). Prospecting parties advanced along proposed rights-of-way ahead of construction in order to identify locations

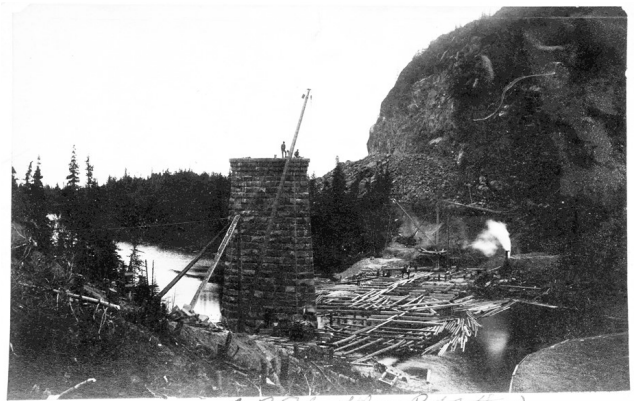


Figure 5. CPR construction across the Little Pic River, circa. 1884. Photo compliments of the Thunder Bay Historical Society.

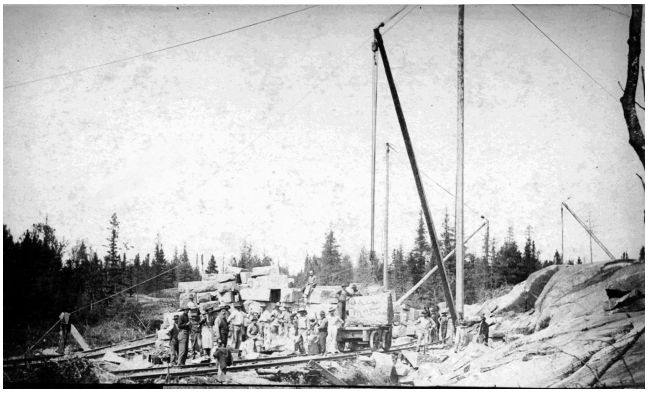


Figure 6. Little Pic River Quarry, circa. 1884. Photo compliments of the Thunder Bay Historical Society.

of quarriable stone. This quarry, previously unknown to Ministry staff, was one such location where the stone was quarried and land transported to the bridge construction site. Fig. 6 shows a work crew at the Little Pic River Quarry during the construction of the C.P.R., circa. 1884.

References

Alexander, M. 2007. The mineralogy of NYF pegmatites from the Coldwell Alkaline Complex, northwestern Ontario; unpublished MSc thesis, Lakehead University, Thunder Bay, Ontario.

Cannon, W.F., Green, A.G., Hutchinson, D.R., Lee, M., Milkereit, B., Behrendt, J.C., Halls, H.C., Green, J.C., Dikas, A.B., Morey, G.B., Sutcliffe, R. and Spencer, C. 1989. The North Midcontinent Rift beneath Lake Superior from GLIMPCE seismic reflection profiling; Tectonics, v.8, p.305-332.

Heaman, L.M. and Machado, N. 1987. Isotope geochemistry of the Coldwell alkaline complex: 1. U-Pb studies on accessory minerals; Geological Association of Canada–Mineralogical Association of Canada, Joint Annual Meeting, Saskatoon, Saskatchewan, Program with abstracts, p.54.

Hinz, P., Landry, R.M. and Gerow, M.C. 1994. Dimension stone occurrences and deposits in northwestern Ontario; Ontario Geological Survey, Open File Report 5890, 191.p.

Kerr, H.L. 1910a. Geological map of part of the north shore of Lake Superior, District of Thunder Bay; Ontario Bureau of Mines, Annual Report Map 19B, scale 1:63 360.

Kerr, H.L. 1910b. Nepheline syenites of Port Coldwell; Ontario Bureau of Mines, Annual Report, v.19, p.194-232.

Laderoute, D.G. 1987. The petrology, geochemistry, and petrogenesis of alkaline dyke rocks from the Coldwell Alkaline complex; unpublished M.Sc. Thesis, Lakehead University, Thunder Bay, Ontario, 89p. Tectonophysics, v.184, p.73-86.

Laughlin, R., Carlson, S.M., Olds, T.A. and Miller 2018. A New Find of Fluorescent Sodalite From Michigan's Upper Peninsula. Mineral News, Vol. 34, No. 5, May, 2018.

Lukosius-Sanders, J. 1988. Petrology of the syenites from Center III of the Coldwell alkaline complex, northwestern Ontario; unpublished MSc thesis, Lakehead University, Thunder Bay, Ontario, 141p.

MacTavish. A. and Smyk, M.C. 2017. Archean and Proterozoic geology of the Marathon-Hemlo area, 63rd Institute on Lake Superior Geology Proceedings, v. 63, Part 1, Field Trip Guidebook, p. 1-31.

Mitchell, R.H. and Platt, G. R. 1978. Mafic mineralogy of ferroaugite syenite from the Coldwell alkaline complex, Ontario, Canada; Journal of Petrology, v.19, p.627-651.

Mitchell, R.H. and Platt, G. R. 1982a. The Coldwell alkaline complex; in Field Trip Guidebook, Proterozoic geology of the northern Lake Superior area, Geological Association of Canada–Mineralogical Association of Canada, Joint Annual Meeting, Winnipeg, Manitoba, p.42-61.

Mitchell, R.H. and Platt, G. R. 1994. Aspects of the geology of the Coldwell alkaline complex: Field trip A2, Geological Association of Canada–Mineralogical Association of Canada, Joint Annual Meeting, Waterloo, Ontario, 36p.

Mulja, T. 1989. Petrology, geochemistry, sulphide- and platinum-group element mineralization of the Geordie Lake intrusion; unpublished MSc thesis, Lakehead University, Thunder Bay, Ontario, 234p.

Paterson, W.P.E., Lichtblau, A.F., Ravnaas, C., Lewis, S.O., Tuomi, R.D., Fudge, S.P., Pettigrew, T.K. and Wiebe, K. 2019. Report of Activities 2018, Resident Geologist Program, Red Lake Regional Resident

Geologist Report: Red Lake and Kenora Districts; Ontario Geological Survey, Open File Report 6351, 127p

Puskas, F.P. 1967. Geology of the Port Coldwell Area, District of Thunder Bay; Ontario Department of Mines , Open File Report 5014, 92p.

Puskas, F.W. 1970. The Port Coldwell alkali complex; in Proceedings, 16th Institute on Lake Superior Geology, Thunder Bay, Ontario, p.87-100.

Puumala, M.A. 2018. Geological description of the Coldwell Alkaline Complex. Personal correspondence. Unpublished Report, p.1.

Rayleigh, Lord. 1923. Studies of Iridescent Colour, and the Structure Producing It. III; The Colours of Labrador Feldspar. Proceedings of the Royal Society (Londaon) 103A, p.34-45.

Ribbe, P.H. (1983) Chemistry, structure and nomenclature of feldspars. in: Feldspar Mineralogy. (P.H. Ribbe, editor). Reviews in Mineralogy 2. Mineralogical Society of America, Washington, D.C. p. 1-19.

Sage, R.P. and Watkinson, D.H. A. 1995. Alkalic Rocks of the Midcontinent Rift, 41st Institute on Lake Superior Geology Proceedings, v. 41, Part 2a, Field Trip Guidebook, 79p.

Schnieders, B.R., Smyk, M.C. and Hinz, P. 1991. Schreiber-Hemlo Resident Geologist's District; in Report of Activities 1990, Resident Geologists, Ontario Geological Survey, Miscellaneous Paper 152, p.141-171.

Thomson, J.E. 1931. Geology of the Heron Bay Area, District of Thunder Bay; Ontario Department of Mines, v.XL, pt .2, p.21-39. Accompanied by map 40d.

Thomson, J.E. 1933. Geology of the Heron Bay Area, Thunder Bay District, Ontario; Ontario Department of Mines, Annual Report 1932, v.XLI, pt.6,,p.34-37.

Walker, E.C., Sutcliffe, R.H. , Shaw, C.S.J. , Shore, G.T. and Penczak, R.S. 1992. Geology of the Coldwell Alkaline Complex; in Summary of Field Work and Other Activitie s 1992, Ontario Geological Survey, Miscellaneous Paper 160, p. 108-119.

Walker, E.C., Sutcliffe, R.H., Shaw, C.S.J., Shore, G.T., and Penczak, R.S. 1993. Precambrian geology of the Coldwell Alkalic Complex; Ontario Geological Survey, Open File Report 5868, 30p.

Field trip 8 - Geology of the past-producing Winston Lake Cu-Zn Mine

Robert W.D. Lodge

Department of Geology, University of Wisconsin-Eau Claire, WI 54702-4004

Mark Smyk and Mark Puumala

Resident Geologist Program, Ontario Geological Survey, Ministry of Energy, Northern Development and Mines, Thunder Bay, Ontario, P7E 6S7, Canada

Introduction

The Winston Lake greenstone belt is best known for hosting economic volcanogenic massive sulphide (VMS) deposits totalling ~ 6 million tons of Zn-Cu-Pb ore (Ontario Geological Survey, 2011). The belt is located along the northern margin of the Wawa Subprovince of the Wawa-Abitibi terrane and is about 20 km north of Schreiber, Ontario (Pye, 1964; Severin et al., 1991). The Winston Lake greenstone belt is tectono-stratigraphically equivalent to ca. 2720 Ma greenstone belts along the northern margin of the Wawa Subprovince, such as the Shebandowan (Corfu and Stott, 1998), Manitouwadge (Zaleski et al., 1999), and Vermilion (Peterson et al., 2001) greenstone belts (Fig. 1). Regional metamorphic grade in the belt is lower amphibolite facies (Williams et al., 1991).

The Winston Lake Greenstone Belt (Fig. 2) is a small belt located directly north of, and almost connected to the Schreiber-Hemlo greenstone belt (Williams et al., 1991); however, the contact relationship of these belts is poorly constrained (Carter, 1982b, a). Unlike the many other greenstone belts in the region, the Winston Lake greenstone belt has not been mapped at a regional scale since the 1960's (Pye, 1964). The belt is bound to the north by the Quetico Subprovince, to the west by the Winston Lake batholith, and to the south by the Crossman Lake Batholith (Severin et al., 1991). Rocks in the western part of the belt that host the past-producing Winston Lake Mine were initially interpreted as metasedimentary rocks because of the presence of aluminosilicate minerals (Pye, 1964). They were later interpreted to be hydrothermally altered felsic and mafic volcanic assemblages.

The Winston Lake greenstone belt and its VMS-hosting strata have received a considerable amount of research at a property scale (e.g., Osterberg, 1993; Schandl et al., 1995), a belt scale (Lodge et al., 2014), and a subprovince scale (e.g., Polat et al., 1999; Kerrich et al., 2008; Lodge et al., 2015). There are also several field trips and published guidebooks (Severin et al., 1991; Smyk and Schnieders, 1995; Lodge, 2012). The previous research in these areas has been extremely valuable throughout the planning of this field trip and preparation of the guidebook. Note that, in the descriptions of some of the units, primary igneous names are used rather than their metamorphic names (e.g., gabbro versus amphibolite). The geochemical and isotopic data presented in this guidebook are available for download through the Ontario Geological Survey (Lodge and Chartrand, 2013).

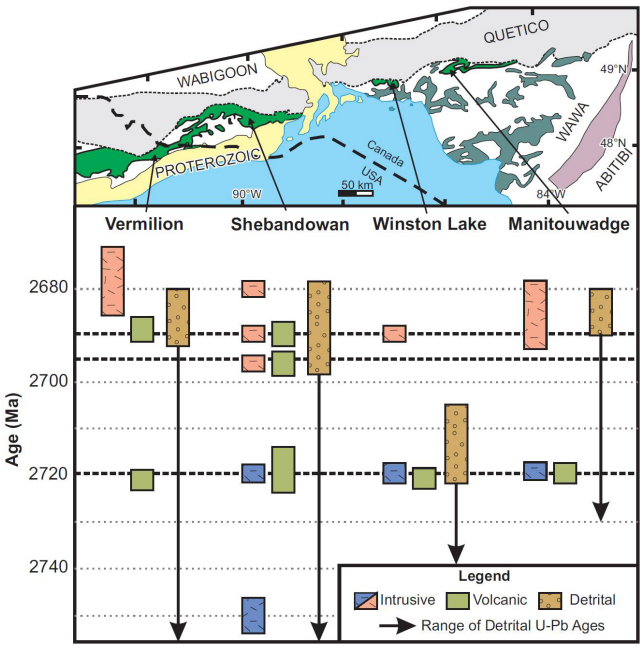


Figure 1. Geochronology of northern most greenstone belts in the Western Wawa Subprovince. Most of the belts have experienced most of their formation ca. 2720 Ma. Figure from Lodge et al. (2014) and was compiled from numerous geochronological studies (Corfu and Stott, 1998; Zaleski et al., 1999; Peterson et al., 2001; Lodge et al., 2013, 2014).

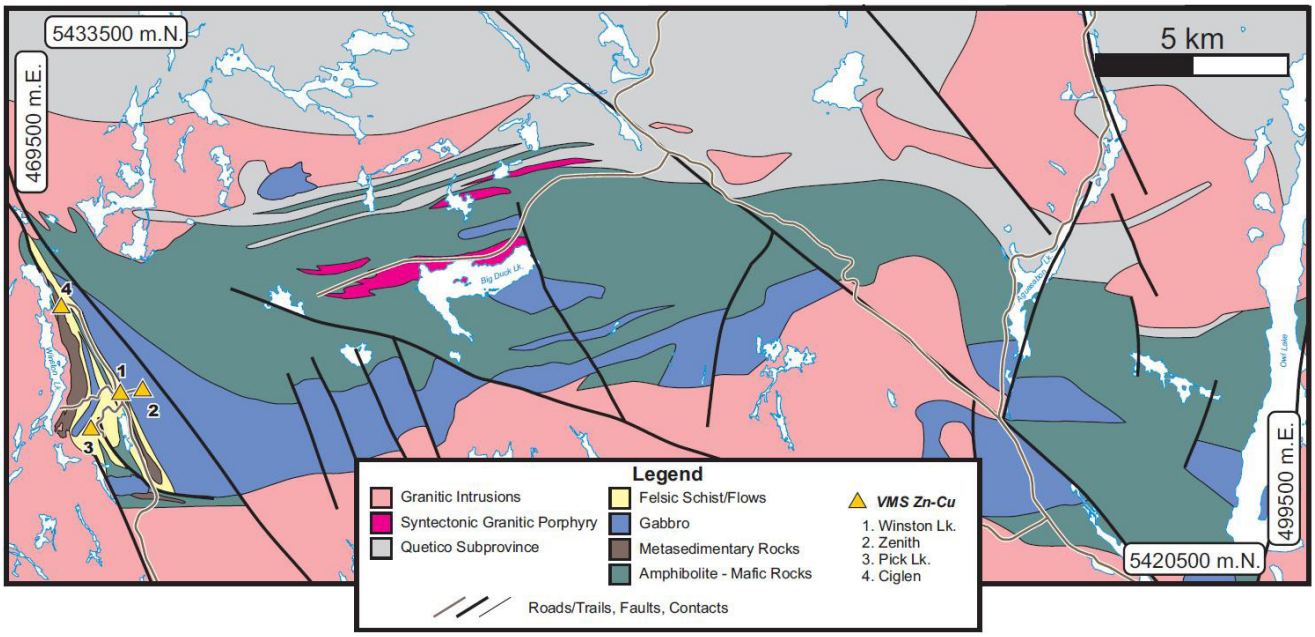


Figure 2: Geology of the Winston Lake greenstone belt. Figure compiled by Lodge et al. (2015) from various published and unpublished maps (Pye, 1964; Ritcey, 1992; Osterberg, 1993).

Regional Geology

The Winston Lake belt has been informally subdivided into two main lithotectonic assemblages: the Winston Lake Assemblage (Fig. 3A) and the Big Duck Lake Assemblage (a thick mafic unit composing most of the belt in Fig. 3B; Severin et al., 1991; Polat et al., 1999; Lodge et al., 2014). The Winston Lake Assemblage is host to the VMS deposits and is composed of calc-alkaline, bimodal volcanic and siliciclastic rocks (Gorton and Schandl, 1995). The Big Duck Lake Assemblage consists of Mg- to Fe-tholeiitic basalts, quartz-feldspar porphyry dykes and sills, and their brecciated equivalents (Ritcey, 1992; Polat et al., 1999). It has been assumed that the Big Duck Lake Assemblage conformably overlies the Winston Lake Assemblage and that the contact was intruded by a thick differentiated gabbro (Osterberg, 1993). This field trip will not examine the Big Duck Lake Assemblage and therefore it will not be discussed further. If interested, please consult the references cited above (in particular: Ritcey, 1992).

Prior to the research of Lodge et al. (2014), only one U-Pb age of 2723 ± 3 Ma was obtained from a felsic volcanic rock associated with the Winston Lake orebody (Davis et al., 1994). More recent geochronological data indicate that the entire Winston Lake Assemblage and the Zenith gabbro are all ca. 2720 Ma (Lodge et al., 2014). The structural history of the belt is also poorly constrained and two main structural events are

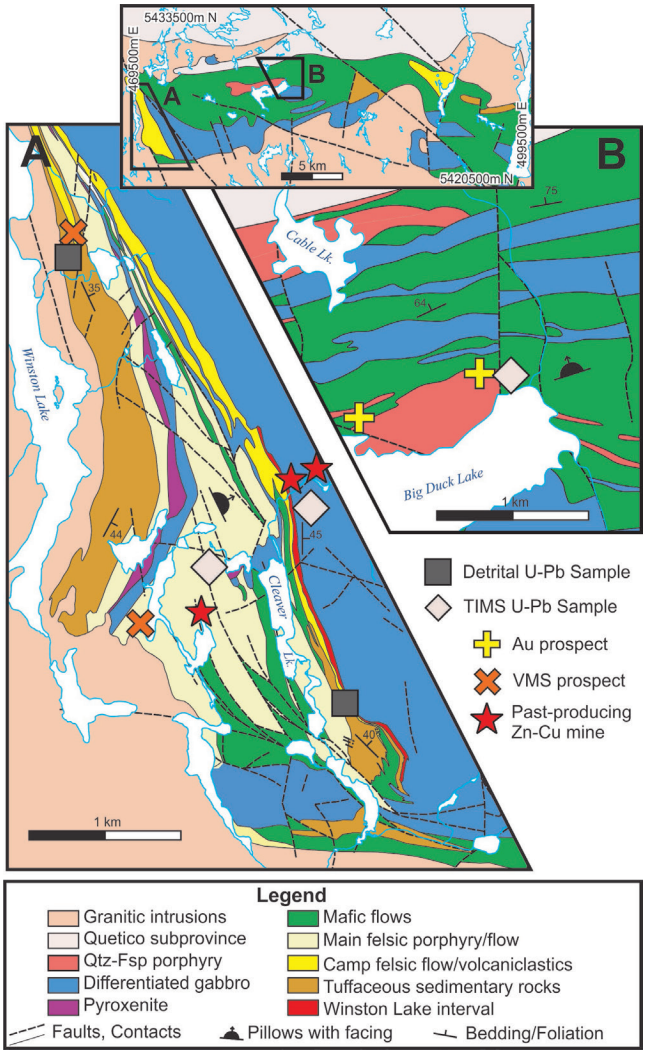


Figure 3: Geology of the Winston Lake greenstone belt. The belt is subdivided into the VMS-hosting Winston Lake Assemblage (A) and Big Duck Lake Assemblage (B). Figure compiled by Lodge et al. (2014).

interpreted: D1 manifested as tilting of stratigraphy and a foliation development (north-northwest striking foliation in the Winston Lake Assemblage; west-striking foliation in the Big Duck Lake Assemblage), and D¬2 represented by minor folds and faulting that offset contacts at the map scale (Osterberg, 1993).

The VMS-hosting Winston Lake Assemblage is dominated by felsic volcanic and siliciclastic rocks. Despite the high degree of metamorphism and relatively high degree of deformation, many primary volcanic features are preserved in the volcanic rocks. Reliable younging directions obtained from pillowed flows and cross-bedding in volcaniclastic rocks suggest an eastward-younging stratigraphy. The oldest supracrustal strata in this part of the belt are felsic volcaniclastic and siliciclastic rocks. These are conformably overlain by a quartz-feldspar porphyry flow that is associated with the Pick Lake VMS deposit. Altered mafic flows (named Ladder and Middle mafic units) are interlayered with the Camp and Main felsic units that host the Winston Lake VMS deposit. The feldspar-phyric felsic volcanic rocks were then presumably overlain by mafic flows of the Big Duck Assemblage, which was followed by the emplacement of a thick, synvolcanic differentiated gabbro at that contact; the gabbro sill hosts the Zn-rich Zenith orebody. The general stratigraphy of the Winston Lake Assemblage is illustrated in Figure 4.

History of Mining and Mineral Exploration

Much of the mining and exploration history for the Winston Lake greenstone belt is published internally within the companies that have explored and mined these deposits. Most of these are not externally available. However, the Mineral Deposit Inventory published by the Ontario Geological Survey (2019) has summarized current and historical information available for these deposits. Much of the historical information provided in this section is summarized from this database. The size and grade of the deposits in the Winston Lake area are summarized in Table 1.

Massive Zn-mineralization, in what is now interpreted to be a synvolcanic gabbroic sill, was first discovered in 1879 by prospectors and became the Zenith Mine. A total of 1065 tons of ore, averaging approximately 45% Zn, was shipped to a smelter between 1891 and 1899. Between 1899 and 1901, 2700 tons of sphalerite-rich ore was mined and concentrated by Grand Calumet Mining Company Limited (Ontario Geological Survey, 2019) Very little exploration was undertaken in the area until the grounds were claimed by Zenmac Metal Mines Ltd. in 1952. In the late

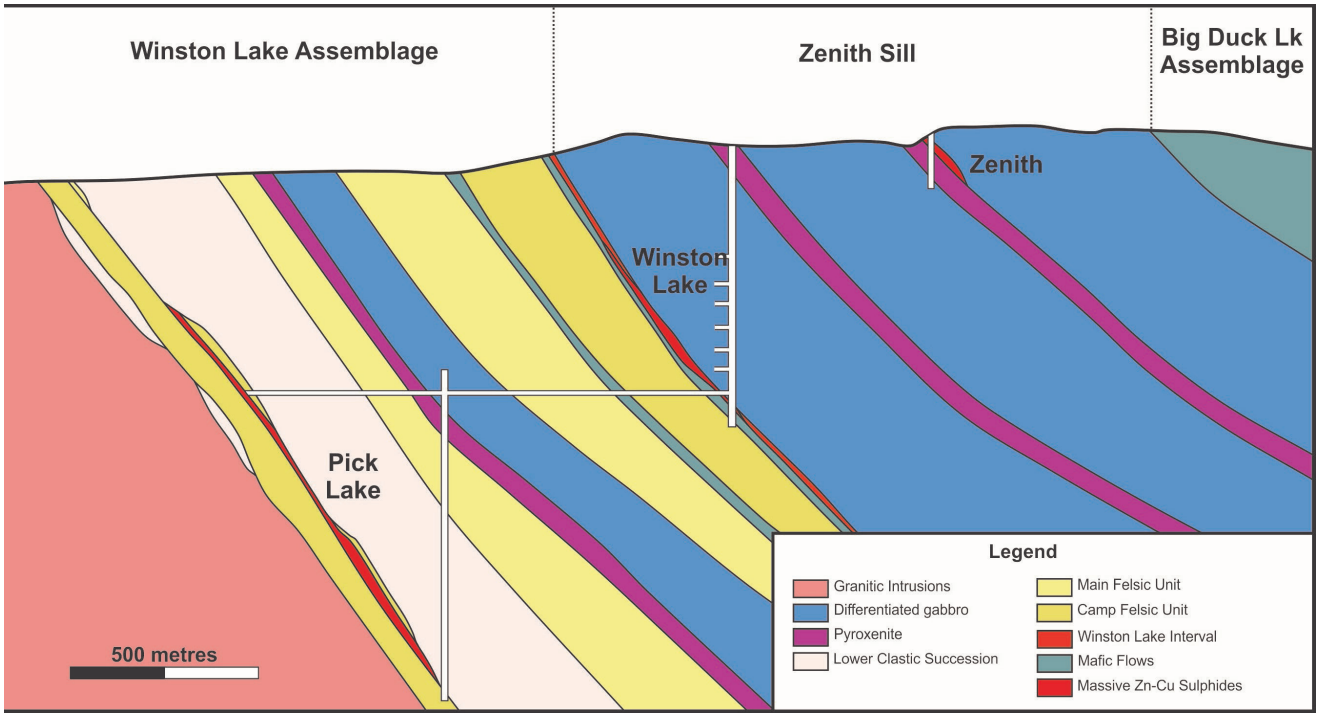


Figure 4. Schematic cross-section looking north-northwest through the strata hosting the VMS orebodies of the Winston Lake area. Figure modified from unpublished Inmet Mining Corp. figures based on stratigraphic terminology from Lodge et al. (2014).

Table 1. Summary of mining activity in the Winston Lake area (Resident Geologist's Files, Thunder Bay South District, Thunder Bay).

Mine	Years of Production	Ore Milled (tonnes)	Commodities and Grade
Winston Lake	1988-1999	3 268 698	1.04% Cu, 14.56% Zn, 32.32 g/t Ag, 1.41 g/t Au
Zenith	1891–1901	3416	45% Zn
Zenmac	1966–1970	164 200	16.5% Zn

1960's, almost 165,000 t at a grade of 16.5% Zn were mined from the Zenmac deposit.

After the Zenith Mine closed, the property was stagnant until 1978 when Corporation Falconbridge Copper (CFC) completed reconnaissance geological mapping and lithogeochemical sampling in the region. The "metasediments" (Bartley, 1940; Pye, 1964) were re-interpreted as metamorphosed felsic volcanics. This was followed by more detailed property mapping, lithogeochemistry, and geophysical surveys, which defined the alteration zone that is in the immediate footwall to the gabbro. Areas of Na_2O depletion and FeO, MgO, and Zn enrichment were outlined in the calc-alkaline volcanic rocks. CFC geologists also realized that the presence of massive sphalerite in the gabbro was unusual. The presence of VMS-like lithogeochemical signatures in the footwall to the gabbro led to the interpretation that the Zenith orebody was likely a large xenolith from a larger VMS orebody hosted at the top of the calc-alkaline felsic volcanic strata below the gabbro. With this newly recognized VMS potential, diamond drilling began in 1981 and targeted the felsic volcanic rocks at the base of the gabbro. In 1982, after only drilling five holes, CFC intersected 2.1 metres of massive sulphides containing 1.1% Cu, 19.1% Zn, 22.2 g/t Ag and 0.73 g/t Au. Mining began in 1988 and continued until the mine was officially closed in 1998. Later research by Osterberg (1993) and Lodge et al. (2014) outlines the lateral extent of alteration in the Winston Lake camp (Fig. 5).

The surface expression of the Pick Lake orebody, the Anderson occurrence, was first reported by local prospectors in 1952. There was some shallow diamond drilling completed in the area but nothing materialized. CFC picked up the claims following the discovery of the Winston Lake deposit in 1982. In 1984, diamond

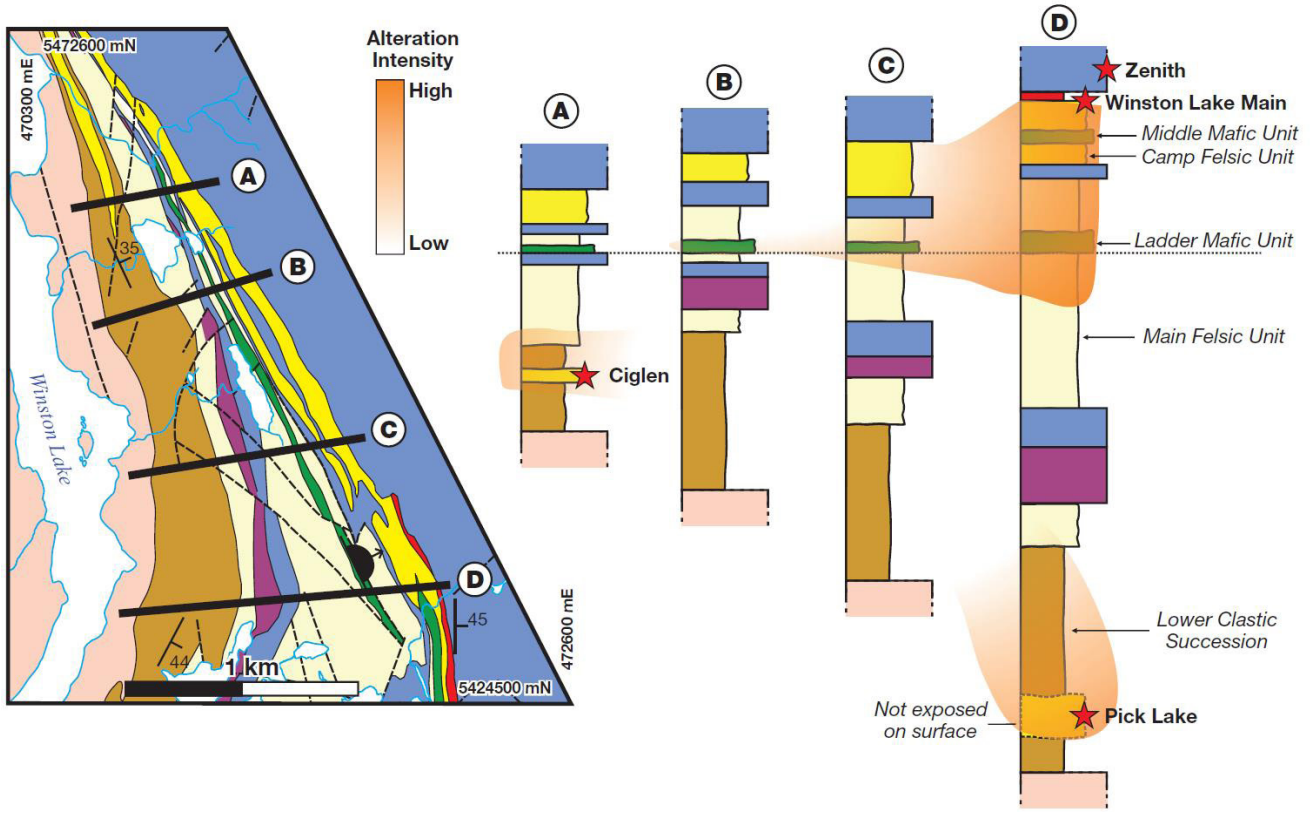


Figure 5. Lateral variations in the stratigraphic thicknesses in the Winston Lake assemblage. Distance between sections is not to scale. Strata are hung from the bottom of the Ladder mafic unit. Figure from Lodge et al. (2014). For location of figure and legend, refer to Figure 3.

drilling testing the down-dip extension of the Anderson occurrence discovered the Pick Lake orebody. In 1993, Metall Mining (formally Minnova, and operators of the mine at the time) began a 2200 metre drift to mine the Pick Lake deposit through the mine workings at Winston Lake. Doiron et al. (1997) proposed that the dyke-like nature of the deposit, combined with durchbewegung ore textures and sulphide injection structures, suggested that the Pick Lake deposit was a remobilized massive sulphide ore body. The Pick Lake Mine was abandoned when the Winston Lake Mine shut down in 1998.

After the shut-down of the mine limited exploration was carried out on the property. There were several mapping and geophysical projects carried out on select parts of Superior Lake Resources' current property between 2000-2011 by various exploration companies, but no further resources were outlined. In 2017-18, the mineral properties overlying the Pick Lake and Winston Lake deposits were acquired by Superior Lake Resources Limited. Superior Lake have completed new drilling programs that updated the resources at the Pick Lake and Winston Lake deposits (Table 2) and ground geophysical surveys that defined new targets for future exploration (Fig. 6).

Field Trip Stops

All coordinates are reported in NAD 83, Zone 16

The purpose of this portion of the field trip is to introduce the geological setting of strata hosting the VMS ore bodies at Winston Lake. As most of the lithofacies of the greenstone belt are difficult to access, this part of the trip will focus on camp-scale features and what role they played in the discovery of the orebodies. The stops will focus on the immediate footwall strata to the Winston Lake deposit and will highlight some of the geochemical and geochronologic data obtained from recent studies (Lodge et al., 2014). The field stops are illustrated in Figure 7.

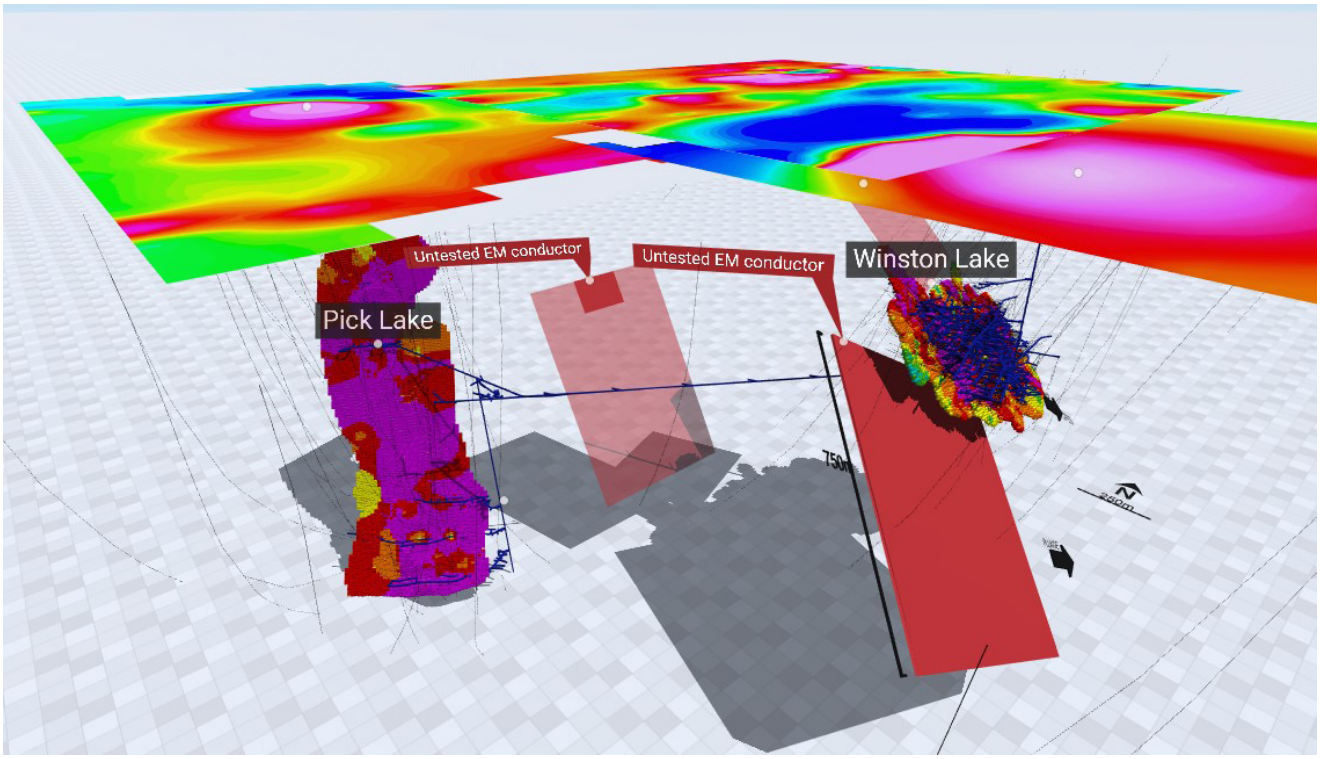


Figure 6. Recent ground EM geophysical results in the vicinity of the Winston Lake and Pick Lake ore bodies. Figure obtained from Superior Lake Resources website (www.superiorlake.com.au).

Table 2. Updated resources at the Pick Lake and Winston Lake deposits (www.superiorlake.com.au).

Resource Category	Tonnage (Mt)	Zn (%)	Cu (%)	Au (g/t)	Ag (g/t)
Indicated	2.07	18.0	0.9	0.38	34
Inferred	0.28	16.2	1.0	0.31	37
Total // Weighted Average	**2.35**	**17.7**	**0.9**	**0.38**	**34**

(News Release, Superior Lake Resources Limited, March 7, 2019)

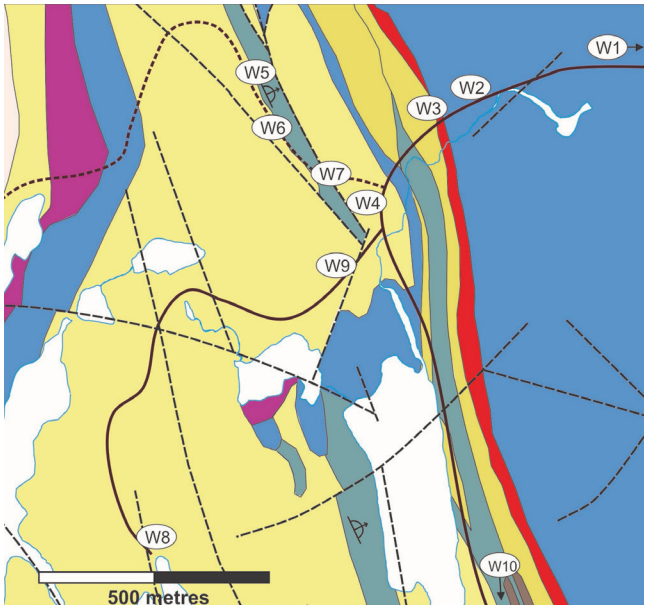


Figure 7. Geology of the Winston Lake mine area highlighting the location of field trip stops. Figure modified from Lodge (2012) based on data presented by Lodge et al. (2014). For location of figure and legend, refer to Figure 3.

Stop 1 – Zenith Mine Open Pit

UTM Coordinates 473182E 5424996N

This stop is inside of the main Winston Lake Mine gate. It is a short drive along mine property roads. From where we park, walk along the base of the cliff toward the lake. **WARNING**: The walk into the main pit area is on a narrow and steep-sided path. Walking to the exposures of sulphides in a large group is discouraged.

This stop represents the remnants of the original discovery in the Winston Lake area. The gabbro (now amphibolite) in this area is massive with some low-angle shears cutting up the outcrop. The gabbro is differentiated and consist of phases ranging from leucocratic gabbro to pyroxenite (this is more apparent at Stop 2). The Zenith orebody appears to be associated with the transition from gabbro to pyroxenite.

The Zenith orebody is essentially mined out but there are a few metre-scale slivers of massive sphalerite remaining. The ores are strictly Zn-rich and contain only minor amounts of pyrite, pyrrhotite, and chalcopyrite. Like most zinc-rich ores, they commonly are coated by white chalky zinc oxide minerals. The grain size of the sphalerite is generally coarse, most likely recrystallized during regional metamorphism.

Stop 2 – Differentiated Gabbro

UTM Coordinates 472337E 5425082N

This stop is on the main road about 100 metres back from the Winston Lake mine gate along the side of the road. The different phases of the gabbro intrusion are well-exposed on either side of the road. This outcrop is very large and is dissected by a stream. We will not be crossing the stream.

This stop highlights the complexity and multiple phases of the gabbro. On either side of the road, near the gate to the Winston Lake mine site, are perfectly exposed road cuts and stripped exposures of the gabbro that hosts the Zenith orebody. At this stop, we are less than 100 metres from the base of the intrusion.

Particularly on the south side of the road toward the creek, the gabbro has a layered appearance with layers of pyroxenite (now mostly hornblende) and more plagioclase-rich leucocratic layers. In other areas, there are pegmatitic patches with large centimetre-scale plagioclase crystals. The compositional layering in this intrusion ranges from centimetre-scale to metre-scale



Photo 1. (Left) Zenith mine open pit. (Right) Sphalerite-rich xenolith in gabbro.



Photo 2. Differentiated gabbro showing melanocratic and leucocratic layers.

layers. Most of these variations are not mappable.

A leucocratic pegmatitic phase of the gabbro was sampled for U-Pb geochronology to determine the age of the gabbro. Zircons separated from the gabbro were low-U, typical of gabbroic zircons, indicating that they were magmatic in origin rather than xenocrystic. These grains were analyzed using TIMS analysis at the University of Toronto, yielding a U-Pb age of 2719.2 ± 4.0 Ma. This age indicates that the gabbro that intruded and entrained the Winston Lake VMS body is synvolcanic, and the same age (or slightly younger) as the host rocks.

Stop 3 – Winston Lake Horizon

UTM Coordinates 472200E 5425057N

This stop is along the main road about 100 metres west from Stop 2. It is a large roadcut outcrop of the contact between the gabbro and the underlying felsic volcanic rocks.



Photo 3. Bedded felsic volcaniclastic unit known as the Winston Lake Horizon.

At this stop, the contact between the gabbro and the underlying volcanic rocks is exposed along road cuts leading toward the mine property. Immediately below the contact with the gabbro is a layered siliceous tuff unit that is known as the Winston Lake Interval. About 450 metres down dip of this unit is the Winston Lake main orebody.

The finely laminated layers range in thickness from a few millimetres to 1-2 centimetres and range in composition from felsic tuff, chert, and lesser mafic tuff. This unit is laterally extensive (Fig. 3) and continues almost the entire length of the Winston Lake assemblage. Trace element and REE patterns suggest that this ash layer has an FII to FIII type felsic composition (Hart et al., 2004). There is little variation in this volcaniclastic unit, both compositionally and texturally, although it is locally interlayered with mafic flows.

Stop 4 – Altered Felsic Volcanic Rocks in Footwall

UTM Coordinates 472123E 5424987N

Continue south(west) along the road for about 150 metres to the next stop. This stop is near the trail entrance to stops W5 to W7. There is about 100 metres of roadcut outcrop of variably altered felsic volcanic rocks here to examine.

This stop, and nearby outcrops typify the alteration facies (assemblages) found within the uppermost Main and Camp felsic units. These altered units are laterally extensive, but relatively thin (Figs. 3 & 4) and it is not known how many flows are represented within this unit. Unaltered equivalents of this rock are usually massive, coherent units that are quartz- and plagioclase-phyric,



Photo 4. Altered felsic volcanic rock now a quartz-muscovite-sillimanite-biotite schist.

and locally contain flow banding. Minor felsic tuffs and tuff breccias have also been described in this unit elsewhere in the camp (Osterberg, 1993). This unit has a U-Pb age of 2723 ± 3 Ma (Davis et al., 1994).

Altered versions of these quartz- and feldspar-phyric flows contain variable amounts of biotite, muscovite, sillimanite, and cordierite. Phenocrysts may be locally preserved, but are more difficult to see. Lesser altered equivalents contain quartz-muscovite-biotite-feldspar assemblages. With increasing degree of alteration, the rocks contain cordierite, sillimanite knots, garnet and anthophyllite. Major element geochemistry shows extensive Na_2O depletion and local Fe-Mg enrichment. Trace element and REE patterns indicate that this unit is a FIII-type felsic volcanic (Fig. 8).

Stop W5 – "Ladder" Mafic Flow

UTM Coordinates 471800E 5425200N

From the last stop, enter the trail that leads westward from the main road. The next stop is approximately 500 metres in along the trail. This is the furthest stop from the main road and we will be returning on the same trail and we will look at the lithofacies passed over on the return trip. **WARNING**: This is an ATV trail and there are many wet places and irregular surfaces. Please walk with caution and try and stay dry.



Photo 5. (Top) Coarse grained orthoamphibole. (Bottom) Orthoamphibole-garnet-biotite schist.

This outcrop of the Ladder Mafic Unit contains some of the most spectacular features that will be observed

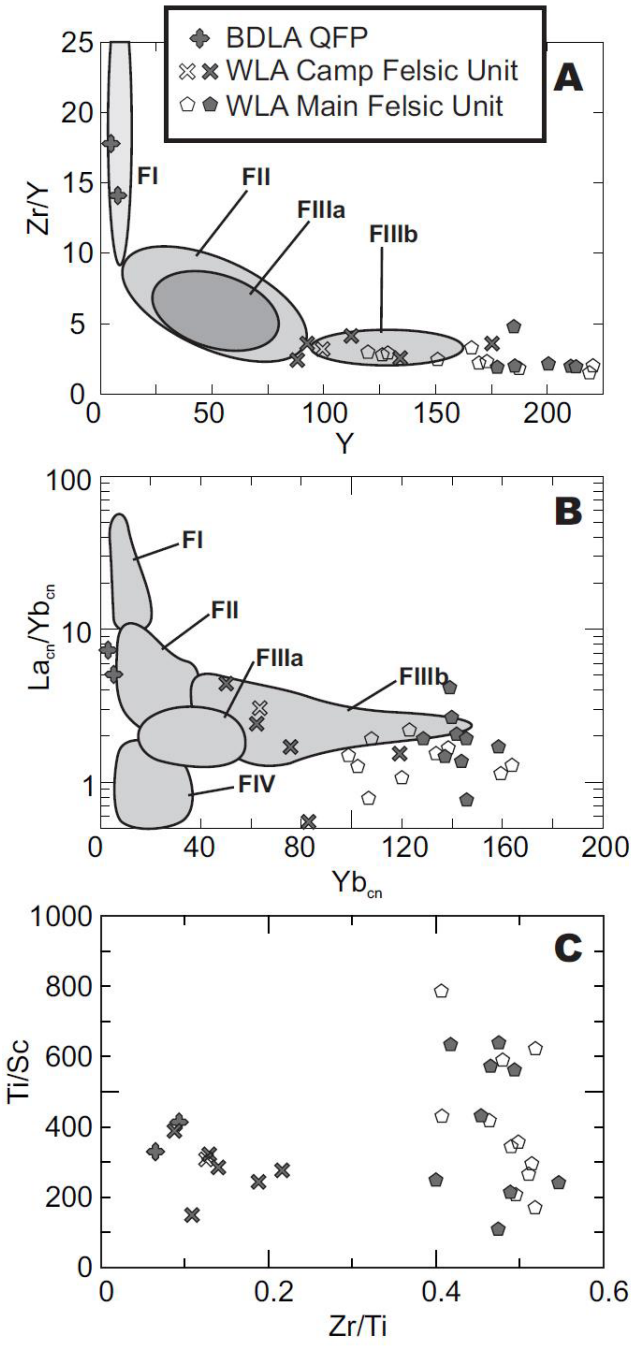


Figure 8. Geochemical discrimination plots for the felsic units in the Winston Lake greenstone belt. One notable geochemical distinguisher for the different felsic units in the Winston Lake Assemblage is the differences in Zr/Ti. Figure from Lodge et al. (2014). Fields in plots A and B are from Lesher et al. (1986) and Hart et al. (2004).

during this field trip. In addition to the coarse-grained mineral assemblages associated with metamorphosed hydrothermal alteration, the overall lack of significant deformation in this area has preserved the volcanic textures in the rock (Fig. 9). Younging directions are still determinable in this unit despite strong alteration and they indicate an eastward younging of the strata. As with most units in the Winston Lake assemblage, this unit is laterally extensive, but relatively thin. Unaltered equivalents of the Ladder Flow contain plagioclase phenocrysts.

At the eastern limit of this outcrop are spectacular exposures of an orthoamphibole-cordierite assemblage within the altered pillowed mafic flows. The pillows are metre-scale and their selvages are resistive weathering. There appears to be very little compositional difference between the pillow interior and the selvages, with the exception of slightly more biotite. Stratigraphically below the pillows is a 10 metre thick massive basalt flow. This massive flow is very homogeneous and the only variation are gradational changes in the size of the orthoamphibole crystals. These crystals can be up to 10 centimetres in size and are usually randomly oriented. The matrix is mostly medium grained cordierite and minor biotite in this massive lithofacies.

Near the lower contact with the altered felsic volcanic rocks, the Ladder Flow contains abundant clots, sheets, and veins of porphyroblastic garnet. In addition to garnet-orthoamphibole-cordierite, there are also local concentrations of biotite and chlorite. This alteration style is interesting, but difficult to interpret. In some places it appears as if the garnet clots represent altered clasts in a breccia. In other locations, they may be altered pillow margins or may be deformed veins. Regardless, the sharp transition to massive orthoamphibole-cordierite altered flow into a more chaotic orthoamphibole-garnet-cordierite zone may indicate the transition from a massive to breccia facies of this unit. It may also represent a different chemical gradient within the alteration zone. Geochemically, the garnet-bearing rocks are still mafic in composition.

The geochemical characteristics from the Ladder Mafic Unit, as well as other mafic units throughout the greenstone belt, are summarized in Figure 10. All of the mafic flows in the footwall to the Winston Lake mine have similar geochemical characteristics. Most noteworthy is that they are all calc-alkalic to transitional in their magmatic affinities and have pronounced negative Nb anomalies. In the hangingwall strata (i.e. Big Duck Lake Assemblage), the flows are tholeiitic and have flat rare earth and trace element patterns on normalized element plots (Lodge et al., 2014).

Stop 6 – Trail Showing

UTM Coordinates 471867E 5425051N

From the previous stop, return eastward back toward the main road for approximately 150 metres. This stop is a flat, rusty outcrop that we walked over to get to the

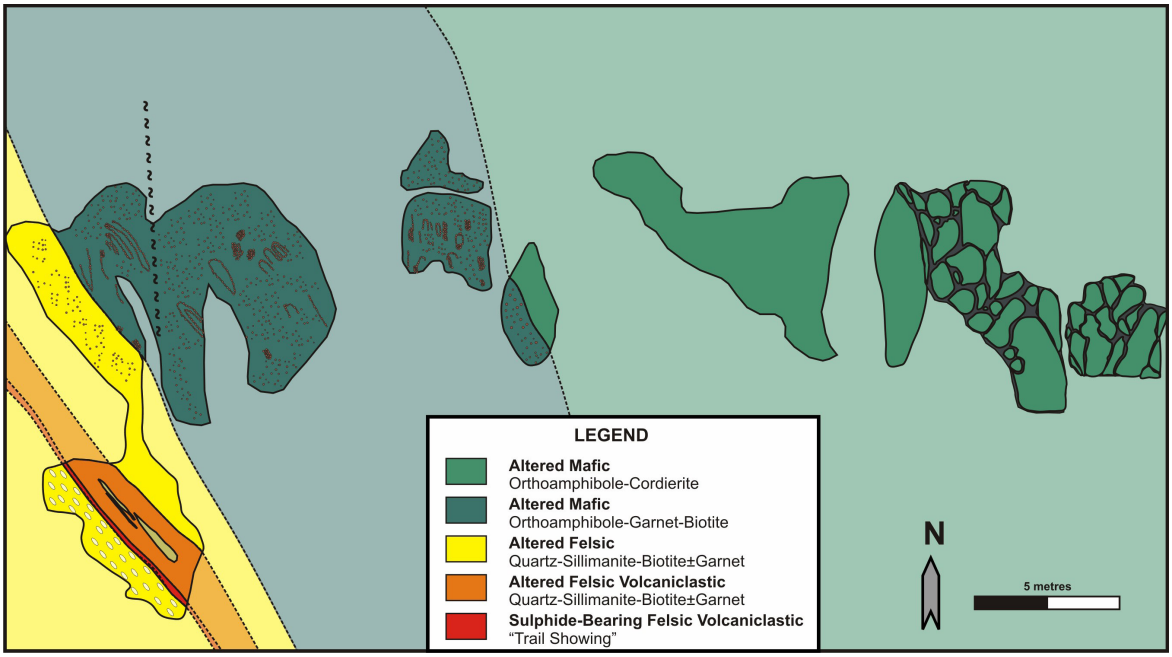


Figure 9. Outcrop sketch of the contact between the altered mafic "Ladder flow" and the underlying altered felsic volcanics in the Winston Lake area. Sketch only incorporates areas that were cleaned and there are additional outcrops in the area.

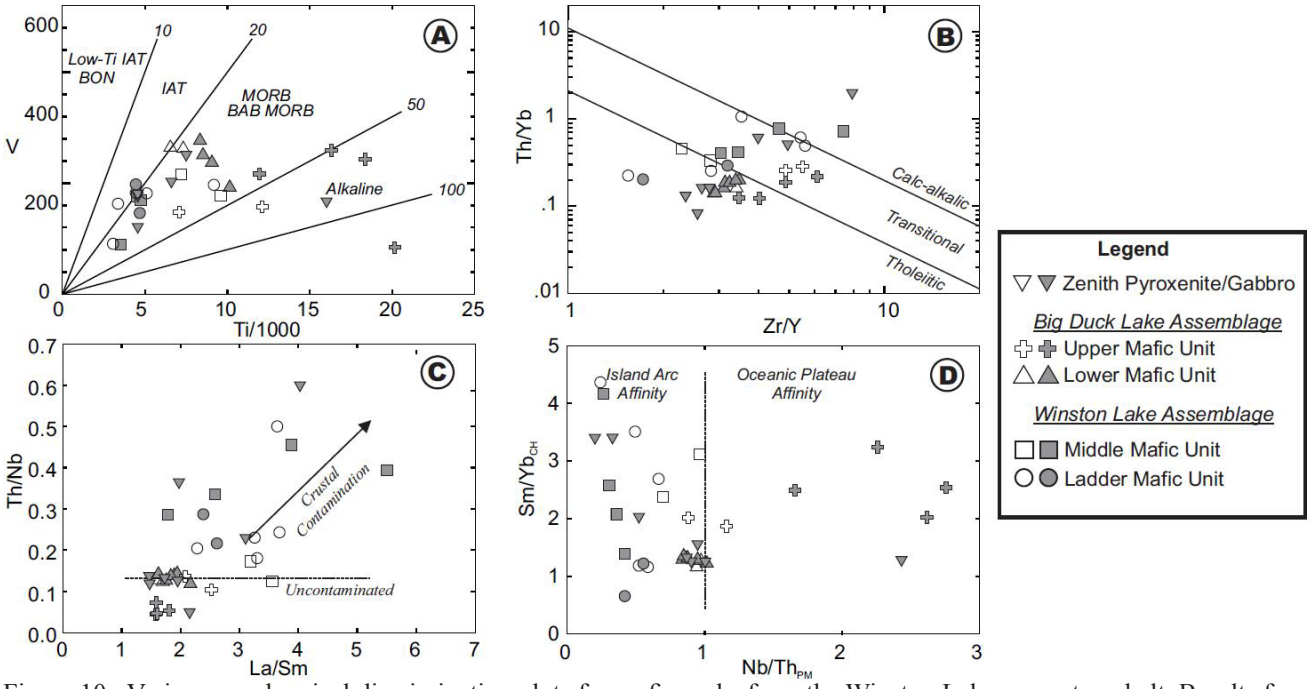


Figure 10. Various geochemical discrimination plots for mafic rocks from the Winston Lake greenstone belt. Basalts from the Ladder and Middle units tend to be have more calc-alkalic to transitional magmatic affinities. Sills and flows from the Big Duck Lake assemblge are mainly tholeiititc. Figure from Lodge et al. (2014). Fields in A from Shervais (1982). Fields in B from Ross & Bedard (2009). Fields in C from Piercey et al. (2002). Fields in D modified from Polat (2009).

Ladder Flow.

This stop represents one of the many smaller mineralized intervals in the Winston Lake camp. The mineralization in the "Trail Showing" is located near the contact between the "Ladder Flow" and underlying felsic volcanic rock and it is hosted within a siliceous, bedded volcaniclastic unit up to 15 centimetres thick. It contains over 6000 ppm Cu and Zn-bearing metamorphic minerals such as gahnite are also present.

The bedded volcaniclastic unit is altered to a quartz-cordierite-biotite-garnet mineral assemblage containing variable amounts of orthoamphibole and sillimanite. The layering in the rock appears to be relict primary volcanic texture.



Photo 6. Felsic volcaniclastic rock hosting disseminated sulphides.

This unit is distinct and is present at the contact between the Ladder mafic flow and the underlying massive, altered quartz-feldspar-phyric Main felsic flow, which the trail passes over from there to the main road. The alteration assemblages in the massive flow are the same as those observed at Stop 4.

Stop 7 – Contact of Ladder Flow and Altered Felsic Volcanic Rocks

UTM Coordinates 471918E 5424992N

Continuing back toward the main road along the trail, this stop is approximately 100 metres from the previous stop. This is the last stop on the trail before returning to the main road.

This stop shows the contact between the Ladder mafic flow and the overlying altered Main felsic volcanic rocks, which constitute the immediate footwall strata to the Winston Lake deposit. Cleaning of this otherwise black and featureless exposure resulted in a near-perfect exposure of an altered basaltic flow top breccia that is intermingled with the overlying felsic tuff. This is one of a few places where these flow features are exposed at surface. The variety of flow facies exposed within



Photo 7. Upper contact of altered mafic flow (Ladder Flow) and altered felsic volcanic.

the Ladder mafic flow indicates that the contact at this stop is not a peperite caused by a sill mingling with overlying unconsolidated tuff. Rather, it is more likely that the felsic tuff settled into on top of the basaltic flow top breccia.

The flow here is altered to an orthoamphibole-garnet assemblage with retrograde chlorite and biotite. The garnet porphyroblasts are evenly distributed and occur in the felsic volcanic above the contact. This suggests some chemical exchange between the lithofacies at the contact during metamorphism, as previously suggested by Gorton and Schandl (1995). The overlying felsic tuff is altered to a quartz-muscovite-sillimanite-biotite mineral assemblage.

Stop 8 – Pick Lake Vent Raise Area

UTM Coordinates 471579E 5424177N

About 150 metres south of the trail entrance on the main road is the gate to the Pick Lake deposit. The Pick Lake vent raise, and the next stop are about 1.1 kilometres from the gate. There are plenty of outcrops around the former vent raise to examine that show a variety of alteration facies. **WARNING**: Although the shaft has a concrete cap and is safe to walk on, please do not walk directly on old mine workings.

This stop is in the middle of the thickest part of the quartz-feldspar-phyric felsic flow that forms the Main felsic unit of the Winston Lake assemblage and the hanging wall to the Pick Lake orebody. The Pick Lake deposit is about 300 metres directly below the mine workings near this stop. The orebody is not associated with the rocks exposed here, rather is associated with felsic volcaniclastic and siliciclastic rocks that dip eastward underneath this unit (Fig. 4). We will not see the host rocks to the Pick Lake deposit on this trip because they are not easily accessible. The surface expression of the Pick Deposit is known as the Anderson Occurrence and is 850 m west of this location.

Based on this location alone, it is not clear whether this part of the Main Felsic Unit is definitively an intrusion or extrusion (e.g. Osterberg, 1993). There appears to be very little textural variation in the unit throughout the area. The unit is massive and the only variations are in the degree of alteration and mineral assemblages. The alteration is pervasive and mineralogical changes are gradational and do not appear to represent primary compositional layering. If it is an extrusive unit, it is a very massive flow with only a thin brecciated carapace (seen at Stop W9). Stratigraphically above the Ladder Mafic Unit, the Main Felsic Unit appears to exhibit phenocryst sizes in unaltered parts of this unit that are much larger (3-4 millimetres) compared to the Camp Felsic Unit in the footwall to the Winston Lake orebody.

A sample of this unit was submitted for U-Pb dating by TIMS analysis at the University of Toronto. The sample yielded a homogeneous population of zircon that produced an age of 2721 ± 1 Ma. This confirms that the unit is the same age as the host rocks to the Winston Lake orebody. The Main felsic unit has a notably higher Zr/Ti ratio that the Camp felsic unit. All the felsic magmas in this camp are FIII type felsic magmas.



Photo 8. Quartz-muscovite-biotite-garnet schist near the Pick Lake mine shaft.

Stop 9 – Pick Lake Felsic Breccias

UTM Coordinates 471998E 5424667N

This stop is a roadside outcrop on the Pick Lake road approximately 100 metres away from the gate. This is the last stop inside the Pick Lake gated road.

At this stop, the monolithic breccia phase of the felsic quartz-feldspar-phyric flow from the Main Felsic Unit is well exposed on the roadside. It is not certain if this breccia is a volcanic or structural texture. Given that the main part of this body is thick, massive and homogeneous, and that it has been confirmed to be the same age of the surrounding volcanic rocks, it is possible that this may represent the synvolcanic intrusion that was the feeder for the overlying felsic flows and volcaniclastic units above the Ladder mafic unit. It is common for hypabyssal synvolcanic intrusions to be brecciated at their margins. Alternatively, it could represent the breccia margin of a flow. Opinions are encouraged!

The fragments are lenticular and stretched defining a pronounced stretching lineation. They contain quartz and plagioclase phenocrysts that compose up to 15% of the fragment. The anastomosing matrix is composed of quartz-biotite-muscovite mineral assemblages and composes up to 25% of the rock. There is no obvious layering in the rock but there is some variation in the abundance and size of the clasts that may represent crude bedding.

Stop 10 – Tuffaceous Metasedimentary Rocks

UTM Coordinates 472699E 5423145N

This stop is 1.8 kilometres southward on the main road from the Pick Lake gate and is adjacent to the power lines. There are several roadcut outcrops that are worth checking out.



Photo 9. Matrix-supported quartz-phyric felsic volcanic breccia.

This is the final stop of the field trip. The tuffaceous metasedimentary rocks are along strike and south from the orebodies, and do not contain mineral assemblages indicative of significant hydrothermal alteration. They were classified as "intermediate volcaniclastics" by Osterberg (1993). There are many sedimentary structures in this unit, such as cross-bedding, that suggesting it is a reworked volcaniclastic deposit. The composition of the rock suggests that the provenance is mostly mafic with only a minor felsic component.

In this stop, mineral assemblages range from biotite-quartz-garnet to biotite-quartz-hornblende and even local concentrations of lapilli-sized clasts of mafic composition. These compositional variations are on the metre- to outcrop-scale.



Photo 10. Low-angle cross-bedded mafic-intermediate tuffaceous metasedimentary rock.

A sample of this unit within the finer-grained, cross-bedded part of the exposure was sent for detrital zircon analysis at the LA-ICP-MS lab at Laurentian University. The results show a single peak centered around 2720 Ma, suggesting that the source of detritus was local and from 2720 Ma volcanic units (Lodge et al., 2014). The composite, mafic-felsic composition of these rocks suggests that they are not primary volcanic deposits. They may represent distal, reworked facies of slump fans deposited during rifting and sourced from bimodal volcanic units within the Winston Lake assemblage.

Acknowledgements

The guidebook represents a revised version of a field trip guidebook published by the Ontario Geological Survey (OFR 6282). Much of the text and images has been re-used from this publication. A complete citation for that publication is below:

Lodge, RWD (2012). Winston Lake and Manitouwadge revisited: Modern views of two volcanogenic massive sulphide (VMS)-endowed greenstone belts: A field trip guidebook. Ontario Geological Survey, Open File Report 6282, 37 p.

In addition, the authors would like to thank management of Superior Lake Resources for allowing members of the Institute on Lake Superior Geology to access their mineral exploration property.

References

Bartley, M.W. 1940. Geology of the Big Duck-Aguasabon Lakes area. Ontario Geological Survey, Map 49k.

Carter, M.W. 1982a. Precambrian geology of the Terrace Bay area, northeast sheet, Thunder Bay District. Ontario Geological Survey, Preliminary Map 2557.

Carter, M.W. 1982b. Precambrian geology of the Terrace Bay area, northwest sheet, Thunder Bay District. Ontario Geological Survey, Preliminary Map 2556.

Corfu, F. and Stott, G.M. 1998. Shebandowan greenstone belt, western Superior Province: U-Pb ages, tectonic implications, and correlations. Geological Society of America Bulletin 110, p. 1467-1484.

Davis, D.W., Schandl, E.S., and Wasteneys, H.A. 1994. U-Pb dating of minerals in alteration halos of Superior Province massive sulfide deposits; syngenesis versus metamorphism. Contributions to Mineralogy and Petrology 115, p. 427-437.

Doiron, D., Siddiqui, M., and Smyk, M.C. 1997. Preliminary investigations of the Pick Lake deposit, Winston Lake Mine, Ontario: A remobilized massive sulphide orebody; 43rd Institute on Lake Superior Geology, Program with Abstracts, Sudbury, Ontario, p.17-18.

Gorton, M.P. and Schandl, E.S. 1995. An unusual sink for rare earth elements: the rhyolite-basalt contact of the Archean Winston Lake volcanogenic massive sulphide deposit, Superior Province, Canada. Economic Geology 90, p. 2065-2072.

Hart, T.R., Gibson, H.L., and Lesher, C.M. 2004. Trace element geochemistry and petrogenesis of felsic volcanic rocks associated with volcanogenic massive Cu-Zn-Pb sulfide deposits. Economic Geology 99, p. 1003-1013.

Kerrich, R., Polat, A., and Xie, Q. 2008. Geochemical systematics of a 2.7 Ga Kinojevis Group (Abitibi), and Manitouwadge and Winston Lake (Wawa) Fe-rich basalt-rhyolite associations: Backarc rift oceanic crust? Lithos 101, p. 1-23.

Lesher, C.M., Goodwin, A.M., Campbell, I.H., and Gorton, M.P. 1986. Trace-element geochemistry of ore-associated and barren, felsic metavolcanic rocks in the Superior Province, Canada. Canadian Journal of Earth Sciences 23, p. 222-237.

Lodge, R.W.D. 2012. Winston Lake and Manitouwadge revisited: Modern views of two volcanogenic massive sulphide (VMS)-endowed greenstone belts. A field trip guidebook., Ontario Geological Survey Open File Report 6282, p. 37.

Lodge, R.W.D. and Chartrand, J.E. 2013. Establishing regional geodynamic settings and the metallogeny of volcanogenic massive sulphide mineralization of greenstone belt assemblages (circa 2720 Ma) of the Wawa Subprovince via geochemical comparisons, Ontario Geological Survey, Miscellaneous Release - Data 306.

Lodge, R.W.D., Gibson, H.L., Stott, G.M., Franklin, J.M., and Hamilton, M.A. 2014. Geodynamic reconstruction of the Winston Lake greenstone belt and VMS deposits: New trace element geochemistry and U-Pb geochronology. Economic Geology 109, p. 1291-1313.

Lodge, R.W.D., Gibson, H.L., Stott, G.M., Franklin, J.M., and Hudak, G.J. 2015. Geodyamic setting, crustal architecture, and VMS metallogeny of ca. 2720 Ma greenstone belt assemblages of the northern Wawa subprovince, Superior Province. Canadian Journal of Earth Sciences 52, p. 196-214.

Lodge, R.W.D., Gibson, H.L., Stott, G.M., Hudak, G.J., and Jirsa, M. 2013. New U-Pb geochronology from Timiskaming-type assemblages in the Shebandowan and Vermilion greenstone belts, Wawa Subprovince, Superior Craton: Implications for the Neoarchean development of the southwestern Superior Province. Precambrian Research 235, p. 264-277.

Ontario Geological Survey 2019. Mineral Deposit Inventory; Ontario Geological Survey, Mineral Deposit Inventory (April 2019 update), online database.Osterberg, S.A. 1993. Stratigraphy, physical volcanology, and hydrothermal alteration of the footwall rocks to the Winston Lake massive sulfide deposits, northwestern Ontario. University of Minnesota at Minneapolis, 351 p..

Peterson, D., Gallup, C., Jirsa, M., and Davis, D.W. 2001. Correlation of the Archean assemblages across the U.S.-Canadian border: Phase I geochronology, 47th Annual Meeting, Institute on Lake Superior Geology, Proceedings Volume 47, Part 1 - Program and Abstracts, p. 77-78.

Piercey, S.J., Mortensen, J.K., Murphy, D.C., Paradis, S., and Creaser, R.A. 2002. Geochemistry and tectonic significance of alkalic mafic magmatism in the Yukon-Tanana terrane, Finlayson Lake region, Yukon. Canadian Journal of Earth Sciences 39, 1729-1744.

Polat, A. 2009. The geochemistry of Neoarchean (ca. 2700 Ma) tholeiitic basalts, transitional to alkaline basalts, and gabbros, Wawa Subprovince, Canada: Implications for petrogenetic and geodynamic processes. Precambrian Research 168, p. 83-105.

Polat, A., Kerrich, R., and Wyman, D.A. 1999. Geochemical diversity in oceanic komatiites and basalts from the late Archean Wawa greenstone belts, Superior Province, Canada: trace element and Nd isotope evidence for a heterogeneous mantle. Precambrian Research 94, p. 139-173.

Pye, E.G. 1964. Mineral deposits of the Big Duck Lake area, district of Thunder Bay, Ontario Department of Mines Geological Report 27, 58 p..

Ritcey, D.J. 1992. Geology and mineralization in the vicinity of Big Duck Lake, Ontario. Unpublished MSc. thesis, University of Ottawa, 235 p..

Ross, P.-S. and Bédard, J.H. 2009. Magmatic affinity of modern and ancient subalkaline volcanic rocks determined from trace-element discriminant diagrams. Canadian Journal of Earth Sciences 46, p. 823-839.

Schandl, E.S., Gorton, M.P., and Wasteneys, H.A. 1995. Rare earth element geochemistry of the metamorphosed volcanogenic massive sulfide deposits of the Manitouwadge mining camp, Superior Province, Canada; a potential exploration tool? Economic Geology and the Bulletin of the Society of Economic Geologists 90, p. 1217-1236.

Severin, P.W.A., Balint, F., and Sim, R. 1991. Geological setting of the Winston Lake massive sulphide deposit, Mineral Deposits in the Western Superior Province, Ontario, Geological Survey of Canada Open File 2164, p. 58-73.

Shervais, J.W. 1982. Ti-V plots and the petrogenesis of modern and ophiolitic lavas. Earth and Planetary Science Letters 59, p. 101-118.

Smyk, M.C. and Schnieders, B.R. 1995. Geology of the Schreiber greenstone assemblage and its gold and base metal mineralization; 41st Institute on Lake Superior Geology, Proceedings volume 41, pt.2c, Marathon, Ontario, 77 p.Williams, H.R., Stott, G.M., Heather, K.B., Muir, T.L., Sage, R.P., 1991. Wawa Subprovince, in: Thurston, P.C., Williams, H.R., Sutcliffe, R.H., Stott, G.M. (Eds.), Geology of Ontario, Ontario Geological Survey, Special Volume 4, Part 1, p. 485-541.

Zaleski, E., van Breemen, O., and Peterson, V.L. 1999. Geological evolution of the Manitouwadge greenstone belt and Wawa-Quetico subprovince boundary, Superior Province, Ontario, constrained by U-Pb zircon dates of supracrustal and plutonic rocks. Canadian Journal of Earth Sciences 36, 945-966.